Electric Technology U.S.S.R.

ЭЛЕКТРИЧЕСТВО

Volume I, January, 1959

Selected papers from

Elektrichestvo Nos. 3 and 4, 1958

Published by

ERGAMON PRESS *NE*

for Pergamon Institute, New York and

SPEEDY, ACCURATE AND
ECONOMICAL TRANSLATION SERVICE
You can now obtain speedily translation of a
article published in the open literature of the USS
or abstract thereof at a reasonable price. Wh
there is a need for a speedy, accurate and economic
translation, please write to The Administrati
Secretary, Pergamon Institute—in London or Ne
York at:

ELECTRIC TECHNOLOGY, U.S.S.R.

EDITORIAL BOARD

H. M. Barlow, *London*; F. W. Bowden, *San Luis Obispo*; F. Brailsford, *London*; G. S. Brown, *Cambridge, Mass.*; F. M. Bruce, *Glasgow*; C. C. Carr, *Brooklyn*; G. W. Carter, *Leeds*; A. G. Conrad, *New Haven, Conn.*; G. F. Corcoran, *College Park, Md.*; J. D. Craggs, *Liverpool*; A. L. Cullen, *Sheffield*; G. E. Dreifke, *St. Louis*; V. Easton, *Birmingham*; A. R. Eckels, *Vermont*; W. Fishwick, *Swansea*; C. Froehlich, *New York*; C. G. Garton, *Leatherhead*; J. Greig, *London*; L. D. Harris, *Salt Lake City*; J. D. Horgan, *Milwaukee*; E. C. Jones, *Morgantown*; E. C. Jordan, *Urbana*; I. H. Lovett, *Rolla, Missouri*; J. M. Meek, *Liverpool*; J. H. Mulligan Jnr., *N.Y.*; W. A. Murray, *Blacksburg, Virginia*; J. E. Parton, *Nottingham*; H. A. Peterson, *Madison*; A. Porter, *London*; J. C. Read, *Rugby*; W. G. Shepherd, *Minneapolis*; W. P. Smith, *Lawrence, Kansas*; Philip Sporn (Chairman), *New York*; J. A. Strelzoff, *East Lansing*; F. W. Tatum, *Dallas, Texas*; C. V. O. Terwilliger, *Monterey*; D. H. Tompsett, *Stafford*; A. Tustin, *London*; S. Reid Warren Jnr., *Philadelphia*; A. R. van C. Warrington, *Stafford*; A. H. Waynick, *Pa.*; E. M. Williams, *Pittsburgh*; F. C. Williams, *Manchester*; H. I. Wood, *Manchester*; C. M. Zieman, *Ohio*.

PERGAMON INSTITUTE

A NON-PROFIT FOUNDATION FOR THE FURTHERANCE
AND DISSEMINATION OF SCIENTIFIC KNOWLEDGE

President of the Board of Governors:

Sir Robert Robinson, O.M., F.R.S.

Executive Director: Captain I. R. Maxwell

4 & 5 Fitzroy Square, London W.1
122 East 55th Street, New York 22, N.Y.

Pergamon Institute can occasionally use additional translators for science and engineering material to assist with this programme of translation from Russian and other Slavonic languages.

Scientists and engineers who have a knowledge of Russian, and who are willing to assist with this work, should apply to the Administrative Secretary of the Institute. They should write to either New York or London for rates of payment and other details.

Financial assistance has also been received from A.S.E.A., Sweden

Four volumes per annum. Approximately 700 pages per annum.
Annual Subscription Rate £20 ($56).
Single volumes may be purchased for £6 ($14).

Orders should be sent to the distributors at either of the following addresses

4 & 5 Fitzroy Square, London W.1

122 East 55th Street, New York 22, N.Y.

PUBLISHED BY

PERGAMON PRESS LTD.
LONDON · NEW YORK · PARIS · LOS ANGELES

February 1959

ELECTRIC TECHNOLOGY, U.S.S.R.

VOLUMES 1—4, 1959

Selected papers and abstracts from *Elektrichestvo*, Nos. 3—12, 1958

EDITORIAL BOARD

H. M. Barlow (London)
F. W. Bowden (San Luis Obispo)
F. Brailsford (London)
G. S. Brown (Cambridge, Mass.)
F. M. Bruce (Glasgow)
C. C. Carr (Brooklyn)
G. W. Carter (Leeds)
A. G. Conrad (New Haven, Conn.)
G. F. Corcoran (College Park, Md.)
J. D. Craggs (Liverpool)
A. L. Cullen (Sheffield)
G. E. Dreifke (St. Louis)
V. Easton (Birmingham)
A. R. Eckels (Vermont)
W. Fishwick (Swansea)
C. Froehlich (New York)
C. G. Garton (Leatherhead)
J. Greig (London)
L. D. Harris (Salt Lake City)
J. D. Horgan (Milwaukee)
E. C. Jones (Morgantown)
E. C. Jordan (Urbana)
I. H. Lovett (Rolla, Missouri)
J. M. Meek (Liverpool)
J. H. Mulligan Jnr. (N.Y.)
W. A. Murray (Blacksburg, Virginia)
J. E. Parton (Nottingham)
H. A. Peterson (Madison)
A. Porter (London)
J. C. Read (Rugby)
W. G. Shepherd (Minneapolis)
W. P. Smith (Lawrence, Kansas)
Philip Sporn (Chairman) (New York)
J. A. Strelzoff (East Lansing)
F. W. Tatum (Dallas, Texas)
C. V. O. Terwilliger (Monterey)
D. H. Tompsett (Stafford)
A. Tustin (London)
S. Reid Warren Jnr. (Philadelphia)
A. R. van C. Warrington (Stafford)
A. H. Waynick (Pa.)
E. M. Williams (Pittsburgh)
F. C. Williams (Manchester)
H. I. Wood (Manchester)
C. M. Zieman (Ohio)

PERGAMON PRESS LTD.
LONDON · NEW YORK · PARIS · LOS ANGELES

PERGAMON INSTITUTE

A DIVISION OF PERGAMON INTERNATIONAL CORPORATION,
OPERATED IN THE PUBLIC SERVICE FOR THE FURTHERANCE
AND DISSEMINATION OF SCIENTIFIC KNOWLEDGE

President of the Scientific Advisory Council:
Sir Robert Robinson, O.M., F.R.S.
Executive Director: Captain I. R. Maxwell, M.C.
Scientific Secretary: Dr. D. J. Hughes

1404 *New York Avenue, N.W. WASHINGTON, 5 D.C.* (*Telephone No. Metropole No. 8-5382*)
Headington Hill Hall, OXFORD (*Telephone No. Oxford 64881*)

Financial assistance has also been received from A.S.E.A., Sweden

Elektrichestvo

Editor-in-Chief: N. G. DROZDOV

Deputy Editor-in-Chief: I. A. SYROMIATNIKOV

EDITORIAL BOARD

K. A. ANDRIANOV, N. I. BORISENKO, G. V. BUTKEVICH, M. G. CHILIKIN, A. A. GLAZUNOV, V. A. GOLUBTSOVA, E. G. KOMAR, M. P. KOSTENKO, L. R. NEIMAN, I. I. PETROV, V. I. POPKOV, A. M. FEDOSEEV, M. A. SHATELEN

ELECTRIC TECHNOLOGY, U.S.S.R.

CONTENTS OF VOLUMES 1–4, 1959

Vol. 1

PAGE

I. M. Postnikov: A method of calculating the performance of compound synchronous motors . 1

B. I. Nornevskii, V. F. Batko, V. E. Malishevskii, P. V. Kuropatkin and E. I. Rosin: Comparison of two-stage and three-stage rotary amplifiers with axial field 18

V. D. Afanas'ev and Ivobotenko: Speed control of a d.c. motor fed from a magnetic amplifier . 28

Yu. E. Efroimovich: Model installation for remote control of electric parameters in arc furnaces . 39

L. Ia. Stanislavskii: Turbogenerators of 30 to 300 MV power built by Khetz factory . . . 50

V. G. Fastovskii and Iu. V. Petrovskii: On the possibility of intensification of cooling of turbogenerators 61

A. P. Geppe: On the surface resistance of dielectrics 68

K. F. Guba: The dependence of frequency of the rochelle salt piezo-electric vibrators on temperature 77

A. M. Kakhelnik: The use of electric locomotives with rectifiers—A review 81

I. A. Glebov and S. F. Zonov: Service tests—Tests of the experimental installation of an ionic excited hydrogenerator 89

T. A. Suetin: Ignition IVS-200/2 97

B. Konorskii: Discussion: Modification of the heaviside formula 102

K. A. Andrianov: Synthetic compounds of high molecular weights as dielectrics 110

P. V. Sakharov: Apparatus for low-voltage distribution gear 127

G. V. Ostroumov: Investigation of transient processes in linear circuits by the method of loci . 137

I. G. Shubov: Determination of the level of magnetic noise of d.c. machines by the method of electromechanical analogy 146

Yu. P. Petrov: Transient processes in an electric drive for an exponential variation of the magnetic flux 156

T. A. Glazenko: The use of electromagnetic powder couplings for frequent reversals of a driven mechanism 164

A. A. Sakovich: The increase of the reliability of conversion networks 177

A. B. Oslon: Calculation of certain types of compound earthing devices 187

A. G. Mirer: Service tests—A method of calculation of mechanical characteristics of asynchronous motors under conditions of dynamic braking 198

S. Ia. Berezin: Experimental determination of parameters of elements of automatic control systems 201

Vol. 2

F. I. Butaev, N. S. Klimov, M. F. Kostrov and A. A. Sakovich: The high-power high-voltage rectifier 209

B. L. Konstantinov: The problem of the approximate analytical solution of oscillations of a synchronous machine 224

V. M. Matiukhin: The influence of the law of the excitation control on the damping of oscillations of a synchronous machine 230

M. M. Akodis: Artificial methods of obtaining high power for the investigation of arc extinction devices 240

O. G. Vegner: Increase of stability of a welding a.c. arc 252

N. P. Bogoroditskii and I. D. Friberg: Physical processes in electrical ceramics and rational methods of development 259

G. I. Poliuk: Automatically controlled series excitation for generators 271

A. B. Vitanov: Negative sequence filters with independent arms 284

PAGE

V. V. Artamonov: Calculation of the characteristics of an electric drive with frequency control by the equivalent resistance method 294

B. M. Shkolnikov and I. I. Sud: Properties and design of a multi-motor drive system with a mechanical differential 302

Vol. 3

V. L. Fabrikant: The utilization of semiconductors in relay protection 313

I. S. Bruk: Controlled reactors for long-distance transmission 322

I. K. Khrustalev: New methods of connecting starter-control resistances of asynchronous motors. 334

R. A. Lipman and I. B. Negnevitskii: Transient processes in a magnetic booster working in a relay system 337

Abstracts of papers published in *Elektrichestvo* No. 7, 1958 353

V. A. Prevezentsev: Heat resistant winding conductors 358

Ia. N. Shtrafun and M. S. Rostovtseva: An investigation for an automatic system of excitation for large turbogenerators using semiconductor power rectifiers 373

N. S. Siunov, B. K. Gavrilov and V. N. Breev: The excitation of synchronous motors of normal construction by the application of mechanical rectifiers 384

T. V. Stepnov: Directional protection from short-circuits to earth 392

Abstracts of papers published in *Elektrichestvo* No. 8, 1958 403

M. A. Panasenkov: Surface effect in solid ferromagnetic bodies taking non-linearity into account . 408

L. Ia. Stanislavskii: An experimental turbogenerator with internal hydrogen cooling of stator and rotor windings at a pressure of 3 atm 425

G. M. Kasprzhak: Calculation of the reduction of voltage on the terminals of high-power current collectors with strong actuating currents 435

V. T. Renne, N. N. Kaliazina and M. N. Morozova: Dielectric losses in condenser paper . . 445

Abstracts of papers published in *Elektrichestvo* No. 9, 1958 458

Vol. 4

I. M. Postnikov: Eddy currents in synchronous and asynchronous machines with unlaminated rotors 463

E. D. Sapir: Compensation of capacitive currents in differential phase carrier protection of transmission lines 480

V. A. Golovanov: The problem of a circuit for a rectifying semiconductor set on electric rolling stock of a.c. single-phase—d.c. transmission 494

O. B. Bron and D. S. Itenberg: Problems of liquid cooling in electrical equipment . . . 503

Abstracts from papers published in *Elektrichestvo* No. 10, 1958 513

N. A. Poliak: Short-circuits, asynchronous drive and turbogenerator resynchronization . . 519

V. V. Kaplan, V. M. Nashatyr' and V. L. Ivanov: A synthetic method of testing high-voltage circuit-breakers 533

L. L. Rotkop: The energy properties of an asynchronous motor with a system of impulse speed regulation 545

A. S. Kurbasov: On the conditions of the formation of flashover or arcing on to the framework of traction motors 556

Abstracts from papers published in *Elektrichestvo* No. 11, 1958 564

E. M. Tseirov: The electrical properties of compressed air in an air-blast circuit-breaker . . 570

M. G. Portnoi: The occurrence of sub-harmonic resonance in unbalanced line conditions . . 589

M. F. Iudov: Experimental investigation of deformations and vibrations of the stator windings . 599

P. S. Livshits: Calculation of losses in the sliding contacts of electric machinery 610

Abstracts from papers published in *Elektrichestvo* No. 12, 1958 619

ELEKTRICHESTVO

Editor-in-Chief: N. G. DROZDOV

Deputy Editor-in-Chief: I. A. SYROMIATNIKOV

EDITORIAL BOARD

K. A. ANDRIANOV, N. I. BORISENKO, G. V. BUTKEVICH, M. G. CHILIKIN, A. A. GLAZUNOV, V. A. GOLUBTSOVA, E. G. KOMAR, M. P. KOSTENKO, L. R. NEIMAN, I. I. PETROV, V. I. POPKOV, A. M. FEDOSEEV

Pergamon Press are also the publishers of the following journals:

JOURNAL OF NUCLEAR ENERGY (*including* THE SOVIET JOURNAL OF ATOMIC ENERGY *on behalf of Pergamon Institute*)

REACTOR TECHNOLOGY (*Journal of Nuclear Energy, Part B*)

HEALTH PHYSICS (*The Official Journal of the Health Physics Society*)

JOURNAL OF INORGANIC AND NUCLEAR CHEMISTRY

TETRAHEDRON (*The International Journal of Organic Chemistry*)

INTERNATIONAL JOURNAL OF APPLIED RADIATION AND ISOTOPES

BIOCHEMICAL PHARMACOLOGY
*BIOPHYSICS

*JOURNAL OF MICROBIOLOGY, EPIDEMIOLOGY AND IMMUNOBIOLOGY

*PROBLEMS OF HEMATOLOGY AND BLOOD TRANSFUSION

*PROBLEMS OF VIROLOGY

*PROBLEMS OF ONCOLOGY

*SECHENOV PHYSIOLOGICAL JOURNAL OF THE U.S.S.R.

*RADIO ENGINEERING

*RADIO ENGINEERING AND ELECTRONICS

*TELECOMMUNICATIONS

ARCHIVES OF ORAL BIOLOGY

HUMAN FACTORS

*PAVLOV JOURNAL OF HIGHER NERVOUS ACTIVITY
ELECTROCHEMICA ACTA

*THE PHYSICS OF METALS AND METALLOGRAPHY

*THE ABSTRACTS JOURNAL OF METALLURGY
  PART 1. THE SCIENCE OF METALS
  PART 2. THE TECHNOLOGY OF METALS

*APPLIED MATHEMATICS AND MECHANICS

CHEMICAL ENGINEERING SCIENCE

JOURNAL OF ATMOSPHERIC AND TERRESTRIAL PHYSICS

PLANETARY AND SPACE PHYSICS

GEOCHIMICA ET COSMOCHIMICA ACTA

BULLETIN GÉODÉSIQUE

ANNALS OF THE INTERNATIONAL GEOPHYSICAL YEAR

SPECTROCHIMICA ACTA

JOURNAL OF THE MECHANICS AND PHYSICS OF SOLIDS

ACTA METALLURGICA (*for the Board of Governors of Acta Metallurgica*)

INTERNATIONAL JOURNAL OF THE PHYSICS AND CHEMISTRY OF SOLIDS

DEEP-SEA RESEARCH

JOURNAL OF NEUROCHEMISTRY

JOURNAL OF PSYCHOSOMATIC RESEARCH

JOURNAL OF INSECT PHYSIOLOGY

JOURNAL OF AIR POLLUTION

INTERNATIONAL ABSTRACTS OF BIOLOGICAL SCIENCES (*for Biological and Medical Abstracts Ltd,*)

RHEOLOGY ABSTRACTS

VACUUM

OPERATIONAL RESEARCH QUARTERLY

ANNALS OF OCCUPATIONAL HYGIENE

*Translations of the Russian journals published on behalf of Pergamon Institute.

Leaflets giving further details and subscription rates of each of these journals are available on request.

ELECTRIC TECHNOLOGY, U.S.S.R.

1959 VOLUME 4 DECEMBER

CONTENTS

PAGE

I. M. Postnikov: Eddy currents in synchronous and asynchronous machines with unlaminated rotors 463

E. D. Sapir: Compensation of capacitive currents in differential phase carrier protection of transmission lines 480

V. A. Golovanov: The problem of a circuit for a rectifying semiconductor set on electric rolling stock of a.c. single-phase—d.c. transmission 494

O. B. Bron and D. S. Itenberg: Problems of liquid cooling in electrical equipment . . 503

Abstracts from papers published in Elektrichestvo No. 10, 1958 513

N. A. Poliak: Short-circuits, asynchronous drive and turbogenerator resynchronization . 519

V. V. Kaplan, V. M. Nashatyr' and V. L. Ivanov: A synthetic method of testing high-voltage circuit-breakers 533

L. L. Rotkop: The energy properties of an asynchronous motor with a system of impulse speed regulation 545

A. S. Kurbasov: On the conditions of the formation of flashover or arcing on to the framework of traction motors 556

Abstracts from papers published in Elektrichestvo No. 11, 1958 564

E. M. Tseirov: The electrical properties of compressed air in an air-blast circuit-breaker . 570

M. G. Portnoi: The occurrence of sub-harmonic resonance in unbalanced line conditions . 589

M. F. Iudov: Experimental investigation of deformations and vibrations of the stator windings 599

P. S. Livshits: Calculation of losses in the sliding contacts of electric machinery. . . . 610

Abstracts from papers published in Elektrichestvo No. 12, 1958 619

NOTICE

Readers wishing to acquire translations or a copy of the original of any article abstracted or mentioned bibliographically in this journal, should sent their order or request for a quotation to:

The Secretary,
Pergamon Institute, Headington Hill Hall, Oxford
or
1404, New York Avenue, N.W., Washington 5, D.C.
where their order or enquiries will receive immediate attention

Made and printed in Great Britain by Pergamon Printing & Art Services Ltd.

five

A METHOD OF CALCULATING THE PERFORMANCE OF COMPOUND SYNCHRONOUS MOTORS*

I.M. POSTNIKOV

(Received 13 November 1956)

General characteristics of motors and of methods of connexion

Excitation of synchronous motors through semiconductor rectifiers was first used in the U.S.S.R. in the DAG network [5]. This network was used for synchronization purposes, and the application of rectifiers fed from transformers was planned; or in the case of the low voltage grid, rectifiers had to be connected directly to the grid. It proved later that the DAG system cannot ensure satisfactory working characteristics of synchronous induction motors (small maximum torque in the case of increased load, low efficiency).

The situation changes radically if we make use of compounding. Synchronous induction compounded motors, with a d.c. exciter (Fig.1a) are widely used in foreign countries, particularly in England [3]. The use of synchronous induction compound motors without exciter but fed through a semiconductor rectifier was suggested by Iuditskii [1] and Tsiganek [6].

In 1954, Inosov [2] proposed exciting a network (Fig.1b) with rectifiers fed from current transformers. This system was tested on experimental synchronous salient-pole machines, and quite satisfactory working characteristics were recorded (constant cos ϕ, possibility of considerable overloading). Inosov and Krutikova gave a method of calculating the overload capacity and stability of these machines, as well as a method of calculating rectifying devices. At the same time, synchronous induction motors, constructed on this system, were investigated and calculations of synchronous motors,using the AK series, were performed by a method different from the method suggested by Inosov.

Calculations and tests showed that the use of rectifiers with a compounding device was expedient both for synchronous induction motors and for synchronous motors.

In the first case it is advisable to design these motors on the basis of AK series for powers above and below 100 kW. In the second case, for powers less than 100 kW, it is advisable to design motors with mixed excitation on the basis of series generators ESG, SM and others; and for powers above 100 kW, on the basis of the unique series of big synchronous and asynchronous machines.

---

* *Elektrichestvo*, No.3, 1-9, 1958.

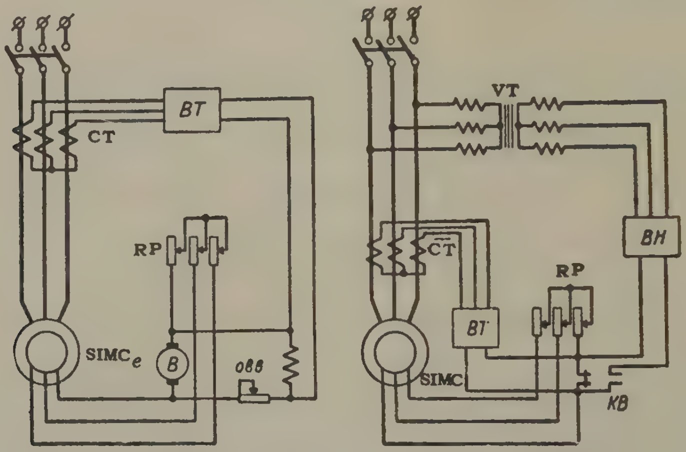

a)

b)

FIG.1. Basic networks for connecting a synchronous induction compounded motor with a d.c. exciter (SIMC$_e$) (a); and a synchronous induction compounded motor excited through 4 rectifiers (SIMC) (b).

The use of synchronous induction motors with compounding (abbreviated as SIMC; if the separate compounded exciter generator is used for excitation, it is convenient to introduce the notation SIMC$_e$)is economically justified in all cases when conditions of drive allow the use of synchronous motors. It is particularly desirable to use them when we have to start at heavy initial torques avoiding considerable current fluctuations; also where high reactances are present in the network, and consequently the increase of cos ϕ is desired without introducing special compensating devices (condensers, synchronous condensers and others).

The use of the excitation compounded network (Fig.2) for a normal salient-pole synchronous motor (SMC) is also recommended. In this case the absence of exciters makes the motor cheaper.

Compounding permits us automatically to keep a high value of cos ϕ when the load varies, and to obtain higher annual average efficiency and higher torques for rapidly varying loads. The use of compounded synchronous motors with separate exciters is recommended in the cases when the motor power is considerable and selenium rectifiers are less reliable than exciters. Nevertheless, with the improvement of semiconductor rectifiers, they may also be used for high-power motors.

The use of machines of SMC and SMC$_e$ types for powers less than 100 kW, based on the design of synchronous generators, needs an economic justification.

Lower cost of a set, due to the absence of an exciter, is partly offset by an increase in the cost of the motor itself, due to the introduction of an auxiliary winding on the poles and due to increased service costs in comparison with asynchronous motors. The use of SMC-type machines of power less than 100 kW is justified in cases when economy, due to the increase of cos ϕ, repays in two to five years their greater initial capital costs and additional operating costs compared with asynchronous motors.

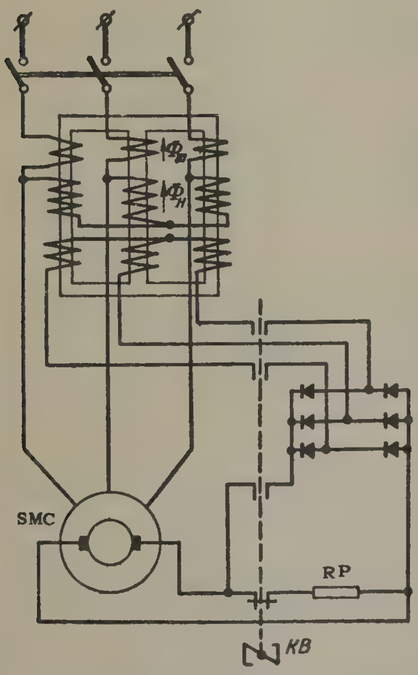

FIG.2. Basic network for connecting a compounded synchronous motor excited through rectifiers (SMC).

The use of SIMC-type motors of power less than 100 kW may also be advantageous in the following conditions. In certain cases it may be necessary to decrease the power of the motor of a given size by 15 - 20 per cent or to use a better rotor insulation of an increased thermal and electric strength. The main advantage of motors of SIMC type is that, without any change in the construction of series-made asynchronous machines, we may get synchronous motors by addition of compounding and rectifying devices. In the case of damage to these additional devices, the motors may continue working without interruption as asynchronous motors, until the defective rectifiers are repaired or replaced.

Methods of calculation for motors of SMC and SIMC type

In carrying out the calculations, it is advisable to begin with the existing types of synchronous and asynchronous machines.

The main problems in calculations are:

(a) to determine voltages and currents in the system of excitation;

(b) to determine parameters of current and voltage transformers and of rectifiers, that will ensure the required working characteristics of the motor and the necessary torques for overloads (with minimum dimensions of additional devices and sufficient service reliability);

(c) to obtain the required calculated working characteristics of the motor, and a good efficiency-load characteristic for the given rectifier and transformer parameters;

(d) to determine overloading;

(e) to verify stability;

(f) to calculate conditions in starting and in synchronizing;

(g) to determine whether overheating of the excitation winding and of the rectifying device takes place.

Inosov and Krutikova worked out methods for calculating the overload capacity of SMC motors, for calculating rectifying devices and for selecting current and voltage transformers. Nevertheless, so far as the overload capacity and motor characteristics are concerned, these methods give wrong results in certain cases.

The determination of the maximum torque, based on resistance, was given by Inosev by the formula: $M_{\max} = U^2/4a - b$, where a represents the relative copper losses proportional to the square of the stator current at the rated current value, and b the relative losses in the stator steel.

This formula is only valid in the case when the compounding device ensures the constancy of $\cos\phi$ at limit loads, or, for low-power machines, when the overloading capacity is determined mainly by resistance.

Basic initial assumptions in choosing a practical

In order to simplify calculations for both synchronous induction (SIMC type) and synchronous (SMC type) motors, it is expedient to start from the theory of a motor with a cylindrical rotor, i.e. to assume that

$$x_d = x_q = x_g$$

In investigating general relationships it is advisable to neglect the influence of saturation on motor parameters, particularly in the determination of the limiting overload.

Saturation may be accounted for by constructing Potier diagrams and a series of auxiliary adjusting characteristics (Fig.3).

It is expedient to calculate motor operating conditions in the following way:

(1) to determine by ordinary methods, experimentally or by calculation, stator and rotor parameters: (a) leakage reactances of the stator x_s and of the rotor x_f, x_{kd}, x_{kq}; (b) synchronous reactance, neglecting saturation x_d and $x_{ad} = x_d - x_s$, (c) resistances of the stator r_1 and of the rotor r_f, r_{kd}, r_{kq};

(2) to calculate or to determine experimentally characteristics in no-load and short-circuit conditions;

(3) to choose a value of overload capacity ($M_{\max}$);

(4) to choose a value of $\cos\phi_N$ at the rated load;

(5) from the torque equation

$$M = \frac{UE_f}{z}\sin(\theta + \rho) - \frac{E_f^2 R}{z^2}$$

for $\theta + \rho = \frac{\pi}{2}$ to get:

$$M_{\max} = \frac{UE_{f\max}}{z} - \frac{E_{f\max}^2}{z^2}R. \tag{1}$$

For a given value of $M_{\max}$ from (1), the maximum value of the excitation e.m.f. is determined:

$$E_{f\max} = \frac{Uz}{2R} - \sqrt{\left(\frac{Uz}{2R}\right)^2 - M_{\max}\frac{z^2}{R}}, \tag{2}$$

where $z = \sqrt{x^2 + R^2}$; $x = x_d + x_l$;

x_l is the reactance of the line; $rR = r, + r_{ct} + r_r + r_f$, the sum of resistances of the stator winding, of the current transformer, of the rectifier and of the excitation winding, expressed in fractions of unity;

(6) to have current in fractions of unity at $M = M_{\max}$

$$I_{\max} = \sqrt{\frac{E_{f\max}^2 + U^2}{z^2}}. \tag{3}$$

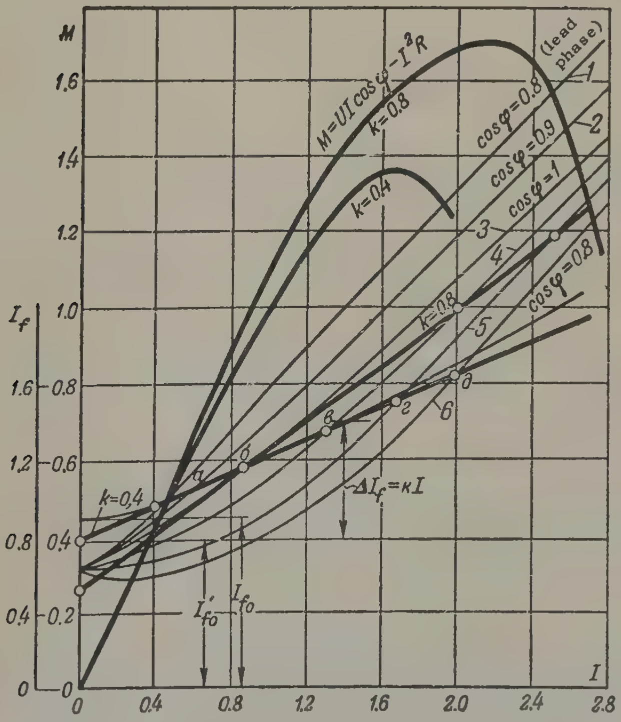

FIG.3. Determination of overloading and of working characteristics of motors SIMC and SMC, with saturation accounted for (1-6); characteristics in relative units constructed by Potier method.

(7) to have compounding factor

$$k=\frac{E_{f\,\max}-E_{fN}}{(I_{\max}-1)\,x_{ad}}, \qquad (4)$$

where, for $\cos\phi_N = 1$

$$E_{fN}=\sqrt{U^2+(I_N x)^2}. \qquad (5)$$

(8) to have e.m.f. E'_{fo} for the stator current equal to zero (Fig.3), (a conventional value),

$$E'_{fo}=E_{f\,\max}-\frac{E_{f\,\max}-E_{fN}}{I_{\max}-1}I_{\max} \qquad (6)$$

and the corresponding excitation current

$$I'_{fo}=\frac{E'_{fo}}{x_{ad}} \qquad (7)$$

in fractions of the stator current;

(9) to have transformation ratio of the current transformer

$$k_{c.t}=\frac{w_1}{w_2}=k\,\frac{i_{f(1)}}{1.3I_N}, \qquad (8)$$

where $i_f(1) = i_{f\delta}\,X_{ad}$, the nominal excitation current from the rectilinear characteristics in amperes, corresponding to the e.m.f.

$$E_{f(1)}=I_N x_{ad}. \qquad (9)$$

Factor 1.3 is the ratio of the rectified current to the alternating current (network in Fig.2);

(10) to show that the number of the parallel connected disks of the current

$$m_I=\frac{k i_{f(1)}}{i_1},$$

where $i_1 \approx 3.5$ - 4 A the current in one disk ($d = 100$ mm);

(11) to find the number of parallel connected disks of the voltage rectifier

$$m_U=\frac{i'_{fo}k_e}{i_1},$$

where i_1 is the permissible permanent current in one disc; $k_l \approx 1$ - 1.5 is the load factor; $i_{fo} = E_{fo}\,i_{f\delta}$;

(12) to show that the number of the series-connected disks of the voltage rectifier

$$n_U=\frac{i'_{fo}r_f}{U_1},$$

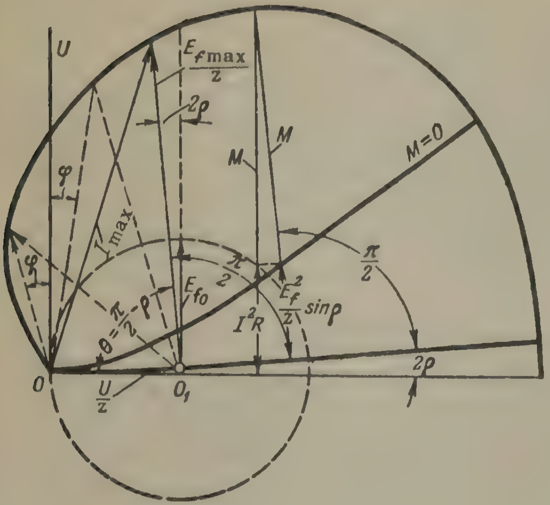

FIG.4. Hodograph of current of motors SMC and SIMC and determination of the maximum torque and of characteristics neglecting the influence of saturation.

where $U_1 = 12\text{-}15$ V, the permissible continuous back voltage across one disk; and r_f is to be expressed in ohms;

(13) to find the transformation ratio of the voltage transformer

$$k_{mn} = \frac{2.34U_p}{i'_{fo}r_f + \Delta U_v} \approx \frac{2.34U_p}{1.2i'_{fo}r_f}, \quad (11)$$

where U_p is given in volts, and r_f in ohms; $\Delta U_v \approx 2\, n_U$ is the voltage drop in the rectifier in volts; Factor 2.34 is the ratio of the rectified voltage to the alternating phase voltage (Fig.2); and

(14) to find the number of the series-connected disks in the network of Fig. 1 b

$$n_I = n_U$$

Construction of characteristics and determination of the overload capacity while taking into account saturation.

We construct a series of auxiliary adjusting characteristics for different values of $\cos\phi$, using the Potier diagrams (Fig.3). We draw the curve $I_f = f(1)$ and obtain the points of intersection a, b, c, d etc. Using the points of intersection we draw curves $\cos\phi = f(1)$ and $m = UI\cos\phi - I^2 R$, whence we determine the value of the maximum torque taking into account saturation (in Fig.3 for $k = 0.4$ and $k = 0.8$).

Locus of points of the motor current while neglecting the influence of saturation and accounting for it.

Neglecting the influence of saturation from the diagram on Fig.4 we get:

$$E_f^2 + U^2 - 2E_fU\cos\theta = (Iz)^2. \quad (11a)$$

For
$$E_f = E'_{fo} + kx_{ad}I = E'_{fo} + k_1 I \quad \text{we get:}$$

$$I = \frac{k_1(E'_{fo} - U\cos\theta)}{z^2 - k_1^2} + \sqrt{\left[\frac{k_1(E'_{fo} - U\cos\theta)}{z^2 - k_1^2}\right]^2 + \frac{E'^2_{fo} + U^2 - 2UE'_{fo}\cos\theta}{z^2 - k_1^2}}. \quad (12)$$

In this case $E'_{fo} \leqslant U$.

From equation (12), it follows that for $k_1 = z$, $I = \infty$. Therefore, it is necessary to choose $k_1 < z$. Usually in this case $k \approx 0.8-0.9$.

The current hodograph may be easily constructed by points. For this purpose, on a curve $I_f = f(1)$ [or $E_f = f_1(I)$] we choose a series of values of I and the corresponding values of I_f. Striking from points 0 and 0_1 arcs of radius I and $I_f = E_f/z$ (Fig. 4), we find a point on the hodograph and the corresponding value of cos ϕ. Plotting current values and cos ϕ taken from Fig. 3, we may plot a hodograph taking the influence of saturation into account.

Angle - torque characteristic

Characteristics showing the dependence of torque on the power angle θ (angle between the rotor and stator fields) may be obtained from the hodograph in Fig.4, in a form shown in Fig.5. As may be seen, it differs slightly from the characteristic $M = M_{\max} \sin \theta$, obtained at a constant excitation. If we assume a certain definite value of $M_{\max}$, then for the motors of SMC or SIMC types we may, in many cases, use the equivalent sinusoid of the torque (moment) as a function of the angle.

Dynamic and static stability

To determine the dynamic loads for normal non-compounded synchronous motors we use the method of areas. Both static and dynamic angle characteristics (with regard to extra currents in the rotor) may be used. By constructing an angle characteristic for a motor with a mixed excitation (Fig.5), from Fig.4 we may approximately apply the method of areas in this case as well. The influence of extra currents is to be accounted for with quickly varying loads, lasting not more than the time constant T'_d of transient currents; this may be done in the ordinary way by replacing the synchronous reactance x_d by a transient reactance x'_d and the e.m.f. E_f by E'_{fd}.

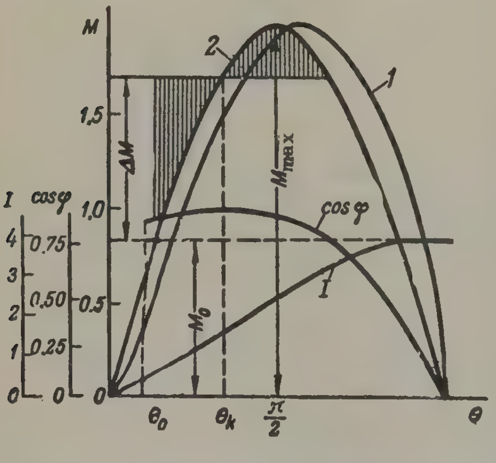

FIG.5. Comparison of angle characteristics for equal maximum torques. 1: for SMC and SIMC types; 2: for a synchronous motor with constant excitation.

For a shock load, not exceeding the limit of static stability and remaining afterwards constant during a period of time considerably greater than T'_d, we may disregard the extra currents and use a static angle characteristic. The additional limiting dynamic torque ΔM from the angle characteristic, which may be represented in a form of equivalent sinusoid in Fig.5, is the condition of equality of shaded areas, approximately determined by:

$$\Delta M \approx \frac{M_{\max}}{\sqrt{2}}\left(1 - \frac{M_0}{M_{\max}}\right). \qquad (13)$$

The limit of static stability is determined by the curve $M = f(\theta)$. But in this case we disregard the possibility of self-excited rotor oscillations. The problem of permissible values of compounding factors, which are restricted to the possibility of oscillations, requires theoretical and experimental investigations. Investigations carried out by Inosov [7], are subject to criticism because they neglect the smoothing torque due to damping windings.

Starting and synchronizing a motor

If a motor with a mixed excitation is designed as an asynchronous motor with slip rings (for instance of AK type), then it starts as an asynchronous motor and usually has a sufficiently high subsynchronous torque. If in this case semiconductor rectifiers are used they should be disconnected during the start. When an exciter generator is present, starting may be done without commutation in the secondary winding; i.e. as if starting a short-circuited asynchronous motor.

If a motor with a mixed excitation is designed as a salient pole synchronous machine, it is necessary to include an additional winding for starting. In this case, if semiconductor rectifiers are used, the excitation winding should be connected to a suitable discharge resistance (in some cases it may be left open, if no danger exists of breakdown of the insulation of the excitation winding during the start).

In practice, the idea of subsynchronous torque usually refers to the torque at the slip $s = 5$ per cent. It is usually accepted that for synchronization, it is necessary that subsynchronous torque should be greater than the shaft torque at subsynchronous speed. Experiments and calculations given below show that a motor may be synchronized at initial slips greater than subsynchronous slip, for example $s_0 = 10$ per cent and more, if the period of synchronization is correspondingly increased. Sometimes a slip, for which rotor windings are to be supplied with d.c., is determined from conditions of synchronization during the first hunting cycle by the Edgerton formula [4]:

$$s_{cr} = \frac{247}{n_s}\sqrt{\frac{P_{\max}}{fGD^2}}. \qquad (14)$$

This formula is not valid for determining self-synchronization conditions of synchronous motors with starting winding in cases of difficult starting, because it gives the value of a critical slip for synchronization during the first hunting cycle and does not allow the determination of the time for synchronization, in the case when s_0 is different from s_{cr} given by (14). We may obtain a formula for s_{cr} that approximately takes into account the influence of the asynchronous torque, of the external load torque and of the rotor position, by an approximate solution of the equation of rotor motion.

Attempts at a rigorous analysis of a synchronization process of a synchronous motor lead to very complicated non-linear equations. Nevertheless, a solution, sufficiently accurate in practice in most cases, may be obtained if we neglect the influence of idle currents and torques and consider electromagnetic moments as known functions of θ and $d\theta/dt$. In this case, only one equation of motion is to be considered.

The equation of the rotor motion may be written in this form:

$$H\frac{d^2\theta}{dt^2}+D\frac{d\theta}{dt}+M_c(\theta)=M_v, \tag{15}$$

where H is an inertial constant in radians. The angle characteristic $M_c\ (\theta)$ may be approximately represented, disregarding parametric moment (torque), in the form of an equivalent sinusoid:

$$M_c(\theta)\approx M_{\max}\sin\theta. \tag{16}$$

From the previous discussion (see Fig.5), we may assume this to be true for ordinary synchronous motors and for motors with mixed excitation, thus determining $M_{\max}$ by (1).

Damping torque per unit slip $s = d\theta/dt$ may be expressed, disregarding the salient pole motor properties, as in the case of symmetrical multiphase rotor winding*

$$D\approx\frac{U^2r_2'}{c_1^2(r_2'^2+s^2x_d''^2)}\approx\frac{U^2}{r_2'c_1^2(1+s^2T_d''^2)}. \tag{17}$$

Here $U_0\,r_2'$ and x''_d are expressed in fractions of unity;

$$c_1=1+\frac{x_s}{x_{ad}}.$$

For small slips $s \ll 1/T''_d$, the value of D may be assumed to be constant, i.e. independent of the slip $D\approx\dfrac{U^2}{C_1^{\,2}\,r_2}$, or its mean value within a given range of the slip may be taken.

Torque due to external load M_{ex}, generally speaking, is a function of slip, but during the synchronization process within narrow limits of speed variation, it may be taken as a constant.

For asynchronous starting, the torque $M_c\ (\theta) = 0$, and the established slip may be determined as a function of M_{ex} and D from the asynchronous characteristic (Fig.6);

$$s=\frac{M_{\text{ex}}}{D}=S_a,$$

---

* For synchronous salient-pole motors $D = M_{in}/0.05$, where M_{in} is an input torque.

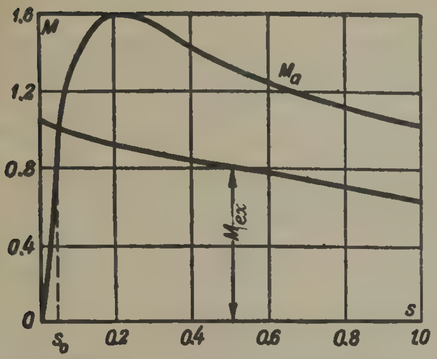

FIG.6. Asynchronous characteristics of motors SIMC or SMC and determination of the established slip S_0 before switching on a d.c.

whence

$$D = \frac{M_{ex}}{s} \tag{18}$$

At this slip, let us apply d.c. to the rotor. Let us consider conditions under which a motor will be pulled into step, and how long it will take. Conditions will differ according to the value of the initial slip $s_0 = s_a$ and the position of the axis of the rotor m.m.f. at the instant of switching on the current; i.e., according to the value of θ_0. The most unfavourable case will be when $\theta_0 = -\pi$. Therefore, if a motor is pulled into step in this case, then this will be so in all cases. To determine the conditions for synchronization we write equation (15) in the form:

$$\frac{d^2\theta}{dt^2} = f(\theta), \tag{19}$$

where

$$f(\theta) = \frac{1}{H}[M_{ex} - M_c(\theta) - D_s].$$

Here $s = d\theta/dt$ is an unknown function of the angle θ. Equation (19) is solved by multiplying both sides by $2\, d\theta/dt$:

$$\frac{d}{dt}\left[\frac{d\theta}{dt}\right]^2 = 2f(\theta)\frac{d\theta}{dt},$$

where

$$s^2 - s_0^2 = 2\int_{\theta_0}^{\theta} f(\theta)\cdot d\theta = \tag{20}$$

$$= \frac{2}{H}\int_{\theta_0}^{\theta} [M_v - M_c(\theta) - Ds]\, d\theta.$$

Here s_0 is a slip when $t = 0$, i.e. at the instant when d.c. is switched on. This slip should be at least 1.5 - 2 times smaller, than pull-out slip, $S_k = r_2/x_d$. If switching-on takes place during established asynchronous running (characteristic in Fig.6), then

$$s_0 = s_a = \frac{M_{ex}}{D} \ll s_k.$$

From (20), slip s for $M_c(\theta) = M_{max} \sin\theta$ will be:

$$s = \sqrt{\frac{2}{H}\left[M_{\max c}(\cos\theta - \cos\theta_0) + \int_{\theta_0}^{\theta}(M_{ex} - Ds)\,d\theta\right] + s_0^2}\,. \tag{21}$$

Synchronization will be assured if the slip s becomes equal to zero at a positive value of the synchronous torque, i.e. at the beginning or in the middle of any positive half-period of the sinusoid $M_{\max}\sin\theta$, and this happens according to (21), when

$$s_0 = \sqrt{\frac{2}{H}\left[M_{\max}\;(\cos\theta_0 - \cos\theta_c) + \int_{\theta_0}^{\theta}(Ds - M_{ex})\,d\theta\right]}\,. \tag{22}$$

We shall call angle $\theta = \theta_S$ the angle of synchronization. Obviously, it will be equal to

$$\theta_S = 2\pi X + \alpha, \tag{23}$$

where X is an integer;

$$\alpha = \frac{\pi}{2} \;\ldots\; \frac{\pi}{3}$$

Equation (22) enables us to find a criterion of pulling a synchronous motor into step.

Let us consider the case when d.c. is switched on at $\theta_0 = -\pi$. On condition that $\theta_0 = -\pi$, a motor will be syncronized if, for any value of the angle of synchronization $\theta_S = 2\pi X + \pi/2$, corresponding to a positive value of a half-cycle of the synchronous torque, slip s becomes zero. From (22) it follows that for this to happen it is necessary that s_0 should not exceed a certain value. Supposing $\theta_0 = -\pi$ and $\theta = \theta_S$, when $\theta_S = \pi/2 + 2\pi X$, we get:

$$s_0\sqrt{\frac{H}{2}} = \sqrt{\int_{-\pi}^{\theta_S} Ds\,d\theta - [M_{ex}(\theta_s + \pi) + M_{\max}\;]}. \tag{24}$$

Introduce the average value of the asynchronous torque during the period of synchronization:

$$M_{aav} = Ds_{av} = \frac{1}{\theta_c + \pi}\int_{-\pi}^{\theta_S} Ds\,d\theta, \tag{25}$$

Pulling into step will be achieved if the work performed by this torque during the period of synchronization is greater than the sum of the work, performed by the external torque, by the synchronous torque and by the moment of inertia of the rotor, i.e.

$$(\theta_s+\pi)\,Ds_{av} \geqslant \frac{Hs_0^2}{2}+M_{\max}+M_{ex}(\theta_s+\pi)=$$
$$=A+M_{ex}(\theta_s+\pi),$$

where

$$A=\frac{1}{2}Hs_0^2+M_{\max}, \tag{25a}$$

or alternatively:

$$\left.\begin{aligned} Ds_{av} &\geqslant M_{ex}+\frac{A}{\vartheta_s+\pi};\\ s_{av} &\geqslant s_0+\frac{A}{D(\theta_s+\pi)}, \end{aligned}\right\} \tag{26}$$

this means that the average asynchronous torque and the average slip should be greater than certain definite values.

It is seen from (26) that the longer the process of synchronization (large number of periods of oscillations κ), the smaller is the average synchronous torque required.

For example, let us verify the possibility of synchronizing a motor, if $H = 1000$ rad, $s_0 = 5$ per cent and $M_{\max} = 2$ for two periods of oscillations ($\chi = 2$) and the torque on the shaft $M_{sh} = 1$. In accordance with (26) $Ds_{av} = 1 + \frac{0.5 \times 1000.0 \times 0.05^2 + 2}{2\pi \times 2 + 3\pi/2} = 1.2$ where $s_0 = 0.05$ and $M_{ex} = 1$, we get $D = M_{ex}S_0 = 1/0.05 = 20$. Therefore, the average slip should be not less than $s_{av} = 1.2/20 = 0.06$; i.e. about 6 per cent. Is it possible to get such a value?

The solution of equation (15) by the method of successive approximations, which is given below, suggests that the average slip during the period of synchronization varies within very narrow limits. In fact, the maximum possible slip occurs when $\theta_0 = -\pi$, and if we neglect the value of D from (21), when $\theta = 0$:

$$s_{\max}=\sqrt{\frac{4M_{\max}}{H}+s_0^2}. \tag{27}$$

The average value of the slip for a half-period under these conditions will be:

$$s_{av1}=\sqrt{\frac{2M_{\max}}{H}+s_0^2}. \tag{28}$$

For an infinite period of synchronization:

$$S_{av2} = S_0. \tag{29}$$

Thus the value of s_{av} lies within the limits:

$$S_{av1} > S_{av} > S_0 \tag{30}$$

A more accurate value of the average slip may be obtained from (21). In fact, for an interval from $-\pi$ to θ_s

$$(s^2)_{av} = \frac{2}{H}\left[M_{\max}\left(1+\frac{\sin\theta_s}{\pi+\theta_s}\right)+(M_{ex}-Ds_{av})\frac{\pi+\theta_s}{2}\right]+s_0^2. \tag{31}$$

If we introduce the square of the shape factor of the curve $k^2_{sh} = \frac{(s^2)_{av}}{s^2_{av}}$, then from (31) we get:

$$s_{av} = -\frac{D(\theta_s+\pi)}{2Hk^2_{sh}} + \sqrt{\left[\frac{D(\theta_s+\pi)}{2Hk^2_{sh}}\right]^2+\frac{2M_{\max}}{Hk^2_{sh}}\left(1+\frac{\sin\theta_s}{\theta_s+\pi}\right)+\frac{s_0^2}{k^2_{sh}}+\frac{Ds_0}{Hk^2_{sh}}(\theta_s+\pi)}. \tag{32}$$

In this case, we may assume $k^2_{sh} \approx 1.1-1.2$ according to Fig.7.

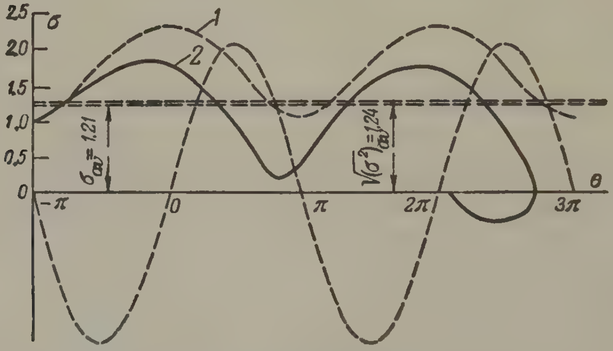

FIG.7. Curves of relative slip-angle θ (1) for $D = 0$; (2) for $D = 20$.

Above we have determined the value S_{ar} for which during the interval from $\theta = -\pi$ to $\theta = \theta_s$, the slip becomes zero (equation (26)). Equating (26) and (32), we find for given values of D, H and s_0, the number of rotor oscillations:

$$\gamma = \frac{A}{2\pi D\left[-\left(s_0-\frac{DM_{\max}}{HAk^2_{sh}}\right)+\sqrt{\left(s_0-\frac{DM_{\max}}{HAk^2_{sh}}\right)^2+\frac{1}{2}\left(\frac{2M_{\max}}{Hk^2_{sh}}-s_0^2\right)}\right]}-\frac{3}{4}, \tag{33}$$

which is approximated to the nearest integer. From equation (33), it follows that the time of synchronization becomes infinite, if

$$s_0 = \sqrt{\frac{2M_{\max}}{Hk^2_{sh}}} = s_{cr}.$$

The last equation gives the limiting value of the slip for which synchronization of a motor is still possible. Inserting the value S_{cr} from (34) into (33) and rejecting the term $-\frac{3}{4}$, we get:

$$\varkappa = \frac{A}{2\pi D\left[-\left(s_0 - \frac{D}{2A}s_{cr}^2\right) + \sqrt{\left(s_0 - \frac{D}{2A}s_{cr}^2\right)^2 + \frac{1}{2}\left(s_{cr}^2 - s_0^2\right)}\right]} \tag{33a}$$

For the case, when

$$\frac{1}{2}\left(s_{cr}^2 - s_0^2\right) \ll \left(s_0 - \frac{D}{2A}s_{cr}^2\right)^2,$$

from (33a) we get

$$\varkappa = \frac{2}{\pi}\cdot\frac{A}{D}\left[\frac{s_0 - \frac{D}{2A}s_{cr}^2}{s_{cr}^2 - s_0^2}\right], \tag{34}$$

or

$$\varkappa = \frac{2}{\pi}\left[\frac{\varepsilon^2(1+\varepsilon^2) - 0.5m}{(1-\varepsilon^2)m}\right], \tag{35}$$

where

$$\varepsilon = \frac{s_0}{s_{cr}}; \quad m = \frac{Ds_0}{M_{\max}}.$$

The value of the slip from (26), (33), and (35):

$$s_{av} = s_0 + \frac{A}{D\left(2\pi\varkappa + \frac{3}{2}\pi\right)}. \tag{36}$$

The time of synchronization from (36) is:

$$t_s = \frac{2\pi\varkappa + 1.5\pi}{s_{av}2\pi f}\ [\text{sec}]. \tag{37}$$

In the above example we get, according to (26), (33), (36) and (37), when $k_{sh}^2 \approx 1$:

$$A = \tfrac{1}{2}Hs_0^2 + M_{\max} = \tfrac{1}{2}\,1000\times 0.05^2 + 2 = 3.25;$$

$$D = 20; \quad s_0 = 0.05; \quad s_{cr} = 0{,}0632; \quad X = 2.1.$$

Using the approximate formula (35), we have

$$\epsilon = 0.79; \quad m = 0.5; \quad X = 2.5.$$

The average slip for $\kappa = 3$ will be $S_{av} = 0.0569$. Time of synchronization $t_s = 1.33$ sec. The approximate method given above was verified by solving equation (15), by the method of successive approximations. For this purpose it is convenient to decrease the number of equation constants by introducing the relative value of slip

$$\sigma = \frac{s}{\omega_{sw}} \tag{38}$$

where $\omega_{sw} = \sqrt{\frac{M_{\max}}{H}}$, the angular speed of free oscillations of the rotor in a magnetic field. The equation (15) assumes the form:

$$\frac{d\sigma}{d\theta}\sigma + k_A(\sigma - \sigma_0) + \sin\theta = 0, \tag{39}$$

where,

$$k_A = \frac{D\omega_{sw}}{M_{\max}}; \quad \sigma_0 = \frac{s_0}{\omega_{sw}}; \quad k_A\sigma_0 = \frac{M_{ex}}{M_{\max}} = m.$$

In the above example,

$$D = 20; \; H = 1000; \; M_{\max} = 2; \; s_0 = 0.05;$$

$$k_A = 0.5; \; \sigma_0 \approx 1.$$

If $M_{sh} \neq Ds_0$ the equation (39) will have the form:

$$\frac{d\sigma}{d\theta}\sigma + k_A\sigma + \sin\theta = \frac{M_{ex}}{M_{\max}} = m, \tag{40}$$

or

$$\frac{dw}{d\theta} + \sqrt{2}\,k_A\sqrt{w} + \sin\theta = m, \tag{41}$$

where, $w = \frac{1}{2}\sigma^2.$

Fig. 7 shows the curve of the relative slip σ. The solution for σ neglecting D, i.e. when $k_A\sigma = 0$, is also given in this figure (curve 1):

$$\sigma = \sqrt{-2\int_{\theta_0}^{\theta}\sin\theta\, d\theta + m} = \sqrt{2(\cos\theta - \cos\theta_0) + m}. \tag{42}$$

In this case, equation (21) will have, in relative units, the form:

$$\sigma = \sqrt{2\left[(\cos\theta - \cos\theta_0) + \int_{\theta_0}^{\theta}(m - k_A\sigma)\right] + \sigma_0^2}. \tag{43}$$

The analysis of equation (43) enables us to determine the criterion for entering into synchronization:

$$k_A\sqrt{2} > m, \quad \text{or} \quad D > m\sqrt{\frac{HM_{\max}}{2}}. \tag{44}$$

Conditions for synchronization found above allow the solution of the inverse problem: to find the value of the relative resistance r_2' of the symmetrical starting winding for a motor with an inertial constant H, torques $M_{\max}$ and M_{ex} for the time of synchronizing t. For instance, let us take: $H = 500$ rad., $M_{sh} = 0.5$, $t_s =$ sec. We determine the critical slip by formula (34) for $k^2_{sh} = 1.2$:

$$s_{cr}=\sqrt{\frac{2M_{\max}}{1.2H}}=\sqrt{\frac{2\cdot 2}{1.2\cdot 500}}=0.081.$$

The value of s_0 should be less than s_{cr}. Let $s_0 = 7$ per cent; in this case

$$D=\frac{M_{ex}}{s_0}=\frac{0.5}{0.07}=7.1 \quad \text{and} \quad r_2' \approx \frac{1}{D}=\frac{1}{7.1}=0.14.$$

Verification by formula (33) when $A = \frac{1}{2} \times 500 \times 0.07^2 + 2 = 3.25$; $S_{cr} = 8.1$ per cent, gives:

$$\kappa = 10.8.$$

By the approximate formula (35), for $\epsilon = 0.86$, $m = 0.25$, we find $\kappa = 11.4$. By formula (36), $s_{cr} = 0.76$, and by formula (37) for $\kappa = 11$ we have

$$t_s = \frac{\pi\,(2 \times 11 + 1.5)}{0.076 \times 314} = 3.1 \text{ sec},$$

i.e. a value greater than assumed. Therefore, it is necessary to diminish s_0 to the value $s_0 = 6$ per cent and the resistance of the starting winding r_2 in the ratio 6/7, i.e. to the value of 12 per cent.

The real conditions of synchronizing will be more favourable, since for switching on at $\theta_0 = -\pi$, the exciting current does not reach its full value instantaneously due to the winding reactance, and the work of braking from $-\pi$ to zero will be smaller.

The experimental verification of the conditions determined above agree with results obtained in practice using the calculated data; the use of the above methods may therefore be recommended.

Translated by S. Szymanski

REFERENCES

1. S.B. Iuditskii; *Sinkhronnye mashiny s poluprovodnikovymi vypriamiteliami (Synchronous machines with semi-conductor rectifiers),* Gosenergoizdat (1954).
2. V.L. Inosov and V.E. Krutikova; *Electrichestvo,* No.6 (1956).
3. Griffin; *The synchronous induction motor,* London, MacDonald Co. Ltd. (1954).
4. *J. Inst. Elect. Engrs.* vol. 6, 1205 (1930).
5. O merakh povysheniia koeffitsients moshchnosti elektroustanovok promyshlennykh predpriiatii (Methods for increasing the power factor of electrical installations in industrial establishments), *Elektrichestvo,* No.2 (1953).
6. Ziganek; *Electricke stroje Praha, sixth edition* (1951).
7. V.L. Inosov; Sinkhronnyi dvigatel smeshannogo vozbuzhdeniia i teoriia ego raboty (Synchronous motor with mixed excitation and the theory of its action), in symposium, *Tr. inst. elektro-tekh, Akad Nauk Ukr. SSR* No.14 (1956).

COMPARISON OF TWO-STAGE AND THREE-STAGE ROTARY AMPLIFIERS WITH AXIAL FIELD *

B.I. NORNEVSKII, V.F. BATKO, V.E. MALISHEVSKII, P.V. KUROPATKIN
and E.I. ROSIN

Ulianov Lenin Institute of Electric Technology, Leningrad

(Received 21 May 1957)

Electric rotary amplifiers with a cross and axial field belong to the class of quick acting and highly sensitive regulators. The rate of voltage increase of these machines, at a control power of a few watts, reaches a value of 1000 - 2000 V/sec at the rated voltage of 230 V; the voltage amplification factor varies within limits of tens up to hundreds of units.

Investigations show that the amplifiers with an axial field have many important advantages in comparison with amplifiers with a cross field. Multistage amplifiers with an axial field have higher amplification factors and efficiencies and can act more quickly [2].

An additional advantage of these amplifiers is their wide range of power output, which makes possible their use in high power control systems as main exciters. It is known that the construction of high power amplifiers with a cross-field is limited by serious difficulties connected with commutation.

Amplifiers with an axial field may have one, two or more amplification stages according to the network and number of poles.

The work of the amplifier with an axial field is discussed in a series of articles by Soviet and foreign authors [1, 2, 4, 5, 6].

The three-stage rotary amplifier is at present the least investigated. Only a comparatively small number of works is devoted to its investigation [3, 7].

Recently in the laboratories of the LETI, LYIMU and LIIZhT, a series of investigations was carried out on a three-stage amplifier with an axial field. Some of the results obtained are discussed in the present article.

---

* *Elektrichestvo*, No. 3, 9 - 14, 1957.

The working principle of a three-stage amplifier

A three-stage rotary amplifier with an axial field is similar in its construction to an ordinary d.c. generator. Its magnetic system, like the system of the majority of other amplifiers, is usually unsaturated, since a satisfactory performance of an amplifier, from the point of view of the quality of regulation-amplification and quick action, is possible within the linear part of the magnetization curve. The armature winding of the amplifier is of the lap type without compensating windings.

Let us consider how the amplification stages are realized in a three-stage amplifier taking as an example a four-pole machine. Fig. 1 shows the network of this amplifier.*

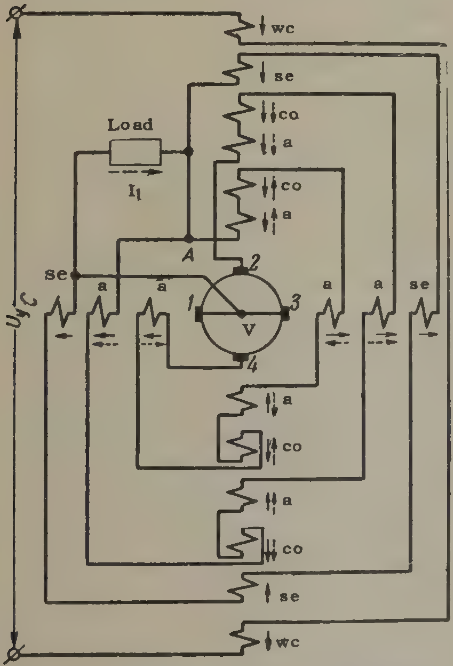

FIG. 1. Network of a three-stage amplifier

The basic four-pole flux Φ_3 in this amplifier is induced by a self-excitation winding $S\theta$ and an amplifying winding a. These windings are wound on four poles. Control windings are situated on the poles of the same polarity for a four-pole excitation system (for example 1-3).

Flux Φ_1, induced by m.m.f. of the control winding, induces a potential difference between brushes 1-3 when the armature rotates. The armature network between brushes 1-3 and the control winding constitute the first amplification stage, for which the input factor is the voltage, applied to the control winding, and the output is the e.m.f. E_{13}.

The second stage of amplification is produced by using the cross-reaction of the armature due to the compensating current i_{13}, which flows when the circuit of brushes 1-3 is completed. The armature reaction flux Φ_2, induced by the compensating current i_{13}, induces an e.m.f. $E24$ between brushes 2-4. The e.m.f. $E24$ is the output factor of the second amplification stage.

The third stage is achieved by connecting the four-pole amplifying winding to the brushes 2-4. The resultant output of this stage is the e.m.f. E_3 between the adjacent brushes.

---

* Interpoles are not shown on Fig. 1, 6 and 7. For a three-stage amplifier the number of sections of the interpole windings and the network of connections remain the same, as for a two-stage amplifier [1].

When the compensating current l_{24} flows between brushes 2-4, a two-pole flux of the armature reaction is induced in the amplifier armature, this flux being directed against the flux of the control winding. To neutralize this reaction a compensating winding C, wound on poles 1-3, is connected in series with the amplifying winding.

The load and the parallel self-excitation winding are connected to the midpoints of the network of brushes 1-3 and 2-4. When the amplifier is on load, the load current and the current of the parallel winding of self-excitation flow in the networks of the amplifying and compensating windings.

To neutralize the influence of these currents on fluxes, set up by the compensating currents, windings a and c are arranged in such a way that for the compensating winding these sections are connected in series aidings and for the load current and the current of self-excitation they are connected in series opposing. The self-excitation winding of the amplifier is adjusted to a resistance near to the critical.

For $R_{se} = R_{se.c}$ we can assume <(cf. straight line, Fig. F), that the volt-ampere characteristic of the self-excitation winding coincides with the rectilinear portion of the magnetizing curve. For $R_{se} = R_{se.c.}$, n = const., and in the absence of an input signal, the amplifier is not self-excited, and its output voltage may assume any value within the limits of the rectilinear portion of the no-load characteristic in the case of idle running, or of the load characteristic, if the load is present. For open circuit conditions of the amplifier and with manual control, the voltage required on its terminals, for such an arrangement of the self-excitation winding, is obtained by voltage impulses applied to the control winding.

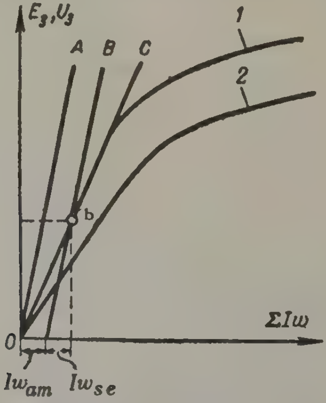

FIG. 2. Characteristics of idle running (1) and on-load (2) for R_{ρ} = const.

In the closed loop system the change of voltage is realized by means of a measuring device and a feedback coupling. An amplifier, working on load near the critical value, can be considered as an astatic regulator. Investigations which have been carried out [4] show that the work of the amplifier under these conditions is entirely stable, while, from the point of view of the stability of the amplifier itself, this occurrence is the limiting case.

An amplifier with an axial field can work with the resistance of the self-excitation winding *se* above the critical value, if the volt-ampere characteristic lies above the magnetization curve. Under these conditions it may be considered as a static regulator: for a definite value of the current in the control winding there corresponds a strictly determined value of the output voltage (lines A and B, Fig. 2).

A comparison of qualities of three- and two-stage amplifiers with an axial field

In comparing qualities of rotary amplifiers it is customary to consider their amplification factors and their ability to respond quickly. The notion of the static amplification factor may be applied to an axial amplifier; it has a theoretical meaning in the arrangement of the circuit of the self-excitation winding to a resistance larger than the critical one.

Considering an amplifier as an unsaturated machine and using the well-known relationship between m.m.f. and e.m.f., we may establish the relationship between e.m.f. at the amplifier output E_3, and the voltage U_c, applied to the control winding. The equations of e.m.f. and m.m.f. of a three-stage amplifier, for the steady-state conditions, are:

(a) for the first stage

$$E_{13} = c\Phi_1 = \frac{c}{a} Iw_{13}; \tag{1}$$

$$Iw_{13} = 2w_c \frac{U_c}{r_c} + 2w_a{}^{\varepsilon} \frac{E_{24}}{r_{24}}; \tag{2}$$

(b) for the second stage

$$E_{24} = c\Phi_2 = \frac{c}{a} Iw_{24}; \tag{3}$$

$$Iw_{24} = 2w_a i_{13} = 2w_a \frac{E_{13}}{r_{13}}; \tag{4}$$

(c) for the third stage

$$E_3 = c\Phi_3 = \frac{c}{a} Iw_3; \tag{5}$$

$$Iw_3 = 2w_a \frac{E_{24}}{r_{24}} + 2w_{se} \frac{E_3}{r_{se}}, \tag{6}$$

where lw_{13}, lw_{24} and lw_3	are the m.m.f.'s of the first, second and third amplifying stages;
c	factor of the proportionality between the e.m.f. and the flux;
a	the factor of the proportionality between the m.m.f. and the flux;
i_c, i_{se}, i_{13}, i_{24}	currents in the following windings: control, self-excitation and in the circuits of brushes 1-3 and 2-4;
r_c, r_{se}, r_{13}, r_{14}	resistances of the following windings: control, self-excitation, and in the circuits of brushes 1-3 and 2-4;
w_c, w_a, w_{co}, w_{se}	number of turns per pole of the following windings: control, amplifying, compensating and self-excitation;
$w_a = \frac{N}{16}$	equivalent number of turns of the armature winding per pole;
N	number of active conductors of the armature winding,
$\epsilon = \frac{2w_{co} - 2w_a}{2w_a}$.	degree of compensation of the armature reaction due to the compensating current i_{24}.

Solving equations (1 – 6) with respect to E_3 and dividing both sides of the formula so obtained by U_c, we have the following expression for the amplification factor of a three-stage amplifier.

$$K = \frac{E_3}{U_c} = \frac{\overset{c}{K_c} K_1 K_a}{(1 - T_{se})(1 - K_1 K_2 \epsilon)}, \qquad (7)$$

where

$$K_c = \frac{2w_c c}{ar_c}; \; K_1 = \frac{2w_a c}{ar_{13}}; \; K_\epsilon = \frac{2w_c c}{ar_{24}};$$

$$K_{se} = \frac{2w_{se} c}{ar_{se}}; \; K_2 = \frac{2w_a c}{ar_{24}}.$$

Similary we get the expression for the amplification factor of a two-stage amplifier

$$K' = \frac{K_c K'_a (1 + K_{op})}{(1 - K_{se})(1 + K_{op} + \epsilon_1 \epsilon_2 K'_1 K'_2)},$$

where

$$K'_a = \frac{2w_a c}{ar'_{13}}; \; K'_1 = \frac{2w_a c}{ar'_{13}}; \; K'_2 = \frac{2w_a c}{ar'_{24}}; \qquad (8)$$

$$K_{op} = \frac{2w_{op} c}{ar_{24}};$$

$\epsilon_1 = \frac{2w_a - 2w_{co_{13}}}{2w_a}$; $\epsilon_2 = \frac{2w_a - 2w_{co_{24}}}{2w_a}$; degrees of compensation of the armature reaction due to the compensating currents i_{13} and i_{24}.

From the above formulae (7) and (8) we find the expression for the ratio of the amplification factors of two- and three-stage rotary amplifiers with an axial field:

$$\frac{K}{K'}=\frac{K_1(1+K_{op}+\varepsilon_1\varepsilon_2K'_1K'_2}{(1-K_1K_2\varepsilon)(1+K_{op})}. \qquad (9)$$

In the case of total compensation of the armature reaction, when $\epsilon = \epsilon_1 = \epsilon_2 = 0$, ratio K/K' corresponds to the amplification factor K_1 of the second stage of a three-stage amplifier. The value of this factor is of the order of a few units or tens of units. This fact shows that it is possible, for a given set of conditions, to obtain a much greater voltage amplification in a three-stage amplifier than in a two-stage one, and consequently a much greater power amplification.

In the case of undercompensation of the armature reaction, $K/K' < K_1$. The nature of the influence of the degree of compensation on the amplification factors of the amplifiers in question is shown in Fig. 3, in the form of a curve $K/K' = f(\epsilon)$. This curve is plotted for the linear part of the magnetization curve by using the data from an experimental amplifier, assuming that $\epsilon = \epsilon_1 = \epsilon_2$. Usually the undercompensation of the armature reaction in the amplifier with an axial field does not exceed 1 - 6 per cent. For these values of E the amplification factor of a three-stage amplifier is 2.5 - 5 times greater than the a.f. of a two-stage amplifier.

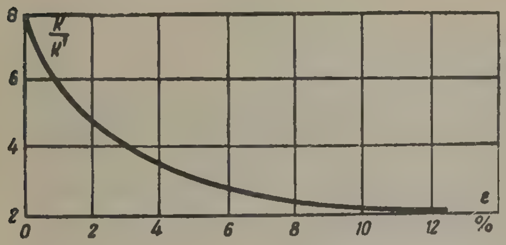

FIG. 3. The influence of the degree of compensation on the ratio of amplification factors of two-stage and three-stage amplifiers.

When the amplifier works as an astatic regulator, i.e. when the circuit of the self-excitation winding is arranged for a resistance equal to the critical one, the notion of the static amplification factor becomes meaningless, since under steady-state conditions the intermediate stages do no work. To evaluate the quality of an amplifier working under these conditions, we usually introduce the conception of the minimum control power and of the dynamic amplification factor. As a minimum control power we usually accept such a value, for which an amplifier begins to reverse its polarity. The value of the minimum control power characterizes a region of the amplifier insensibility and is determined by the width of the hysteresis loop. The minimum control power of existing amplifiers with an axial field is of the order of milliwatts.

The dynamic amplification factor is determined as a ratio of the rate of increase of e.m.f. at the output of the amplifier to the value of U_c of the voltage applied to the control winding; it characterizes the speed of the amplifier reaction to a unit disturbance.

Under conditions of total compensation of the armature reaction by the compensating current i_{24}, and neglecting the saturation and the reaction of commutation currents, we may write the expression for the dynamic amplification factor in the following form: (a) for the three amplification stages

$$K_{\text{dyn}} = \frac{\frac{dE_3}{dt}}{U_y} = \frac{K_c K_1 K_a}{T_a + T_{se}}, \tag{10}$$

where T_a and T_{se} are time constants of the amplifying winding and self-excitation winding;

(b) for the two amplification stages

$$K_{\text{dyn}} = \frac{\frac{dE'_3}{dt}}{U_y} = \frac{K_c K'_a}{T_a + T_{se}}. \tag{11}$$

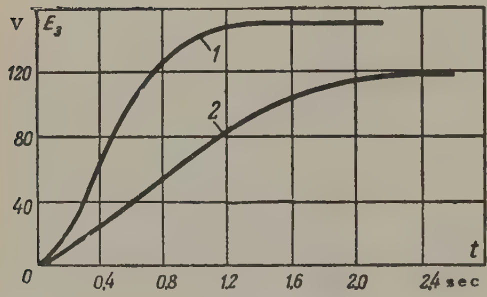

FIG. 4. Curves of a transient process for three (1) and two (2) amplification stages (i_{co} = 75 m A).

The ratio of these two factors and also the ratio of the amplification factors correspond to the amplification factor of the second stage of a three-stage amplifier;

$$\frac{K_{\text{dyn}}}{K'_{\text{dyn}}} = K_1 \tag{12}$$

The comparison of the quick operation of the two- and three-stage amplifiers with an axial field was carried out on the experimental model of 1.8 kW power, U_l = 60 V, I_l = 30 A, n = 1450 rev/min.

This amplifier, constructed in accordance with the design of the ordinary d.c. generator model PN, was made so that it was possible to arrange either two or three amplification stages by changing the winding connexions. This was done in order to carry out comparative tests under the same conditions. In both cases the resistance of the self-excitation winding was adjusted to its critical value. The same control winding was used (r_c = 30 Ω). The transient processes were recorded by an oscillograph at U_c = const.

The results of these comparative tests are shown in Fig. 4 and 5.

Fig. 4 shows the curves of the transient processes, plotted on the basis of oscillogram data, for two- and three-stage amplification, for the same degree of compensation of the armature reaction ϵ = 5.5 per cent, and the same control current equal to 75 m A. Fig. 5 shows the main values of the rate of increase of the e.m.f. at the output for various values of currents in the control winding.

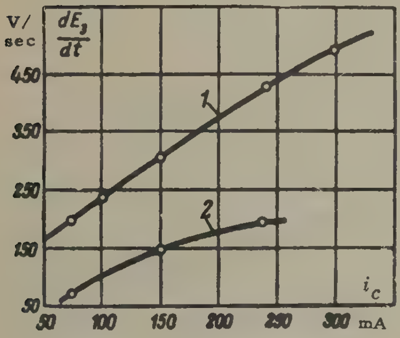

FIG. 5. Rate of increase of e.m.f. E_3 at the output for three (1) and two (2) amplification stages.

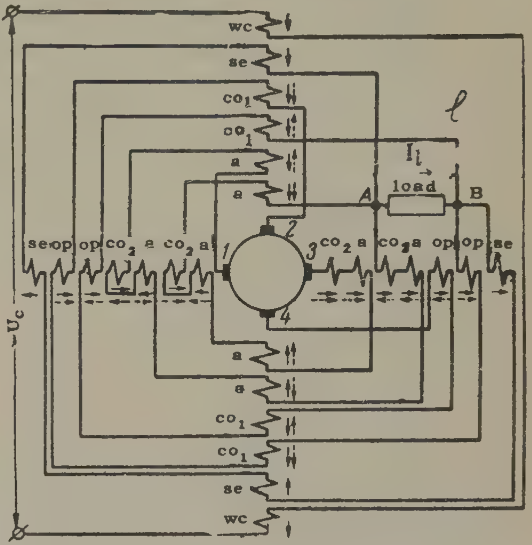

FIG. 6. The network of a two-stage amplifier with an oxide field.

From the above experimental data it follows that, for the same magnetic system and for approximately the same weight of active materials and for the same values c and l_c the rate of increase of the e.m.f. at the output is approximately 2-2.5 times greater in a three stage amplifier than in a two-stage one.

Amplification and quick response are not the only criteria in the evaluation of amplifier qualities. It is necessary to consider such properties as the tendency to oscillate and the complexity of the networks.

A three-stage amplifier in comparison with a two-stage one has a greater tendency to oscillations and to self-excitation, which is due to the increase in the total amplification factor and the phase delay. However, experimental investigations showed that the working of a three-stage amplifier may be quite stable; possible causes of instability, which are common in the amplifiers and were compared (magnetic asymmetry, accelerated commutation and over-compensation of the armature reaction) may be entirely eliminated, or their influence reduced to a minimum.

The influence of magnetic asymmetry in an amplifier with an axial field may be compensated by varying the value of the resistance of the self-excitation winding, of the degree of compensation of the armature winding, and also by increasing the air gap [3]. For the adjustment of the required degree of compensation of the armature winding, we use a variable resistance, which is connected in parallel to the compensating winding. The commutation adjustment is done in the same way as in an ordinary d.c. machine.

In comparing the networks of the two- and three-stage amplifiers (Fig. 6, 1) we may point out that a three-stage amplifier has a somewhat simplified network. In a two-stage amplifier the armature reaction, due to the equalizing current i_{13}, must be compensated rather accurately by the compensating winding co_2 and by the series opposing winding *op*, wound on poles 2-4, whereas in a three-stage amplifier this reaction is used for further amplification, and the additional windings co_2 and *op* on poles 2-4 are absent.

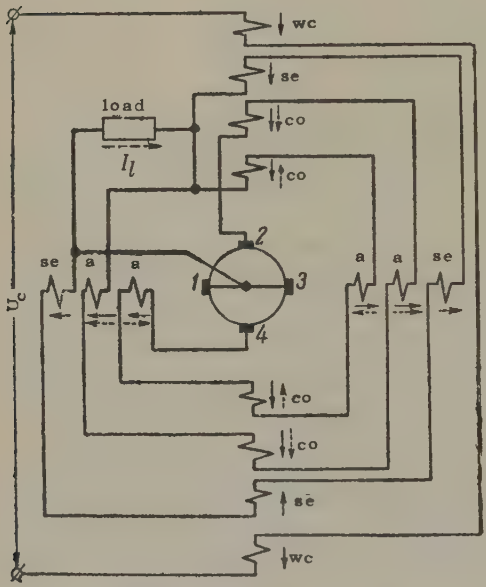

FIG. 7. Simplified network of a three-stage amplifier.

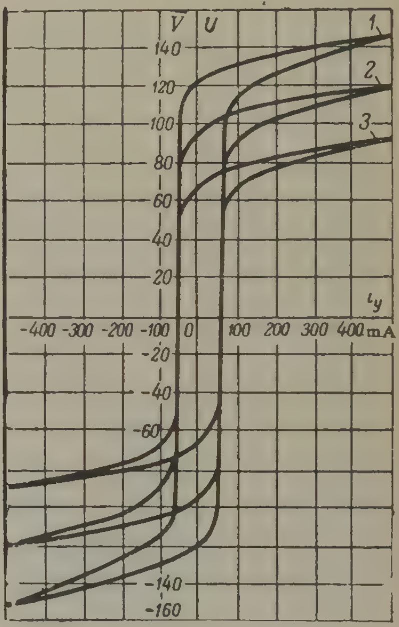

FIG. 8. Characteristics of an experimental three-stage amplifier of 5.5 kW power. 1 - characteristic idle running 2 – for R_e = 1.7 Ω; 3 – for R_e = 0.83

This last feature permits a further simplification of the network of a three-stage amplifier as well as a reduction in the number of windings on poles 1-3; this is very desirable in order to improve the conditions of the distribution of control windings. The arrangement of the amplifying winding as shown in Fig. 7 may also be recommended.

As distinct from the network shown in Fig. 1 here the sections of the amplifying winding *a* are situated only on poles 2-4, but, since these windings are connected in series opposing, a four-pole excitation flux of the third stage is produced. This method of connexions was used on two experimental models of 4-5.5 kW power, constructed basically according to the design of the machine model PN-100.

Fig. 8 shows the characteristics of the idle and load working of one of these amplifiers of 5.5 kW power, running under conditions of astatic regulation.

Conclusions

(1) A three-stage amplifier has a number of advantages in comparison with a two-stage one. Its response is quicker for the same control power. For the same speed of response, a three-stage amplifier is controlled by a smaller power.

(2) A three-stage amplifier has a simpler network than an amplifier with two amplification stages.

Translated by S. Szymanski

REFERENCES

1. V.F. Baiko and A.A. Vavilov; Perekhodnye protsessy v dvukhstupenchatom usilitele s samovozbuzhdeniem (Transient processes in a two-stage rotary amplifier with self-excitation), *Elektrichestvo*, No. 10 (1956).
2. F.A. Goriainov and B.Ia.Gusev; Issledovanie dvukhstupenchatogo regulatora prodolnogo polia (Investigation of a two-stage regulator with an axial field), *Tr. Moscow Power Inst.*, XV (1955).
3. F.A. Goriainov and B.F. Tokarev; Vliianie magnitnoi nesimmetrii na rabotu trekhstupenchatogo elektro-machinnogo usilitelia (The influence of the magnetic asymmetry on the working of a three-stage rotary amplifier), *Elektrichestvo*, No. 8 (1949).
4. R.S. Piasetskii; Elektromachinnyi regulgator c kriticheskim samovozbuzhdeniem (Rotary regulator with a critical self-excitation), *Elektrichestvo*, No. 8 (1949).
5. W.R. Harris; The industrial application of regulators of the rototrol type. *Trans Amer., Inst. Elect. Engrs.* 118-123 (1945).
6. A.W. Kimbal; A two-stage rototrol for a low-power control system *Trans. Amer Inst. Elect. Engrs.* 66, 1507 (1947).
7. M. Liwshits, The multistage rototrol. *Trans Amer. Inst. Elect. Engrs.* 66, 564-568 (1947).

SPEED CONTROL OF A D.C. MOTOR FED FROM A MAGNETIC AMPLIFIER *

V.D. AFANAS'EV and IVOBOTENKO

Central Scientific Research Institute for Machine Technology

(Received 18 October 1957)

In automatic control systems of electric drive, controlled small-power motors are being used more frequently; they constitute an integral part of control systems. The use of magnetic amplifiers for the feeding of these motors may ensure their speed control within large limits, and enables us to obtain rigid mechanical characteristics, similar to the characteristics of speed control in the generator-motor system. For this purpose it is necessary to choose an appropriate magnetic amplifier and a control system with a feed-back.

Simple methods for designing such systems are of considerable practical importance, provided they enable us to find characteristics with sufficient accuracy for practical use, and to determine the necessary parameters of the control networks.

The method described below is an approximate but very simple method of calculation; it permits the easy determination of the mechanical characteristics of the system amplifier-motor using the catalogue operational characteristic of an amplifier, which gives the dependence of the mean load current upon the magnetization current at the nominal load resistance.

$$I_1 = f(I_y) \text{ and } R = R_l.$$

For calculations of the static characteristics of a d.c. low-power motor, fed through a magnetic amplifier from a grid of line frequency, we may neglect the armature inductance and replace it by an equivalent resistance.

$$R_e = \frac{U_m}{I_m} = \frac{k_e \phi n}{I_m} + R_a , \tag{1}$$

---

* *Elektrichestvo*, No. 3, 14-19, 1958.

where U_m and I_m are the motor voltage and current,
R_a is the armature resistance,
n is the speed of rotation;
ϕ is the excitation flux;
k_e is the motor constant.

The equivalent resistance R_e may be easily determined from formula (1) for the given arbitrary operational conditions of the motor. If the amplifier characteristic, obtained for a load resistance $R = R_e$, is available, it is possible to determine the magnetization current corresponding to the given conditions (n, I_m) of work of the motor. Thus the problem is reduced to obtaining the artificial characteristics of the amplifier running at different load resistances, differeng from the nominal value of the load.

For calculating the necessary artificial characteristics of an amplifier we shall use the notion of its *universal characteristic* [1]. We shall construct the amplifier characteristic in relative units, but not as a function of the total magnetization current, [1], but as a function of the control current, i.e. taking into account a positive feed-back of the amplifier.

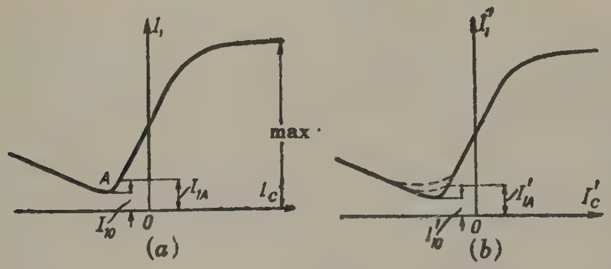

FIG. 1. Characteristics of a magnetic amplifier (a) in absolute units (b) in relative units.

Let the curve in Fig. 1a represent a catalogue or an experimentally obtained working characteristic of the amplifier in nominal conditions. We replot the amplifier characteristic in relative units (Fig. 1b),

$$I_1' = \frac{I_1}{I_m}; \quad I_c' = \frac{I_c}{I_{c.u}}, \tag{2}$$

where I, I_c are the current values in absolute units
Unit values of currents are:

$$\left.\begin{aligned} I_{1u} &= \frac{U_\sim}{1{,}11 R_{1u}}; \\ I_{c.u} &= \frac{I_{1u}}{k}\cdot\frac{w_1}{w_c}, \end{aligned}\right\} \tag{3}$$

where U is the effective value of the applied voltage;
R_{1u} is the total resistance of the load network, including the resistance of rectifiers and of amplifier windings;
W_1 is the number of turns of the a.c. winding;
W_c is the number of turns of the control winding;
$k = 1$ is for networks with a series connexion of windings w_1.
$k = 2$ is for networks with a parallel connexion of windings w_1 and networks with an internal feed-back.

With sufficient accuracy we may assume:

$$I_{1u} = I_{1\max}$$

where $I_{1\max}$ is the maximum value of the load current(according to the nominal amplifier characteristic, Fig. 1a).

We determine unit resistance of the load network where the amplifier saturation is:

$$R_{1u} = \frac{U_{\sim}}{1.11 I_{1u}}. \qquad (4)$$

By changing the load resistance by ΔR, we determine the unit resistance, corresponding to another value of load resistance $R_{II} = R + \Delta R$.

$$(R_{1u})_{II} \approx R_{1u} + \Delta R, \qquad (5)$$

whence the new unit values of current will be:

$$(I_{1u})_{II} = I_{1u} \frac{R_{1u}}{(R_{1u})_{II}}; \qquad (6)$$

$$(I_{c.u})_{II} = I_{c.u} \frac{R_{1u}}{(R_{1u})_{II}}.$$

Choosing a certain value of the control current I_c, we determine its new value in relative units:

$$(I_c')_{II} = \frac{I_c}{(I_{c.u})_{II}}. \qquad (7)$$

From the amplifier characteristic in relative units (Fig. 1b) we find the new relative expression for the load current $(I_1)_{II}$, corresponding to $(I_c)_{II}$, and then its absolute value.

$$(I_1)_{II} = (I_1')_{II}\,(I_{1u})_{II}. \tag{8}$$

Thus we have found the value of the load current for the new value of the resistance $(R)_{II}$, corresponding to the control current I_c. In this way we may construct artificial characteristics of an amplifier for different values of the load resistance R.

In determining $(R_{1u})_{II}$in formula (5) we neglected the variation of value resistances with the variation of unit current, since usually it does not exceed a few per cent of the total resistance R_{1u}. For large variations of R it is necessary to take into consideration the variation of valve resistances from the curves valve resistance-load current. The minimum current I_{10} at the output of the amplifier is determined by its inductance x_{10}, which is considerably greater than the load resistance R. Therefore in varying R, current I_{10} remains practically unchanged.

The part of the artificial characteristic of an amplifier, in the region of minimum currents, has to be constructed while taking this fact into account. For every value of R, the universal characteristics of an amplifier in the region of minimum currents will be different (dotted curves on Fig. 1b).

If we assume, as is recommended [1] that the minimum current I_{1A} of the linear portion of the amplifier characteristic is equal to 1.55 I_{10}, then the portion of the characteristic in relative units between I_{10} and I_A can be approximately obtained by joining it smoothly with linear portions of the characteristic.

Fig. 2 shows experimental and calculated characteristics of the magnetic amplifier model PMU-1 for different values of the load resistance. The network of the amplifier connexions during the tests is also shown.

From Fig. 2 it follows that there are differences between the calculated and experimental values of characteristics of up to 10 per cent. Nevertheless, taking into account that the dispersion of characteristics is unavoidable, owing for example to the instability of rectifiers, we may assume that the method recommended for constructing artificial characteristics of an amplifier, while varying its load resistance, gives sufficiently accurate results in practice. Calculations for other amplifiers give similar results.

Construction of artificial characteristics of an amplifier, in varying resistance R, may also be carried out, as a first approximation, using as a basis the condition that, for a constant control current I_c, current I_1 at the amplifier output varies inversely as the unit load resistance R_{1u} of the load network, i.e.

$$(I_1)_{II} = I_1\,\frac{R_{1u}}{(R_{1u})_{II}}. \tag{9}$$

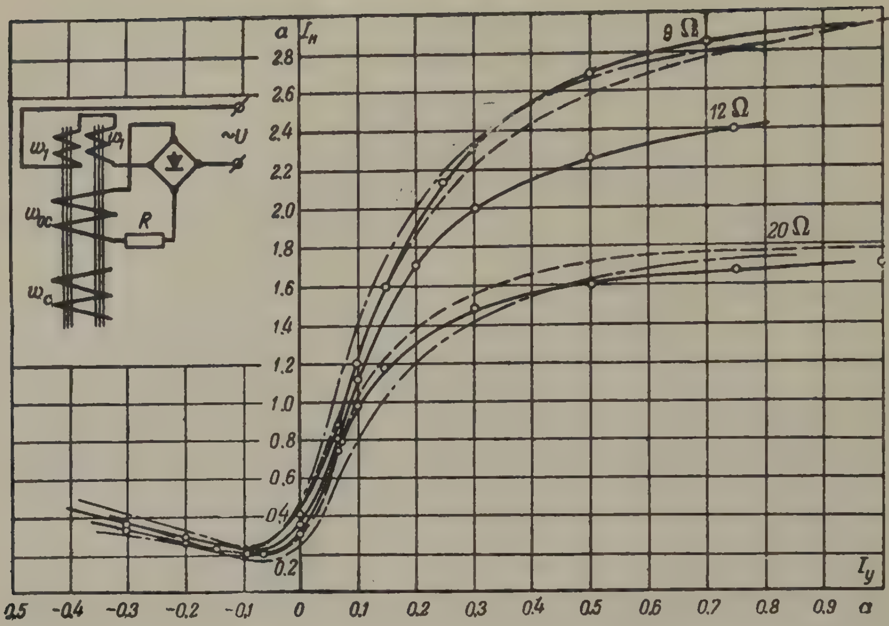

FIG. 2. Experimental and calculated characteristics of the amplifier PMU-1 ($U_{\sim}$ = 55 V, w_1 = 250; w_{oc} = 220; w_c = 450, selenium rectifier; into each leg of the rectifier two disks were series-connected, of d = 100 mm. ——— – experimental characteristics; — — — calculated characteristics (calculations in relative units); — . — . — . calculated characteristics (calculations by formula (9).

This method of verifying calculations gives satisfactory results only for the working portion of the amplifier characteristics. Utilization of amplifier artificial characteristics, obtained by this method, in replacing an actual motor load by an equivalent resistance, calculated from equation (1), permits the easy determination of the mechanical characteristics of the amplifier-motor system as well.

Experimental verification of the possibility of replacing an actual motor load by an equivalent resistance was carried out in the following way.

The amplifier was assembled from three magnetic amplifiers, model BKN-1, in a three-phase bridge circuit. Characteristics were taken for different values of load resistances (dotted curves on Fig. 3). Then the armature of a d.c. motor (110 V, 9A, 4500 rev/min, was connected into the network instead of the load resistance (Fig. 4).

A rotary amplifier was used as the load, on the motor output shaft; the load was varied by using the resistance 9R.

TABLE 1.

I_c (mA)	− 5.0				0					5.0			10,0
I_1 (A)	2.5	5.0	5.3	5.95	3.0	5.0	5.5	6.0	8.0	6.5	6.9	7.5	8.0
n rev/min	1950	1250	1190	1040	2650	2130	2020	1885	1510	2620	2510	2400	2980
R_l (Ω)	17.5	7.0	6.0	5.0	20.0	10.0	9.0	8.0	5.0	10.0	9.0	8.0	9.0
R_e (Ω)	18.15	6.5	5.95	4.85	20.5	10.37	7.97	7.97	5.15	9.88	9.0	8.05	9.2

For control currents -10, -5, 0,5 and 10 mA, the load on the motor shaft was so chosen that the magnetic amplifier current was equal to the current corresponding to the load resistance.

The results of the measurements of the motor speed ($k_e\ \phi \approx 0.022$ V rev/min, $R_a = 1.0\ \Omega$) and of calculations of the equivalent resistance R_e from formula (1), shown in the table, confirm the possibility of replacing the motor by an equivalent resistance R_e. The error due to this lies within the limits 0-7 per cent. Experiments, which were carried out with other magnetic amplifiers and motors, gave similar results.

Thus, the replacing of a motor by equivalent resistances and constructing for these values artificial characteristics of the magnetic amplifier for different load resistances permit us to calculate the drive static characteristics.

The analysis of expression (1) shows, that the amplifier characteristics, obtained for a certain value of load resistance R_1 is the locus of points, for which the motor speed n is proportional to the load current I_1.

Amplifier characteristics for different values of R enable us to solve a series of other problems. Thus, for a constant magnetization current I_c, and choosing different load currents I_1, we may easily find by equation (1), putting $R = R_e$, corresponding values of the motor speed, i.e. we may easily construct the motor speed characteristic $n = f\,(I_m)$ for a given magnetization current I_c of the amplifier.

We may also solve the inverse problem: to determine the magnetization current, necessary to keep a constant speed n, when the load current of the motor varies.

The constant speed curves on Fig. 3 are shown as continuous lines.

Having obtained these relationships we may calculate the feed-back parameters, and the feed-back coupling will automatically maintain the desired speed of rotation. As follows from formula (1) and Fig. 3, the constant speed characteristic intersects the amplifier characteristic. This means that for a constant speed of rotation, a decrease in the equivalent resistance R_e corresponds to an

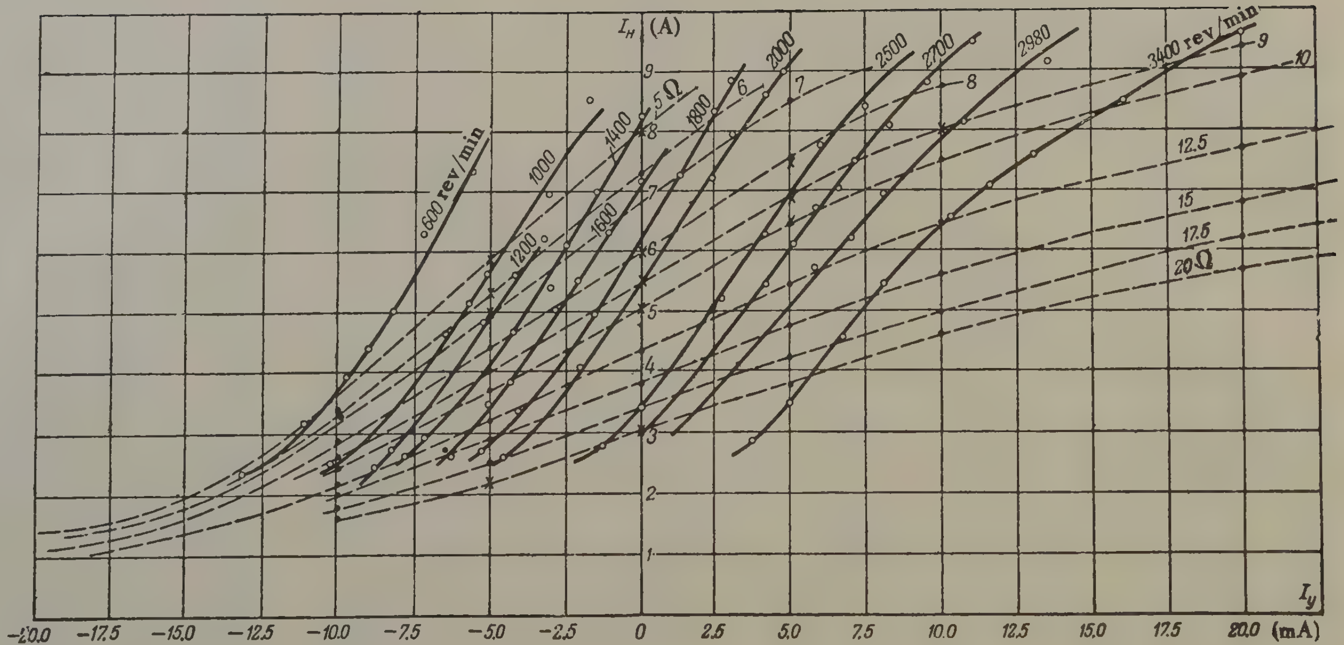

FIG. 3. Characteristics of an amplifier assembled in a three-phase bridge circuit from magnetic amplifiers BKN-1 ($U_{\sim ph.i}$ = 130 V; w_1 = 400; w_{oc} = 1500); – – – amplifier characteristic for load resistance; —— constant speed characteristics.

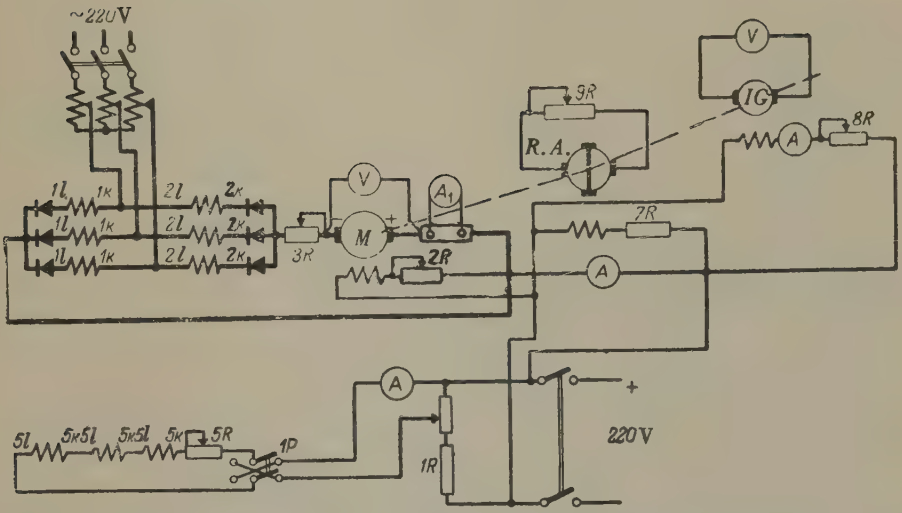

FIG. 4. Network for feeding a motor from magnetic amplifiers assembled in a three-phase bridge circuit.

increase in the motor current.

The constant speed characteristic may be considered as a straight line only in a restricted part of the curve. In the region of maximum and minimum currents this characteristic is obviously non-linear.

Comparison of the amplifier characteristic and the constant speed characteristic of the motor shows that by using linear feed-back in the amplifier-motor system we may obtain rigid motor speed characteristics, while varying the motor load within those limits of the amplifier characteristic, which are approximately rectilinear. Strictly determined values of the feed-back amplification coefficients correspond to this region.

From Fig. 3 we see that the constant speed characteristics have different slopes with respect to the coordinate axes: for greater speeds they are less steep. Hence, it follows that for the same range of load variation ($I_{\min} - I_{\max}$) to maintain a high constant speed we need a greater variation of the magnetization current than to maintain a smaller speed. Therefore, an invariable feed-back coupling in the amplifier-motor system does not ensure the constant characteristic rigidity of the motor at all speeds. If the feed-back network is designed to obtain rigid mechanical characteristics of the motor for certain mean speeds, then with the increase of speed the rigidity of mechanical characteristics will decrease, and with the decrease of speed will increase. In the latter case with the load (current) increase the motor speed may increase. Therefore, to ensure rigid mechanical characteristics of the motors a positive feed-back of current is not sufficient. Besides a positive feed-back of current, it is necessary to provide also for a negative feed-back from the motor voltage.

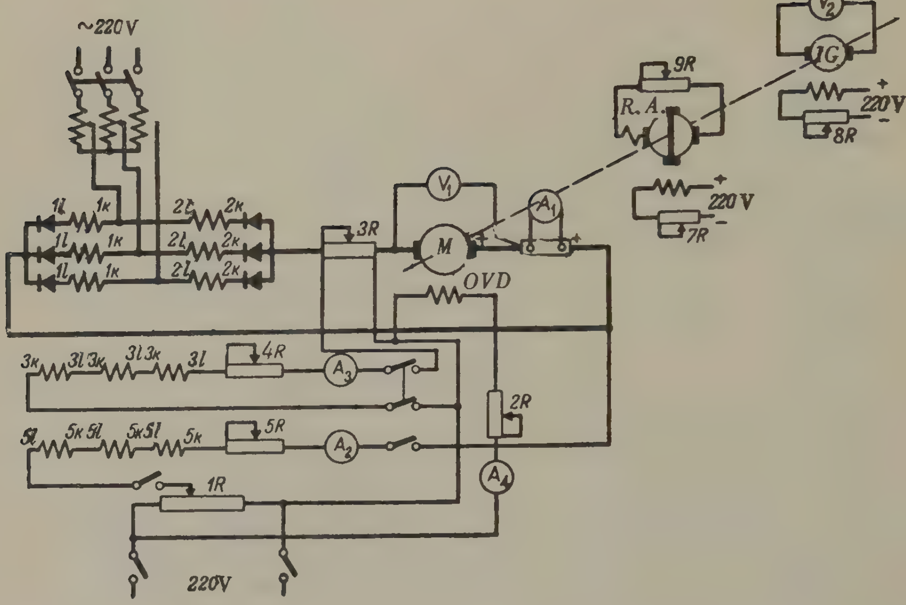

FIG. 5. Network for feeding a motor from magnetic amplifiers assembled in the three-phase bridge circuit with feed-back current and current couplings.

Experiments show that in networks with a magnetic amplifier, provided with an internal feed-back, it is necessary to use an additional small winding for external positive feed-back of the current in order to increase the coefficient of the positive feed-back of current by 3 - 5 per cent; in this way the realization of the negative feed-back from the motor voltage is facilitated.

Fig. 5 shows the network for feeding a d.c. motor in the amplifier-motor system with a positive feed-back of current and a negative feed-back from the motor-voltage(motor data: U= 110 V, I= 9A, n = 4500 min; magnetic amplifier model BKN-1).

The potential difference between the motor and the control potentiometer 1 R, was applied to windings 5 l – 5 k, ie. they were used simultaneously as control windings and as the feed-back windings from the motor voltage. As follows from Fig. 6, feeding of the motor in network 5 ensured the obtaining of rigid mechanical characteristics within the regulation limits 10: 1 (dotted curves).

In feeding the same motor from the amplifier BKN-1, connected in a single phase and with the use of similar feed-back couplings (for different values of feed-back amplification coefficients), rigid mechanical characteristics of the motor could not be obtained, for the same range of speeds and loads. This is due to the fact that the equivalent motor resistance R_e, under given conditions, cor-

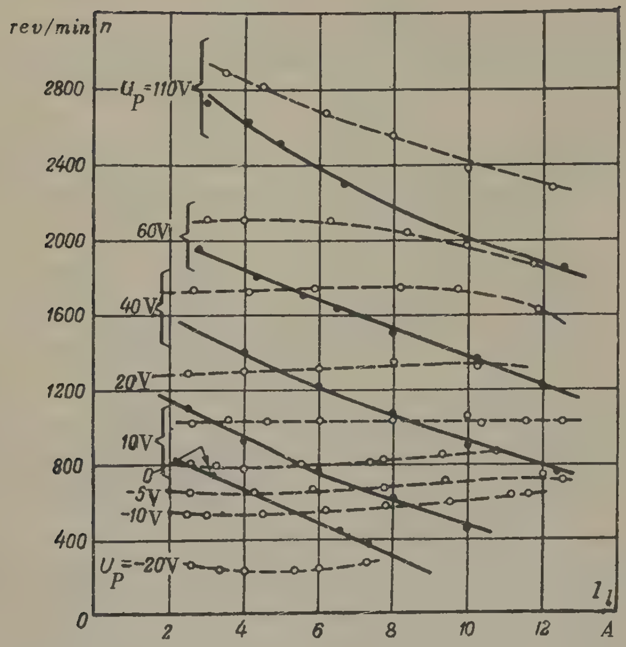

FIG. 6. Experimental characteristics of a motor connected in the network of Fig. 5. *Up* is the voltage of potentiometer 1*R*; 1 —— for coefficient of current feed-back equal 1; 2 — — — for coefficient of current feed-back equal 1.026.

responded to the work of the amplifier in the region of non-linear portions of the constant speed characteristics (Fig. 3).

Thus a proper choice of the amplifier is very important, to obtain the required characteristics of the drive to be controlled. Besides general considerations, the fundamental problem in choosing a magnetic amplifier for feeding a motor is a choice of an amplifier with a proper nominal load resistance. On the basis of the above discussion we may conclude that, if the nominal load resistance of the amplifier is equal or nearly equal to the equivalent resistance R_e of the motor, for its nominal current and a certain mean speed, then the conditions for obtaining rigid motor characteristics will be most favourable. Nominal amplifier resistance R_e should lie between the values of the equivalent motor resistance R_e for two sets of conditions: (a) $I_{\max}$, $n_{\max}$ and (b) $I_{\min}$, $n_{\min}$. If R_l is considerably smaller than R_e, corresponding to $I_{\max}$ and $n_{\max}$, or considerably greater than R_e corresponding to $I_{\min}$ and $n_{\min}$, then obtaining rigid characteristics will be difficult: in the first case in the region $I_{\max}$, $n_{\max}$, and in the second case in the region $I_{\min}$, $n_{\min}$. According to concrete requirements the necessary value R_l may vary somewhat within specified limits.

Translated by S. Szymanski

REFERENCES

1. T.Kh. Stefanovich; Raschet magnitnykh usilitelei i magnitnykh rele pri pomoshchi universalnoi kharakteristiki (Calculation of data for magnetic amplifiers and magnetic relays by means of a universal characteristic) *VEP*, No. 6 (1956).

MODEL INSTALLATION FOR REMOTE CONTROL OF ELECTRIC PARAMETERS IN ARC FURNACES*

Yu.E. EFROIMOVICH

(Received 21 June 1957)

A system of automatic remote control of the parameters of the secondary winding of electric arc furnaces, of arc voltage and of useful power in each phase is necessary for the application of rational methods of regulating the complex technological processes of melting steel in these furnaces.

The solution of these problems is possible by using special model installations; a characteristic feature of these installations is the electrical relationship existing between the model and the object under investigation.

The theory and principle of model installations

Fig. 1 shows two equivalent networks of a three-phase electric furnace installation. In Fig. 1 the e.m.f. of the mutual induction $e_{ik} = M_{ik}\, di_t/dt$ is taken into account by introducing two suitable generators with negligible impedances. In Fig. 1b, their influence is accounted for by a proper choice of the phase inductances of the secondary network [3]. According to Fig. 1b and [3], the arc voltage in any one phase will be:

$$e_{di} = u_{ti} - r_{\kappa ci} i_i - L_{\kappa ci} \frac{di_i}{dt} - (u_0'' - u_0') - u_0', \tag{1}$$

where

$$u_0'' - u_0' = L_1' \frac{di_1}{dt} + L_2' \frac{di_2}{dt}; \quad L_1' = M_{12} - M_{23}; \quad L_2' = M_{12} - M_{13};$$

u_{ti} is the secondary voltage ith phase of the furnace transformer; u_0', u_0'' are respectively: potential difference between zero points O of the metal in the furnace, or O of the installation equivalent network and the zero voltage point of the secondary of the transformer.

Fig. 2 shows the basic network of the model installation for measuring resistances r_{kci} and inductances L_{kci} of the phases of the secondary network, voltages on arcs e_{ai} and differences between mutual phase inductances L_1' and L_2'. In the upper part of this figure the furnace transformer TF, the furnace itself and the secondary network, which feeds the powerful furnace arcs, are shown diagrammatically. The

---

* *Elektrichestvo*, No. 3, 22 – 27, 1958.

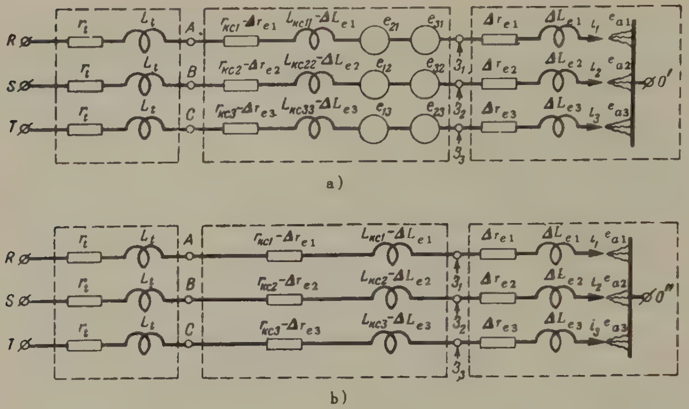

FIG. 1. Equivalent network of a three-phase-arc furnace, r_t and l_t arc phase resistance and inductance of a furnace transformer; r_{kc} and L_{kci} the same but for a phase of the secondary; Δr_{ei} and ΔL_{ei} the same but for the electrode section situated inside the furnace; L_{kcii} the inductance of the i-phase; e_{ik} the e.m.f. of mutual induction, induced in phase k by current in phase i; e_{a1} and i_i the voltage and current of the ith phase.

equivalent model of the secondary network of the installation, corresponding to the network on Fig. 1b is shown below.

Let us assume that the values of the parameters r_{kci} and L_{kci} of the model are made equal to the instantaneous values of resistances and inductances of the furnace phases, and that real non-sinusoidal currents i_i of the corresponding furnace phases flow in them. Let us also assume that, between points $O''$of the equivalent network and O' of the furnace, inductances L_1' and L_2' are connected, through which real furnace currents i_1 and i_2 flow. In this case potential differences, measured between the corresponding leads A, B, C of the secondary of the furnace transformer and the model leads A′, B′, C′, will, according to (1), exactly represent the non-sinusoidal arc voltages e_{a1}, e_{a2} and e_{a3} in the furnace.

In order to decrease electric losses in the model network k_m times in comparison with the losses in the secondary of the furnace and to obtain a proper scale for the model voltages, it is necessary to increase resistances and inductances in the model k_m times, and to decrease the values of the currents in the model networks k_m times.

Fig. 3 shows the basic network of a model installation for remote measurement of resistances r_{kci} - Δr_{ei} and inductances L_{kci} - ΔL_{ei} and of differences of mutual inductances $L_1''$and L_2'' of the sections of the secondary network, which are situated outside the furnace. On the left side of the figure networks of the furnace are shown; on the right side, networks of the model.

Contact-rods S_i are used to tap the potential of each electrode at the place where it emerges from the furnace. If the values of the model parameters correspond to the instantaneous values of the required parameter of the sections of the furnace secon-

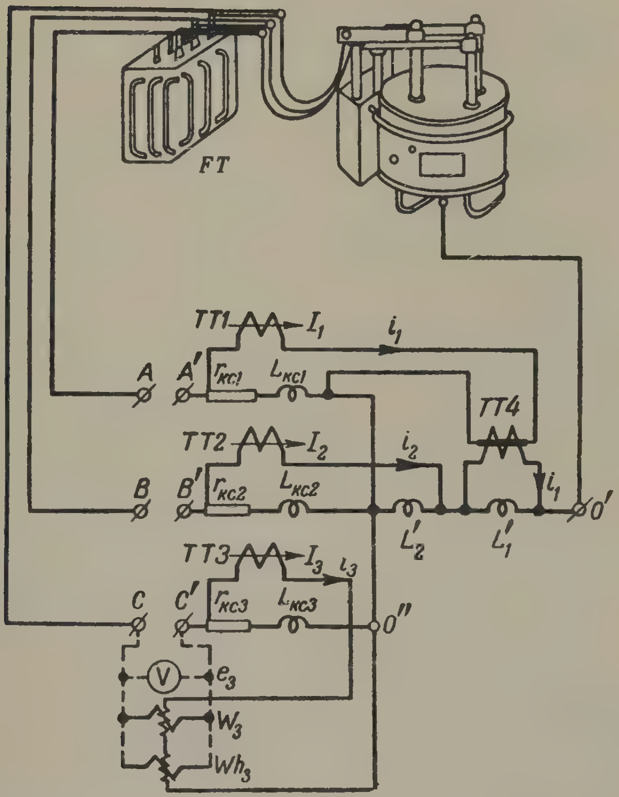

FIG. 2. Network of the model installation of the low-voltage part of an electrical melting furnace.

dary, and the currents in the network models correspond to the real non-sinusoidal currents in the furnace,* then the p.d. measured between points S_1 and E_1 will be equal to zero.

Introduction of contact-rods S_i enables us to measure directly the useful power of each phase of the furnace, equal to the sum of powers developed in the arc and on the portion of an electrode inside the furnace. If the parameters of the model shown in Fig. 3 are determined, the useful power say of Phase 1 may also be remote-controlled by means of a model by measuring p.d.s between points E_1 of the model and O' of the furnace.

Arranging models according to Figs. 2 and 3 on the furnace benchboard we have

---

* On Fig. 1 only networks for the phase current of Model 1 are shown.

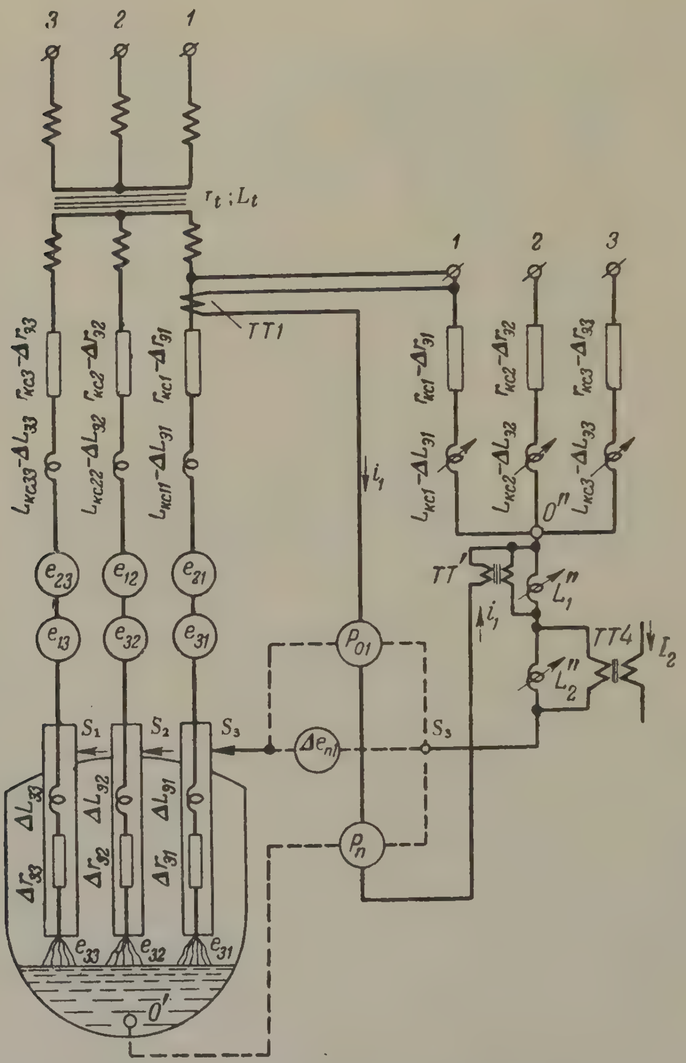

FIG. 3. Network of model installation of sections of the secondary, which are situated outside the furnace.

as 19 unknowns to be determined, L_{kci}, $L_{kci} - \Delta L_{ei}$, $r_{kci} - \Delta r_{ei}$, e_{ai}, r_{kci}, L_1', L_2', L_1'', L_2'', where $i = 1,2,3$.

Determination of the first 12 quantities may be made entirely automatic, since it can be performed under normal conditions when electrodes of all the three phases are arcing.

Experiments showed that, for the equal working lengths of the three electrodes: $L_1' \approx L_1''$, $L_2' = L_2''$ – this being due to the positioning of the electrodes in the furnace at the apices of an equilateral triangle.

Values of L_1'', and L_2'', may be experimentally determined from a series of experiments by breaking one of the arcs, while the electrodes of two other phases are arcing under normal conditions. The order, in which these experiments are to be performed, is as follows.

We set $L_1'' = 0$ and break the arc in Phase 2. From the following equations:

$$(e_{d1} + i_1\Delta r_{e1}) - [u_{t1} - (L_{\kappa c1} - \Delta L_{e1})\frac{di_1}{dt} - L_1''\frac{di_1}{dt} - \qquad (3)$$

$$- L_2''\frac{di_2}{dt} - i_1(r_{\kappa c1} - \Delta r_{e1})] = \Delta e_{n1} = 0; \qquad (4)$$

$$i_1 = -i_3; \qquad i_2 = 0,$$

and varying either automatically or by hand the values of $L_{kc1} - \Delta L_{e1}$ and $r_{kci} - \Delta r_{e1}$ on the model, we may set and determine the values of $L_{kc1} - \Delta L_{e1} + L_1''$ and $r_{kc1} - \Delta r_{e1}$.

Striking the arc in Phase 2 and breaking it in phase $3 (i_1 = - i_2, i_3 = 0)$, and by condition (3), leaving the model parameters in Phase 1 unchanged, we may set up in Phase 2 the value L_2''.

After this, striking the arc in Phase 3 and breaking it in Phase 1, from the conditions required to satisfy equations

$$(e_{d2} + i_2\Delta r_{e2}) - \Big[u_{t2} - (L_{\kappa c2} - \Delta L_{e2})\frac{di_2}{dt} - L_1''\frac{di_1}{dt} - \qquad (5)$$

$$- L_2''\frac{di_2}{dt} - i_2(r_{\kappa c2} - \Delta r_{e2})\Big] = \Delta e_{n2} = 0; \qquad (6)$$

$$i_2 = -i_3; \qquad i_1 = 0,$$

we may set up on the model, values of $L_{kc2} - \Delta L_{e2}$ and $r_{kc2} - \Delta r_{e2}$, and taking into account the equation

$$(e_{d3} + i_2\Delta r_{e2}) - \Big[u_{t3} - (L_{\kappa c3} - \Delta L_{e3})\frac{di_3}{dt} - L_1''\frac{di_1}{dt} - \qquad (7)$$

$$- L_2''\frac{di_2}{dt} - i_3(r_{\kappa c3} - \Delta r_{e3})\Big] = \Delta e_{n3} = 0$$

we may set up on the model values of $L_{kc3} - \Delta L_{e3}$ and $r_{ke3} - \Delta r_{e3}$. Further, by setting up the conditions satisfying equations (4), on the basis of equations (3), we may set up on the model values of $L_{kc1} - \Delta L_{e1}$ and L_1''.

Having determined by the above method values of L_1'' and L_2'' and keeping the electrodes arcing on all three phases in the furnace, we may determine values of $L_{kci} - \Delta L_{ei}$ and $r_{kci} - \Delta r_{ei}$, by equations (3), (5) and (7) and by measuring continuously these values on the model. The process of measuring may be made entirely automatic. For certain known values $L_1' = L_1''$ and $L_2'' = L_2''$, set on the model, we may, by touching the metal alternatively with each electrode, determine values L_{kci} and r_{kci} for every phase by means of the model (Fig. 2); after this, under normal conditions of electrode arcing in all three phases, we may measure p.d.s between leads A - A′, B - B′, C - C′ and the power in every phase of the furnace.

Inductances L_{kci} may be determined by means of the model under normal conditions of electrode arcing on all three phases of the furnace. The method in question is based on a known physical phenomenon, that in continuous arcing the instantaneous current values and arc voltages simultaneously change polarity, passing through zero values. Therefore, observing on Phase 1, say, the moments of passing through the zero value of the arc current and of the voltage between leads A - A of the model (Fig. 2), and adjusting the value of L_{kc1}, so as to obtain the simultaneous passing through zero both of current and voltage, we may find the value of L_{kc1}. Varying the values of currents in the furnace by ± 20 ... 30 per cent, while keeping all three electrodes arcing, or performing the series of experiments discussed above by breaking in turn one of the arcs, we may determine the values of L_1' and L_2' as well.

The values of resistances r_{kci} set up on the model and measured by this method may differ considerably from the true values, but this does not affect the accuracy of measurement of furnace inductances.

Instruments, constructed in the Central Automation Laboratory,* for automatic and manual measuring values of L_{kci}, are based on this principle.

We may investigate the influence of different factors on the parameters of the furnace secondary network by applying the above methods of measurements in various ways: we may feed the furnace by a three-phase and a single-phase current, or keep all electrodes arcing or short-circuit them by keeping them in contact with the metal, or vary currents at symmetrical and asymmetrical loads on phases.

Fig. 4 shows one of the oscillograms of arc voltages e_{1m} and e_{2m}, of Phases 1 and 2; these oscillograms were recorded by using a model installation on a furnace of 20 tons capacity.

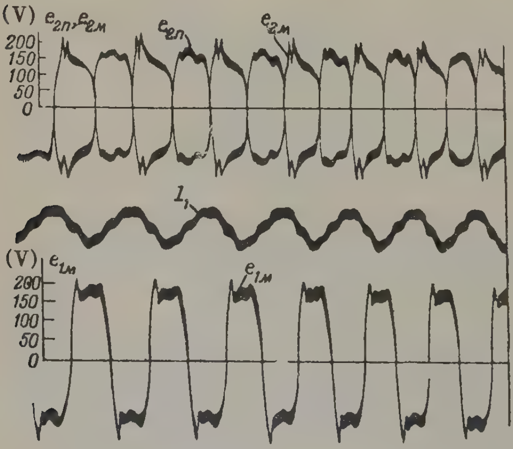

FIG. 4. Oscillograms of arc voltages.

In this figure, the oscillograms of true arc voltages e_{2n} of Phase 2 are shown for comparison; these voltages were directly measured by using two rods, introduced into the furnace: one rod was in contact with the electrode above the arc, the other in contact with the metal near to the arc and slightly below it.

Investigations of an industrial furnace carried out by using a model installation

A series of investigations was carried out by using an experimental specimen of a model installation on an industrial furnace of 20 tons capacity. By these investigations the character of variation of parameters of the furnace secondary network and of the useful power in phases during the melting was first studied; the influence of furnace currents and of the load asymmetry on the values of parameters of the secondary network was also determined, as were several other characteristics.

---

* A.N. Kotikov, B.N. Znamenskii and V.B. Tikhmenev (Engineers of the Central Automation Laboratory) took part in the development of model installations and in carrying out investigations.

Some conclusions, which were made on the basis of the results obtained from these experiments, are given below.

(1) A comparison of many arc voltage oscillograms, obtained on the furnace and on the model, confirmed their complete identity, even in the case when disturbances occur in the arc voltage; these are characterized by a very steep slope on the oscillogram. The differences in voltage values were about 1 per cent of the measured value.

(2) During the process of melting and from one charge to another, the phase resistances $r_{kci} - \Delta r_{ei}$ may vary by more than 20 - 30 per cent; this is due to the contact instability, to the redistribution of currents among parallel branches of tubular conductors and so on.

For different phases these quantities, during weeks and months, may differ by more than 30 per cent.

The use of apparatus for the control of these quantities during service will contribute to the study of the causes of increased losses in the furnace secondary networks and will help in averting these losses.

Resistances of the electrode sections situated inside the furnace constitute more than 40 per cent of the total resistance of the secondary network. Thus, the true value of the electric efficiency of furnaces is considerably greater, and the real losses of electrical energy are 40 per cent smaller than those which are usually assumed, when only the total resistance of the secondary is measured.

(3) The difference in inductances of the extreme phases of the secondary network (for 20 ton furnace) usually does not exceed 4 per cent. The inductance of the middle phase of the secondary is smaller than inductances of extreme phase by approximately 30 per cent, and this is the cause of considerable difference in useful power of phases. The variation of the inductance of the section of the secondary, which is situated outside the furnace, $L_{kc1} - \Delta L_{e1}$, does not exceed 10 per cent, when an electrode is moved from its uppermost position into the lowest one; the variation of the value of inductance between one charge and another is of the same order. After the charge is melted, the values of inductances of the electrode portions situated inside the furnace are practically equal for all phases, do not vary with time and represent less than 15 per cent of the mean value of the inductance of the whole installation. Whilst the ferro-magnetic charge is still solid in the furnace, the inductance increases considerably.

(4) Values of the differences between the phase mutual inductances L_1' and L_2' are determined practically only by the influence of sections of the secondary, which are situated outside the furnace; they are approximately equal to 5 - 15 per cent of the mean value of the inductance of a phase. These values vary with time only during

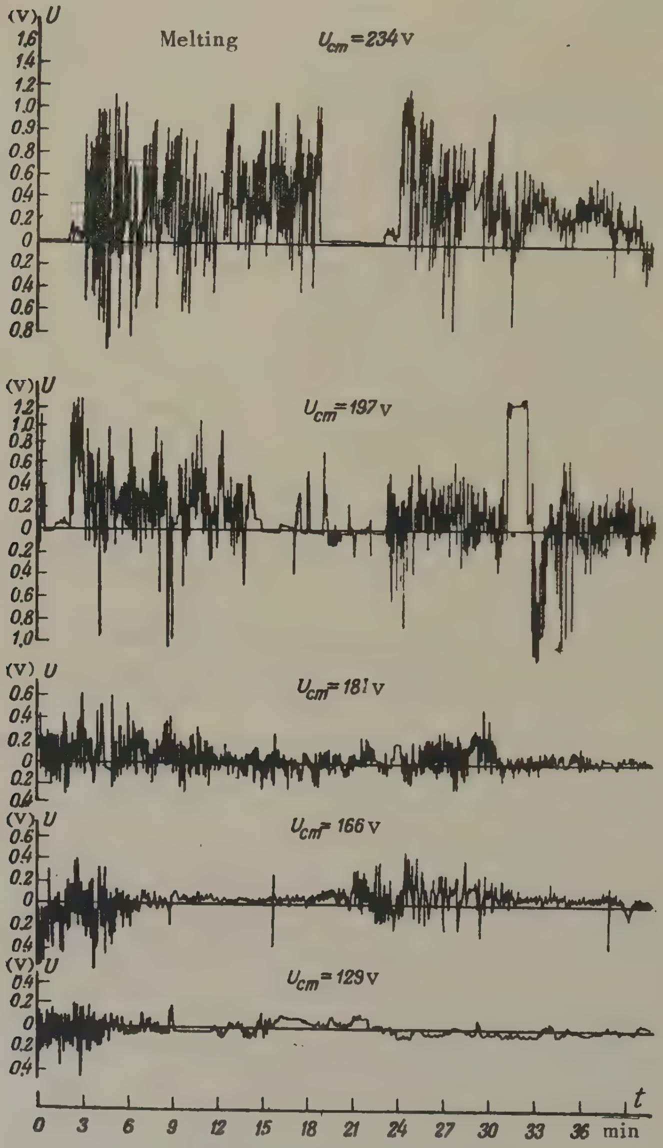

FIG. 5. Variation of voltage drop on the ohmic resistance of a section of the secondary, which is situated outside the furnace during the melting process.

the period when the electrodes are melting the cold charge.

(5) Only the reactance of the middle phase varies considerably with the current, and increases with an increase in current. Asymmetry in electric conditions has only slight influence on the variation in the reactances of a given furnace. Variation of phase resistances, caused by the influence of conditions of contact, is comparable to the influence of current variations and of the load asymmetry between phases.

This fact prevented an exact determination of the influence of each one of these factors.

(6) A d.c. component is present in the arc current; this component may be equal to 15 - 30 per cent of the current during the period of melting, while arcing occurs between an electrode and solid metal. The character of variation of currents during the process of melting is shown in Fig. 5. Directions and values of direct currents in the arc often vary.

The appearance of these currents is due to rectifier action of the arc [4, 5] and to the difference in the d.c. voltage components in arcs of different phases.

Fig. 6 shows the data which characterizes the real electric parameters of the work of an arc furnace of 20 tons capacity; these data were recorded during ten meltings at the higher value of the voltage (236 V).

For every melting, r.m.s values of the phase currents I_i, mean values of the furnace useful power ΣP_u, mean values of useful phase power P_{ui} and average values of the installation power factor cos ϕ are given.

Results of these investigations and of similar investigations carried out during meltings in another furnace of 20 tons capacity allow us to draw the following conclusions.

During melting the difference between mean values of phase useful power may exceed 20 per cent. This difference is still greater for various intervals of melting periods. Slightly small differences are observed during the process of metal refining. The results of this are: non-uniform rate of metal melting, delay in melting, the increase in energy consumption and non-uniform heating of the surface of the molten metal.

The mean value of the total useful phase power may vary from one charge to another by more than 10 per cent; this is due to different factors; delays in melting, increase in energy consumption because of electric conditions in the furnace, which differ from optimum conditions, and also because of abnormal melting conditions, which bring about the deterioration in the quality of the metal.

From one melting to another, power factors and electric efficiencies may vary within the limits 0.01 - 0.03.

Conclusions

1. The model installations, designed for non-sinusoidal currents and for electromagnetic transmissions of power from one phase to another, enable manual or automatic remote control of parameters in conductors carrying heavy currents, of voltages on arcs of useful powers in every phase of the installation.

2. During the normal work of installation, automatic and continuous control is possible of the following quantities: resistances and inductances of the low-voltage conductors, situated outside the furnace, total inductance of conductors, arc voltage and useful electric power. It is possible to control automatically conductor resist-

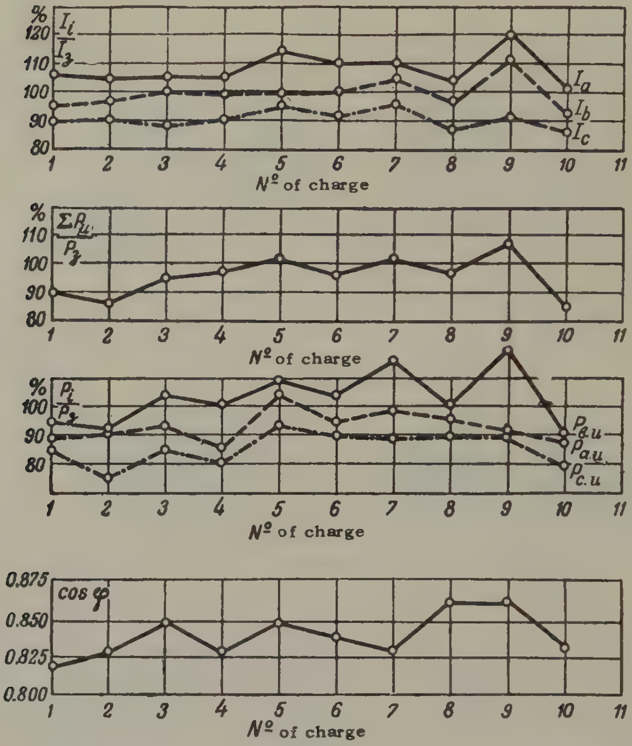

FIG. 6. Mean values for a period of melting of electric parameters in a furnace, recorded for ten charges; I_a, I_b and I_c are phase currents, P_{au}, P_{bu}, P_{cu} are useful phase powers, ΣP_u total useful electric power consumed by a furnace.

ances in each phase and the differences of coefficients of the phase mutual induction.

3. Experimental investigations carried out by using model installations show that there are considerable possibilities for decreasing electric losses and specific consumption of electric energy and for increasing power factors of arc furnaces, which are big consumers of electric energy.

The use of the installations described above offers prospects for the application of new methods of control of the useful power of the installation by computers [1].

4. The application of model installations may prove useful for the measurement of parameters of industrial sets and the control of technological processes which cannot be directly controlled.

Translated by S. Szymanski

REFERENCES

1. Yu. E. Efroimovich; *Kempleksnaia mekhanizatsiia i avtomatizatsiia protsessa vyplavki stali v dugovykh pechakh. Doklad na Vsesoiuznom soveshchanii po avtomatizatsii proizvodstvennykh protsessow (Complex mechanization and automation of processes of steel melting in arc furnaces. Report read at the All-Union Conference on automation of production processes)*, Metallurgizdat (1956).
2. *Avtomatizatsiia proizvodstvennykh protsessov, gl. IV. Elektrostaleplavilnye dugovye pechi. (Automation of production processes, Ch. IV. Electric arc furnaces for steel melting)*, Akademizdat (1956).
3. Iu.E. Efroimovich; *Elektrichestvo*, No.1 (1951).
4. V.N. Nikolskii; *Elektrichestvo*, No. 11 (1951).
5. Iu.E. Efroimovich; *Elektrichestvo*, No. 3 (1954).

TURBO-GENERATORS OF 30 TO 300 MW POWER BUILT BY KhETZ FACTORY *

L. Ia. STANISLAVSKII

Khar'khov Electrical Equipment Diesel Works

(Received 26 July 1957)

The production of turbo-generators in Khar'khov began in 1936 in the turbo-generator factory, (Khar'khov Turbo-generator Plant), built during the second five-year plan. During these years, the problem of organizing the production of turbo-generators of 50 MW at 1500 rev/min has been solved. In this factory, not only the problem of the output of these machines, which were unique at the time, was solved, but also in 1938 the first four-pole turbo-generator of 100 MW power was made in the Soviet Union; its rotor, weighing 100 tons, consisted of three parts [1]. In this factory, reconstructed after the war, a turbo-generator mark TGV-25, of 25 MW power and 3000 rev/min, was designed and production began.

In 1954 the production of turbo-generators was transferred to the Khar'khov factory of Diesel)electrical equipment, where the biggest generator unit in the world at that time was installed and fitted with first class nationally-made equipment. The production of large hydro-generators was also organized in these works.

In this article, the main topic is the description of new powerful turbo-generators with direct hydrogen cooling of the stator and rotor windings; a short account is also given of experience in building and using an experimental turbo-generator of 25-30 MW power.

In designing the construction of the turbo-generator mark TGV-25, of 25-30 MW at 3000 rev/min (Fig. 1) with hydrogen cooling at 0.04 a.t.g. (a.t.g = atmosphere gauge pressure) the following problems were posed. It was necessary to ensure the performance and service characteristics, required by G.O.S.T. standards; furthermore, an attempt was made to introduce several new constructive solutions, which might be useful in construction of turbo-generators of much greater power.

For the first time in the U.S.S.R. and to a certain extent for the first time in the world, welded stator shields with built-in bearings were used in this

---

* *Electrichestvo*, No. 3, 27-32, 1958.

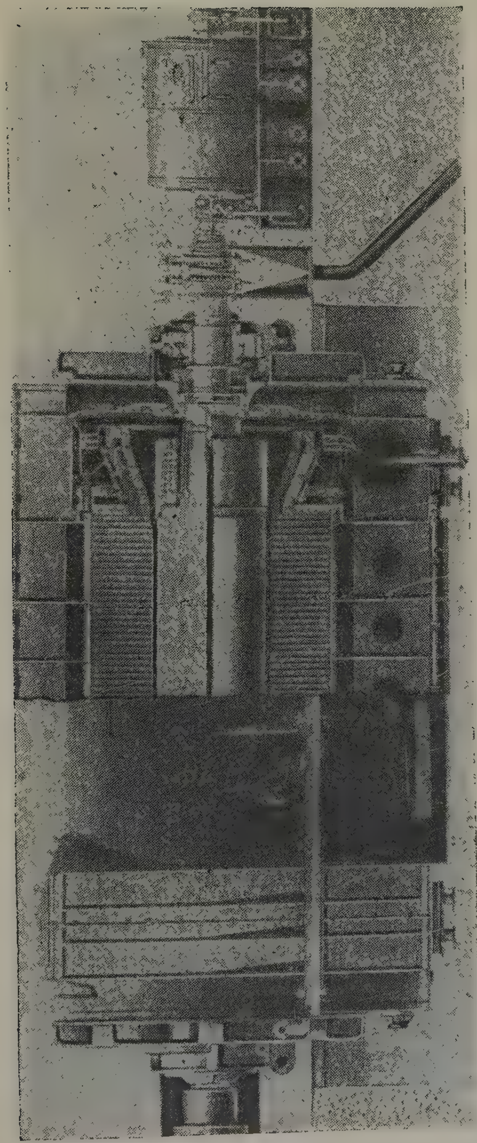

FIG. 1. Turbo-generator mark TGV-25, 25-30 MW, 6.3/10.5 kV. 3000 rev/min.

generator, as well as disk seals with small oil consumption and propeller ventilators. The vertical disposition of coolers and bracket fixing of retaining rotor rings was used. Moreover, at the author's suggestion, the stator cores and windings were produced in repetitive manufacture, and the stator winding was made for voltages of 6.3 and 10.5 kV by using a delta or star-connexion. The use of disk seals dispenses with a cumbersome and complicated vacuum purification of oil.

At present, since a large number of such generators has been made, and a considerable number of them has been in service for some years, we may draw certain conclusions.

Some apprehension, which was expressed concerning the ability of a generator with shield bearings to withstand vibration, did not materialize.

The results of measurements of double amplitudes of vibrations are given below; these vibrations were recorded on the covers of bearings built in the end shields of the generator type TGV-25. These measurements were taken on 50 turbo-generators, working on load and in normal service conditions. On 19 machines out of the total number, vibrations were measured in the transverse, vertical and axial directions; on the remaining machines only transverse vibrations were recorded.

No. of turbo-generators	Maximum double amplitude of vibrations (mm)
32	0.02
7	0.03
5	0.04
4	0.05
1	0.06
1	0.09*

* The generator was coupled to a foreign-made turbine, the critical speed of rotation of which was unknown.

The data show that the vibrations of turbo-generators are insignificant. In practice, the axial vibrations of the bearing from the exciter side are entirely eliminated, these vibrations being extremely undesirable, but unfortunately a common phenomenon in machines with the pedestal (external) bearings.

The experiment of making and using a turbo-generator mark TGV-25 gave an opportunity for improving the shield construction and for increasing the reliability of the electrical insulation of the shaft by protecting it from currents in the bearings; easier access in the assembly of stuffing boxes was achieved as well.

A disk seal permits the sealing of the rotor shaft, with the oil consumption inside the stator casing not exceeding 1 litre per minute. For this rate of consumption no necessity arises for separating oil from hydrogen.

The vertical arrangement of coolers is the most convenient with respect to conditions of assembly, working and inspection. The suppression of vibrations of the tubes of the cooler is achieved by fixing these tubes in appropriate places.

Because of this the vibrations of tubes decreased from 2 to 0.02 mm.

The use of propeller ventilators proved to be entirely justified; moreover, their cost was considerably reduced due to production by drop forging. Bracket fixing of retaining rings of the rotor prevents the breaking of the teeth of the rotor body or the wearing down of the places of setting, which happens, for instance, when a split set binding ring or elastic centring rings are used.

More than half the machines of mark TGV-25 already made are delta-connected. No extra overheating or other losses were recorded. The advantage of repetitive manufacture of stator cores and windings is obvious.

In 1956 the production of turbo-generators mark TVS-30, of 30 MW power at 3000 rev/min [2] began. In the design of this generator, the main problem was the creation of a unified machine based on the construction of turbo-generators marks TGV-25, TV2-30-2 and T2-25-2 produced in the Soviet Union. In this generator, all valuable improvements made in the generator TGV-25 were applied. The hydrogen pressure is 0.05 - 0.5 a.t.g. No doubt the hydrogen pressure will be raised in future up to 1 a.t.g., thus increasing the power of the generator by 10 - 15 per cent.

The generator mark TVS-30 is made with couplings of unified dimensions, so that it can be directly coupled with turbines, made in all turbine-making factories of the Soviet Union. The systems of oil distribution, of protection and of the generator voltage regulation are all standardized; a silicone insulation is used for the rotor winding; for insulating the retaining rings the compressed glass fabric is used, the aluminium saddles in the front part being absent.

Due to difficulties encountered during the first period of service of generators of mark TGV-25, external bearings (on the outside pedestals) are used in generators TVS-30, this being, in the author's opinion, their disadvantage.

In the design of turbo-generators of 200-300 MW power the basic trends which appear in the development of the construction of generators were taken into account.

One of the most important problems in the construction of high power generators, while keeping their size within reasonable limits, is the increase of the hydrogen pressure inside the machine. On the basis of the tests carried out by the factory for turbo-generators mark TGV-25 [2], it was found that, by increasing the gas pressure from 0.05 to 0.5 a.t.g. and keeping the load constant, the rise in temperature of the generator is decreased in the ratio of 1.5 to 1, and by increasing the pressure up to 1 a.t.g. the corresponding decrease is more than two to one, i.e. instead of 32.6°C it becomes only 15° (taking into account the lowering of losses in the generator windings due to the drop in their temperature). Table 1 shows the results of the measurements of the temperature rise of generator windings as different hydrogen pressures.

For high-power generators the pressure of the cooling gas was fixed at 3a.t.g.

TABLE 1.

Hydrogen pressure (a.t.g.)	Temperature rise (°C)	
	Rotor winding	Stator winding
0.05	94.6	60.3
0.5	80.7	40.3
0.75	75.1	37.5
1.0	71.5	34.8

The values of the power, developed by a 200 MW generator in relation to the hydrogen pressure, are shown below:

Hydrogen pressure (a.t.g.)	Power of the generator (MW)
0.5	100
1	140
2	170
3	200

Nevertheless, by solely increasing the hydrogen pressure the problem of the construction of high-power generators cannot be solved. In the rotor windings and in the stator bars of ordinary design, the temperature distribution at the hydrogen atmospheric pressure is such, that 50-60 per cent of the temperature drop occurs in the insulation. The remaining part occurs in gaps, the surface gas layer and the steel of teeth, their thermal conductivity considerably increasing with the increases of the hydrogen pressure.

The thermal conductivity of the insulation, however, does not increase with increasing hydrogen pressure; therefore the use of external cooling does not permit an increase in the power of the generator by more than 30 per cent.

The use of direct internal cooling of the rotor and stator copper, permits the construction of the 200 MW generator (Fig. 2) of smaller dimensions than those of the turbo-generator TV2-150-2 of 150 MW.

This is due to the fact that direct cooling permits a more efficient use of th active materials of the machine. At present the next outstanding problem is the beginning of repetitive manufacture of turbo-generators, with direct cooling of the stator and rotor windings. This will result in an economy of up to 50 per cent in the materials required at present, and by slightly increasing the number of the working hours needed for production, the productive capacity of the turbo-generators factories will be nearly doubled, and the capital expenditure in building ele tric plants will be considerably lowered.

With metallurgy at the standard it is today, it is possible to make a rotor of 1,100 mm diameter and a body length of 6,500 mm for a generator rotating at a speed of 3000 rev/min. For this case, the limiting values of the power developed by generators with different methods of cooling are as follows:

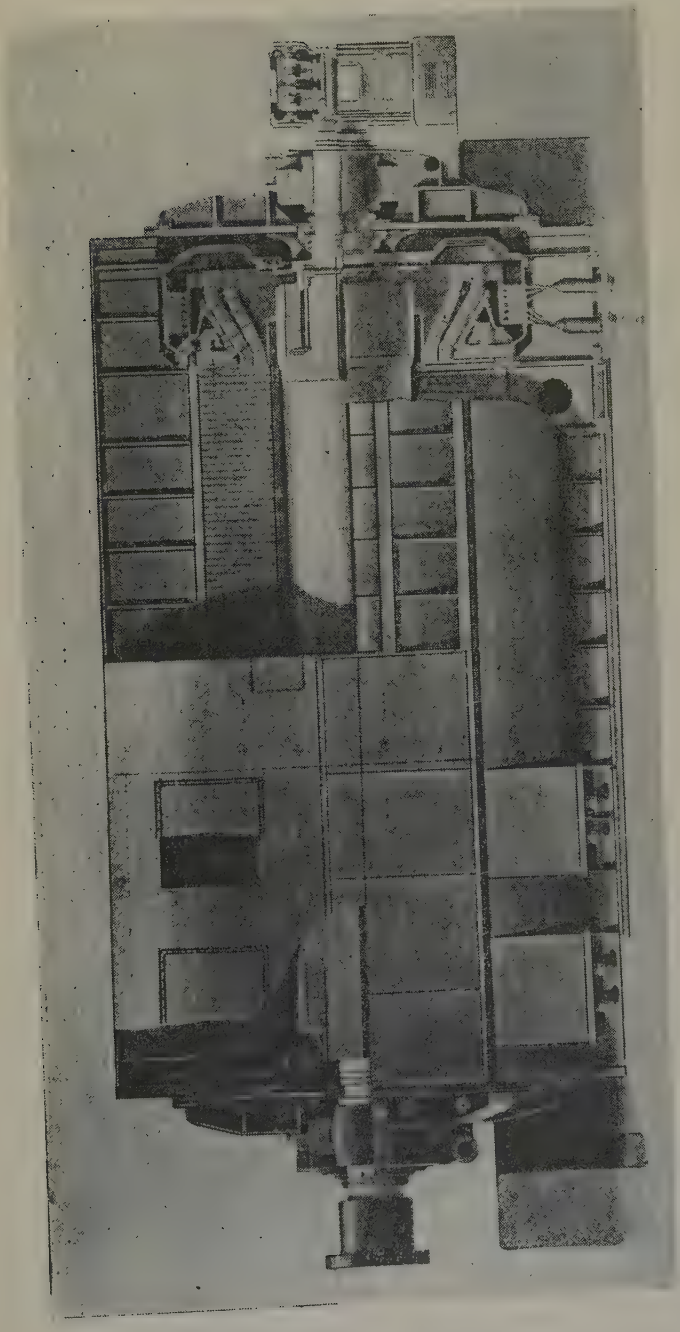

FIG. 2. Turbo-generator mark TGV-200, 200 MW, 15.75 kV, 3000 rev/min.

Method of cooling	Power (MW)
Air cooling	140
Surface hydrogen cooling at the gas pressure 0.03 a.t.g.	210
Surface hydrogen at the gas pressure 3 a.t.g.	270
Internal hydrogen cooling at the gas pressure 3 a.t.g.	350-400

The considerable increase in power of generators with direct hydrogen cooling is possible due to the fact that the internal cooling of the rotor and stator windings permits a considerable increase of the current density in the windings. For comparison, in Table 2 the values of current densities are given for generators of different marks.

TABLE 2.

Generator mark	Nominal power (MW)	Nominal voltage (kV)	Current density (A/mm^2)	
			Stator	Rotor
TGV-25	30	10.5	3.53	3.88
TV2-30-2	30	10.5	3.53	3.88
TV2-50-2	50	10.5	3.17	3.36
TV2-100-2	100	13.8	2.80	3.40
TV2-150-2	150	18.0	2.50	3.50
TGV-200	200	15.75	3.17	7.06

In the turbo-generator TGV-200 an axial-radial system of ventilation is used. A centrifugal pressure compressor, situated at the slip ring end of the rotor, delivers the gas at 3 a.t.g. into the hollow rotor windings and into the ventilating tubes situated in the stator windings. The hydrogen stream leaving the compressor is divided into three parts: one part flows into the ventilating tubes of the stator bar winding, the second part under the retaining ring from the side of rotor slip rings and further into the hollow rotor conductors, the third part also enters the hollow rotor conductors from the turbine side.

The gas, leaving the ventilating tubes of the stator bars, enters the axial ventilator, situated on the turbine side. The gas, which entered the gaps after leaving the hollow rotor conductors and hollow stator cores, comes into the same ventilator. The axial ventilator sends the hydrogen into a gas cooler; on leaving this cooler a part of the hydrogen stream cools the stator core and the stator and rotor surfaces, after which it passes into the gap and enters the axial ventilator. The second part of the gas stream comes into the centrifugal compressor.

The ventilating channels of the bar winding are made in the form of thin-walled non-magnetic steel tubes situated between the two rows of glass-insulated conductors. Investigations have shown that the temperature drop in the 0.3 mm thick insulation of such a bar is only 3°C, a rather small value.

At a gas speed in the bar channels of more than 30m/sec, the temperature drop between the channel walls and the gas is equal to 3°C. Thus the excess of the temperature of the stator copper winding over the gas temperature is only 6°C, hence the temperature of the copper depends mainly on the gas temperature.

The ventilating ducts of the rotor winding are formed by two conductors of channel sections. The investigations on the temperature distribution and on the flow of the gas in the ducts for internal cooling, which were carried out by ourselves together with the Scientific and Research Institute of the Electrical Industry and with the Chair of Blade Machines and Applied Gas Dynamics of the Khar'khov Aviation Institute, gave a result for the optimum cross-section of the windings and of their ventilating channels [3].

The shaft seals are the most important constructional details of a modern turbo-generator.

The study of the performance of these seals, which was carried out by this factory for many years, showed that a properly designed seal of the disk type may work safely at pressures up to 3 a.t.g. and more. The method of decreasing the load, carried by the packing of stuffing boxes which was designed by this factory, is very important, since it allows for a sharp decrease in overheating of the boxes and in the losses in packing.

Table 3 shows the experimental data of the work of one of these stuffing boxes.

TABLE 3.

Gas pressure in the chamber (kg/cm^2)	Oil pressure at the stuffing box inlet (kg/cm^2)	Oil temperature at the stuffing box inlet (°C)	Babbit temperature in the stuffing box (°C)	Oil consumption by the stuffing box (l/min)	
				Inside the stator body	On the outer side of the box
00	0.2	38	51	0.14	36
0.05	0.4	36	50	0141	36
0.5	0.9	35	49	0.64	38
1.0	1.4	36	48.5	0.43	46.5
2.0	2.4	36	47.0	0.21	53
3.0	3.4	36	46.5	0.15	58.5
3.0	3.6	36	46.0	0.5	62.5
3.0	3.8	36	44	1.9	72.0

The turbo-generators made by the factory have built-in bearings in the end shields; these bearings have many advantages in comparison with the external bearings.

This arrangement permits a large decrease in the distance between the centre lines of bearings; for example, in 200 MW turbo-generators this distance is cut by nearly 800 mm. In consequence the static sag of the rotor is considerably reduced, and this increases the critical speed of rotation. This reduction is very desirable, since both in the world at large and in home practice some cases of fracture of rotors of big generators are known. These accidents were caused by excessive sags, the second critical speed of rotation being smaller than the normal working speed.

The use of built-in shield bearings for turbo-generators weighing up to 250 tons

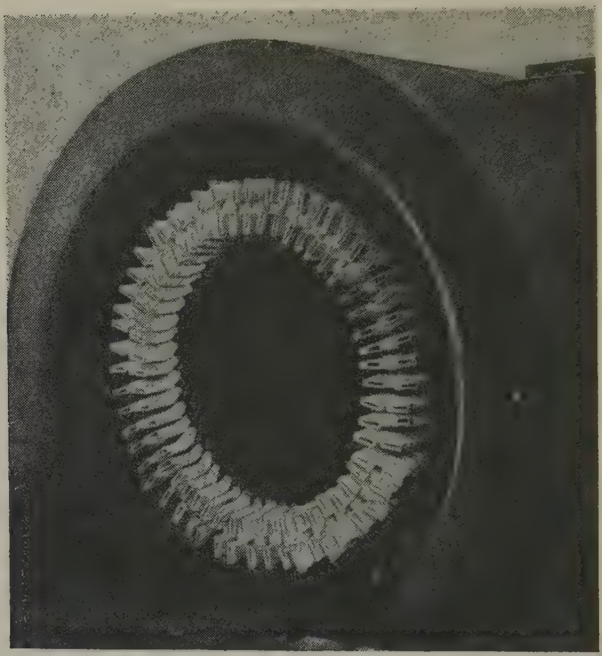

FIG. 3. Silicon rubber caps for the inlet and outlet of the cooling gas.

permits their transport in a completely assembled form (together with the rotor), and this fact permits assembling and sealing of the generator in the factory, thus shortening the time required for assembly 4-5 times.

By using built-in shield bearings we reduce the weight of a turbo-generator and its size, the amount of vibration and the resistance of bearings as well. Difficulties connected with the unavoidable axial vibrations of bearings situated on the exciter side disappear when these vibrations occur with the majority of big generators with external bearings.

The use of built-in shield bearings makes the accurate machining and assembling of the generator much easier, due to the presence of centring grooves in the shield and cover, in bushes and stuffing boxes; it also ensures a complete interchangeability of parts. The construction of front shields with built-in bearing bushes permits the examination of bushes without letting out hydrogen and examination of packing without dismantling the bearing. Shield bearings permit the examination of frontal parts without dismantling the bearings; for this purpose only the upper part of the shield is removed. By the use of "biscuits" for the insulation of the bush covers the suppression of currents in bearings is greatly simplified.

The turbo-generator of 200 MW power has the following nominal characteristics: voltage 15.75 kV, current 8.63 kV, the power factor cos $\phi = 0.85$, 3000 rev/min.

For the same power factor for the 300 MW turbo-generators the stator winding voltage is taken as 20 kV. In both cases these generators have single-coil windings, thus permitting their use at 10 kV. The field winding of the generators, according to the design, will be fed from the generator terminals through gas rectifiers. The welded, gas-tight frame of the stator is calculated on the basis of long use at a gas pressure inside the stator of 3 a.t.g. The test pressure is 10 a.t.g. Two vertical gas coolers are situated at the side of the turbine. The stator core together with the winding is elastically attached to the stator body by means of flat springs, and this excludes the possibility of transmitting vibrations of double frequency to the stator body.

The stator winding is of the bar, basket type.

The inlet and outlet of the cooling gas into the ventilating tubes is made in the bar heads through the silicon-rubber caps (Fig. 3). For the bar insulation silicon plastic is used, a heat-resisting insulation of increased mechanical strength devised jointly with the All-Union Lenin Institute of Electrical Technology.

Bars with new insulation have been used in the stator of an experimental turbo-generator. Preliminary tests have shown that, so far as electrical strength and tangent of the loss angle are concerned, the new insulation is not inferior to the compound one and has a greater mechanical strength. There are, however, still some difficulties in the repetitive production of these windings.

For the rotor winding, copper is used with the addition of some silver. This increases the mechanical strength of the copper, which is essential for securing reliable working of the rotor. In the system of ventilation adopted, teeth and slots of the rotors have no holes.

The rotor of the 200 MW turbo-generator is of smaller dimensions than the rotor of the 150 MW generator mark TV2-150-2, due to internal cooling of windings.

To solve a series of problems connected with the design and production of 200 and 300 MW turbo-generators, an experimental turbo-generator of 30 MW power was made. In the stator and rotor of this generator about 200 resistance thermometers, thermistors, tensometers and thermocouples were inserted, and valuable results were obtained.

Some parameters of the 200 MW turbo-generator mark TGV-200 are shown below.

Efficiency	98.87
Short circuit ratio	0.58
Subtransient reactance (%)	19
Transient reactance (%)	29.5
Synchronous reactance (%)	203.5
Mean temperature rise of the stator winding (°C)	38
Mean temperature rise of the rotor winding (°C)	38
Distance between bearings (mm)	8200
First critical speed of rotation (rev/min)	1340

Second critical speed of rotation (rev/min)	4380
Specific copper consumption (kg/kVA)	0.076
Specific active steel consumption (kg/kVA)	0.436
Total weight of the generator (tons)	287

Translated by S. Szymanski

REFERENCES

1. L. Ia. Stanislavskii; 100,000 Turbo-generator Khar'khov S.M. Kirova Turbo-generator Plant,*Vestnik elek. prom.*, No. 5 (1941).
2. L.Ia. Stanislavskii, Seriinyi turbo-generator s vodorodnym okhlazhdeniem tipa TVS-30 (Series-produced turbo-generator with hydrogen cooling, mark TVS-30) *Vestnik elek. prom.*, No. 2 (1956).
3. Raspredelenie temperatury i technik okhlazhdaiushchei sredy v provodnikakh vnutrennego okhlazhdenia.(Temperature distribution and flow of the cooling medium in a conductor with internal cooling) *Trud. Khar'khovskogo aviatsionnogo inst.* No. 2 (1957).

ON THE POSSIBILITY OF INTENSIFICATION OF COOLING OF TURBO-GENERATORS

V.G. FASTOVSKII and IU.V. PETROVSKII

Lenin All-Union Institute of Electrical Technology

(Received 1 April 1957)

The dimensions of modern turbo-generators, of 150-200 MW power with hydrogen cooling of the surface, reach limiting values (rotor diameter 1.10-1.15 m, rotor length 6.3 m), determined by the permissible stresses in the rotor material and by conditions, occuring when the machine passes through the critical speed of rotation at the start. It is well known that an increase in power of a turbo-generator, its dimensions being unchanged, is possible only by an intensification of the process of heat dissipation, the amount of heat developed increasing with the increase of current density in the machine windings.

In view of this fact, it follows that it is desirable to consider briefly some problems connected with methods of intensification of cooling of turbo-generators. Let us remember that the first important step in this direction was the use of hydrogen cooling, which permitted a decrease in the overheating of active parts of a machine and a reduction in the friction and windage losses in the rotor.

With surface cooling of the rotor, the increase of hydrogen pressure reduces the temperature difference between the rotor surface and the gas stream, this lowering constituting 17-22 per cent of the total temperature drop. In the limiting case, this permits an increase in the power of a turbo-generator by 20-25 per cent.

The system of internal hydrogen cooling of the active copper of the rotor and stator windings makes possible a considerable increase in power. Furthermore, the increase of hydrogen pressure is a very efficient method for the intensification of cooling, since the coefficient of thermal conductivity at a constant gas speed varies proportionally to $p^{0.8}$ (p is the gas pressure in abs atm). The permissible current density increases accordingly, and with it the power of a turbo-generator.

The problem of maximum output of a turbo-generator, with internal copper cooling, is of considerable interest. Calculations show that, at a hydrogen pressure of 5 abs atm and a speed in the channels of the excitation winding (where the major quantity of heat is developed) of the order of 80 m/sec, the coefficient of thermal conductivity from the copper surface to the gas is equal approximately to 1200 k cal/m²hr°C. At a current density of 10 A/mm² the increase of hydrogen temperature is about 31°C. For the hydrogen temperature at the channel inlet of 40°C, the maximum copper temperature is 85°C, which is considerably lower than the permissible temperature of 120°C. Under such conditions, which can certainly be realized, the power of a turbo-generator increases up to 350-400 MVA [1].

---

* *Elektrichestvo*, No. 3, 32-35, 1958.

The actual importance of the problem of cooling gave rise to a series of new propositions for intensification of the process of internal cooling of excitation windings. Thus, evaporation cooling, based on the principle of using the latent heat of a volatile liquid, pumped directly into the channels of the excitation winding, is of considerable interest. With this method the rotor will rotate in the vapour of the cooling liquid, since a perfect sealing of the circulating system is rather difficult. To reduce the windage losses inside the body of a turbo-generator it is necessary to maintain a vacuum. For this purpose a powerful vacuum pump and surface condenser, to liquify the vapour and to return the liquid into the circulating system, will be needed. The liquid must have many specific properties: dielectric strength, large latent heat, a convenient boiling point, chemical inertness, non-inflammability etc. To find such a liquid, especially for cooling of the stator winding, is a difficult problem, and the cooling system becomes complicated.

The use of a liquid (for example of transformer oil) was also suggested for cooling the rotor; such a liquid must be a good dielectric and must not destroy the insulation, since hermetic sealing of the circulating system is impossible in practice, and a part of the liquid penetrates into the gap between the rotor and the stator. But in this case there is a danger of destroying the stator surface opposite the rotor, by the oil drops projected at a great speed from the rotating rotor.

Another suggestion was to use the so-called convection-evaporation cooling, which consists in injecting the liquid into the circulating hydrogen.

The result of the evaporation of the liquid is a drop in the hydrogen temperature, consequently the temperature difference between the copper to be cooled and hydrogen increases, thus increasing the process of heat dissipation. The condensation of the vapour of the liquid takes place at the surfaces of the gas coolers, from where the condensed liquid returns into the circulating system.

Obviously, we cannot expect a considerable increase in the rate of cooling from such a system since only a small proportion of the liquid will evaporate from the surface to be cooled.

The liquid cooling of a rotor is a complicated technical problem, the satisfactory solution of which would permit a considerable increase of the limiting power of turbo-generators, while keeping their dimensions unchanged.

Calculations show that particularly favourable conditions of heat dissipation can be achieved by using water for cooling of the rotor.

Liquid cooling of the stator is easier to solve and in this case the distilled water is very efficient; but during the process of circulation, the electric conductivity of water increases. By introducing into the circulation system an ion-exchange apparatus, it is possible to keep water resistivity at the level of $10^6 - 10^7\ \Omega$ cm [2].

The most serious attention should be paid to the technical design of water cooling systems for turbo-generators. Recently articles have appeared concerning the realization of the water cooling system of the stator winding of a turbo-generator at 11.8 kV [3].

Using a liquid system for cooling, power losses due to the circulating of the cooling agent are greatly reduced. Thus, for oil cooling of the stator winding of a 500 MW turbo-generator, in which the losses are approximately equal to 1.2 MW, a pump, driven by a 10 kW motor, will be required. The power needed for ventilation with hydrogen cooling is of the order of hundreds of kW.

Let us consider in greater detail the problem of the usefulness of forced hydrogen cooling [4].

If the temperature of the hydrogen after passing the water coolers is taken to be equal to 40°C under normal conditions, its temperature may be reduced considerably by the use of artificial cooling. In this case, however, it must be borne in mind that the power of the cooling devices increases rapidly as the cooling temperature is reduced.

The forced hydrogen cooling may be used to achieve one of two objects:
1. while keeping the dimensions of the active parts of a generator unchanged, to increase its output; in this case, the conditions of work of copper remain unchanged as regards temperature; the copper temperature remains at the previous limiting level, but heat dissipation increases due mainly to an increase in the temperature difference between copper and hydrogen;
2. while keeping the dimensions of the active parts of a turbo-generator and its power unchanged, to increase the efficiency of the machine by decreasing the copper temperature, which in turn decreases the copper resistivity; the advantage of this solution depends upon the relation between the decrease of losses in the windings and the power required for forced cooling.

The first problem is of greater interest. As an example, let us analyse the cooling conditions of a 200 MW generator. We assume that the hydrogen temperature at the inlet is 0°C; let the increase of the gas temperature be 40°C. The total losses of such a machine are estimated at 1.77 per cent of its nominal power [1], i.e. 3540 kW. Excluding losses in bearings (0.2 per cent), we find that the losses, to be dissipated by hydrogen, are 3240 kW, or in thermal units 2.7×10^6 kcal/h. – Assuming that the gas pressure inside the machine is equal to 4 abs atm and taking the specific heat of hydrogen, at the mean temperature of 20°C, as equal to 3.4 kcal/kg °C, we find the total weight of the circulating hydrogen to be approximately equal to 20 t/hr, or 6 x 10^4 m^3/hr. We have to design the ventilators for this output.

If the rotor winding has ventilating channels of rectangular cross-section, then the value I of the current in the winding conductors exceeds the value I_0 of the current in the conductor of the full section [1] by the ratio:

$$\frac{I}{I_0} = 12\alpha^{1/2}, \tag{1}$$

where a is the coefficient of thermal conductivity (W/cm^2. °C).

For the forced cooling of hydrogen the temperature difference between copper and hydrogen increases; for the same pressure and gas speed in channels, the value of the coefficient of thermal conductivity varies only slightly. Therefore, equation (1) may be written in such a form as

$$\frac{I}{I_0} = 12\left(\alpha \frac{\theta}{\theta'}\right)^{1/2}, \tag{2}$$

where θ is the temperature difference for the forced cooling of hydrogen, and θ' the temperature difference for the water cooling of hydrogen. Assuming the copper temperature is equal to 120°C, then $\theta = 100$°C and $\theta' = 60$°C. In this case

$$\frac{I}{I_0} \approx 15.5\alpha^{1/2}. \tag{3}$$

Thus, for the chosen set of parameters, the ratio I/I_0 increases approximately by 30 per cent.

By substituting external cooling of the rotor by internal cooling of the excitation winding, at the increased hydrogen pressure, we may increase the m.m.f of the excitation 2-3 times. In the case of forced cooling of hydrogen up to 0°C, we may further increase the m.m.f. of the excitation winding 2.5-4 times in comparison with its value, when the rotor slots remain without cooling.

Let us now consider the second problem – reducing the copper losses by decreasing the copper temperature. As a first approximation we may assume that the decrease of the mean hydrogen temperature by 40°C will bring about the same decrease of the copper temperature. Using the well-known relationship between the resistivity of copper and its temperature, it is easy to show that the decrease of the temperature by 40°C results in a decrease of copper losses by 17 per cent, thus increasing the effective power of a generator by 220 kW (the total copper losses in this machine are estimated at 1270 kW). It is quite obvious that the power required to drive the cooling system will be greater than the economy achieved.

Let us consider possible methods for the forced cooling of hydrogen up to 0°C: the use of a liquid evaporation and cooling installation with a compressor, an absorption cooling installation and a turbo-exhaust pump.

In a compressor cooling installation, working in vapour cycle, evaporation of the cooling agent takes place at a constant temperature and pressure. To cool hydrogen up to 0°C, the temperature of evaporation of the cooling medium should not exceed – 5°C, since, for smaller difference of temperature, the dimensions of gas coolers increase considerably.

Let us consider an installation working on freon-12 at an evaporation temperature 5.5°C, a pressure in the evaporator of 267 abs atm, a temperature of condensation 30°C, and a pressure in the condenser of 7.6 abs atm. For such an installation the effective specific cooling capacity is 37200 kcal/k Whr [5].

For the amount of heat to be dissipated, which we assumed above to be equal to 2.7 x 10^6 kcal/hr, the power of the cooling installation will be

$$P = \frac{2.7 \cdot 10^6}{3720} = 730 \text{ kW}.$$

This corresponds to a decrease in the efficiency of the turbo-generator of 0.4 per cent.

Taking into account the greater cooling capacity of a freon installation, it is advisable to use a turbo-compressor set.

Russian industry does not at present produce a cooling installation of this power but, according to published data [5], a turbo-compressor set of the cooling capacity 2.5 x 10^6 kcal/hr occupies an area 7-9 m^2, and the weight of the turbo-compressor is 4-7 tons. In the conditions of power stators driven by heat engines, where powerful turbo-generators are usually installed, we may use an absorption cooling system working on the exhaust steam at a pressure of 1.5-2.5 abs atm. Assuming that the amount of heat to be dispersed is equal (as above) to 2.7 x 10^6 kcal/hr, we find that the heat consumption in the absorption cooling installation, working in the water ammonia cycle, will be 5.3 x 10^6 kcal/hr, which corresponds to a steam consumption of 10 tons/hr [6].

This steam consumption at a pressure of 2.5 abs atm is equivalent to 1060 kW of power, if the steam condenses at a pressure of 0.04 abs atm, as happens in turbine condensers; the turbine efficiency is assumed to be 0.8, the generator efficiency 0.98 and the mechanical efficiency 0.98.

It is also necessary to take into account that the power of the circulating pump is about 100 kW.

The consumption of the cooling water is estimated at 515 m^3/hr, i.e. approximately the same as the water consumption in the turbine compressor set.

From the above consideration it follows that from the point of view of power economy, the absorption cooling installation has no advantage whatsoever in comparison with a compressor installation. The absence of machine equipment may be considered a certain advantage in the absorption installation (there is only one small circulating pump of rather small dimensions). The size of the absorption cooling installation is much bigger than the size of the compressor installation.

The lowering of the hydrogen temperature may be achieved by its expansion in a turbo-exhaust pump, after a preliminary compression. Let us assume that the hydrogen pressure inside the turbo-generator is 4 abs atm and the temperature of the compressed gas at the outlet of the cooler, situated after the turbo-compressor, is 30°C. In order that the hydrogen temperature be lowered to 0°C after expansion in the turbo-exhaust pump, the gas should be compressed to 6 abs atm, if the efficiency of the turbo-exhaust pump is 0.8.

The energy required to compress 1 kg of hydrogen from 4 abs atm to 6 abs atm is equal to 0.209 kWhr. Since, for the heat dissipation of a 200 MW generator, the total amount of hydrogen required is 20 tons/hr, then the total power required for the compression of hydrogen will be 4180 kW. It is necessary to point out that part of the work, performed by the gas expanding in the turbo-exhaust pump, may be usefully employed, but the amount so recovered does not exceed 10 to 12 per cent of the work spent in compressing the gas. Thus, the power required for the cooling of hydrogen in the turbo-exhaust pump will be 3700 kW, i.e. 5 times more than the power required to drive a compressor cooling installation. Moreover, the production of such a cooling system would require additional complicated equipment: a turbo-compressor to compress the hydrogen, coolers for the compressed gas and a turbo-exhaust pump for its expansion.

From the above discussion it follows that the development and realization of liquid cooling, first of the stator winding, and then of the rotor, offers the best prospects for increasing the power of a turbo-generator while keeping its dimensions unchanged.

The forced cooling of hydrogen by cooling installations does not produce the desired effect because of the great expense of running the installation and the necessary capital investment. It may prove advantageous in particular cases, for instance, when a considerable quantity of low temperature exhaust heat is available and when this heat may be used in an absorption installation.

Translated by S. Szymanski

REFERENCES

1. E.G. Kumar; *Voprosy proektirovaniia turbogeneratov (Problems concerning the design of turbo-generators)*, Gosenergoizdat (1955).
2. G.P. Monet; *Chemical Engineering Progress*, 52, No. 7, 299 - 302 (1956).
3. Water-cooled alternator windings. Successful system developed by Metropolitan-Vickers *Elect. Engng.*, 159, No. 24, 1089-1090 (1956).
4. Itogi raboty sektsii elektricheskikh mashin Tekhnicheskogo soveta MEP za 1955g

(Summary of the works of the section of electric machines of the Technical Council of MEP in 1955), *VEP*, No. 3, 76-78 (1956).

5. L.I. Rozenfeld and A.G. Tkachev; Kholodilnye mashiny i apparaty (Cooling machines and apparatus), Gostorgizdat, 426, 177-178 (1955).
6. Kaltetechnik, 8, No. 8, 1956, Arbeitsblatt.

ON THE SURFACE RESISTANCE OF DIELECTRICS*

A.P. GEPPE

Moscow Power Institute

(Received 4 July 1957)

Although the specific surface resistance ρ_S is one of the five fundamental characteristic electrical properties of dielectrics along with ϵ, ρ_v, tan δ and E_{b1}, it is not yet however fully characterized and the term "surface conductance" is not clearly defined.

The term "surface conductance" usually means the electric conductance of the surface layer of a substance, but the thickness of this layer remains undetermined in those cases where the dielectric is covered by a film of increased conductance. Consequently, the physical meaning of the surface conductance $\gamma_S = 1/\rho_S$ is not sufficiently clear. The fundamental equation, relating the value of the surface resistance R_S to the geometrical dimensions of a specimen (the length of electrodes l and the distance between them b)

$$R_S = \rho_S \frac{b}{l} \tag{1}$$

is often applied without sufficient physical foundation. For instance, on the basis of this equation the following definition is deduced: "The surface resistivity is numerically equal to the resistance of a square (of arbitrary dimensions), imagined to be constructed on the surface of a substance when the current flows through two opposite sides of this square" [1]. The second formal deduction is the "principle of similarity"; the meaning of this principle is that with geometrically similar configurations of electrodes (b/l = const.), the quantity R_S remains constant [2].

The nature of the conducting surface is usually connected with the presence of a film of moisture on the surface of the dielectric. The influence of moisture on the surface, usually enhanced by the presence of soluble ions, has been convincingly proved by many investigators of the phenomena of surface conductance [3 - 7]. Hydrophilic substances, however, do not always function in an atmosphere of increased humidity. Moreover, high quality hygrophobic dielectrics have recently been widely used, for example fluoroplastics, organic silicon compounds, polyethylene etc. The surface electric conductance of many of these substances deserves more detailed study.

---

* *Elektrichestvo*, No.3, 60 – 65, 1958.

A very important starting-point for theoretical research and for the measurement of surface electric conductance is the exact definition of such a term as the surface current (or the current surface leakage). The existing definition which defines a surface current as the current flowing on the surface of insulation (or in the surface layer) is not clear. It is necessary, however, to keep in mind that this current is of practical importance. The necessity for its determination has posed the problem of the study of the phenomenon of surface conductance. Consequently, the notion of surface current should be completely adapted to practical requirements. In practice it is necessary to know the current between the electrodes situated on one side of the insulator surface. This current should be considered as the surface current, without restricting the domain of its flow by a layer of any definite thickness. It is necessary that this definition should also include dimensions of the electrodes, i.e. their width and length, for determination of the surface current. At present we take into account only the length. This is the consequence of the formal character of the initial assumption.

The definition of the term "surface electric conductance" may be clearly deduced on the basis of the above definition of the term "surface current". This conductivity, therefore, means the conductance of the dielectric between the electrodes situated on the same side of its surface. In investigating the flow of the current between such electrodes we must distinguish two strictly different cases: the first, when electric conductances of the superficial and internal layers of the substances are equal, and the second, characterized by the presence on the surface of the dielectric of a layer with considerably increased conductance in comparison with the conductance of the internal region.

Let us consider the first case and deduce the equation for the calculation of the value of the surface resistance R_S when a current is flowing between the flat electrodes A and B, of length l and width a, placed on the surface of the dielectric at a distance B apart (Fig. 1).

We assume that the volume resistance ρ_v has the same value on the surface layers and inside the dielectric.

Calculation can be carried out by an approximate method, assuming, for simplicity, that the boundary lines of the current tubes are semicircles.

In the absence of a strongly conducting layer on the surface, the resistance between the electrodes (surface resistance R_S) will be determined by the geometrical dimensions of the current tube (dimensions a, b and l), and by the value of $\rho_v = 1/\gamma_v$ of the dielectric.

The electric conductance dG of the elemental area $kstu$ will be:

$$dG = \frac{dF}{\rho_v d},$$

where $dF = l dr;$

$$d = r d\varphi.$$

The conductance of the portion *pqnm*,

$$G=\int dG=\int_{b/2}^{a+b/2}\frac{l\,dr}{\rho_v r\,d\varphi}=\frac{l}{\rho_v r\,d\varphi}\ln\frac{2a+b}{b},$$

and its resistance

$$dR=\frac{1}{G}=\frac{\rho_v}{l\ln\dfrac{2a+b}{b}}\,d\varphi.$$

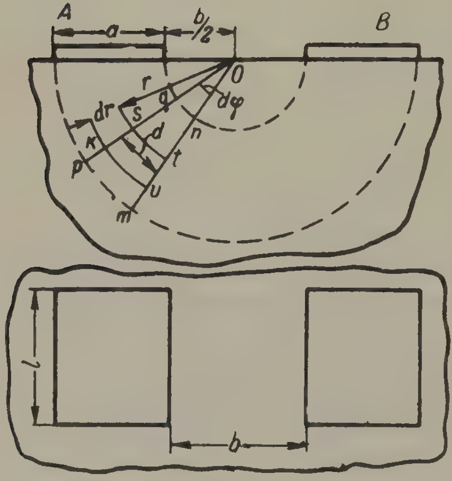

FIG. 1. Diagram for calculation of the surface resistance of a dielectric without surface film of increased conductance.

Now we can easily find the resistance encountered by the current between the electrodes *A* and *B* (i.e. R_S)

$$R_S=\int dR=\int_0^{\pi}\frac{\rho_v}{l\cdot\ln\dfrac{2a+b}{b}}\,d\varphi,$$

or

$$R_S=\frac{\pi\rho_v}{l\ln\dfrac{2a+b}{b}}\,. \tag{2}$$

The comparison of equation (2) with equation (1), which at present is normally used, shows that only the electrode length *l* has the same influence in both cases on the value of R_S.

The dependence of R_S on the distance between the electrodes *b*, in equation (2), is, however, of a more complex nature than in equation (1). It should be particularly pointed out that in equation (2), as opposed to equation (1), the dependence of the electrode width *a* on R_S is taken into account.

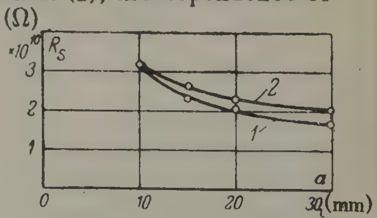

FIG. 2. Dependence of the surface resistance R_S on the electrode width *a*, for $b = 5$ mm and $l = 80$ mm; (1) experimental curve obtained by testing a specimen of getinax 10.4 mm thick, at 55 per cent relative humidity, (2) calculated (from equation (2)).

The resistance R_S according to equation (2) does not increase linearly with the distance between the electrodes as it does in equation (1), but increases considerably less rapidly. Calculations show that, for instance, by increasing *b* from 1 to 20 mm, the value of R_S, according to equation (1), increases 20 times, and according to equation (2) only 3.3 times (the width of the electrodes *a* is taken as 20 mm) since its value enters into equation (2). Experimental investigations of specimens of genitax and textolite, performed with electrodes 80 mm long and 20 mm wide, show that, by increasing the inter-electrode distance *b* within the stated limits (from 1 to 20 mm), the resistance R_S in various experiments increased 1.75 - 4.25 times.

The experimental verification of the dependence of R_s on the electrode width shows a sufficiently close agreement between the experimental results and the values calculated by equation (2) (See Fig. 2).

Thus, despite certain simplifications, assumed in the deduction of equation (2), this equation correctly accounts for the influence of the geometric dimensions of the electrode and the distance between them on the value of the surface resistance of the dielectric, in the absence of the film of increased conductance on the surface. The current between electrodes situated on one side of the surface in this case flows through the bulk of the substance, and not only in a thin surface layer. The density of the current will be greater in the upper layers of the substance. In a sufficiently thick specimen, currents flowing in internal regions may be so small that we can neglect them. In consequence, we may consider the depth of penetration of the current into the specimen when the current flows between the electrodes situated at the surface. Experiments have shown that this depth is of the order of a few mm.

Calculating the value of R_s by equation (2), and afterwards finding the value of ρ_s by formula (1), we get

$$\rho_S = \frac{\pi}{b \ln \frac{2a+b}{b}} \rho_v \quad \text{or} \quad \rho_S = k\rho_v .$$

Hence, it follows that ρ_s is not a specific constant of a given substance (since the factor k depends on dimensions a and b), but this contradicts equation (1). Moreover, taking $a = 10$ mm and $b = 2$ mm, these being the usual dimensions of ordinary electrodes, we have $k = 6.55$ cm^{-1}. For other values of a and b found in practice, the factor k will be within the limits 1 - 10 cm^{-1}. Hence, we may conclude that, in the absence on the surface of the dielectric of a conductive film, the value of ρ_s determined by the above method should be expressed by a number of the same order as the value of ρ_v(for instance, for various types of getinax, $\rho_v = 10^{11} - 10^{12}$ ohm.cm, $\rho_s = 10^{11} - 10^{12}$ ohm., etc.).

In fact, it is well known that many hydrophilic dielectrics in a comparatively low relative humidity (60 - 70 per cent), and hydrophobic dielectrics in a high relative humidity have the values of ρ_v and ρ_s expressed by approximately the same number, although given in different units; consequently this coincidence of numerical values is not accidental, but caused by the flow of the surface current through the internal region of the substance.

For the above case, the surface resistance R_s is determined, not only by the geometric dimensions, but also by the value ρ_s of the substance. The influence of these factors is quite satisfactorily accounted for by equation (2). The investigation described above leads to the conclusion that formula (1) is not valid for this case; and its modification for widely used round electrodes is also invalid. In the absence from the surface of the insulation of the film with the increased conductance (or when the thickness of the film is very small), such a characteristic of the substance as ρ_s proves to be superfluous.

Although the surface conductance of dielectrics in presence of the layer with the increased conductance has been investigated very thoroughly, nevertheless it is desirable to consider some aspects of this phenomenon. Fig. 3 shows a diagrammatic cross-section of a portion of a dielectric, on the surface of which is a film with a thickness of δ; the volume conductance γ_{vf} is much greater than the conductance of the internal regions of the substance ($\gamma_{vf} >> \gamma_v$).

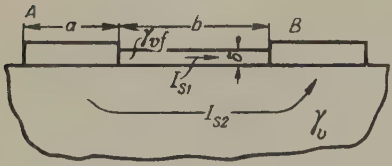

FIG. 3. Diagram for determining the value of the surface resistance R_S of a dielectric in the presence on its surface of the film of increased conductance.

Let us determine for this case the value of the surface resistance R_S, when a current flows between the flat electrodes A and B of length l and width a, situated at a distance b apart. The current between the electrodes, which is a surface current, can be considered as a sum of the currents, one flowing in the surface layer and the other inside the dielectric $I_s = I_{s1} + I_{s2}$. In this case, for a film of a sufficient thickness, δ $I_{s1} >> I_{s2}$, so we may assume that $I_s = I_{s1}$. Then $R_s = R_f$, (R_f is the resistance of the film). Obviously, $R_f = \rho_{vf} b/F$, where $\rho_{vf} = 1/\gamma_{vf}$, and $F = l\delta$ (the area of transverse section of the film).

Hence

$$R_S = \frac{\rho_{vf}}{\delta} \frac{b}{l}. \tag{3}$$

If the thickness of the film is uniform, the ratio ρ_{vf}/δ is a constant.

If we denote this ratio

$$\rho_S = \rho_{vf}/\delta (\Omega) \tag{4}$$

then equation (3) transforms into equation (1). Thus, the realm of applicability of equation (1) is made clear. Using this equation we may determine the surface resistance; but this is possible only when on the surface of the dielectric there is a film of increased conductance γ_{vf}, and of a sufficient thickness δ, i.e. when we may neglect the current I_{s2}. Such conditions occur in the case of hydrophilic dielectrics in an atmosphere of increased humidity, when the thickness of the humid layer on the surface sharply increases. The presence of the soluble ions in the substance, of various gases in the surrounding air and of surface impurities, giving soluble ions, decreases the value of R_s still more, since the volume resistance of the film γ_{vf} decreases.

For the case in question, the physical meaning of the surface conductance $\gamma_S = 1/\rho_S$ becomes clear. From equation (4) it follows that $\gamma_S = \delta/\rho_{vf}$, or

$$\gamma_S = \delta \cdot \gamma_{vf}. \tag{5}$$

The volume electric conductance of the film

$$\gamma_{vf} = nKq, \tag{6}$$

where n is the number of ions in 1 cm³, q the ion electric charge, K the ion mobility. Equation (6) is given for the case when the film contains ions of the same polarity and mobility. After substitution of (6), equation (5) becomes

$$\gamma_S = \delta \cdot n\ K \cdot q. \tag{5a}$$

The product $\delta . n = n_{\text{sur}}$ represents the number of ions in a portion of the surface layer with an area of 1 cm² (ion surface density). Taking this into consideration, we obtain the expression for γ_S in its final form:

$$\gamma_S = n_{\text{sur}} \cdot K \cdot q. \tag{7}$$

If the film thickness δ is comparatively small (for instance in the presence of slightly though not excessively increased air humidity), we cannot neglect the current I_{S2}. In determining the surface conductance G_S it is necessary to consider the conductance of the upper layer $G_1 = 1/(\rho_S b/l)$, on which the current I_{S1} depends, and the conductance of the internal region of substance $G_2 = \dfrac{1}{\dfrac{\pi \rho_v}{l \cdot \ln \dfrac{2a+b}{b}}}$, which determine the value of the current I_{S2}:

$$G_S = G_1 + G_2 = l\left(\frac{1}{\rho_S b} + \frac{\ln \frac{2a+b}{b}}{\pi \rho_v}\right).$$

For the case in question, the surface resistance is

$$R_S = \frac{1}{G_S}$$

or

$$R_S = \frac{1}{l\left(\dfrac{1}{\rho_S b} + \dfrac{\ln \frac{2a+b}{b}}{\pi \rho_v}\right)} \tag{8}$$

Equation (8), for the determination of R_S, is of a more general character, and equations (1) and (2) are its particular cases.

The surface resistance of substances with an open porous surface will decrease very sharply in an atmosphere of high humidity, since in this case the volume resistance ρ_v considerably decreases. As follows from the previous discussion, the surface resistance is determined by the value of ρ_S only in the presence on the surface of the substance of a film of increased conductance. Moreover, if the thickness of the film is small, then R_S, according to equation (8), also depends on the value of ρ_v of the substance. As has already been stated, for a very thin film or in the absence of a film, we do not need to know the property ρ_S at all. In cases when it is important to a certain extent, it is necessary to bear in mind, that the value of ρ_S depends on properties of the surface film. Certainly, the film thickness δ and its volume resistivity ρ_{vf} depend to a considerable degree on the properties of the dielectric, but we also have to reckon with the possible influence of various objective factors. All this leads to the conclusion that the existing cautious opinion about the factor ρ_s, as a characteristic of insulating materials is sufficiently justified.

Since the surface resistance of dielectrics is important in practice, we can find its value not from the value of ρ_s, but by measuring the surface resistance of specimens of dielectrics by using round electrodes of strictly specified dimensions, thus ensuring the attainment of comparable results.

The methods of determining R_s (ρ_s), recommended by standards GOST 6433-52, are basically incorrect and therefore subject to criticism.

The tendency to measure not the total current, flowing between the electrodes A and B situated on the surface (Fig. 4), but only the part of it I_{s1} which flows in the surface layer of the specimen, and which is considered by GOST authors as the surface current, has resulted in a natural tendency to lead away the current I_{s2} so that it is not recorded by a galvanometer G. For this purpose, an electrode C is fixed to the lower surface of the specimen and the earthing of this should ensure the desired result. At a first glance everything seems to be correct: first, the galvanometer measures only the current required; secondly, such an arrangement of electrodes permits the use of the same specimen for the determination of ρ_v and ρ_s, this being convenient.

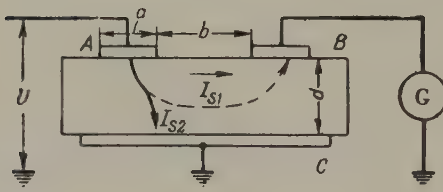

FIG. 4. Diagrammatic lay-out of electrodes for determination of the surface resistance by the standard method.

In fact, however, the presence of the electrode C and still more the fact that it is earthed are not only undesirable, but often quite inadmissible. If we accept the definition of the surface current which is recommended in this article, then the uselessness of the electrode C becomes obvious. Still more, this electrode cannot perform its function in the actual method of measurement of the surface current. In fact, why should the electrode C lead away the total so-called "volume current" I_{s2}? It is quite clear that for the same substance the value of the current I_{s1} will vary with the specimen thickness *d*, other things being equal (equal voltages *U* and dimensions *a* and *b*). For sufficiently thick specimens (8-10 mm and more) and for the recommended standard distance between the electrodes $b = 2$ mm, a very considerable part of the "volume current" will nevertheless flow towards the electrode B. Thus, both the thickness of the layer, in which the current flows between electrodes A and B, and the current I_{s1} itself are determined, and this corresponds to the vagueness of the existing definition of the term "surface current".

When a film of considerably increased conductance is present on the surface of the dielectric, the electrode C will be superfluous, since in this case we can neglect the current I_{s2} in comparison with I_{s1}.

The experimental determination of R_s for thin fabrics should be particularly considered (i.e. for lacquered fabrics and substances in the form of a thin film).

In this case $b >> d$, and this is very important as the electrode B is far away from the electrode A, while the electrode C is very close to the electrode A along the whole length of the latter.

Taking into account that the potentials of B and C, the latter being earthed, are almost equal ($\phi_B = \phi_C = 0$), it becomes clear that the electrode C entirely screens the electrode B, which finds itself practically outside the electric field. When a voltage is applied to the specimen, the total current from the electrode A in fact flows towards the electrode C, by-passing the electrode B. As a result, the use of the standard method creates the false impression that thin insulation fabric has a very high surface resistance. For instance, in tests on specimens of various cotton lacquered fabrics, carried out according to the above method, no surface current could be detected even when these specimens were heated up to 120°.

Yet the test on the same specimens carried out without the electrode C resulted in the measurement of R_s even at room temperature; and this resistance was far from infinity (10^{10} - 10^{11} Ω), decreasing at 120° approximately to 10^8 Ω.

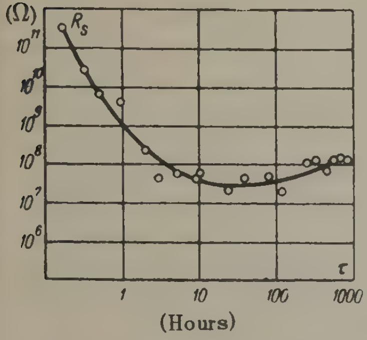

FIG. 5. Relationship between the surface resistance R_s of the lacquered fabric LKh - 2, 0.17 mm thick, and the time of keeping specimens in water. Tests carried out by the standard method.

A paradoxical result also was obtained in finding the relationship between the surface resistance of the lacquered fabric LK_h - 2 0.17 mm thick, and the time of keeping the specimens in water, when carrying out this experiment by the standard method. The graph of this dependence (see Fig. 5) shows that at the beginning the resistance R_s sharply decreases and after passing through a minimum, increases slowly, a result which is entirely unexpected.

This behaviour is also due to the experimental method. The sharp decrease in R_s for the initial stages when the specimens were kept in water is caused by the moistening of the substance. Further, the difference in conductance of outer and inner layers begins to decrease, and this is due to the penetration of moisture inside the specimen, this penetration being helped by the tissue structure of the material. In consequence, the current flowing towards the electrode C sharply increases, and the screening action of this electrode becomes effective. This, in turn, brings about the decrease of the current I_{s1}, and the apparent increase of the value of R_s.

Hence it is advisable to carry out the measurement of the surface resistance without the lower electrode C, because only in this case is it possible in fact to measure the current between the electrodes situated on the same side of the specimen surface, i.e. the surface current. The specimen under test should be placed on an insulated base avoiding any metal supports, even non-earthed, when the current between the electrodes A and B (Fig. 4) will flow not directly but by a path A C B.

Translated by S. Szymanski

REFERENCES

1. N.P. Bogoroditskii; V.V. Pasynkov and B.M. Tareev; *Elektrotekhnicheskie materialy (Electrotechnical materials)* Gosenergoizdat (1955).
2. B.M. Tareev; Osnovy fiziki dielektrikov (Principles of the physics of dielectrics), *Izd. Vses.Zauch. energ. inst.* (1954).
3. P.A. Florenskii; Dielektriki i ikh tekhnicheskoe primenenie (Dielectrics and their technical applications), *Red.-izd. otd. Glovelektro Vys. Sov. narod. khoz.* (1924).
4. N.N. Semenov and N.M. Chirkov; O poverkhnostnoi elektroprovodnosti dielektrikov (On the surface conductance of dielectrics), *Dokl. Akad. Nauk SSSR*, 51, No.1 (1946).
5. N.P. Bogoroditskii and I.D. Fridberg; *Vysokochastotnye neorganicheskie dielektriki (High frequency inorganic dielectrics)*, Izd. "Sovetskoe radio" (1948).
6. M.M. Mikhailov; *Elektromaterialovedenie (Electrical materials reference book)* Gosenergoizdat (1953).
7. Le Clerc; Variation with time of the surface electrical conductivity of glasses in a conditioned atmosphere, *Silicates industr.*, 19, No. 6/7 (1954).

THE DEPENDENCE OF FREQUENCY OF THE ROCHELLE SALT PIEZOELECTRIC VIBRATORS ON TEMPERATURE*

K.F. GUBA

Lvov Institute of Forest Technology

(Received 30 October 1957)

We have investigated twelve orientations of the Rochelle salt piezo-plates with respect to X, Y, Z co-ordinate axes; nine orientations were investigated on metallized plates, and three orientations were tested under the influence of electric field, with metallized as well as non-metallized plate surfaces.

The experimental investigation of the dependence of the frequency of vibrations of a piezoelectric plate on temperature at different orientations led to the exact determination of temperature frequency coefficients of different cuts, and this is of practical industrial importance.

Fig. 1 shows temperature-frequency characteristics of the Rochelle salt piezoelectric vibrators with the basic surface perpendicular to the X-axis. The curves are: (1) for a metallized vibrator of length $l = 2.073$ cm, width $b = 0.253$ cm and thickness $d = 0.08$, its long side being inclined to the Y-axes at an angle $\theta = 22° 30'$; (2) for a metallized vibrator of dimensions $l = 1.60$ cm, $b = 0.20$ cm, $d = 0.09$ cm and $\theta = 45°$; (3) for metallized vibrator of dimensions $l = 2.17$ cm, $b = 0.194$ cm, $d = 0.071$ cm, and $\theta = 67° 30'$; (4) for non-metallized vibrator of dimensions $l = 2.59$ cm, $b = 0.449$ cm, and $d = 0.11$ cm its long side being parallel to the Z-axis; (5) this vibrator differs from 4 only in that it is non-metallized.

Plates characterized by curves 1-3 are excited by a longitudinal force, therefore their frequency is determined by their longitudinal dimensions (length). [1]. The frequency of the plate, characterized by curves 4 and 5 (Fig. 1) is determined by its linear dimensions along the crystallographic "b"-axis of a Rochelle salt monocrystal [2].

Curves 1-3 (Fig. 2) correspond to the three metallized vibrators with their basic surface perpendicular to the Y-axis; the vibrators are inclined to the X-axis at angles $\theta = 22° 30'$, $45°$ and $67° 30'$.

---

* *Electrichestvo*, No. 3, 71-72, 1958.

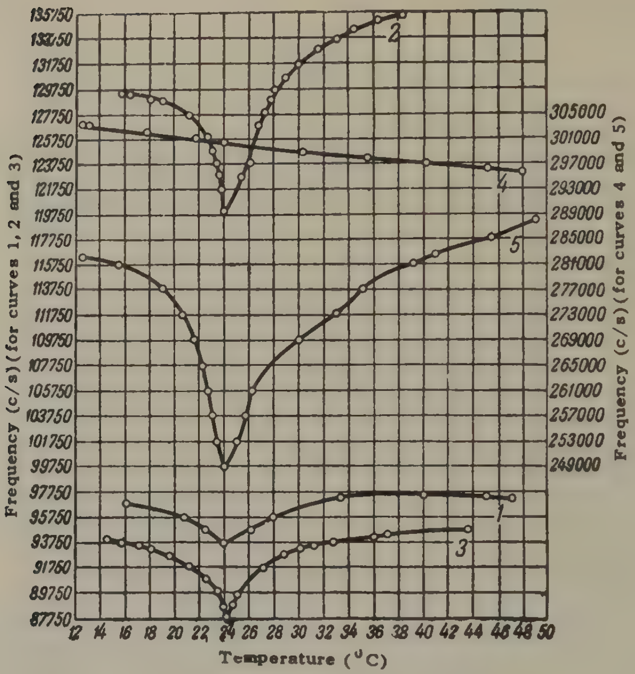

FIG. 1.

Linear dimensions of the specimens are respectively equal to:
length, 2.795, 2.266 and 2.655 cm; width, 0.21, 0.235 and 0.24 cm; thickness, 0.096, 0.091 and 0.09 cm. The frequency of plates characterized by curves 1-3 is a function of their length. Curves 4 and 5 (Fig. 2) are temperature-frequency characteristics of the same vibrator; non-metallized (curve 5) with its basic surface perpendicular to the Y-axis. The linear dimensions of the specimen are $l = 2.51$ cm, $b = 0.46$ cm, $d = 0.345$ cm. The length of the plate is parallel to the Z-axis. The frequency of the plate, characterized by curves 4 and 5 (Fig. 2), is a function of its dimensions along the crystallographic "a" axis of a Rochelle salt monocrystal.

Curves 1-3 (Fig. 3) show the influence of temperature on the frequency of vibrations of the three Rochelle salt piezoelectric vibrators, cut with their lengths at angles $\theta = 22° 30'$, 45° and $67° 30'$, respectively, to the X-axis; the basic surface of plates is perpendicular to the Z-axis. The linear dimensions of specimens are respectively: length, 2.469, 2,512 and 3.13 cm; width, 0.282, 0.328 and 0.348 cm; thickness, 0.082, 0.131 and 0.158 cm. The frequency of vibrations is a function of the plate length.

The last result (curves 4 and 5, Fig. 3) is related to investigations of the frequency of the same Rochelle salt plate in the absence of metallization (curve

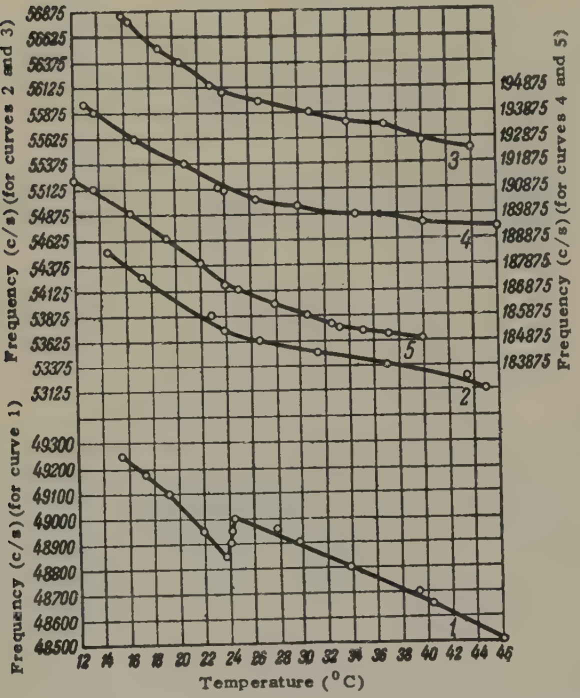
Frequency (c/s) (for curves 2 and 3)
56875
56625
56375
56125
55875
55625
55375
55125
54875
54625
54375
54125
53875
53625
53375
53125
Frequency (c/s) (for curve 1)
49300
49200
49100
49000
48900
48800
48700
48600
48500
Frequency (c/s) (for curves 4 and 5)
194875
193875
192875
191875
190875
189875
188875
187875
186875
185875
184875
183875
1
2
3
4
5
12 14 16 18 20 22 24 26 28 30 32 34 36 38 40 42 44 46
Temperature (°C)

FIG. 2.

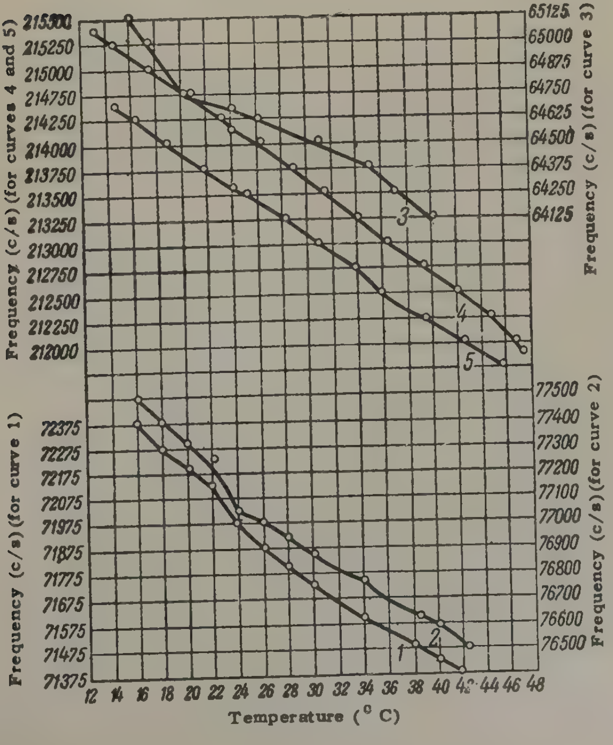
Frequency (c/s) (for curves 4 and 5)
215500
215250
215000
214750
214250
214000
213750
213500
213250
213000
212750
212500
212250
212000
Frequency (c/s) (for curve 3)
65125
65000
64875
64750
64625
64500
64375
64250
64125
Frequency (c/s) (for curve 1)
72375
72275
72175
72075
71975
71875
71775
71675
71575
71475
71375
Frequency (c/s) (for curve 2)
77500
77400
77300
77200
77100
77000
76900
76800
76700
76600
76500
1
2
3
4
5
12 14 16 18 20 22 24 26 28 30 32 34 36 38 40 42 44 46 48
Temperature (°C)

FIG. 3.

4) and in the presence of metallizations, (curve 5). The length of the specimen is parallel to the X-axis and its basic surface is perpendicular to the Z-axis. The dimensions of the plate are: $l = 4.13$ cm, $b = 0.569$ cm, $d = 0.17$ cm. The frequency of the plate is determined by its dimensions along the crystallographic "b"-axis of a Rochelle salt monocrystal.

In recording the temperature frequency characteristics, the crystal temperature was varied at the rate of 0.1° C in 5-10 min. In the vicinity of the Curie-point the rate of variation did not exceed 0.05° C in 10-12 min [3].

Translated by S. Szymanski

REFERENCES

1. W.P. Mason; *Phys. Rev.*, 55, 775 (1939).
2. G.P. Mikhailov; *Zh. tekh. fiz.* VI, 7 (1936).
3. K.F. Guba; K voprosu opredelenia dielektricheskoi pronitsaemosti p'ezokristalla segnetovoi soli (Problem of determination of the permittivity of a Rochelle salt piezocrystal). *Tr. Vses. zaoch. lesotekhnicheskogo inst.* II Leningrad, (1956).

THE USE OF ELECTRIC LOCOMOTIVES WITH RECTIFIERS – A REVIEW *

A.M. KAKHELNIK

(Received 15 October 1957)

The beginning of the use of electric traction may be ascribed to the year 1837, when the Russian Academy of Science considered a scheme of the Russian scientist B.S. Iakobi, "The application of electric power for ship propulsion," It is known that in 1838-39 an electrically propelled ship navigated on the Neva river with 14 passengers on board. F.A. Pirotskii, in September 1880, after some preliminary experiments, set in motion the first electric carriage in the world with 40 passengers. Later, with a centralized production of electrical energy, electric traction using a d.c. current found wide application in many countries.

With the development of the electric d.c. traction and of public electric grids the idea of using a.c. current for the railway traction arose.

The first attempts abroad to use a.c. current for electric traction relate to the last decade of the nineteenth century, when Werner Siemens in 1892 tried to use three-phase a.c. current for this purpose; in 1895 a Swiss firm Brown-Boveri opened the first electric railway (of the urban type) in Lugano using three-phase current.

In 1899 the main-line electric a.c. locomotive – the first in Europe – was built for the Burgdorf – Thun line (Switzerland). It was fed by a three-phase current of the frequency 40 c/s. Simultaneously with this, electric traction of lower frequency was developed: in Europe at 15 and 16 2/3 c/s, in the U.S.A. at 25 c/s. This is a short and very incomplete summary of the development of a.c. electric traction; this period preceded the appearance of an electric locomotive with devices for converting a.c. energy into d.c. energy. Such a conversion may be realized either by means of a rotary convertor (motor-generator), or by using a static converter. By this method we may have both the advantages of an a.c. supply system and the good traction qualities of a d.c. motor.

In 1904 in Switzerland on the Seebach-Vettingen section the Oerlikon firm was the first in the world to attempt to use a single-phase current of normal frequency 50 c/s, by converting it, on the electric locomotive, by means of a synchronous motor-generator.

---

* *Elektrichestvo*, No. 3, 73-76, 1958.

This 400 h.p. locomotive, type Bo - Bo, underwent successful tests on the above mentioned section. But further development of this construction was abandoned since the electric machine industry at that time was unable to produce an electric locomotive, with a rotary a.c.-d.c. convertor, within reasonable weight limits. Later, with the improvement of production methods and with the weight reduction of the motor-generator set, electric locomotives of this type were used.

In the search for reducing the convertor weight, attention was drawn to the mercury rectifier.

First experiments in the use of a static convertor were carried out by the Westinghouse firm, which in 1914 built a motor coach, with a multi-anode exhaust-type mercury rectifier, for the New-Kanaon branch of the New York - New Haven railway. These tests proved unsuccessful, since at that time technical ability was insufficient to produce rectifier tanks with sufficiently strong and tight seams to withstand travel shocks. Moreover, this system caused disturbances in the telephone network. This carriage was withdrawn after a 35,000 km run.

Tests which were carried out by the same firm with mercury rectifiers with welded tanks did not give more successful results because of the lack of effective protection of the tanks from vibrations.

Thus, more than 20 years elapsed from the first attempts to use a.c. for railway traction up to the first application of a static a.c. - d.c. convertor on the locomotive itself.

It is necessary to add that besides the single-phase a.c. - d.c. system, other systems were investigated such as: a three-phase single-phase, electric locomotives with single-phase commutator motors and others.

After unsuccessful attempts in 1914, the problem of using mercury rectifiers on electric locomotives did not arise until 1925, when Reichel (Germany) presented the plan of such a locomotive. This plan was never realized since it was based on the three-phase method of feeding, and such a system offered no advantage.

The progress in making welded seams in metallic tanks and the experience accumulated in production and exploitation of mercury rectifiers in the traction substations brought about the renewal, by the Brown-Boveri firm in 1930, of work on the application of mercury rectifiers for the system of traction using a single-phase a.c.

For this purpose an old electric locomotive type 1-C_0-1 of the Simplon line was provided with a multi-anode rectifier, capable of working on frequencies from 15 to 60 c/s.

In the same year, 1930, Siemens-Schuckert built a contact-accumulator electric locomotive, which was fed from a single-phase grid at 15 kV, 16 2/3 c/s through two glass mercury rectifiers. This locomotive was destined for repair, for inspection of the grid and for shuntling work.

In 1932 Reichel renewed his proposal, but this time he suggested single-phase a.c. feeding with control-grid rectifiers. However, this system with a low frequency (16 2/3 c/s) does not offer any particular advantages in comparison with electric locomotives, equiped with single-phase commutator traction motors.

In June 1932, the first All-Union Conference on railway electrification decided to press for work concerning the practical use of electric traction, based on a single-phase normal frequency current.

In this year "Elektrosila" ("Electric power") factory mastered the production of mercury rectifiers with control grids. As a further step, such a rectifier was used for the equipment of an electric locomotive, built by the "Dinamo" factory; it was fed by the single-phase industrial frequency current.

In 1933 the Directorate of the German railways decided to begin trials on traction using a single-phase, 50 c/s, 20 kV current; the trials were to be carried out on the Hollentall line in Schwarzwald. Work on the project for electrification of this line started in 1930, but the initial intention was to use a current of 16 2/3 c/s frequency.

In 1936, of the four electric locomotives which were put in service on this line for trial, two locomotives were fitted with the multi-anode exhaust type mercury rectifiers, with water cooling. Locomotive E 244.01 was built by the A.E.G. Co., and locomotive E 24411 by Brown-Boveri.

Simultaneously with this, in the U.S.S.R., both research and design were carried out with a view to building a similar electric locomotive. In September 1938 the Kirov "Dinamo" works jointly with the V.V. Kuibyshev locomotive factory at Kolomna, built the first Soviet electric locomotive mark OR-22-01, for the single-phase a.c.-d.c., fitted with the 12-anode mercury rectifier model RV-20, which is used on traction substations.

During the period between the two World Wars, electric high-power grids were developed on a large scale, and feeding of a railway single-phase grid from a three-phase grid was made much easier. In 1942 the construction of the ignitron rectifiers was greatly improved; these improvements greatly contributed to the wide use of ignitrons in the metallurgy of non-ferrous metals during the Second World War, particularly in aluminium and magnesium production. These two circumstances gave a new impetus to the development of the single-phase-d.c. system of electric traction with the use of static convertors.

The results of trials, carried out on the Hollental line, which after the War was placed under French occupation, drew the attention of French Railways. A few weeks after the occupation of Germany the Society appointed a commission to carry out tests on this line. The conclusions of the commission led to electrification in 1950 of the 78 km line Aix-les-Bains — La-Roche-sur-Fauron in Savoy

(France), in view of the final investigation of problems, arising with the single-phase 50 c/s system.

Positive results of the experiment with exploitation of this line led to the large-scale electrification of the north-eastern French Railways region, which carries much goods traffic; a single-phase current of line frequency is used throughout.

In 1948, in the U.S.A., trials were undertaken: first on a stand, and later on an experimental el-motor coach built by the Westinghouse Company, with a mercury rectifier. This carriage started its running tests on 15 July 1949, and after completing 4000 km was assigned for the normal service on the Pennsylvania railway (25 c/s). The results of this trial led to the conclusion that rolling stock of the single-phase d.c. system with mercury rectifiers had passed the stage of laboratory tests.

The outcome of these experiments was the order of the New York-New Haven railway of the Westinghouse Co. for 100 such el-motor coaches.

On the trial section of French Railways in Savoy a motor coach, mark Z-9055, with the single-anode ignitron rectifiers of American construction was tested; these rectifiers were made in France on licence. In July 1955, the Alstom firm delivered for this line an electric locomotive mark VV-8051 with mercury rectifiers of the same type.

In November 1957 the first of the two electric locomotives with rectifiers built for the Pennsylvania railway was delivered for use. In 1957 the A.E.G. Co. equipped electric locomotives, fed by 50 c/s. a.c., with a bridge circuit system; and the Brown-Boveri Co. performed an experiment for the first time with two single-anode air-cooled rectifiers, installed on the locomotive E-244.11 of the Hollental line.

At the beginning of 1952, two double-section electric locomotives, built by the Westinghouse Co., were delivered for the Pennsylvania railway; they were fitted with ignitron rectifiers 2/VVV/ and 2/SS/, their power was 6000 h.p.

In December 1952, on the Lancaster-Morecambe-Heysham line, a motor-coach, with a mercury rectifier fed by a single-phase, 50 c/s current at 6.6 kV, was sent on experimental runs. A regular passenger service began in August 1953. For this purpose three three-coach sets were equipped with a d.c. installation fed through mercury rectifiers.

In 1953, the Administration of Peat Transport of the Shatur Administration of the Ministry of Electric Stations in the U.S.S.R. electrified the ten-kilometer Baksheevo-Lidino section, and at the end of 1956 the length of the electrified line run by the Shatur Administration was more than 20 km. For this line an electric locomotive, with a six-anode, controlled, non-exhaust mercury rectifier mark P-KO-1 was built by the S.M. Budennyi electric locomotive factory in Novocherkassk; this locomotive was fed by a single-phase, 50 c/s current at 6 kV. This locomotive is still in service at the present time.

On 1 April 1954 a ten-motor-coach train with mercury rectifiers was delivered for the New York-New Haven line. It was equipped by the Westinghouse Co. and worked on a multi-unit system. In 1955 this line received a hundred more coaches.

In December 1954 the delivery of ten high-speed electric passenger locomotives, of rectifier power 4000 h.p., began for this railway; delivery by the General Electric Co. was finished in March 1955. These motor-coaches and locomotives work equally well on the 25 c/s a.c. or on d.c. at 650 V. In 1954, in the U.S.S.R., the Novocherkask electric locomotive factory built two electric locomotives of the NO series, which were equipped with the ignitron single-anode rectifiers. These rectifiers were designed and constructed by the All-Union V.I. Lenin Institute of Electric Technology and were tested on the experimental ring of the All-Union Railways Scientific and Research Institute. These locomotives are fed by a single-phase 50 c/s a.c. and have the same power as the Soviet main line d.c. locomotives VL 22m.

In June 1955 the Virginia Railway ordered 12 electric locomotives of the type supplied by the General Electric Co. for the New York-New Haven line. These locomotives will replace the 36 old electric locomotives with asynchronous motors, since these locomotives are already 30 years old.

It is necessary to point out that an ionic convertor usually works as a rectifier, converting a.c. into d.c. At present, the work of an ionic convertor acting as an inverter i.e. as a device for converting the a.c. energy into the d.c. energy, is explained theoretically and verified in practice. This opens up the possibility of the use in practice of the regenerative braking of electric locomotives with mercury rectifiers. In this case an appreciable amount of energy is returned to the grid and the specific consumption of energy decreased.

At the beginning of 1955 only one out of the 17 electric locomotives, which were ordered from the Brown-Boveri Co. for open-cast brown coal mines in the Rhineland, was to be fitted with a mercury rectifier with regeneration; at the end of 1955, locomotives for the same purpose were in production, and these were equipped with pumpless air-cooled valves, capable of regenerating the energy.

M. Tessier, in his lecture delivered at the conference in Lille (France) on problems of electric single-phase traction at line frequency, stated that nearly half the rolling stock of the north-eastern French Railways will consist of electric locomotives with mercury rectifiers.

In October 1955 tests began on the Japanese State railways, on two electric locomotives of type Bo-Bo, of the ED 451 series, with mercury rectifiers to be fed from the 20 kV, 50 c/s grid.

On 1 December 1955, for the first time in the world, a motor-coach with a semiconductor germanium 750 kW rectifier was put into service on the Lancaster-Heysham line. The rectifier was made by the British Thomson-Houston Co.; it is of the two half-period system and is air-cooled.

In the U.S.S.R. from the beginning of 1956 electric locomotives of the NO series, produced by the locomotive factory in Novocherkassk, have been in service on the Ozherel'e-Mikhailov section, and since the end of 1956 they have been used on the Ozherel'e-Mikhailov-Pavelets section of the Moscow-Kursk-Donbas railway.

In 1956, the British Transport Commission recommended, for the electrification of British railways, a single-phase line frequency current at 25 kV, and decided to accept in principle electric locomotives with rectifiers.

The good characteristics of the locomotives fitted with rectifiers, their ability to cope with different traction conditions, as well as experience in service with electric locomotives of other systems led to the decision of French National Railways to suspend completely orders for locomotives with motor-generator sets or with single-phase commutator traction motors. The table given below clearly proves the accuracy of this statement and gives a picture of trends in the distribution of orders for the north-eastern French railways.

For the Lisbon-Oporto line of the Portugese railways, which was electrified at the end of 1956 on an industrial frequency a.c., 15 ignitron electric locomotives Bo-Bo were ordered together with other items of rolling stock.

Year of order	Number of electric locomotives			
	Motor generator type with electric traction motors		With a.c. commutator traction motors	With rectifiers feeding d.c. series traction motors
	on d.c.	on three-phase a.c.		
1952	20	65	15	5
1954	—	37	9	9
1955, first half	—	—	29	38
1955, second half	—	—	—	75
1956	—	—	—	130

As early as 1932 in Hungary, the Budapest-Hodieshalom section was electrified on a single-phase line frequency current; electric locomotives of the Kando system were used on this line. But, because of defects which were recorded during service, construction of these locomotives was abandoned.

Taking into account progress achieved during recent years, the Hungarian State Railways intend in future to buy single-phase locomotives, fitted with rectifiers and d.c. motors.

On 27 May 1957 in Munich a six-axle shunting electric locomotive came into service; on this locomotive, instead of two mercury rectifiers, a silicon semiconductor rectifier made by the Siemens-Schuckert Co. was fitted. With air-cooling and a continuous power $P_{\infty} = 800$ kW, this rectifier is remarkable for its small dimensions. It is necessary to point out the advantages which silicon rectifiers offer in electric traction, because of their greater reliability in service, under difficult temperature conditions, in comparison with germanium rectifiers.

At present British Railways have ordered 35 complete germanium semiconductor rectifiers from the British Thomson-Houston Co. for some sections of the Manchester-Crewe line.

On 1 October 1957 in Japan an electric locomotive with rectifiers of the series ED 70 at 20 kV, 60 c/s came into service.

At the end of 1957 in the U.S.S.R. the first model of the main-line series electric locomotives was delivered; it works on a single-phase line frequency current and is fitted with ignitron rectifiers, series N 60. This locomotive with an axle formula Ho - Ho, a power 4000 kW and with six-pole traction motors is one of the best locomotives of this type in the world.

Thus we may draw the conclusion that during recent years electric locomotives, fed by a.c. and fitted with static rectifiers, are more widely used than other types. This is due to great improvements, which were made in the production of rectifiers during the last 15-20 years, and also to the good traction qualities of electric locomotives fitted with rectifiers.

Translated by S. Szymanski

REFERENCES

1. E.S. Avatkov and A.S. Avatkov; *Elektricheskaia tiuga na odnofoznom toke normalnoi chastoty (Electric traction on a single-phase industrial frequency current)*, Transzheldorizdat (1934).
2. A.E. Alekseev; *K voprosu ob elektrifikatsii zheleznykh dorog v SSSR na odnofaznom toke promyshlennoi chastoty. Materialy nauchno-tekhnicheskogo soveshchaniia po tiagovonu elektrochorudo-vaniiu (The problem of electrification of railways in the U.S.S.R. on a single-phase industrial frequency current. Proceedings of the Scientific and Technical Conference on electrical traction equipment)*, Riga (1955).
3. B.R. Bondarenko, N. Kh. Sitnik and V.A. Stekolshchikov; *Zhelez. Trans.* No. 11, 8, (1955).
4. L.A. Visloukh, *Elektrichestvo*, No. 5, 85 (1952).
5. L.A. Visloukh; Elektrifikatsia zheleznykh dorog Anglii (Electrification of English railways), *Biulleten tekhniko-ekonomicheskoi informatsii*, No. 11, 3 (1956).
6. L.A. Visloukh; *Elektrichestvo*, No. 9, 85 (1953).
7. D.I. Gordeen; *Elektrooborudovanie elektrovozow peremennogo toka (Electrical equipment of a.c. locomotives)*, Transzheldorizdat (1938).
8. S.S. Kalinin; *Zhelez. trans.* No. 10, 84 (1956).
9. *M.P.S. Biulleten tekhniko-ekonomicheskoi informatsii (Bulletin of technical and economic information)* No. 4, p.20 (1957).
10. Novye vidy tiagi na transporte (New aspects of transport traction), *Izd. Akad. Nauk SSSR* (1956).
11. Opytnii motornyi vagon rtutnym wyprianitelem (Experimental motor-coach with a mercury rectifie *Elektrichestvo*, No. 2, p.71 (1951).
12. F.Ia. Slavgorods ; *Opytnye lokomotivy (Experimental locomotives)*, Tranzheldorizdat (1949).

13. V.N. Stasuk; *Gornyi zh.* No. 4, p. 26 (1956).
14. B.M. Shliaposhnikov; *Zhelez. trans.* No. 9, 59 (1952).
15. *Elektricheskaia i teplovaia tiaga (Electric and thermal traction),* No. 5, p. 35 (1957).
16. *Elektrichestvo,* No. 3, 84; No. 6, 86 (1957).
17. *Elektrovozy odnofaznogo toka promyshlemnoi chastoty (Electric locomotives fed by a single-phase industrial frequency current),* Transzheldorizdat (1956).
18. S.B. Iuditskii and S.E. Nemchin; Vypriamitel dla elektrovoza uzkoi kolei (Rectifier for electric locomotives for a narrow-gauge railway),*Elektrichestvo,* No. 5, p.55 (1956).
19. *AEG Mitteilungen,* No. 9/10, 442 (1955).
20. *Trans. Amer. Inst. Elect. Engrs.,* II, p.107 (1954).
21. *Brown-Boveri Mitteilungen* No. 4/5, 167 (1955).
22. La traction electric dans les chemin de fer, *Bull. Ass. Int. Congr. Chem.de-fer.* No. 3, 165 (1956).
23. *Bull. SFE,* No. 9, 544 (1951).
24. *Elect. Engr.* No. 5, 408 (1955).
25. *Elect. Rev.* 158, No. 1, 19 (1956); No. 26, 1159.
26. *Elect. Traction on the Railways* No. 3, 149 (1957).
27. *Elekt. Bahnen,* V, 1 (1956); No.5, 116 (1957).
28. *Genie Civ.* No. 19, 367 (1951).
29. *Gen. Elect. Rev.* 59, No.1, 41-43, 45 (1956).
30. *Rly. Age, N.Y.,* 132, No. 10, 68 (1952).
31. *Rly. Gaz.* 104, No.1, 2 (1956); 107, No. 21 (1957).
32. *Rly. Mech. and Elect. Engr.,* 124 No. 3, 141 (1950).
33. *Rev. Gen. Chem.de-fer,* 7, 595 (1955).
34. Paper, American Society of Mechanical Engineers, No. 55-A-187 (1955).
35. *Tract. Elect. Chem. de-fer* No.6, 228 (1956).

SERVICE TESTS

TESTS OF THE EXPERIMENTAL INSTALLATION OF AN IONIC EXCITED HYDROGENERATOR*

I.A. GLEBOV

Institute of Electromechanics of the U.S.S.R. Academy of Sciences

S.F. ZONOV

Lenergo

(Received 1 November 1957)

Ionic systems of excitation act very quickly and owing to this they are very effective means for increasing the stability of synchronous generators. These systems are also very efficient economically.

In 1951 - 1955 an installation for independent ionic excitation was designed and made for the Hydro Electric Power Station (H.E.P.S.) in Nizhnii Svirsk.† In this installation sealed single-anode rectifiers were used.

Description of the installation

In order to ensure the highest possible service reliability of the installation a six-phase converter system was chosen; the same potential was applied to all cathodes. This system may work with a reduced number of rectifiers, whilst the rectified voltage decreases less than in other systems. It is to be pointed out that the converter may work with or without the ground equalizer.

The system of ionic excitation of Nizhnii Svirsk H.E.P.S. consists of an auxiliary synchronous generator, an ionic converter, a control device, a protection and a signalling device.

Since it was impossible to drive an auxiliary generator directly by the shaft of the main set, a synchronous motor, fed from the station local grid, was used. Nevertheless, this arrangement does not change the principle character of the system, which is a system of independent ionic excitation. As an auxiliary synchronous generator, a synchronous machine type S-15-12-6 of 950 kVA power was used; the stator winding of this machine was rewound for this purpose.

---

* *Elektrichestvo*, No. 3, 77—80, 1958.

† In different stages of work there participated: "Elektrosila" Factory, OKB Ministry of the Electrotechnical Industry, LIAP, Institute of Electromechanics of the U.S.S.R. Academy of Sciences, Lenergo, Central Electrical Research Laboratory.

The parameters of the auxiliary generator, which were determined experimentally, are given below.

The auxiliary generator

U_{ph} (V)	490
I_{ph} (A)	490
$S = 6U_{ph} \cdot I_{ph}$ (kVA)	1440
I_{ex} (A)	87
x_d (ohm)	3.02
x_q (ohm)	2.02
x''_d (ohm)	0.276
x_2 (ohm)	0.037
x_3 (ohm)	0.205
x_4 (ohm)	0.037
x_5 (ohm)	0.312
r_g (ohm)	0.021
x_l (ohm)	0.17

Main generator

U_l (kV)	11
I_l (A)	1730
S (MVA)	33
I_{rn} (A)	900
U_{rn} (V)	300

Remarks:

1. Excitation current I_{ex} is given under no-load conditions.
2. Phase resistance of the stator winding r_g is shown together with cable resistance.
3. Excitation voltage U_{rn} is shown when rotor is warm.
4. Leakage inductance of the stator winding x_l was determined by calculation.

In the case of six-phase construction of the generator, we have to deal with parameters of the first (forward or positive), second, third, fourth and fifth sequences. The stator winding of the generator is designed in such a way as to ensure the sustained action of the excitation system with one rectifier idle and to get a three-fold over-excitation while working with the total number of rectifiers.

The effective value of the phase current under nominal conditions is

$$I_{pn} = g \frac{I_{rn}}{\sqrt{6}} = 0.96 \frac{900}{\sqrt{6}} = 350 \text{ A}$$

where g is the shape factor of the curve of phase current.

In the case of working with an incomplete number of rectifiers $I_{pn} = \sqrt{2} \times 350 = 490$ A, i.e. it is equal to the nominal current of the auxiliary generator.

To increase the reliability of the action of the set, feeding of control networks, including gas-filled rectifiers and thyratrons, is done by an auxiliary generator. A carbon-pile regulator of excitation is used for stabilizing the generator voltage. The ionic converter consists of six ignitrons of VET type I-200 with an average value of rectified current 200 A and a back voltage of 1300 V. Therefore, under nominal conditions of the generator work, ignitron current is 900/6 = 150 A, i.e. about 75 per cent

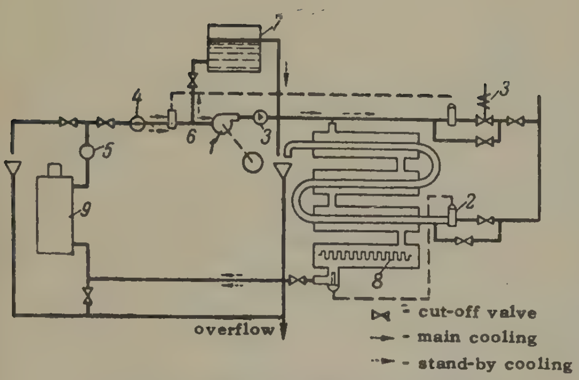

FIG. 1. Diagram of the ignitron cooling: (1) pump; (2) thermo-regulator; (3) return valve; (4) stream relay; (5) water stream indicator; (6) thermo-signalling device; (7) water-tank; (8) water heating resistance; and (9) ignitron.

of its nominal value. Ignitrons are situated in a cabinet divided into six cells; this arrangement allows a quick replacement of the faulty rectifier during the working of the set.

Ignitrons are water-cooled in a closed cycle (Fig. 1). For water heating before the start and for its cooling during the work, a heat exchanger is used with automatic regulation of the water temperature. The cooling system is provided with a stand-by device working in an open cycle. Action of a stream relay or of a thermo-signal device sends an impulse through an auxiliary relay to a contactor, which turns on a solenoidal valve 3; after this the ignitron cooling continues by the flowing water, whilst the temperature of the water leaving the ignitrons is automatically regulated.

Since ignitron ignition requires a considerable pulse power, an independent ignition system is used with a charge-discharge circuit. Control of the instant of the ignition of a thyratron and, consequently, of an ignitron, is made by a magneto-peak system, of which windings for magnetizing peak-transformers are connected to an automatic voltage regulator. The installation is provided with an electro-magnetic compounding system with voltage correction and with an electronic excitation regulator, the so-called "strong action" regulator. In order to force an intensive excitation and to cut it short when the electro-magnetic system is saturated, the magnetizing windings are connected to the operative current grid by the action of the minimum and maximum voltage relay. Besides the automatic regulation of excitation there is a manual control of the generator excitation, which is exerted either by means of phase regulators, or from the station benchboard, or from the machine hall. Elements of the control system are situated in a cabinet divided into six cells in the same way as the ignitron cabinet.

The voltage phase of the igniter with respect to the main anode voltage is so chosen, by means of phase regulators, as to ensure forcing of excitation and cutting off by bringing the converter into inverter action.

The auxiliary generator is provided with axial differential protection. Moreover, to protect its stator windings from overvoltages six dischargers of PVVM-3 type are set up. The protection of ignitrons from flash-back is ensured by the use of quick-acting breakers type VAB-2. To protect the rotor of the main generator from overvoltages a discharger P-100 with a limiting resistance of 1 Ω for 200 A current is provided.

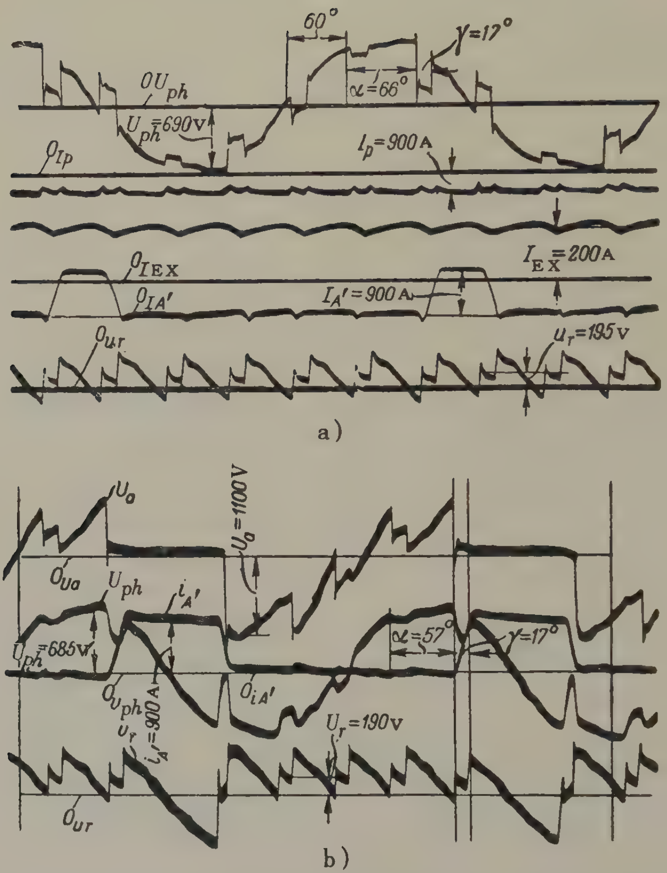

FIG. 2. Nominal condition of the installation: (a) with complete number of the rectifiers; (b) with incomplete number of the rectifiers.

On the benchboard of the station there is a signalling installation that indicates the following undesirable events: flashback in ignitrons, repeated omissions in ignitron firing, stopping of water flow or an excessive water temperature, stoppage of excitation of the main generators and so on. Moreover, an electronic indicator of the voltage on the rotor slip-rings of the hydrogenerator facilitates the control of the performance of the set.

Tests of the installation

Tests were first carried out on an equivalent load with a stalled rotor, and then with a generator running on no-load and on load. The tests showed that the installation ensures forcing of quick excitation and quick braking of exciting current. It may work with an incomplete number of rectifiers, thus permitting the replacement of a faulty rectifier without cutting off the converter. During these tests, the performance of the ignitrons was checked under passing overloads (Table 1). Despite the fact that the amplitude of the p.d. between the rectifier anodes and cathodes in the ionic excitation installation was near to the nominal, forcing of the excitation during one min with a full number of rectifiers and with five rectifiers only, was not accompanied by a flash-back. In certain cases flash-backs were recorded when two adjacent rectifiers were cut off.

TABLE 1.

Conditions	Mean current of the most heavily loaded rectifier (A)	Duration (min)
Forcing with six ignitrons working	330	11
Work with five ignitrons	300	30
Forcing with five ignitrons working	660	1
Work with four ignitrons	450	15
Forcing with four ignitrons working	900	1

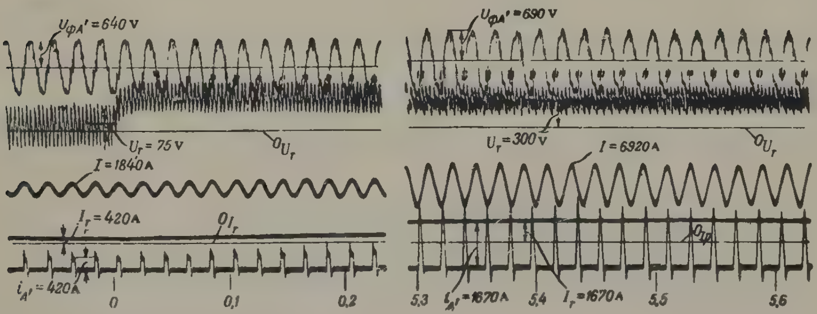

FIG. 3. Forcing of the excitation with the three phases of the main generator short circuited.

Oscillograms were taken at the nominal value of the rotor current of the main generator with a complete (Fig. 2a) and incomplete (Fig. 2b) number of rectifiers. In a converter without a ground equalizer, the normal instant of rectifier igniting was shifted by 60° from the point of passing of the phase voltage through the zero value. Therefore counting of the regulation angle is made from this moment.

In order to show the quickness of response of the system, oscillograms of the forced excitation, with the three phases of the hydrogenerator short-circuited, are shown in (Fig. 3). The minimum regulation angle was limited in such a way as to have the stator current, at the end of the transition period, not exceeding the fourfold normal value. The time necessary to obtain a full value of the voltage, with the forced excitation started and cut off, is approximately equal to 0.01 sec. These oscillograms were recorded during the work without the ground equalizer.

Thermal tests of the auxiliary synchronous generator were carried under two loads with a complete number of ignitrons. Results of these tests are shown in Table 2.

TABLE 2.

I_r (A)	U_l (V)	I_{ex} (A)	Temperature of incoming air (°C)	Increase of temperature (°C)			
				of incoming air	of stator steel	of rotor winding	of stator winding
650	845	163	30	11	44	38	37
800	840	182	29.5	16	56	50.5	46

Temperature of stator and rotor winding was measured by the resistance method. Increase of temperature of the stator steel was measured by a few thermocouples situated on the stator outer surface. Table 2 shows the maximum temperature which was recorded in the middle part of the stator. The maximum increase of temperature occurs in the stator steel.

Experimentally obtained values of voltages and currents and of angles of regulation and commutation were compared with calculated values. For this purpose relationships were determined for various converter networks. For the network without the ground equalizer they are:

$$U_r = \frac{3\sqrt{2}}{\pi} E \cos\alpha - \frac{3}{\pi}\left[x_g + \left(\frac{\pi}{3} - \frac{\gamma}{2}\right) r_g\right] I_d - \Delta U;$$

$$\cos(\alpha + \gamma) = \cos\alpha - \frac{\sqrt{2}\, x_g I_r}{E},$$

where x_g and r_g are the inductance and resistance of a generator phase; E is the effective value of the e.m.f. not distorted by the commutation process; ΔU is the voltage drop in the arc. Inductance x_g may be represented [1] in this form:

$$x_g = \frac{x''_d + 3x_2 + 4x_3 + 3x_4 + x_5}{12}.$$

Taking into consideration that inductances of the second, third and fourth sequences are determined by the stator leakage fluxes and by the higher harmonic components of the flux in the gap, it is convenient to represent reactance x_2 as a sum of two terms:

$$x_g \approx \frac{x''_d + x_5 - 2xl}{12} + \frac{3x_2 + 4x_3 + 3x_4 + 2xl}{12}.$$

The second term determines that part of x_g which is caused by leakage fluxes of the stator winding and by higher harmonics of the flux in the gap.

Fig. 4 shows a vector diagram of the auxiliary salient pole synchronous generator.

On this diagram the fundamental harmonic of the stator current is

$$I_1 \approx \frac{I_r}{\sqrt{2}\pi},$$

and the angle
$$\varphi_1 = \tan^{-1} \frac{\gamma - \sin\gamma \cos(2\alpha + \gamma)}{\sin\gamma \cdot \sin(2\alpha + \gamma)}$$

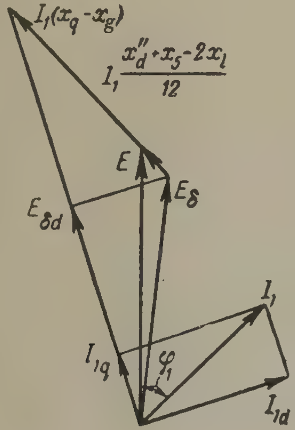

FIG. 4. Vector diagram of an auxiliary generator.

To determine ϕ_1 we may also use a simplified formula. Thus, on the condition of forcing with $\alpha = 0$; $\phi \approx \frac{2}{3}\,\gamma$; when working with high values of α, $\phi_1 = \alpha + \nu/2$

Knowing the longitudinal component of the e.m.f. in the air gap, $E_{\delta d}$, the current in the machine longitudinal axis, and the load characteristic for this current at cos $\phi = 0$, we may determine the exciting current in the auxiliary synchronous generator.

As a certain approximation we may use instead of the load characteristic the no-load characteristic.

Comparison of data calculated by formulae and experimental data (see Table 3) shows that they agree rather well.

TABLE 3.

Quantity	U_r (V)	I_r (A)	α (°C)	γ (°C)	I_{ex} (A)
Experimental value	180	900	65	17	200
Calculated value	180	900	64	17.5	205

Conclusions

The tests showed that the ionic excitation system using sealed single-anode rectifiers ensures a good performance in all service conditions (forcing and cutting off excitation, working with an incomplete number of rectifiers and so on). These tests also showed that the ionic excitation installation acts very quickly (time of growth of the total voltage is of the order of 0.01 sec). The validity of the above method of calculating the currents and voltages of the excitation system is confirmed by experimental results, obtained during tests of installation.

The installation of ionic excitation in the Nizhnii-Svirsk HEPS may be used as an experimental basis for designing new and simpler control systems without gas-discharge devices, with simpler methods of the rectifier protection (grid instead of cumbersome quick-acting breakers), for trial of the new types of rectifier in different service conditions, processes of excitation control and so on.

Translated by S. Szymanski

REFERENCES

1. D.A. Zavalishin and A.Ia. Glebov; Ustanovivshiisia rezhim sinkhronnogo shestifaznogo generatora, rabotaiushchego v skheme ionnogo vozbuzhdeniia (Steady state conditions of

REFERENCES (cont.)

1. a synchronous six-phase generator working in a network with ionic excitation) in symposium "*Elektrosila*", No. 10 (1951).

IGNITRON IVS-200/2*

T.A. SUETIN

All-Union Lenin Institute of Electric Technology

(Received 5 November 1957)

Sealed rectifiers compare favourably with demountable (pump) rectifiers in their electric strength, load capacity, reliability in work, simple construction and smaller size. The use of sealed rectifiers instead of demountable ones permits a considerable cut in working expenses and capital expenses in converter substations. Ignitron IVS-200/2 is now widely used in converter design. At present it is used to equip converter sets of substations for electric urban traction, for ion excitation, electric drive etc.

In the sealed mercury rectifier laboratory of the All-Union Lenin Institute of Electric Technology (V E T), a few types of ignitron IVS-200/2 were developed for mean current 200 A and back-voltage 2500 V. A description is given below of a construction, that is distinguished for its good working qualities and is now widely used.

Fig. 1 shows a general view in section of the ignitron IVS-200/2. The body of the ignitron is made as a welded cylinder with a water jacket. Anode and grid leads of the rectifier are made of glass and metal. Hermetical sealing of lead inlets is achieved by welding molybdenum glass with kovar (fernico) alloy. The anode lead is of high thermal strength and may work for a long time carrying heavy currents. The junction of the rectifier anode is made by using a flexible copper conductor fitted with a terminal, which is screwed into the anode rod. The flexible conductor allows the removal of the mechanical loads, due to the joining of the anode cable, from the glass insulator.

Anode and control grids are made of high quality graphite pressed in closed dies.

Ignitron IVS-200/2 has two igniters and an auxiliary (pick-up) anode. Addition in the ignitron of an auxiliary (pick-up) anode not only facilitates striking of the main arc, or in certain systems unloading the igniter, but also allows for control of the rectified voltage in these ignitrons by a grid, instead of by varying the moment of ignition of a cathode spot by the igniter.

---

* *Elektrichestvo*, No. 3, 80-82, 1958.

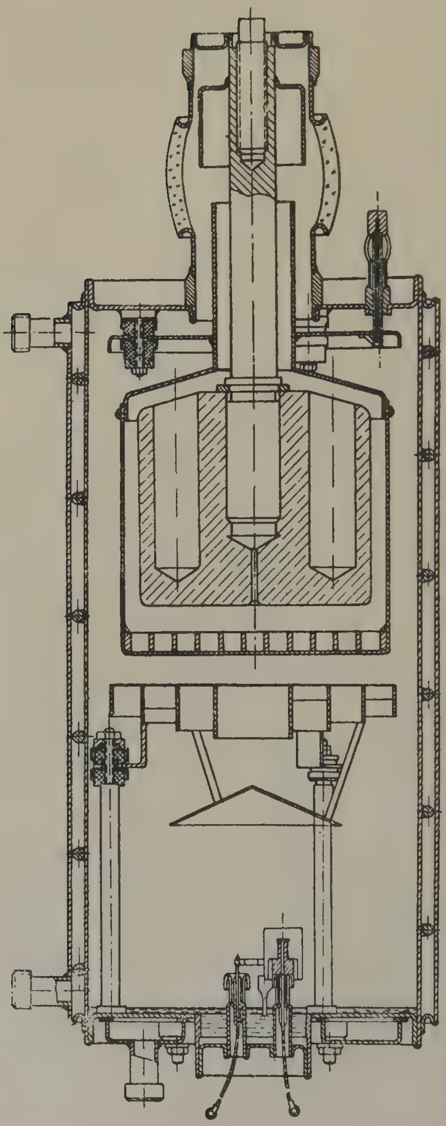

FIG. 1. Cross-section of ignitron IVS-200/2.

In the case when the auxiliary anode is fed by a sinusoidal voltage in phase with the main anode voltage, it is easy to obtain arcing of the auxiliary anode during almost the whole half-cycle of positive anode voltage. The moment of striking of the arc on the main anode depends in this case only on the moment of application to the grid of a positive trigger pulse. Thus, by varying the phase of a positive grid pulse we obtain the control of the rectified voltage in the same way as is done in rectifiers with a permanent exciting arc (excitron).

A steel wafer base with igniters and a pick-up anode is welded together with a steel sleeve of a cathode flange. The presence of the steel sleeve permits quick replacement, when necessary, of igniters in a rectifier without cutting off a whole cathode flange. The cathode of the ignitron IVS-200/2 is water-cooled; during use, water flows around the cathode and the rectifier body.

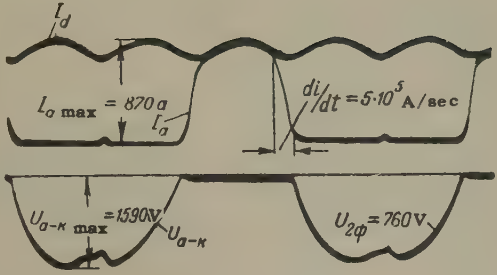

FIG. 2. Oscillograms of rectified current I_d, anode current I_a and p.d. between the anode and the cathode, U_{a-c}, during tests of an ignitron IVS-200/2 under rheostat load (mean rectifier current 240 A.

To prevent hydrogen diffusion from the water jacket into the cylinder, which is inadmissible in sealed (pumpless) rectifiers because of vacuum deterioration, water-cooled rectifiers (i.e. the body and the cathode flange) are made from stainless steel or, in cases when low carbon steel is used, they should be enamelled. Both methods were tested under laboratory conditions and during long periods of normal service and gave equally good results.

In the first samples of ignitrons, igniters were made from silicon carbide. Experience showed that most of these igniters have a short period of service – 1500 - 2000 hr.

At present, in VET ignitrons, igniters are used made from boron carbide. Their electric characteristics are: ignition current not more than 12A, ignition voltage not more than 350 V. The period of service of the boron carbide igniters is estimated as not less than 20,000 hr, as may be assumed from the data obtained at present.

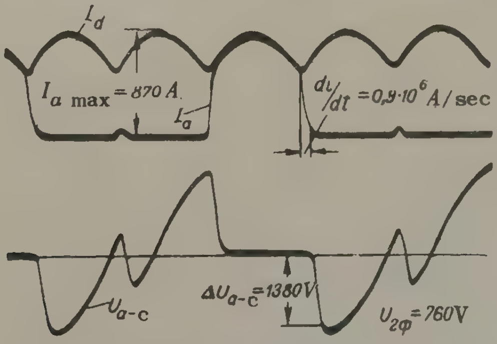

FIG. 3. Oscillograms I_a, I_d and U_{a-c} during the tests of rectifiers under short-circuit conditions (mean rectifier current 240 A).

We may point out that all igniters, even after working 15,000-20,000 hr, continue to work normally and do not require any alterations (forcing) in ignition circuits.

The period of service of sealed ignitrons is determined in practice by the period of service of igniters. Due to the presence of two igniters in ignitrons IVS-200/2 it may be safely assumed that the period of service of these ignitrons will be not less than five years. Technological processes developed by the VET laboratories in production of sealed metallic mercury rectifiers allow a high degree of degassing (exhaustion) of details and of the rectifier as a whole; this ensures stability of its properties during long storage, after which, as experiments have shown, rectifiers may be immediately used for work at the nominal current and voltage without preliminary electrical forming at a low voltage. The weight of the ignitron is 26 kg.

To determine electric parameters of ignitrons and to verify that they satisfy technical specifications, bench tests were carried out in VET. These tests were carried out in a three-phase zero wire network at the nominal phase voltage 760 V under two sets of conditions: using a rheostat as a load and in a short-circuit (Figs. 2 and 3).

Nominal anode currents were drawn for a long time and overloads up to 130 per cent of the nominal current were applied.

As can be seen from these oscillograms tests under short circuit conditions are the hardest ones, since at a high rate of decrease of the anode current ($dI_a/dt = 10^6$ A/sec) the anode back voltage jumps nearly up to the maximum value.

Bench tests were carried out with water-cooled rectifiers; water temperature was within the limits of 20 to 35°C.

On the basis of bench and service tests it has been found that ignitron IVS-200/2 has the following electric parameters

Mean anode current		200 A
Current overload:		
during 10 min		265 A
during 2 min		320 A
during 30 sec		450 A
Maximum back voltage		2500 V
Voltage drop in the arc not more than		16 V
Negative grid bias		150 V
Grid current (amplitude)		150mA
Current of the pick-up anode		1.5-2 A
Igniter parameters		
(a) ignition current	not more than	12 A
(b) ignition voltage	not more than	350 V
Cooling	forced water cooling	
Temperature of cooling water	+ 20 – + 35°C	

Water consumption at $\Delta t = 8°C$ 6 l/min.

During the bench tests ignitrons IVS-200/2 worked smoothly for long periods under nominal currents and under all overloads; grid control worked without failure, direct breaks and back ignitions did not occur.

Translated by S. Szymanski

DISCUSSION

"MODIFICATION OF THE HEAVISIDE FORMULA"* **

B. KONORSKI
Lodz Polytechnic Institute, Poland

The method and formula (12) given by the author of the article are well known; they may be found even in textbooks on operational calculus. The Russian reader may find this formula in the book by Gardner & Burns (translated from English and published in 1951 by Gosizdat. This formula is by no means so universal; it deals only with one particular case, when the denominator $H(p)$ has only one zero root.

It is easy to obtain a more general formula assuming

$$pH(p) = \prod_{k=0}^{n} (p - p_k)^{m_k},$$

where $P_0 = 0$

$$\frac{G}{pH(p)} = \sum_{k=0}^{n} \sum_{s=1}^{m_k} \frac{A_{ks}}{(p - p_k)^{m_k - s + 1}}.$$

With these assumptions we get:

$$L^{-1} \frac{G(p)}{H(p)} = \sum_{k=0}^{n} \sum_{s=1}^{m_k} \frac{A_{ks}}{(m_k - s)!} t^{m_k - s} e^{p_k t},$$

in this case

$$A_{ks} = \frac{1}{(s-1)!} \left\{ \frac{d^{s-1}}{dp^{s-1}} \left[\frac{(p - p_k)^{m_k}}{p} \frac{G(p)}{H(p)} \right] \right\}_{p = p_k};$$

$k = 0, 1 \ldots n;$
$s = 1, 2 \ldots m_k.$

B. SAVIUK Kraiova, Rumania

---

* *Elektrichestvo*, No. 3, 86-89, 1958.
** Cf.O.M. Bogatyrev, *Elektrichestvo*, No. 2 (1957).

The "modification" of the Heaviside formula, proposed by Bogatyrev, has for a long time been in textbooks on Electric Technology (for example, I. Fallon, *Lecons d'electrotechnique*, Paris Gauthier-Villars, 865 (1948); I.S. Antoniu, *Chestine speciale de electrotehnica*, Bucuresti, Ed. Acad. R.P.R. (1956). Bogatyrev's article contains nothing new.

F. CSAKY
Budapest, Hungary.

The article contains a modification of the Heaviside expansion theorem in the case when the denominator of the fraction representing a function has multiple roots. The author uses the following method. The fractional operational equation, the solution of which we want to find, is expanded into partial fractions; coefficients of these fractions are determined, and from tables we find time solutions, corresponding to every fraction.

To determine the coefficients the author recommends expression (12) (Cf. also (1)).

In connexion with the article, I would like to say this. The time solution may be obtained by means of a single universal expression, avoiding the expansion into partial fractions and the use of tables. In different publications (see for example [2], we may find the following expression:

$$F(t)=L^{-1}\{\varphi(p)\}=$$
$$=\sum_{k=1}^{m}\left\{\frac{1}{(n_k-1)!}\,\frac{d^{(n_k-1)}}{dp^{(n_k-1)}}\,[(p-p_k)^{n_k}\varphi(p)\,e^{pt}]\right\}_{p\to p_k}. \qquad (1)$$

where m is the number of different roots of the denominator of the function ϕ (p), and n_k the order of the kth root p_k. Function ϕ (p) is a Laplace transformation of the function F (t), i.e.

$$\varphi(p)=L\{F(t)\}=\int_0^\infty F(t)\,e^{-pt}\,dt.$$

If all roots of the denominator are unequal ($n_k = 1$, $k = 1,2 \ldots m$), then expression (1) assumes the form:

$$F(t)=L^{-1}\{\varphi(p)\}=\sum_{k=1}^{m}\{(p-p_k)\varphi(p)\,e^{pt}\}_{p\to p_k}. \qquad (2)$$

Let us remark that expression (1) is only slightly more complicated than formula (12). Moreover, formula (12) gives only coefficients of partial fractions, but by expression (1) we may determine directly the required time function. The last property constitutes an advantage from a theoretical point of view, and the use of the expression (1) for solving practical problems does not increase the amount of work in comparison with the method based on the expansion theorem.

The correctness of expression (1) may be easily proved by using a theorem on functions of a complex variable:
(a) by the Riemann-Mellin theorem [3],

$$F(t)=L^{-1}\{\varphi(p)\}=\frac{1}{2\pi j}\int_{c-j\infty}^{c+j\infty}\varphi(p)\,e^{pt}dp. \tag{3}$$

(b) by the theorem of residues [3, 4],

$$\frac{1}{2\pi j}\int_{c-j\infty}^{c+j\infty}\varphi(p)e^{pt}dp=\sum_{k=1}^{m}\operatorname{Res}\{\varphi(p)e^{pt}\}._{p=p_k} \tag{4}$$

We assume that the number of poles ϕ (p) to the left of the straight line p-c is equal to m (c is a real number);
(c) If any function ψ (p) at a point $p = p_k$ has a pole of the order n_k, then the residue of the function (p) may be determined by the relationship:

$$\operatorname*{Res}_{p=p_k}\{\psi(p)\}=\left\{\frac{1}{(n_k-1)!}\frac{d^{(n_k-1)}}{dp^{(n_k-1)}}[(p-p_k)^{n_k}\psi(p)]\right\}_{p\to p_k} \tag{5}$$

Let $$\psi(p)=\varphi(p)e^{pt};$$

then, on the basis of (5), (4) and (3), we get expression (1).

Finally, two further remarks:
(1) Expression (1) is nothing other than a generalization of the Heaviside expansion theorem. In fact let

$$\varphi(p)=\frac{G(p)}{pH(p)} \tag{6}$$

and let the equation H (p) = 0 have only m unequal roots p_k equal to zero. From expression (1a) we get:

$$\left\{(p-p_k)\frac{G(p)}{pH(p)}e^{pt}\right\}_{p\to p_k}=\frac{G(p_k)}{p_kH'(p_k)}e^{p_kt}. \tag{7}$$

The term corresponding to the zero root of the denominator will be:

$$\left\{(p-0)\frac{G(p)}{pH(p)}e^{pt}\right\}_{p\to 0}=\frac{G(0)}{H(0)}. \tag{8}$$

In this case, expression (1) leads to the inverse Heaviside expansion theorem:

$$F(t)=\frac{G(0)}{H(0)}+\sum_{k=1}^{m}\frac{G(p_k)}{p_k H'(p_k)}. \tag{9}$$

If the function $H(p)$ has multiple roots[or if $p = 0$ is also a root of the equation $H(p) = 0$], then on the basis of expression (1) we may also get the expression similar to expression (9) (see for instance [1,5, 6]. But in this case the expression becomes complicated; therefore it is more convenient to use expression (1).

(2) If instead of the Laplace transformation we use the Carson [7] and Wagner [6] transformations:

$$f(p)=\varphi\left\{F(t)\right\}=w\left\{F(t)\right\}=p\int_0^\infty F(t)e^{-pt}dt, \tag{10}$$

then, in using expression (1), we have instead of $\phi(p)$ to write everywhere

$$\varphi(p)=\frac{f(p)}{p}.$$

REFERENCES

1. M.F. Gardner and J.L. Burns; *Perekhodnye protsessy v lineinykh sistemakh (Transient processes in linear systems)*, Gostekhizdat (1951).
2. J. Millmann; Laplacian Transform Analysis of Circuits with Linear Lumped Parameters, *Elect. Engrg.* (1942).
3. M.I. Kontorovich; *Operatsionnoe ischislenie i nestatsionarnye iavleniia v elektricheskikh tsepiakh (Operational calculus and transient processes in electric networks)*, Gostekhizdat (1949).
4. V.I. Smirnov; *Kurs vysshei matematiki (Textbook of advanced Mathematics)* VIII, part 2, Gostekhizdat (1951).
5. I.I. Teumin; *Spratochnik po perekhodnym elektricheskim protsessam* (Reference book on transient electric processes), Gosizdat literatury po voprosam sviazi i radio (1951).
6. K.W. Wagner *Operatorenrechnung und Laplacesche Transformation. (Operational calculus and Laplace transformation)*, J.A. Bart Verlag, Leipzig (1950).
7. J.R. Carson *Electric Circuit Theory and the Operational Calculus*, New York (1938).

V.M. GRESHNIAKOV and A.A. MODEROV
Kalinin Polytechnic Institute, Leningrad

Formula (12), recommended in Bogatyrev's article is well known and may be found in books, for instance in the book *Transient processes in linear circuits* by Gardner and Burns. The derivation of formula (12) given by Bogatyrev corresponds to the derivation given by Gardner and Burns. The difference consists in that Bogatyrev derives the formula on a simple particular example, whilst Gardner and Burns deduce the formula for a general case.

The latter deduction is made in a rigorous mathematical way and is distinguished by its clarity; it takes nearly as much or a little more space than Bogatyrev's deduction.

Moreover, as Bogatyrev points out himself, formula (12) gives only the last coefficient $A_k^{(n-1)}$ in the fraction $\dfrac{A_k^{(n-1)}}{p-p_k}$ for the n-fold multiple root. The usefulness of this formula for determination of remaining coefficients is connected with an artificial method of notation used by the author.

Indeed, it is quite unusual in mathematical literature to ascribe to the same index in the same formula different meanings, as was done by Bogatyrev (index n) Thus, in an example given in the Bogatyrev article, he puts in evaluating index A_1, $n = 3$ in one place of the formula (12) [in expression $(p-p_k)^n$], and in other places of the same formula (12) he puts $n = 2$.

It is quite natural that the Gardner and Burns formula, which gives any arbitrary coefficient of expansion, contains, instead of a single index n in formula (12), two indices: m_k, the order of the kth root, and the ordinal index j, taking all integral values from unity to m_k.

Thus, formula (12) in Bogatyrev's article is not new and has the above defects.

P.A. SAPOZHNIKOV and N.D. SAPERSHTEIN
Leningrad Military Mechanical Institute

In dealing with transient processes by operational methods it is necessary to solve the problem of transformation of operational solution of the form $G(p)/H(p)$. It is done by expanding the operational solution into partial fractions, transforms of which are either known or easily found. Bogatyrev considers the expansion of fractional rational expressions of the type $G_k(p)/H_m(p)$ (in the case of the Laplace transformation $K < m$, and in the Carson transformation $K \leq m$) in the presence of single and multiple poles. Having written, as an example, about the expansion of a non-reducible fraction (1), the author of the article makes use of a well-known method of consecutive multiplication of both sides of the identity

$$\frac{G(p)}{H(p)} = \frac{A_0}{p} + \frac{A_1}{(p-p_1)} + \frac{A_2}{(p-p_2)} + \frac{A_2'}{(p-p_2)^2}$$

by denominators of the right hand side terms, i.e. cancels out poles 0, p_1, p_2; and, from the identities so obtained, he determines coefficients A_0, A_1, A_2 A_2'. In the case of absence in the numerator of the Carson expression of the factor p, the author of the article also recommends a well-known method of introducing this factor into the numerator and denominator. But he does not show that expressions (4) and (5) for the coefficients A_0 and A_1 so obtained may be reduced to a more general and more convenient form, namely

$$A_1 = \left[\frac{G(p)}{\frac{H(p)}{p-p_1}}\right]_{p=p_1} = \left[\frac{G(p)}{\frac{H(p)-H(p_1)}{p-p_1}}\right]_{p=p_1} = \left[\frac{G(p)}{H'(p)}\right]_{p=p_1} = \frac{G(p_1)}{H'(p_1)}$$

and similarly

$$A_0 = \frac{G(O)}{H'(O)}.$$

This makes the expression for A_0 and A_1 more similar to the usual form of the Heaviside formula and also allows for the determination of coefficients of partial fractions (for single poles, they are residues as well) in the case when $G(p)$ and $H(p)$ are not polynomials, but arbitrary functions having no common roots. Thence it follows that the transformation of meromorphic forms is possible.

In the last case it often happens that it is easier to evaluate $G(p_1)/H(p_1)$ than

$$\frac{G(p_1)}{\left[\frac{H(p)}{p-p_1}\right]_{p=p_1}}$$

For example, in transforming the operational solution (by the Laplace method)

$$\frac{1}{p}\tanh\frac{p}{2} = \frac{\frac{1}{p}\sinh\frac{p}{2}}{\cosh\frac{p}{2}},$$

$$G(p) = \frac{1}{p}\sinh\frac{p}{2};\quad H(p) = \mathrm{ch}\frac{p}{2},$$

it is much easier to evaluate

$$\frac{G(p_k)}{H'(p_k)} = \frac{\frac{1}{p_k}\sinh\frac{p_k}{2}}{\frac{1}{2}\sinh\frac{p_k}{2}} = \frac{2}{p_k}$$

[$p_k = (2_k + 1)\,\pi i$ – single roots $\cosh p/2$] than "merely to cancel out" in the denominator the factor $(p - p_k)$.

O.M. BOGATYREV
Moscow

Formula (12) is known in different forms in scientific literature, but in textbooks in our country not much attention has been paid to it. For solution of transient processes many various formulae are derived according to the nature of roots and for different applied voltages. These formulae depend upon the kind of transformation, whether Laplace or Carson. The aim of my article is to suggest the use in all cases of the only one and unique universal formula [formula (12)] that is easy to deduce in an elementary way and does not depend upon the type of transformation.

With Konorski's remark that formula (12) "is not as universal as that" I cannot agree. It may seem so if we disregard the fact that the number n in different places in formula (12) has different meanings. Thus, in the expression $(n\text{-}p_k)/n$ index n shows that the root p_k is the nth root, i.e. the number n coincides with the number m_k in the formula given by Konorski and in Gardner and Burns. In other parts of formula (12) n takes all integral values from unity to the number equal to the order of the root p_k; i.e. n coincides with the current index s in the Konorski formula or with the index j in the Gardner and Burns formula.

I have seen two editions of the Gardner and Burns book. The formula in question is encumbered there by indices. The formula given by Konorski, being more general, does not differ in principle from my formula (12), except for the expression for A_{ks} in Konorski's article, where the factor p is inserted in the denominator, probably by mistake.

References given by Saviuk contain nothing new, since the formula in question is not derived there, it is only quoted besides other similar formulae; there is no suggestion whatsoever about the universal use of this formula.

The main point in F. Csaky's comment is this: its author thinks that expression (1) "from the theoretical point of view" has certain advantages and practically does not require more labour than the universal method and the formula recommended in my article. F. Csaky considers that the universal formula gives "only coefficients" of partial fractions, whilst formula (1) gives directly the time solution. This is correct, but the author ignores the fact that the evaluation of coefficients constitutes 95 per cent of the whole problem.

The defects of the formula and of its deduction that are criticized by V.M. Greshniakov and A.A. Moderov, in my opinion are advantages. In fact, what could be simpler than substituting into the binomial $(n\text{-}1)$ (and only into the binomial) of formula (12) the values from unity to n, where n is the order of a given root p_k, and so on for every root. The deduction of the formula is elementary, easy to understand and not tiresome.

The authors write that my notations are artificial. In my opinion they are very convenient, since in the formula there are only two indices, k and n, whilst in the Gardner and Burns notations there are many indices in double sums. It seems to me that their formula is not widely used just because it looks so cumbersome.

I derived formula (12) by a generalization of operations shown in one particular example. I never wrote that this formula is essentially a new one, but I want this formula, that was known in this or another form, to become universal and indispensable in the form that is given in my article.

P.A. Sapozhnikov and N.D. Sapershtein wrongly use the example of evaluation of meromorphic functions, while the theory applies to fractional rational functions (and this point, it follows from their remark, is known to them).

Translated by S. Szymanski

SYNTHETIC COMPOUNDS OF HIGH MOLECULAR WEIGHT AS DIELECTRICS*

K.A. ANDRIANOV

All-Union Lenin Institute of Electric Technology

(Received 28 November 1957)

The progress of modern chemistry of compounds of high molecular weight has reached such a level that the possibility now exists of considerably improving the polymers already known and of producing new ones, not yet obtained, with properties specified in advance. To build the chains of polymer molecules, chemists now make use not only of carbon and silicon but also of other elements: titanium, aluminium etc. All this offers wide opportunities for obtaining many diverse polymers which differ basically in the structure of their molecules and their technical properties. The use of carbon compounds only led to polymers with organic molecular chains. Such polymers have a rather low thermal stability and can be used for a long time at temperatures up to 130°C.

With the use of silicon in combination with organic groups the possibility appeared of building polymers with mineral molecular chains, consisting of atoms of silicon and oxygen surrounded by organic groups.

This development has already resulted in the production of a large group of polymers, polyorganosiloxanes, and in the production of electro-insulating materials with high thermal stability, which can work for a long time at a temperature of 180°C. The use of other inorganic elements, aluminium, titanium, boron and others, greatly increases the prospects of the synthesis of polymers with mineral molecular chains, consisting, for example, of: silicon, oxygen and aluminium; silicon, oxygen and titanium; silicon, carbon, oxygen and aluminium, etc., which are surrounded by organic or silico-organic groups.

This offers good prospects for obtaining new polymers which are similar in their molecular chain structure to silicates but are surrounded by organic or silico-organic groups. Such polymers should combine properties of both kinds; the high thermal stability proper to silicates, and elasticity, which is a characteristic property of the organic part of the molecule.

Along with the above discussed trends in the synthesis of high polymer substances, during recent years new methods of polymerization have been widely developed; these methods make use of new catalysts and they enable us to obtain polymers of a strictly regular structure with great molecular weight and better physical-technical properties than those of the same polymers obtained by the old methods.

---

* *Elektrichestvo*, No.4, 1-10, 1958.

Thus, for example, polyethylene obtained by the old methods melts at 125°C, but that obtained by new methods at 170°C. The use of mechanical chemical methods for production of block- and kraft-polymers on the basis of many very varied polymers enables us to change very considerably the properties of the existing polymers in a desired way.

The use of high-energy particles (γ - rays and others) for changing polymers also enables us to change properties of the known polymers according to our requirements.

Synthetic compounds of high-molecular weight play an important role in electric technology, and their use for the insulation of electric machines, apparatus, cables and other electrical and radio devices increases each year. This is explained by their good electrical and physical-technical properties (particularly their thermal stability and resistance to moisture) compared with natural polymeric substances.

Thus their use enables designers to construct machines and apparatus and to solve problems the solution of which would be impossible using only natural polymers.

Polymeric hydrocarbons

Polymeric hydrocarbons proved themselves as good dielectrics, particularly in the production of high-frequency cables and various types of radio apparatus.

Nevertheless, these polymers which were produced by ordinary methods of polymerization had a low melting point. In consequence, the region of their application, in spite of good electric properties, was limited to temperatures up to 85°C.

Recently new catalysts for polymerization have been obtained, the use of which leads to the production of polymeric hydrocarbons and other polymers with a strictly regular structure; they are now known as "isotactic polymers".

Isotactic polymers possess a regular molecular chain structure; this is due to regular alternation of the carbon atoms with the same space configuration in the main chain. These polymers are characterized by their high melting point and high mechanical strength in the aligned direction in comparison with polymers, produced by the polymerization of monomers by the widely used radical mechanism of polymerization.

Isotactic polymers are produced by the polymerization of monomers in the presence of special catalysts: triethyl aluminium and titanium tetrachloride. The mechanism of polymerization is ionic in nature and, in comparison with the radical one, which is characterized by the branching of molecular chains and the formation of amorphous products, leads to the formation of polymers with strictly regular molecular structure and a high degree of crystallinity. At present the isotactic polyethylene, polypropylene, polybutene, polystyrene and other polymers are synthesized. They are all polymeric hydrocarbons and at ordinary temperature are solid crystalline substances, with small dielectric losses for various frequencies of an electric field.

As opposed to the polymers of the same class, but produced by the ordinary methods, they have a higher melting point and are not soluble in the majority of solvents (Cf. Table 1).

TABLE 1

Polymer	Temperature of the transition of the first kind (softening point) (°C)	Density (g/cm³)
Polyethylene:		
isotactic	170...175	
ordinary	110...125	0.92
Polypropylene:		
isotactic	158...170	0.92
ordinary	75	0.85
Polystyrene		
isotactic	230	1.08
ordinary	70...100	1.04

The properties of isotactic polymers permit a very great extension of the use of polymeric hydrocarbons for electric insulation. Due to the increase of temperature of their melting point they can be used in the form of plastic masses, as cable sheaths and as fibres for working tempertures of 105°C and more.

The regular structure of the isotactic polymer hydrocarbons ensures a high degree of crystallinity and makes them suitable for preparing fibres [2]. The properties of the fibres of the isotactic polymers are shown in Table 2.

TABLE 2

Polymer	Limiting tensile strength (kg/mm²)	Specific strength (g/denier)	Total elongation at breaking (%)	Work of breaking (g/denier)	Density (g/cm³)
Isotactic polypropylene ..	77	9.3	31	1.6	0.92
Nylon	54	5.3	26	0.9	1.14
High strength nylon	78	7.7	14	0.7	1.14
Steel	210	3.0	8	0.2	7.8

Fibres made of such substances as polypropylene or polystyrene do not absorb moisture at all. They posses high electric resistivity greatly exceeding that of other fibres. These fibres have a wide range of application in the insulation of magnetic wires and in the production of different electric insulating materials. The disadvantage of these fibres is their low melting temperature, which prevents their use in insulation above class A.

Table 3 shows the electric properties of the pure polymeric hydrocarbons, which were recorded at a temperature of 20 ± 2°C. Electric strength is shown for a specimen 1.5 mm thick.

TABLE 3

Polymer	ρ_v (Ω cm)	$\tan\delta \times 10^4$	E_{str} (kV/mm)	ϵ
Polyethylene:				
isotactic	$10^{17} \ldots 10^{15}$	$3 \ldots 6$	$20 \ldots 25$	$2.2 \ldots 2{,}3$
ordinary	$10^{17} \ldots 10^{15}$	$2 \ldots 5$	$24 \ldots 26$	$2.25 \ldots 2{,}35$
Polypropylene:				
isotactic	$10^{16} \ldots 10^{14}$	$4 \ldots 8$	$18 \ldots 24$	$2.15 \ldots 2{,}3$
Polystyrene:				
isotactic	$10^{6} \ldots 10^{14}$	$2 \ldots 5$	$20 \ldots 22$	$2.5 \ldots 2{,}55$
block	$10^{17} \ldots 10^{14}$	$1 \ldots 2$	$24 \ldots 28$	2.5

Polytetrafluoroethylene

Among the heat resistant polymers polytetrafluoroethylene is of the greatest interest. It has a regular linear structure of molecules, which ensures its crystalline structure, and possesses a high thermal stability and softening temperature (about 400°C) [12].

Polytetrafluoroethylene is a non-polar polymer; its permittivity within the frequency range $50 - 10^6$ c/s, is equal to 2.0 - 2.2; its tangent of the loss angle, equal to 2×10^{-4}, does not depend upon the field frequency up to 10^8 c/s and varies little with temperature within wide limits. It possesses a high resistivity (up to 10^{17} Ω cm) and its electric properties vary little with temperature and under the influence of moisture.

It is necessary to point out that the electric strength of polytetrafluoroethylene greatly depends on the time of the voltage application. For short periods of application for specimens 1.5 mm thick it is 15 - 20 kV/mm, for long periods it decreases to 6 - 8 kV/mm. Difficult working and ability to creep at low temperature limit its use.

Nevertheless, the high thermal stability of the polymer, which permits its use at temperatures of 250°C and even 280°C, together with its small dielectric losses and high electric resistance, permit its use in the production of high frequency cables, where its tendency to creep at low temperature and its lower electric strength under a long-lasting applied voltage are of no serious importance.

Polyester resins

Polyesters as dielectrics are of great interest; they are known under the name "unsaturated polyester resins" [3-6]. They are produced in the form of liquids, which are solutions of linear unsaturated polyesters in unsaturated compounds stabilized by inhibitors. Such liquid products, when heated in the presence of initiators of the peroxide type, become solid infusible polymers, which possess valuable properties. Polyesters are obtained from diatomic alcohols, glycols and unsaturated dibasic acids, for example, maleic acid.

In order to decrease the polyreactivity of a polyester and to increase its elasticity, the mean distance between double bonds is increased by replacing a part of the unsaturated acid by an equivalent quantity of a saturated dibasic acid: phthalic, adipic, sebacic and others.

Unsaturated polyesters are also modified by monobasic acids and oils (castor oil and others) to obtain less viscous polymers. Such polyesters are usually dissolved in unsaturated compounds, especially in styrene, which acts as a solvent and reacts with the unsaturated ester, thus producing a three-dimensional infusible polymer. This is due to the linking of unsaturated linear ester molecules by styrene. Quinones and amines are used as inhibitors. Peroxides are used as accelerators for solidification.

Industry produces various polyesters, among which KGMS-1 and KGMS-2 are used as dielectrics. Table 4 gives the properties of liquid and solid polyester resins according to the data supplied by the VEI. From the data given in Table 4, it is seen that polymers possess high electric strength and high volume resistivity; the insignificant variation in dielectric characteristics of specimens, after they have remained in a humid atmosphere, proves their rather high moisture stability. This is confirmed by tests of specimens which are kept in an atmosphere with a relative humidity of 98 per cent at temperatures 20°C + 40°C [Fig.1].

The introduction into polymers of fillers decreases shrinking, the coefficient of thermal expansion of the sealing compound and the exothermal heat of the reaction of copolymerization. Therefore, the possibility of cracking decreases and the thermal conductivity of compounds increases.

Table 5 shows dielectric characteristics of polymers with fillers. In electric insulation a polyester made from terephthalic acid and ethylene glycol plays an important role; it is known under the names of lavsan, mylar and Terylene. This polymer, obtained in INEOS of the U.S.S.R. Academy of Sciences, has a comparatively straight linear chain; it crystallizes and forms strong fibres and mechanically strong films. The melting point of lavsan is 220-240°C and breaking stress 400-500 kg/cm². The aligned fibres and films have a greatly increased strength, and breaking stress lies within the limits 350-4500 kg/cm². Electric properties of lavsan are high; for example, the tangent of the loss angle for lavsan films at a frequency of the electric field 50 c/s and temperature 20°C is 0.005-0.01 and

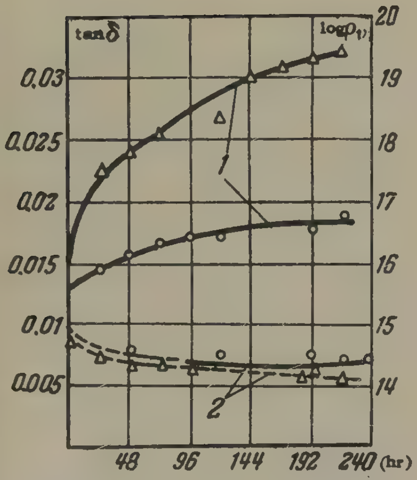

FIG.1. Curves of tan δ (curve 1) and ρ_v (curve 2) as functions of the time of wetting.

varies little up to 100°C in a humid atmosphere. Its volume resistivity is 10^{14}-10^{15} Ω cm. Its permittivity is 3-4. Lavsan is easily made into fibres, films, laminae etc. Lavsan fibres are of great interest since they can be successfully used for the insulation of conductors, and lavsan films, owing to their great mechanical and electrical strength (100 kV/mm for films 0.11 mm thick), can be widely used for insulation of slots in electric machines instead of lacquered fabrics, micanite etc. This results in a much better filling of the slot by copper.

Polyester resins made from terephthalic acid and a mixture of alcohols, glycerine and glycol, have a branched molecular structure. Therefore they cannot crystallize and dissolve in solvents with the formation of lacquers. Such lacquers form mechanically strong films, and, by coating copper conductors with these lacquers, we get enamelled conductors of greater mechanical strength than that of vinyflex enamelled conductors.

TABLE 4. Properties of solid polymers

Characteristics		KCMS-1	KGMS-2
In the initial state	$\tan\delta \times 10^4$ at frequency 50 c/s	142...250	168...190
	Permittivity	3.7...4.3	3.7...4.0
	Volume resistivity (Ω cm)		
	at 20°C	$1.1\cdot10^{14}$...$4{,}0\cdot10^{15}$	$1.7\cdot10^{14}$...$1.5\cdot10^{15}$
	at 120°C	$1.2\cdot10^{11}$...$8{,}9\cdot10^{12}$	$1.8\cdot10^{11}$...$5.8\cdot10^{12}$
	Electric strength (kV/mm)	21.8...29.2	21.1...27.1
After remaining 48 hr in an atmosphere of tropical humidity at +50°C	$\tan\delta \times 10^4$ at frequency 50 c/s	191...292	199...290
	Volume resistivity at 20°C	$1.0\cdot10^{13}$...$3.1\cdot10^{14}$	$5.4\cdot10^{13}$...$7.7\cdot10^{13}$
	Electric strength (kV/mm)	23.2...28.3	25.4...27,5
	Frost resistance	−60°C	−60°C
	Shrinkage at solidification (%)	9.2	9.5

N.B. All properties are shown after heating the specimen for 6 hr at 120°C; thickness of the specimen 0.9 ± 0.1 mm.

IA polyester 124 and a lacquer, modified by the addition of substances binding linear molecules, have been produced in the VEI; this lacquer is used for the production of mechanically strong enamelled conductors which are stable in solvents, and which can work for a long time at a temperature of 130°C in machines with Class B insulation.

TABLE 5

Composition of the sealing compound	Parts by weight	In the initial state			After remaining 48 hr in an atmosphere with relative humidity 97 ± 2 per cent	
		$\tan\delta \times 10^4$	ρ_v (Ω cm)	E_{str} (kV/mm)	$\tan\delta \times 10^4$	ρ_v (Ω cm)
KGMS-2 . . .	100					
Quartz sand .	60	272	$2.8 \cdot 10^{15}$	29.0	1380	$2.8 \cdot 10^{11}$
KGMS-1 . . .	100					
Quartz sand .	60	370	$3.4 \cdot 10^{15}$	30.0	1080	$1.0 \cdot 10^{13}$
KGMS-2 . . .	100					
Mica.	60	308	$8.0 \cdot 10^{14}$	31.4	1350	$3.0 \cdot 10^{12}$
Titanium dioxide. . .	3					

In electric technology, moreover, polyester resins are used as impregnating and casting compositions for the production of textolite. The high impregnating capacity of polyester resins ensures good impregnation of products: on heating a uniform insulation is formed. The use of these resins enables us to avoid the difficulties connected with the porosity of an insulation obtained by impregnation with ordinary lacquers [10]. Articles joined by polyester compounds are distinguished by their good cementation, high electrical and mechanical properties, high vibration stability, frost resistance, increased moisture resistance and operational reliability.

Hermetic sealing of electrical apparatus by filling with polyester resins gives protection from vibration, mechanical damage and atmospheric influence [7].

Epoxide resins

Epoxide resins are obtained by the reaction of different diphenyls with epichlorohydrin and usually have a softening temperature of 40 - 120°C. By treatment with amines they solidify at room temperature and become infusible and insoluble. Anhydrides of phthalic, maleic and other acids cause the epoxide resins to solidify when heated up to temperatures of 120°C and higher. In industry, the epoxide resins made from diphenylpropane are used; they are issued under trade marks E-40, E-37, ED-6.

At temperatures 90 - 100°C epoxide resins become liquid and at these temperatures they can remain unchanged during a rather considerable time [9]. They show good adhesion to metals and non-metallic materials. Electric properties of epoxide resins are high:

$\rho_v = 10^{15} - 10^{17}\ \Omega\,\text{cm}$; $\tan\delta = 0.006 - 0.01$; $\epsilon = 3.7 - 4.2$; $E_{str} = 20 - 24$ kV/cm for a specimen 1.2 mm thick.

In the electrical industry the epoxide resins are mainly used as glues in laminated insulation and as a cast insulation. For filling up current transformers, epoxide-polyester compound E-37 has been developed and is in use; for protection of semiconductor apparatus, epoxide-polyester compounds K-168 and K-239 are used. Compound E-37 consists of epoxide resin E-37 with addition of a polyester as a plasticizer component. Quartz powder serves as a filler. Phthalic anhydride with a small addition of maleic anhydride is used as a solidifying agent.

After the introduction of the anhydrides of acids into an epoxide resin, heated up to 80-100°C, the mixture at first becomes more liquid; after further heating it becomes more viscous, and gradually a solid infusible polymer is formed. The electric properties of Compound E-37 (20 per cent polyester) are given in Table 6.

Compound E-37 with a filler is used as a sealing insulation of current transformers for voltages up to 10 kV.

TABLE 6

Conditions of test	Volume resistivity (Ω cm)	Tangent of the loss angle	Electric strength (kV/mm)
At 20°C	$2.6 \cdot 10^{15}$	0.004	24.5
At 100°C	$7.2 \cdot 10^{11}$	0.083	23.0
After remaining 48 hr in a humid atmosphere	$7.9\ 10^{14}$	0.003	–

Fig.2 shows the dependence of the tangent of the loss angle of a sealing insulation on voltage, and Fig.3 the dependence of insulation resistance on temperature.

Fig.4 shows the electric strength as a function of the thickness of the specimen of the compound E-37.

Tan δ somewhat increases with temperature, but within the range of temperatures 20 ± 80°C it remains within the range 0.02-0.08. Under the continuous influence of a temperature of 120°C, the impact strength of the cast insulation preserves its initial value and even slightly increases, from 5 to 7 kg/cm/cm². The compound is easily cast in moulds and easily machined.

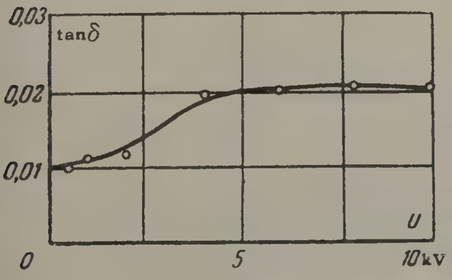

FIG.2. Tan δ as a function of voltage for an epoxide-polyester compound.

Current transformers filled with the fused cast epoxide-polyester compound E-37 with a filler (quartz powder) were tested under short-circuit conditions. These tests showed that they can withstand an electro-dynamic load at short-circuit for a current 500 times above the nominal current, and a thermal load of 1 sec for a current 100 times greater than the rated one. Examination of the sealing insulation of transformers after the short-circuit tests shows a good stability of all characteristics and the absence of any deformations.

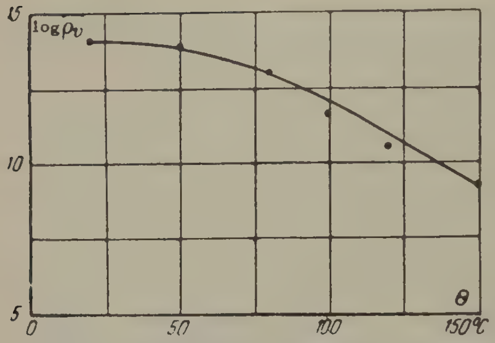

FIG.3. Volume resistivity of an epoxide-polyester compound as a function of temperature.

Epoxide-polyester compounds K-168 and K-293, which are used for hermetic sealing of apparatus, consist of epoxide resin E-37 or ED-6, plasticized by the polyester MGF-9. Compound K-293 contains moreover a filler (quartz powder) and a plasticizer (dybutyl phthalate). As solidifying agents for these compounds hexamethylenediamine or polyethylenepolyamine are used.

Compounds K-168 and K-293 may be used as sealing cold solidifying compounds. They possess the following characteristics: $\rho_v = 10^{12}$-10^{13} Ω cm at 20°C, and 10^{11}-10^{12} Ω cm after reamining 24 hr at + 40°C in a medium of the relative humidity 95 ± 3 per cent; for a frequency 10^6 c/s at 20°C and also after remaining 24 hr at + 10°C in a medium of the relative humidity 95 ± 3 per cent, their tan $\delta < 0.1$ and their resistance to frost is - 60°C.

Polymers based on acrylic and metacrylic esters

Compounds MBK-2 and MBK-3 were developed and are produced on the industrial scale by the All-Union Instrument Scientific Research Institute, Ministry of the Electric Technology Industry; they are based on acrylic and metacrylic esters; they differ from one another in their degree of elasticity, which depends upon the content of plasticizers.

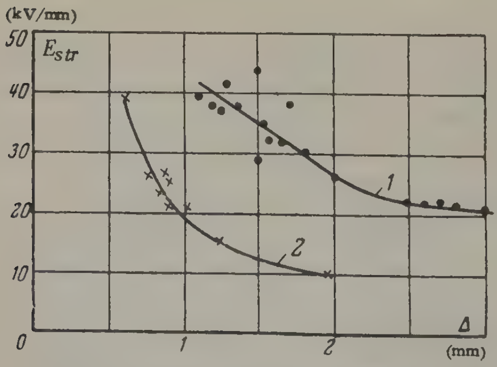

FIG.4. Electric strength of an epoxide compound as a function of its thickness: (1) $\theta = 20°$C; (2) $\theta = 100°$C (puncture in the transformer oil).

Compounds MBK are used in the electrical industry, particularly for insulation in electric motors immersed in water, and also in the radio industry. These compounds are liquids, which polymerize and become solid at temperatures of 100-110°C. By introducing appropriate initiators of polymerization, the MBK compound can be made to solidify even at 20°C.

The principal properties of Compounds MBK, after their polymerization at 70-75°C for 8 hr and after subsequent heating at 100-105°C for 8 hr, are shown in Table 8. The high water-resistance of the compounds MBK permitted their use for the protection of windings of the electric motors immersed in water, which are used for driving water pumps. The windings of these motors successfully withstand a test under hydraulic pressure of 3 atm for 6 hr and the short-circuit conditions in a wet state at - 25°C. After intermittent work in water over more than 1500 hr the insulation resistance of these motors remains at the level of 500 MΩ.

TABLE 7

Characteristics	Epoxide resin	Epoxide polyester compound	Epoxide polyester compound with a filler (quartz powder)
Tangent of the loss angle multiplied by 10^4			
at 20°C	10...20	20...40	100...300
at 80°C	300...500	400...800	600...800
after remaining in water 48 hr	10...30	40...50	—
Volume resistivity, (Ω cm)			
at 20°C	10^{15}	10^{15}	$10^{14}\dots10^{15}$
at 80°C	10^{11}	10^{11}	10^{11}
after remaining in water 48 hr	10^{14}	10^{14}	—
Electric strength (kV/mm)	25...30	25...30	25...30
Permittivity	4.0...4.5	—	5.0...6.0
Impact strength (kg cm/cm^2)	4.0...6.5	6.0...8.0	4.0...6.0
Temporary compression strength (kg/cm^2)	900	—	900
Temporary bending strength (kg/cm^2)	750...1 000	600...750	800...900
Temporary tensile strength (kg/cm^2)	—	—	550
Thermal stability according to Marten's method (°C)	60...70	55...60	60...70

The apparatus coils, which remained for 20 days under conditions of tropical humidity with a periodical dew-fall, show an insulation resistance above 100 MΩ. It has been found that the use of the MBK compounds, which eliminate all cavities in windings, brings about a considerable decrease in overheating of the apparatus coils.

Polyurethane resins

Polyurethane resins recently have found wide practical application in different branches of technology, particularly as adhesive substances. For the manufacture of electric insulation polyurethanes are of great interest; they are compounds of high molecular weight and are based on polyesters and diazocynate. These

TABLE 8

Characteristics	Type of compound		
	MBK-1	MBK-2	MBK-3
Specific gravity	1,06	1,09	1,04
Breaking tensile strength (kg/cm^2)	85...130	–	–
Elongation at fracture (%)	200...250	–	–
Moisture absorption during 24 hr (%)	0.07...0.08	0.07...0.08	0.06...0.08
Moisture absorption during 20 days (%)	0.16...0.17	0.15...0.19	0.10...0.11
Volume resistivity (Ω cm)			
at 20°C	10^{14}	$10^{12}...10^{13}$	$10^{12}...10^{13}$
at 100°C	$10^{12}...10^{13}$	10^{10}	$10^{10}...10^{11}$
after remaining in water for 10 days	$10^{12}...10^{13}$	$10^{11}...10^{12}$	$10^{12}...10^{13}$
Tangent of the loss angle at 50 c/s			
at 20°C	0.06...0.062	0.036...0.042	0.002...0.009
at 100°C	0.005	0.19...0.34	0.010...0.017
after remaining in water for 10 days	0.07...0.08	0.04...0.06	0.007...0.010
for frequency 10^6 - 10^7 c/s			
at 20°C	0.01	–	–
Permittivity at 50 c/s			
at 20°C	2.9...3.1	4.0...5.6	4.0...4.7
at 100°C	4.1...4.3	4.5...5.4	3.6...4.2
after remaining in water for 10 days	3.6...3.7	4.2...5.8	4.1...4.9
Electric strength (for a specimen about 1 mm thick) (kV/mm)	20...28	18...21	18...21

polymers can be obtained in the form of films, resistant to the action of solvents, of rubberlike materials, porous materials etc.

They are of great interest in the production of conductors with an enamel insulation. The high adhesive capacity of polyesteruretanes to copper, good stability in the presence of solvents and comparatively high mechanical strength of the lacquer film ensure the good qualities of enamelled conductors.

Enamelled conductors with polyesteruretane insulation are similar in their properties to conductors insulated by polyvinylacetate resins of the type vinyflex or formex, and they can be used for windings of electric machines and apparatus for a continuous working temperature of up to 120°C.

Silico-organic polymers

Silico-organic polymers – polyorganosiloxanes as opposed to high molecular weight substances discussed above – are compounds in which molecular chains are built not from carbon atoms, but from silicon and oxygen surrounded by organic groups. Such a structure of molecules determines a series of properties which differs from those of the organic polymers already discussed.

In the first place, the non-organic framework of the molecules gives rise to their high thermal stability, photo-stability, and resistance to atmospheric influences. The ratio of organic groups to silicon atoms in polyorganosiloxane resins exerts a great influence on the properties of polymers. In polyorganosiloxane resins the ratio of organic groups to silicon atoms is smaller than in polyorganosiloxane rubbers. This enables us to obtain thermo-setting resins forming lacquer films, which have a considerable number of cross-links between the basic chains of molecules. In consequence these films, as a rule, possess rather low thermoplasticity at high temperatures.

Polyorganosiloxane resins are copolymers, containing alkyl and aryl groups on silicon atoms. By varying the relative proportion of these groups and also the ratio between all organic groups to silicon atoms it is possible to obtain polymers with different degrees of elasticity, starting with an elasticity typical of a rubber, up to a brittleness approaching that of glass. Polyorganosiloxane resins are easily dissolved in ordinary solvents and mix together; in this way we may also give them the properties that we want.

Industry produces various polyorganosiloxane resins and lacquers based on them and also polydimethylsiloxane rubber. All types of materials for working temperatures of 180°C (Class CB) are produced by electrical insulation factories on the basis of polyorganosiloxane resins; these materials are used for insulation of electric machines and transformers [11].

Among new polyorganosiloxanes it is necessary to mention types K-55 and K-43, which are already used in practice. Some properties of polymers are shown below; they were recorded in the All-Union Institute of Electric Technology. Fig.5 shows the electric strength and volume resistivity of polymer films as functions of temperature within a range of 20-350°C; Fig.6 shows some characteristics of pigmented films of a polymer. Non-pigmented films have a volume resistivity more than 10^{12} Ω cm and electric strength about 40 kV/mm at 350°C.

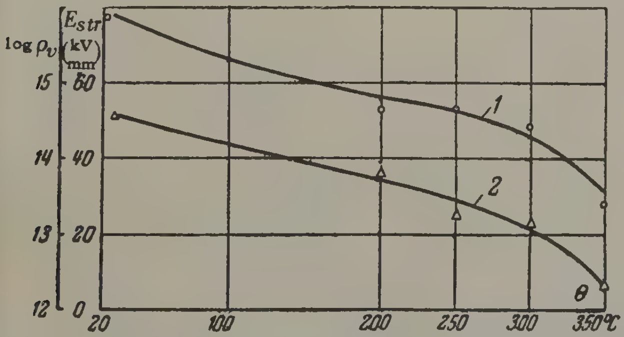

FIG.5. Electric strength E_{str} (curve 1) and volume resistivity ρ_v (curve 2) for films of the polyphenyldimethylsiloxane polymer K-55, as functions of temperature.

Data related to thermal ageing of films of polymers (K-55 and K-43) in a pure state and pigmented bimetal oxides (PKE-14 and

PKE-19) are shown in Table 9. Films were heated to a fixed temperature, and their cracking after ageing was observed. The variation in the electric strength of films on a copper underlayer after ageing at temperatures 250°C and 300°C is shown in Table 10.

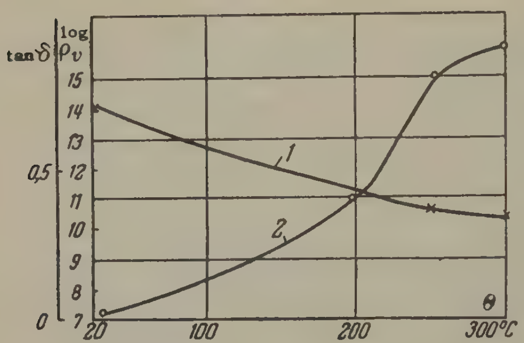

FIG.6. ρ_v (curve 1) and tan δ (curve 2) of films of the polyphenyldimethylsiloxane with a mineral pigment (enamel PKE-19), as functions of temperature.

By using the polyphenylmethylsiloxane resin as a bonding substance we obtain heat-resistant plastic substances. Table 11 shows certain properties of plastic substances with an asbestos filler and a glass-cloth filler. Curves of tan δ, E_{str} and ρ_v as functions of temperatures are shown in Fig.7. Dependence of electrical properties of the polyphenylmethylsiloxane resin with an asbestos filler on temperature is shown in Fig.8; Fig.9 shows the electrical properties of a polymethylsiloxane rubber, deposited on a glass-cloth.

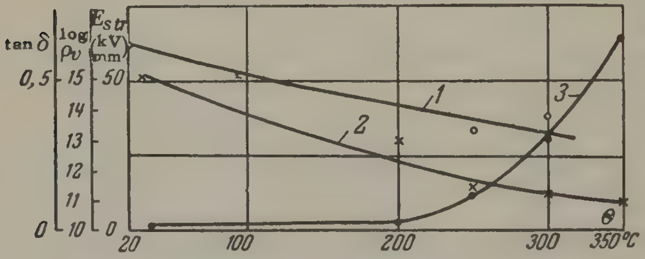

FIG.7. E_{str} (curve 1), ρ_v (curve 2) and tan δ (curve 3) as functions of temperature for polyphenyldimethylsiloxane on a glass cloth (glasslactocloth LSK-7).

Among heat-resistant materials which can be used as electrical insulators, it is necessary to mention the blockcopolymer, which is obtained from polydimethylsiloxane elastomer and polytetrafluorethylene. Fig.10 shows the mechanical properties of a resin based on a blockcopolymer, containing 70 per cent of a metal oxide as a filler, as functions of temperature; Fig.11 shows the variation of its mechanical properties during the process of ageing; tan δ and ρ_v as functions of temperature are shown in Fig. 12.

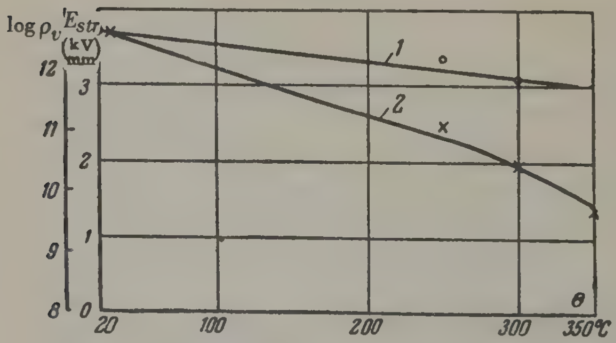

FIG.8. E_{str} (curve 1) and ρ_v (curve 2) as functions of temperature for polyphenylmethylsiloxane with an asbestos filler (plastic material K-41-5).

As can be seen from

these data, polyorganosilaxone polymers and blockcopolymers of a polydimethylsiloxane rubber with polytetrafluorethylene possess high electrical properties even at temperatures 250-300°C and a considerable thermal stability at high temperatures. These properties permit their use in conjunction with asbestos, glass, mica and other inorganic substances for the production of insulation which can work for a short time at temperatures above 200°C.

TABLE 9

Type of the polymer	Underlayer	Time (hr) after which cracks appear on films for temperature of heating shown (°C)		
		250	300	350
K-55	Copper	(more) 240	100	120
	Steel	” 1800	1800	1000
K-43a	Copper	340	100	
	Steel	—	768	120
PKE-14	Copper	240	50	
	Steel	—	—	1200
PKE-19	Steel	2880	1800	840

TABLE 10

Characteristics	Time (hr)				
	0	200	500	10	30
	Temperature (°C)				
	250	250	250	300	300
E_{str} (kV/mm) at 20°C at 250°C	 74.8 57.6	 58.3 50.6	 46.6 25 . . 30	 10 . . 15 —	 7 . . 10 —

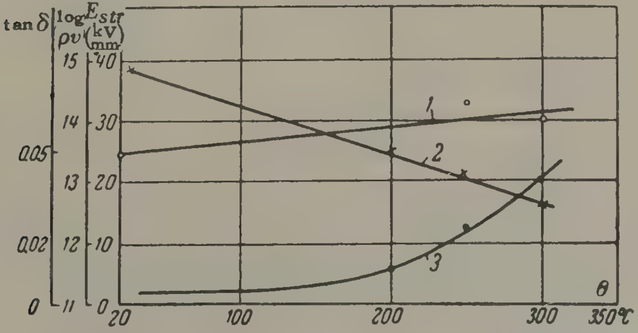

FIG.9. E_{str} (curve 1), ρ_v (curve 2) and tan δ (curve 3), as functions of temperature of resinglass-cloth RSLT.

TABLE 11

	Characteristics	Initial state	At 250 °C	At 350 °C	Temperature (°C)			
					250	300	350	420
					Time of ageing (hr)			
					500	30	20	30
Polyphenylmethylsiloxane with an asbestos filler (plastic material)	E_{str} (kV/mm)	5.2		5.0	4.2	4.4	3.8	2.8
	Static bending stress (kg/cm²)	320		—	264	220	218	257
	Impact strength, (kg.cm/cm²)	5.6			4.5	4.3	4.1	2.7
	Thermal stability, according to Marten's method	400		—	—	—	—	—
Polyphenylmethylsiloxane with a glass-cloth filler (glass-textolite)	E_{str} (kV/mm)	17.8	13.0	9.4	3.3	3.0	—	—
	ρ_v (ohm.cm)	$1.6 \cdot 10^{14}$	$8 \cdot 10^{11}$	$1.6 \cdot 10^{11}$	$1.7 \cdot 10^{14}$	$3.9 \cdot 10^{14}$	—	—
	$\tan \delta$	0.004	0.12	0.8	0.002	0.002	—	—
	Static bending stress (kg/cm²)	1 360	—	—	1 280	1 325	—	—

N.B. Thickness of specimens during tests, 2 mm.

Conclusion

Synthetic polymers discussed in this article cannot satisfy all requirements of modern electrical technology. It is necessary to work on the synthesis of new polymers possessing high mechanical strength, good electrical properties and moisture resistance; this should be done by pursuing investigations in order to obtain new organic polymers, and also polymers containing non-organic elements in molecular chains. Non-organic molecular chains of polymers will make them more similar in their properties to non-organic substances, and surrounding groups, containing carbon, will make them similar to organic polymers.

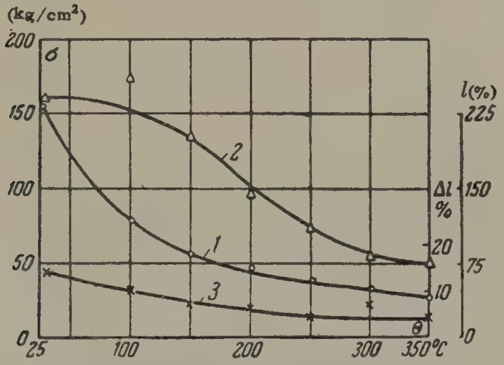

FIG.10. Mechanical properties of a thermostable polymethylpolytetrafluorethylene blockcopolymer with zinc oxide filler as functions of temperature (1) tensile strength σ; (2) of relative elongation l; (3) of total elongation Δl.

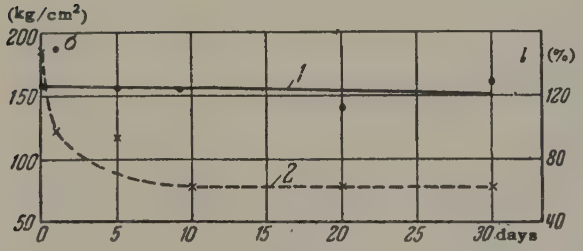

FIG.11. Tensile strength σ (curve 1) and relative elongation l (curve 2) as functions of the time of heating at 350°C.

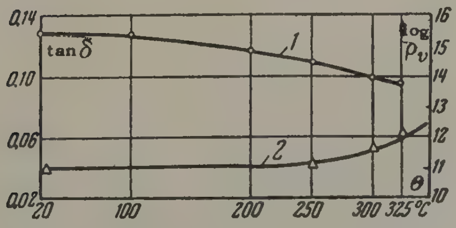

FIG.12. ρ_v (curve 1) and tan δ (curve 2) as functions of temperature.

It is important to work on the development of such polymers, which will decrease the big difference in quality which exists between organic and inorganic polymers in such important properties as thermal stability, elasticity and mechanical properties. Organic polymers, with their exceptionally valuable elastic properties and mechanical strength, do not possess the desired thermal stability; inorganic polymers lack elastic properties.

One of the most important problems which research workers should solve as soon as possible is the synthesis of available polymers, which will possess both a set of properties indispensable for dielectrics and such a thermal stability as would exclude the necessity of limiting the operation of a machine or apparatus by temperatures of Class A, B and even (in many cases) CB.

Such a solution of the problems of insulation would not only facilitate the work of designers, but would also permit the construction of improved and operationally reliable machines, apparatus and other electrical devices.

Translated by S. Szymanski

REFERENCES

1. G. Nata; *Makromol Chem,* No.3, 213 (1955).
2. I. Nearli and W.S. Skinners; *Silk Rayon Record,* 30, No.4, 354 (1956).
3. E. P. Muller; *Kunststoffe,* 41, No.13 (1951).
4. B.S. Parkyns; *British plastics,* 24, No.264, 479 (1951).
5. C.M. Zaffon; *Trans. Amer. Inst. Elect. Engrs.,* 70, 421 (1951).
6. K.A. Andrianov, M.S. Rakitskaia and A.G. Prelkova; Elektroizoliatsionnye kompounndy na osnovye polie' firnykh smol. (Electrical insulating compounds based on polyester resins), *VEP,* No.2 (1956).
7. B. Tolentino; *Moderic plastiche,* 20, No.9, 623 (1954).
8. R. Weller; *Paint Technol.,* 18, No.207, 151 (1954).
9. K.A. Andrianov, L.N. Iukina, A.V. Koval' skaia and M.S. Rakitskaia; Litaia izoliatsia na osnovye epoksidnoi smoly (Sealing insulation based on epoxid resins), *VEP,* No.11 (1956).
10. *Modern Plastics* No.11, 147 (1955).
11. K.A. Andrianov; *Kremniiorganicheskiye teplostoikiye dielektriki (Silico-organic thermostable dielectrics),* Gosenergoizdat (1957).
12. M.I. Garber (Editor); *Ftoroplasty (Fluoroplastics),* Goskhimizdat, Leningrad (1954).

APPARATUS FOR LOW-VOLTAGE DISTRIBUTION GEAR*

P.V. SAKHAROV

All-Union Correspondence Institute of Power Engineering

Uninterrupted and rapid growth of the Russian national economy and steadily increasing production and service requirements pose new problems to our apparatus-making industry; better apparatus for low-tension distribution gear is needed and production should be sharply increased.

During recent years considerable progress has been made in the design and production of this type of apparatus.

In this article, the present situation and the technical level of the design of the basic series of industrial apparatus for low-tension distribution installations made by industry in the Soviet Union are discussed, and comparison is made with the best foreign apparatus. Problems and tendencies in the further development of the design of this apparatus are also discussed with reference to catching up with capitalist countries and overtaking them in the field of production of electrical apparatus.

Basic trends in the development of design

Besides general modern requirements, such as decrease of weight and of dimensions, unification and normalization of details, the use of high protective technological methods and the lowering of cost, basic tendencies in development in the design of distribution installations in the U.S.S.R. and in foreign countries as well are:

(a) increase of the limit switching capacity in connexion with the increased installed power of electric gear;

(b) development of design of separate apparatus with a view to fitting them into complete sets and to quick exchange of the apparatus for inspection and repair; i.e. providing the apparatus with contact connectors and devices, which allow the apparatus to be withdrawn from complete sets;

(c) development and increase of production of the complete low-voltage distribution sets, the major part of all apparatus being produced in the assembled form;

(d) development and manufacture of series additional to the basic series of apparatus, for example in order to increase the range of nominal permissible currents; production of dust- and water-proof apparatus and others; all this should be done in order to satisfy fully the needs of the different branches of the national economy.

---

* *Elektrichestvo*, No. 4, 10–15, 1958.

It is also necessary to mention the tendency in many installations to replace knife switches and protectors by automatic breakers. Such a replacement is desirable in important switchgear, where a rapid restoration of feeding or automatic breaking under abnormal conditions (and not only at over-currents) is necessary, or where remote control is to be used. Moreover, the dimensions of automatic breakers are smaller than those of knife-switches with fuses.

For protection of networks with very large short-circuit currents, fuses are much simpler and more reliable than automatic circuit-breakers. Moreover, the limit breaking-capacity of widely used automatic circuit breakers is considerably smaller than the capacity of breakers with a fusible link and filling for the same rated current. Because of this, in the U.S.A. during recent years automatic breakers with H.R.C. fuses have been widely used. They ensure a reliable protection of networks, by automatic devices, from overloads, and by fuses from short-circuits.

Automatic circuit-breakers for switchgear

Our national industry produces two series of automatic circuit-breakers for switchgear in general industrial use:

(a) automatic breakers, Series A 3100, for currents 15-600 A and voltages up to 500 V a.c. or 220 V d.c. with a limit breaking-capacity up to 50 kA a.c. (shock current), or up to 25 kA d.c.;

(b) automatic breakers, AP 25, for currents 1-25 A and voltages up to 3.80 V a.c. or 220 V d.c. with limit breaking capacity 3 kA a.c. (shock current) and 2 kA d.c.

These automatic devices up to this time were not inferior, so far as their basic technical characteristics are concerned, and particularly in their limit breaking-capacity, to the best foreign constructions. Nevertheless, we have to add that similar apparatus of foreign make is manufactured in a greater variety of models. For instance the Westinghouse Co. (U.S.A.) makes switchgear automatic breakers, Series AB, for rated currents 400 and 800 A – double-pole and four-pole ones with an electrodrive, voltage-reducing relays, distance tripping, block contacts, plug-contacts, and types filled with oil, dust-proof and water-proof, and others. Moreover, in 1956 the I.T.E. Co. (U.S.A.) designed an attachment for switchgear automatic apparatus, containing a fusible link (protector), with a spring mechanism. If the fusible link melts in any of the poles, the trigger is released. This attachment, owing to the current limiting action of fusible links, ensures protection by the automatic breakers of networks in which the short-circuit currents may reach the value of 80 kA (effective value of a symmetrical component), i.e. for a shock current up to 160-190 kA.

Establishments of the electrical industry in the U.S.S.R. are working on the improvement and development of new automatic devices for switchgear. The Khar'khov Electro-mechanical Factory (KhEMZ) has designed new automatic apparatus, Series A 3100, with distance triggers, with block and plug contacts and so on. The Kursk Electrical Apparatus Factory (KEAZ) is now preparing the production of a small single-pole automatic breaker type A015 for current up to 15 A for industrial installations and big buildings; this model was designed by the Science and Research Institute of the Electrical Industry (Fig. 1).

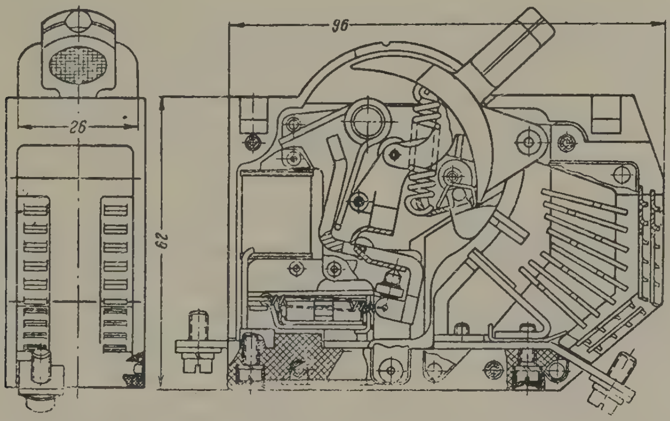

FIG. 1. Automatic single-pole circuit-breaker for currents up to 15 A, Type AO 15.

It is necessary to continue the work in order to increase the breaking-capacity and to develop several additional types of automatic apparatus of Series A 3100. Moreover, it is necessary to develop a small automatic apparatus for currents up to 15 A of a simple construction and to organize its mass production in order to replace the screw fuses in communal and other networks.

Universal automatic circuit breakers

The universal automatic circuit-breakers Series A-2000 for currents 200-1500 A, which were made until recently, are considerably inferior in their basic performance characteristics to the leading foreign constructions and do not satisfy altogether the increased modern requirements for electric supply.

Ul'ianov Apparatus Factory redesigned the construction of automatic apparatus Series A-2000, and started series production of universal-selective automatic breakers Series A 15, A 20 and A 25 for currents 100-1800 A and voltages up to 380 V a.c., 50 c/s with a limit breaking capacity up to 50 kA (shock current) and for voltages up to 440 V d.c., up to 30 kA. Nevertheless, we have to add that this series does not yet satisfy all modern requirements, in particular as regards limit breaking capacity and variety of types, and is inferior to leading foreign constructions.

Among foreign automatic apparatus, the Series AK-1 of the General Electric Co. (U.S.A.) deserves the greatest attention. Apparatus of this series is made for nominal currents of 600, 1600, 3000 and 4000 A, 250 V d.c. and for 600 V a.c., 60 c/s. This equipment has a limit breaking capacity of 25, 50, 75 and 100 kA respectively (effective value with a constant component included), or approximately 40, 80, 120 and 160 kA (shock current).

Greater compactness, in comparison with other similar constructions, has been achieved by using in every pole a few parallel connected contacts, separated by partitions of the arc extinction chamber. In this case, the high limit breaking-capacity of the apparatus was achieved by establishing a current loop by fixed spring contacts; this current loop produces a compensating effect for electrodynamic forces, which rejects the contacts in the case of large short-circuit currents. The apparatus is provided with a spring drive, which is wound by a small electric motor, selective tripping devices for maximum current with various time lags and is capable of instantaneous action.

Fig. 2 shows the protective characteristics of the three automatic breakers of this series. This automatic apparatus may be fitted into the complete gear, and the automatic breakers made for different rated currents are of the same height and depth, owing to the use of unified component parts. Flexible current leads are absent; instead, silvered cylindrical rods are used which conduct the current through the joints of mobile parts equally well.

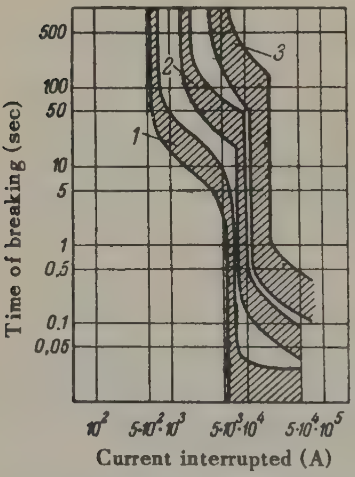

FIG. 2. Protection characteristics of automatic breakers of Series AK-1. (1) AK-1-25, $I_{nom} = 600$ A; (2) AK-1-75, $I_{nom} = 1600$ A; (3) AK-1-100, $I_{nom} = 3000$ A.

The basic constructional solutions mentioned above, such as the parallel contact connexion and the use of the current loop, are applied in other series of foreign automatic breakers, for instance in the automatic apparatus Series R 913/R 914 of the Siemens Co. (Federal German Republic).

It is interesting to mention the use of electromagnetic contactors instead of automatic breakers in low-voltage distribution systems. Telemechanique Electrique Co. (France) make contactors of two types: contactors for currents of 125-2750 A and voltages up to 500 V for work with fusible links, and automatic contactors for currents 800-2750 A and voltages up to 500 V, with limit breaking capacity 30-65 kA, respectively (effective value of a symmetrical component), or approximately 60-130 kA (shock current).

On the basis of the above discussion we come to the conclusion that it is necessary to develop a new series of home built universal selective automatic breakers for currents up to 4000 A. Their design should allow for fitting into the complete distribution gear.

Fusible link protectors

Fusible link protectors are a simple, reliable and cheap means of protecting electrical gear from short-circuits and considerable overloads.

At present in the Soviet Union and in foreign countries three basic kinds of low-voltage fuses are widely used: a tube fuse without a filler, a tube fuse with a filler and a screw fuse. Fig. 3 shows diagrams of the weights of these kinds of fuse, made by our national factories.

Tube fuses without a filler of PR-1 series, made by the Electrical Apparatus Factory, Ufa, have been improved during recent years. A modernized series called PR-2 has ratings, including the limit breaking capacity, not inferior to the best foreign fuses of similar construction.

The factory continues its work for further increase of the limit breaking-capacity by increasing the strength of the tube cartridges.

Substantial disadvantages of tube fuses without a filler – and this also applies to Series PR-2 – are their large size and weight, the considerable amount of labour needed for their manufacture due to the lathe turning and threading operations, and the large amount of non-ferrous metals required. The use of Series PR-2 fuses should be restricted to installations where it is not expedient to use fuses with a filler due to conditions of fuse refilling, for example in mobile installations.

Tube fuses with a filler have, in comparison with fuses without a filler, a considerably higher limit breaking-capacity; they occupy less space, require less labour for their production and are approximately twice as cheap.

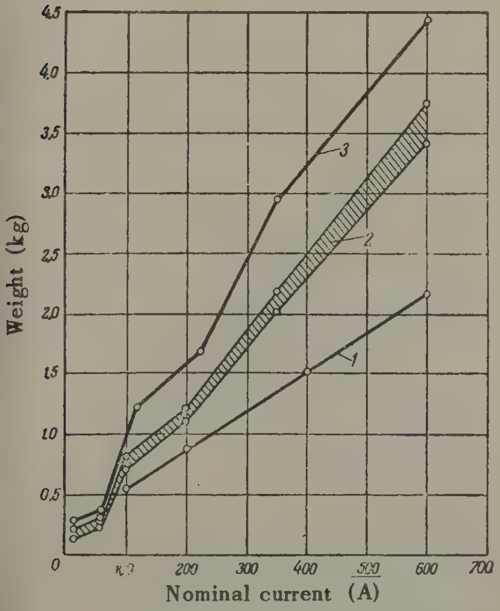

FIG. 3. Weight of protectors. (1) Series PN2; (2) Series PR2 (short and long, with a front-and-back leads connexion); (3) Series PD5.

In the U.S.S.R. until recently fuses with a quartz filler were made of Types NPN, NPR, PNR, A and KP; in these fuses the fusible link is made of copper and not of silver, as in the European constructions. At present the construction of these fuses is already obsolete.

The Factory of Electrical Apparatus, Kursk, has developed demountable fuses with quartz filler of a new series, PN-2, for currents 100, 250, 400 and 600 A and voltages up to 380 V. For putting the cartridges in the contact rack frames and for repair, a plastic detachable handle is provided.

Series PN-2 fuses, according to their basic ratings, are up to the modern technical level, but their limit breaking-capacity is not yet determined. Moreover, fuses of this series are rated only for use on a.c.; the cartridges give no indication that a fuse has "blown". There is no fuse for 1000 A. No construction allows for the back connexion of leads.

Among the best foreign low-voltage fuses with quartz filling, fuses made by

Siemens and A.E.G. (Federal German Republic) deserve the greatest attention. A distinctive feature of these fuses is the use of a fusible wafer link, made of thin copper metal sheet and soldered in the middle by easily melting metal (Fig. 4). The link consists of strips joining all longitudinal bands; when the arc is struck, all longitudinal bands melt. The limit breaking-currents for these fuses, at nominal currents 200, 350, 600 and 1000 A and voltages 380 V a.c. and 440 V d.c., are equal to 70, 50, 50 and 50 kA, respectively (effective value of a symmetrical component), i.e., approximately 140, 100, 100 and 100kA (shock currents). Cartridges are easily taken to pieces and are provided with an indicator for when the fuse has "blown".

The basic problem in the further development of national cartridge fuses with filling is to redesign PN - 2 series in order to eliminate the above defects.

Fuses with a threaded cartridge, which is screwed into a base ("plug"), for currents of 6 - 20A and a voltage of 250V, with a limit breaking capacity of 600 A, are widely used in the Soviet Union for lighting purposes and also in control networks and in low-power installations. During recent years, these fuses have been considerably improved: dimensions of the porcelain base are considerably reduced, and the porcelain cover is replaced by a plastic one. But the most important detail of the fuse – the cartridge itself – was not improved, and the limit breaking-capacity of these protectors is still low; moreover, there is no indicator in the cartridge that the fuse has "blown".

In Western European countries, screw fuses in general use are usually made for currents up to 60A. The fuses have a removable steatite cylindrical cartridge, inside which are inserted fusible links with a quartz filling; the cartridges are provided with an indicator showing whether the fuse has "blown". These fuses are similar to the fuses type PD and PDS which are made by our factories. The limit breaking capacity of Western European fuses is several times greater than that of general fuses made by our national factories.

Since screw fuses, which are manufactured in the U.S.S.R. in tens of millions, are widely used and play an important role in the protection of electric networks and against fires, it is urgent that a new series of general purpose fuses should be developed for currents 6, 10, 15, 25, 40 and 60A.

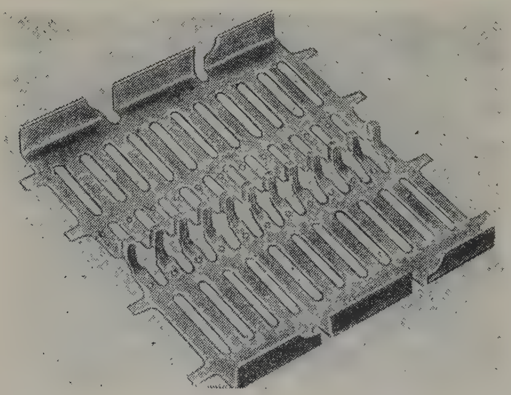

FIG. 4. Fusible link of a protector with fillings, of the Siemens Co. (Federal German Republic).

In foreign countries, particularly in the U.S.A., inertial fuses are widely used, mainly for the protection of synchronous motors from overloads. In these fuses, we may use conductors of smaller cross-section than in ordinary high-speed fuses. Inertial fuses have two elements:

one which melts at overloads, and another which melts at short-circuits; this construction allows us to dispense with a starter with a thermal relay and to replace it by a non-automatic circuit-breaker with such fuses. This brings down the total cost of the apparatus, although inertial fuses are more expensive than ordinary ones.

Non-automatic power circuit-breakers and switches

Among different constructions of power circuit-breakers used in the U.S.S.R. and abroad we may distinguish three basic types: packet-type breakers and switches, knife-breakers and switches, and breaker-protectors.

Packet-type breakers and switches are more and more widely used because of their smaller overall dimensions in comparison with the other power breakers and switches. The smaller dimensions are due to two-stage current-breaking and to arc extinction in a closed chamber with fibre disks.

Tashkent Electrotechnical Factory has recently modernized a series of breakers and switches. The new type, which received the series name PV, is designed for nominal currents 10/6, 15/10, 25/15, 40/25, 60/40, 100/60, 150/100, 250/150 and 400/250 A and voltage 220 V d.c. (the value of the current is shown in the numerator), or for 380 V a.c., (the value of the current is shown in the denominator). In this series three new sizes were included, and in the three other sizes the rated current values were increased.

In switches with complicated circuits, sizes and weights are decreased due to the change in the contact shapes. The technical performance of the new series is not inferior to the performance of the best foreign packet-type breakers and switches.

Among the new foreign constructions the three-pole breakers of the Westinghouse Co. (U.S.A.) and of the Arrow Co. (England) deserve attention. The mobile contact system of these breakers is similar to the construction of the packet-type Series PV breakers, but fixed contacts are situated on a plastic or ceramic flat rectangular base. The advantage of this construction is the use of the easily removable cover which offers access for inspection and repair of the contacts; this is absent in the packet-type breakers of the PV series.

Knife circuit-breakers and switches made by our home factories may be divided into two series. The Electric Apparatus Factory, Ufa, finished the development and started the production of a new series for currents of 100, 250, 400 and 600 A and voltages up to 500 V. Breakers and switches of this series are provided with a side handle with side and central lever drives. The use of arc extinction chambers has greatly increased the breaking capacity of this apparatus.

The second multiampere series for nominal currents up to 30 kA was developed and put into production during the last few years by the Khar'khov Electromechanical Factory. Both series of knife breakers and switches are not inferior to the best similar foreign-made devices.

Breaker-protectors are devices that perform the functions both of cut-outs and protectors, and of knife-breakers and protectors. Such a unification of the two separate pieces of apparatus into a single one permits a decrease in overall dimensions and allows a reduction in the size of complete switchgear. Moreover, an economy in copper is achieved, because the blades of knife-switches or of cut-outs are replaced in such an apparatus by the fuse cartridges. Moreover, in an unified apparatus total circuit-breaking occurs in two stages, and this contributes to the arc extinction. The number of contact junctions is also reduced, and the energy losses due to contact heating are cut. Nevertheless, the complication in contact and kinematic nodes is an obstacle to the wider use of this apparatus.

In the U.S.S.R. only the Saratov factory makes small quantities of breaker-protectors. Because of defects in the design of this apparatus, constructions of a new type are being developed.

In foreign countries in recent years, the use of breaker-protectors has been spreading. The English firm, Lancashire Dynamo, makes breaker-protectors which can be fitted into switchgear. This equipment is made for currents 30-400 A and voltages 660 V a.c. and 250 V d.c. The English firm of Dorman and Smith makes similar apparatus for currents up to 300 A and 500 V with butt-joint contacts (not wedge joint as is usual).

American firms, for example the General Electric Co, also make breaker-protectors. In the German Democratic Republic disconnector-protectors are made.

Taking into account the advantages of breaker-protectors, it is necessary to speed up their development and to organize their production in our national factories.

Complete distribution gear

During recent years, low-voltage apparatus for distribution gear has been made in the form of complete devices, which may be divided into five types.

Complete distribution gear with universal selective automatic apparatus was made by the Moscow Transformer Factory for individual orders as component parts of complete transformer substations. Such complete distribution devices without transformers are needed for the secondary distribution points in industrial plants. Moreover, the existing construction of these devices is already obsolete, and it is necessary to develop new designs of complete distribution gear.

Complete distribution gear with automatic apparatus Series A-3100 are made by the Khar'khov Electromechanical Factory in the form of cubicles Type SU, which are situated in the walls of buildings. Distribution devices of this type, in dust- and water-proof casings, were recently developed by this factory. This apparatus is not inferior to the best foreign-made equipment.

The development of complete distribution gear of a new design, fitted with plug contacts, is required to permit quick exchange of an automatic apparatus which needs inspection or repair.

Boxes, cubicles, cells with fuses, knife switches, knife-switch-protectors, packet-type breakers, all assembled in one complete distribution gear, dust- and water-proof, are needed for many branches of the national economy. In the first place, these branches are: agriculture, building trade, forest, coal, textile, light industry, food and other branches of industry.

At present, boxes and cubicles are made only in limited quantities and only by special order. Their construction does not satisfy the requirements of mass production and use.

At present the building industry trade "Elektromontazhkonstruktsiaa" has developed a series of boxes, which are assembled into complete gear. It is important that their mass production should be organized and that the development of new types of this series should be continued.

Distribution boards for small electric power stations of Type ShUP, developed by the "Armelektrozavod" factory, are now produced in great quantities in connexion with the intensive building of small agricultural and industrial hydraulic power plants and of small electric power stations, driven by steam engines or by gas generators. Distribution boards of Type ShUP are used for the control of synchronous generators of outputs up to 150 kVA, 400/230 V, and for the power distribution in a few feeders.

The construction of these boards satisfies modern requirements and is not in ferior to the best foreign-made apparatus of this kind. Control boards of two types for electric stations and substations are made by our home factories.

The Leningrad factory "Elektropult" has produced control boards for many years. Control boards of the same design are also made by the Khar'khov Electromechanical Factory. During the last few years in the TsKB "Elektroprivod", control and protection boards of a new design have been developed, and their production is carried out by Novosibirsk Turbo-generator Factory and Minsk Electro-technical Factory. These boards differ from those made by "Elektropult"; they are of block construction. In every block the control and protection devices are collected separately for every individual object, generator, transformer, line etc. In the most widely used two-row type on the front panel are placed measuring instruments, control keys and buttons, signalling apparatus and circuit diagram. Protection and automatic relays are located on the back panel.

A passage is provided inside the block. In the single-row construction, the apparatus of the single block is placed on one or two closely situated panels. In comparison with the board designed by "Elektropult", the weight of the board of KU type is on the average 20-30 per cent less, the length is smaller by 15-20 per cent, and the depth in comparison with a two-row board, consisting of two separate panels, control and protection panel assembled together, is smaller by 700 mm. These control boards are not inferior to the best foreign-made boards.

Among the newest solutions in the design of complete distribution boards in foreign countries we have to mention the use of frontal panels made from transparent insulation materials, which enables the operator to watch the apparatus from his place (firms in the Federal German Republic), and also the use of luminous elements in circuit diagrams, including straps representing busbars, (A.S.E.S., Belgium).

Conclusion

During recent years our home factories have developed and put into production a series of apparatus of low-voltage distribution gear. The output of this apparatus has been greatly increased.

Nevertheless, so far as technical characteristics and performances of some series, particularly of automatic breakers, are concerned, this apparatus does not satisfy modern requirements and is inferior to the best foreign-made apparatus.

In order to ensure the further development of the designs under consideration and to organize the production of apparatus for low-voltage distribution gear along the lines discussed in this article, it is necessary, besides the enlargement of the production basis, to take several measures, of which the most important are:

(a) development of the scientific research and laboratory establishments, in particular the setting up of laboratories for the investigation of breaking capacity in the Science and Research Institute of Electrical Industry, and in certain factories, designing and producing apparatus for low-voltage distribution gear, for instance in the Ul'ianov, Ufa and Kursk factories;

(b) the carrying-out of all scientific and research work in accordance with a unified plan; these tasks are to be carried out by all establishments developing low-voltage apparatus, by the research institutes and by the universities; investigations should deal with problems concerning contacts, arc extinction, kinematics and dynamics of the apparatus, and the use of new materials;

(c) the unification, normalization, standardization and development of All-Union series of apparatus for low-voltage distribution gear;

(d) development and production of the new improved electrical insulating, conductive and magnetic material.

Translated by S. Szymanski

INVESTIGATION OF TRANSIENT PROCESSES IN LINEAR CIRCUITS BY THE METHOD OF LOCI*

G.V. OSTROUMOV
Khar'khov Lenin Polytechnic Institute

Received 21 May 1957

The loci method is generally used in the theory of automatic control for the analysis of transient processes in linear networks (the separation of the stability regions with the help of the D-division method [1]. In the present article the method of loci is extended to the problem of finding the roots of the characteristic equation for linear oscillating systems.

The proposed method is the most effective when it is applied to the investigation of the effect exerted by a certain circuit parameter on the transient process. The method is based on a construction on the complex plane which gives the locus of the roots for the characteristic equation of the circuit, when the locus corresponds to all possible (i.e. real) values of the circuit parameters. A general method of finding the analytical equation of the locus is given in the article. The construction of the locus according to its equation avoids the necessity for a numerical solution and considerably reduces the volume of calculation.

Consider the practical application of this method to an example, of the calculation of the transient process in the two-frequency circuit shown in Fig. 1.

The circuit is one of the phases in a three-phase system with a circuit-breaker B, the contacts of which are opened. At the moment when the arc is extinguished, the process of voltage recovery u_B across the contacts of the breaker begins. As usual, a shunt resistor is applied in order to ease the operation of the circuit-breaker, which leads to the reduction of the speed with which the voltage builds up. Now we set out the problem of investigating the influence of the shunt resistor value on the process of building up the voltage u_B. This problem directly arises at the selection of the shunt resistor value.

In the majority of cases the process is so quickly attenuated that we can disregard the variation of the mains voltage during the build-up time of the voltage.

---

* *Elektrichestvo*, No.4, 22-26, 1958.

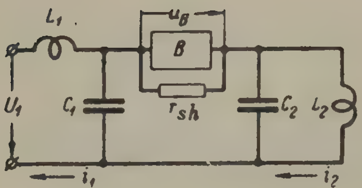

FiG. 1. The calculated circuit.

In addition, after the extinction of the arc the remaining admittance of the gap becomes vanishingly small very quickly. Therefore, we shall assume (as usual in the calculation of a voltage-recovery [2]) that during this process the e.m.f. of the source, and consequently the input voltage U, remains constant and that the residual admittance of the gap is zero. We shall assume furthermore that the extinction of the arc takes place when the arc current goes through zero and that the voltage across the gap at the moment of extinction is zero [2, 3]. Then the initial conditions of the process are expressed by the equations:

$$i_1(0)=i_2(0)=0;\; u_{C1}(0)=u_{C2}(0)=U_1\frac{L_2}{L_1+L_2}. \tag{1}$$

For convenience, we introduce the dimensionless independent variable

$$\tau=\frac{1}{\sqrt{L_1C_1}}t=\omega_{01}t. \tag{2}$$

The form of the voltage recovery $u_B(\tau)$ with the initial conditions (1) has the following form:

$$u_B(p)=U_1\frac{p^2\frac{1+k_C}{1+k_L}+\frac{k_C}{k_L}}{p^4+\varepsilon b_3p^3+a_2p^2+\varepsilon b_1p+a_0}. \tag{3}$$

The coefficients occurring in (3) are the following:

$$k_C=\frac{C_1}{C_2}\quad k_L=\frac{L_2}{L_1};\quad \varepsilon=\frac{\omega_{01}L_1}{r_{sh}};\quad a_0=\frac{k_C}{k_L};$$

$$b_1=\frac{k_C}{k_L}(1+k_L);\quad a_2=1+\frac{k_C}{k_L};\quad b_3=1+k_C.$$

Equating the denominator of (3) with zero, we obtain a characteristic equation of the fourth order:

$$p^4+\varepsilon b_3p^3+a_2p^2+\varepsilon b_1p+a_0=0. \tag{4}$$

The value of the shunt resistor occurs only in coefficient ϵ, which is itself a variable parameter in this particular case. The locus corresponding to the various values of parameter ϵ can be found in the following way.

We solve equation (4) relative to ϵ:

$$\varepsilon=-\frac{p^4+a_2p^2+a_0}{b_3p^3+b_1p}. \tag{5}$$

Assuming that ϵ is a function of $p = x + jy$ (in relative units x is the attenuation factor, y the angular frequency), we separate the real and imaginary parts of (5), for which we multiply the numerator and denominator of the fraction by a polynomial which is the conjugate of the denominator

$$b_3 (x - jy)^3 + b_1 (x - jy).$$

The result of the multiplication can be represented in the following general form

$$\varepsilon = \frac{M(x, y)}{S(x, y)} + j\frac{N(x, y)}{S(x, y)}, \tag{6}$$

where M, N and S are polynomials and are functions of x and y.

Since parameter ϵ, in effect, is a real number, the imaginary part of (6) must be zero. Therefore equation

$$N(x, y) = 0 \tag{7}$$

establishes such a functional relationship between x and y, at which to each pair of x and y values, satisfying equation (7), corresponds a certain real value of parameter ϵ. Consequently equation (7) is the required locus.

Equation (7) is obtained in the form of a polynomial of the sixth order relative to x and y. However, introducing the new variable

$$z = \sqrt{x^2 + y^2} \tag{8}$$

and eliminating one of the independent variables, we can convert the equation of the locus into a form which can be easily solved relative to the other independent variable.

Eliminating y, we find:

$$x^2 = -\frac{b_3}{4b_1} \cdot \frac{z^6 - \left(a_2 + \frac{b_1}{b_3}\right) z^4 + \left(a_0 + a_2 \frac{b_1}{b_3}\right) z_2 - a_0 \frac{b_1}{b_3}}{z^2 - a_0 \frac{b_3}{b_1}}. \tag{9}$$

Thus the co-ordinates of the points on the complex plane are the distance from the imaginary axis (x) and the distance from the origin (z). It is convenient to take z as the independent variable and x as a function of Z. Selecting various values for Z and calculating the corresponding values of x according to (9), we can construct the locus point by point.

Now we note some general properties of the locus.

Since the roots of the characteristic equation are complex conjugate values, therefore the locus is always symmetrical to the real axis and we can confine ourselves to its construction on the upper half-plane. In addition, if the investigated oscillating system is stable, then the real components of the roots are negative or zero. In this case, that part of the locus which is in the right-hand half-plane has no physical meaning and it is sufficient to examine the locus in the second quadrant of the complex plane.

If the investigated system has n degrees of freedom then the characteristic equation has n roots and to each value of parameter ϵ correspond n points on the complex plane. Hence it follows that the locus must have n branches. Each branch, placed in the upper half-plane, corresponds to a conjugate branch in the lower half-plane. If n is an even number then half the branches are placed in the upper half-plane and the other half in the lower half-plane. If n is an odd number then, in the limiting case, one of the roots will be real at any ϵ and the corresponding branch will fall into the real axis.

The locus constructed according to (9) when $k_L = 2$ and $k_C = 0.2$ is shown in Fig. 2. Out of the four branches, numbers 1 and 2 are on the upper half-plane. Both branches start from the imaginary axis at the points for which $\epsilon = 0$. When ϵ increases from zero to infinity, the points representing the roots of the characteristic equation will move along the branches.

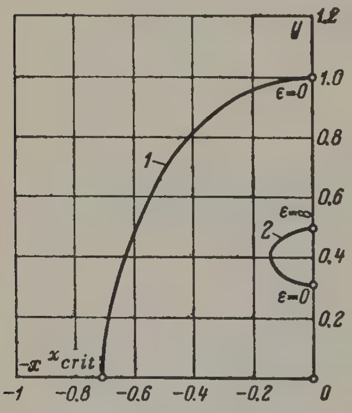

FIG. 2. The locus of the roots of the characteristic equation when $k_C = 0.2$; $k_L = 2$, $z_4 > z_3$; (1) mixed mixed branch; (2) complex branch, $z_1 = 1$; $z_2 = 0.316$; $z_3 = 0.5$; $z_4 = 0.633$; $x_{crit} = 0.707$.

Branch 1 reaches the real axis at the point x_{crit} which corresponds to the critical operating condition for one of the oscillating components of the investigated process (at the critical value of ϵ). At a further increase in ϵ the two conjugated branches meeting at the point x_{crit} (i.e. the branches placed in the upper and lower half-planes) are directed along the real axis in opposite directions.

Branch 2 does not reach the real axis. Consequently, the second pair of roots at all values of ϵ remain complex. This means that with the change in the value of the shunt resistor it is impossible to reach the damping of the second oscillating component of the process; i.e. it is impossible to bring it into the aperiodic condition.

For the complete solution of this problem it is necessary to calculate the ϵ parameter value corresponding to the various points of the locus. Selecting a number of arbitrarily positioned points and substituting the co-ordinates of these points into (5) or (6), we find the value of ϵ for each pair of x and y values.

It is convenient to represent the result of this calculation in the form of $x(\epsilon)$ and $y(\epsilon)$ curves. Such curves, corresponding to the locus given in Fig. 2, are shown in Fig. 2.(To branch 1 in Fig. 2 correspond curves x_1 and y_1 in Fig. 3. To branch 2 correspond curves x_2 and y_2). Since the imaginary components of the conjugate roots differ only in sign and the real components of the roots in this particular case are not positive, in Fig. 3 the curves for the moduli of x and y are constructed. At the critical value of ϵ, branch y_1 is zero and branch x, is doubled.

Some problems can be solved by qualitative analysis of the locus without the point-by-point construction of its branches. One such problem, for example, is the question of damping the oscillations and the conditions necessary for damping.

We shall examine the qualitative analysis in an example.

According to the position of the branches, the place of the characteristic points can be estimated. To the characteristic points belong those points which correspond to the limiting values of ϵ; i.e. $\epsilon=0$ and $\epsilon=\infty$, also the intersection points with the axes. In some cases the first and second types of these special points are coincident.

Now we shall find the characteristic points for the locus defined by (9). Assuming $\epsilon=0$ in formula (4), we obtain two pairs of imaginary conjugated roots:

$$p_1=\pm j;\ p_2=\pm j\sqrt{\frac{k_C}{k_L}}.$$

When $\epsilon=\infty$ the characteristic equation, in addition to the zero root, has a pair of conjugated imaginary roots:

$$p_3=\pm j\sqrt{\frac{k_C(1+k_L)}{k_L(1+k_C)}}.$$

Thus, in this particular case, the points for which $\epsilon=0$ and $\epsilon=\infty$ are simultaneously the intersection points with the axes.

Since the roots p_1, p_2 and p_3 are imaginary and the corresponding points are on the imaginary axis, the moduli of these roots, z_1, z_2 and z_3 must satisfy equation (9). Consequently, the numerator of the right hand side of (9) has the roots $\pm z_1$ $\pm z_2$ and $\pm z_3$, and it can be represented in the following, more convenient, form:

$$x^2=-\frac{b_3}{4b_1}\cdot\frac{(z^2-z_1^2)(z^2-z_2^2)(z^2-z_3^2)}{z^2-z_4^2}, \tag{10}$$

where

$$z_1 = 1,\ z_2 = \sqrt{\frac{k_C}{k_L}};\quad z_3 = \sqrt{\frac{k_C(1+k_L)}{k_L(1+k_C)}};$$

$$z_4 = \sqrt{a_0\frac{b_3}{b_1}} = \sqrt{\frac{1+k_C}{1+k_L}}.$$

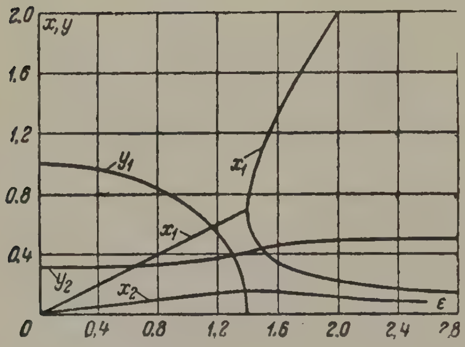

FIG. 3. The real and imaginary parts of the characteristic equation as functions of the variable parameter ε.

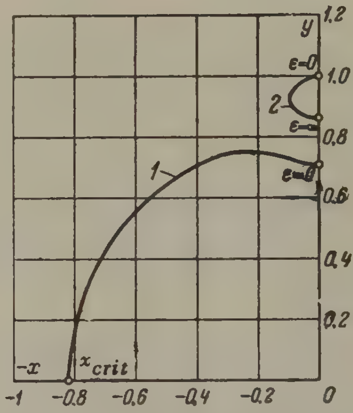

FIG. 4. The locus of the roots of the characteristic equation when $k_C = 1$; $k_L = 2$; $z_4 < z_3$
(1) mixed branch; (2) complex branch;
$z_3 = 0.866$; $z_4 = 0.817$; $|x_{crit}| = 0.814$

For those values of z to which a real value of x corresponds, the right hand side of (10) must be positive. Consequently, the real values of z, i.e. those values which satisfy the physical conditions of this problem, fall into a certain region which is divided into intervals. The region of the real z values can be determined from the conditions that on the boundary of each region one of the four differences $(z^2 - z_k^2)$ is zero, and inside the region the right hand side of (10) is positive.

It can be seen from (10) that to each z value, taken in the region of its real values, corresponds only one negative x value. Therefore to each region of real z values corresponds one branch of the locus.

The comparison of the z_1, z_2, z_3 and z_4 values shows that the two latter values are always between the first two. Two variants of the mutual position of the branches are possible, depending on whether z_3 or z_4 is larger. The branch with the final point p_3 does not reach the real axis. We shall call it complex. The other branch reaches the real axis at the critical point and we shall call it mixed.

To be specific, we assume that $z_1 > z_2$ i.e. $k_C < k_L$. Then the variants of the positions for the complex and mixed branches can be represented as follows.

Variant	Complex branch	Mixed branch
I	$z_2 < z < z_3$	$z_4 < z < z_1$
II	$z_1 > z > z_3$	$z_4 > z > z_2$

In the case when $z_1 < z_2$ $(k_C > k_L)$, it is necessary to interchange the position of z_1 and z_2 in these inequalities.

To the two variants of the branch positions correspond two types of loci, shown in Figs. 2 and 4.

When $z_3 = z_4$, the locus consists of the arc 1:

$$z = z_3 = z_4$$

and curve 2:

$$x^2 = -\frac{b_3}{4b_1}(z^2 - z_1^2)(z^2 - z_2^2).$$

This case is represented by Fig. 5.

The abscissa of point x_{crit} can be found by solving (10) when $|x| = z$. This will be an equation of the third order relative to z^2. For the numerical data, by which Fig. 2 was constructed, we find:

$$x_{crit} = -\frac{1}{\sqrt{2}}; \ \epsilon_{crit} = \sqrt{2}.$$

The regions of the z values will be:

$0.316 \leqslant z \leqslant 0.5$, Complex branch;
$0.633 \leqslant z \leqslant 1$ Mixed branch.

In effect, the complex part of the mixed branch ends at $z = |x_{crit}| = 1\sqrt{2} > z_4$ instead of $z = z_4 = 0.633$; i.e. the region of the real values for the complex part of the mixed branch will be somewhat narrower than that established before.

Now we shall generalize the procedure for finding the analytical expression of the locus to the case of a characteristic equation having an arbitrary form, with the single limitation that the coefficients of the characteristic equation linearly depend on the variable circuit parameter. We denote the variable by ϵ. The characteristic equation in the general case is of the following form:

$$\sum_{k=0}^{n} (a_k + \epsilon b_k) p^k = 0, \tag{11}$$

where

$$p = x + jy.$$

Solving equation (11) relative to ϵ, we obtain

$$\varepsilon = -\frac{\sum\limits_{k=0}^{n} a_k p^k}{\sum\limits_{k=0}^{n} b_k p^k} \tag{12}$$

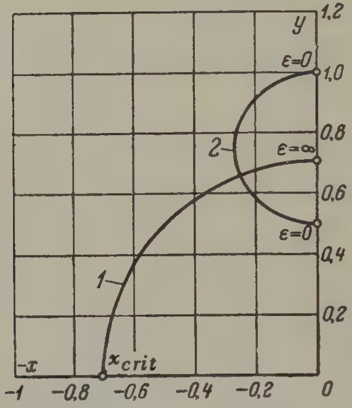

FIG. 5. The locus of the roots of the characteristic equation when $k_C = 0.5$; $k_L = 2$; $z_4 = z_3$ $z_1 = 1$; $z_2 = 0.5$; $z_3 = z_4 = |x_{crit}| = 0.707$

Converting (12) in a similar way, as was done before with (5), we obtain an equation of the form of (6). In this case equation

$$N(x, y) = 0$$

is also the required locus. Introducing the new variable z, we find that the locus will be a polynomial, the order of which is one degree lower than that of the characteristic equation, relative to x. In many cases, however, the coefficients of the higher powers of x are zero and the degree of the locus, relative to x, is two units smaller than that of the characteristic equation. This is especially true in the above case.

We represent the locus in the form of a polynomial relative to x:

$$\sum_{k=0}^{n-1} A_k x^k = 0.$$

Then, for example, for $n = 6$ coefficients A_k will be the following:

$$A_0 = c_{65}z^{10} + (c_{54} - c_{63})z^8 + (c_{43} - c_{52} + c_{61})z^6 + \\ + (c_{32} - c_{41} + c_{50})z^4 + (c_{21} - c_{30})z^2 + c_{10};$$

$$A_1 = 2[c_{64}z^8 + (c_{53} - 2c_{62})z^6 + (c_{42} - 2c_{51} + \\ + 3c_{60})z^4 + (c_{31} - 2c_{40})z^2 + c_{20}];$$

$$A_2 = 4[c_{63}z^6 + (c_{52} - 3c_{61})z^4 + (c_{41} - \\ - 3c_{50})z^2 + c_{30}];$$

$$A_3 = 8[c_{62}z^4 + (c_{51} - 4c_{60})z^2 + c_{40}];$$

$$A_4 = 16[c_{61}z^2 + c_{50}];$$

$$A_5 = 32c_{60}.$$

To reduce the amount of writing, the following notation was introduced

$$c_{ik} = a_i b_k - a_k b_i.$$

The equation of the locus when $n < 6$ will be obtained as a special case of the examined equation, when zero is substituted for the corresponding C_{ik} coefficients.

Finally we note that (12) can be examined as a function of the complex variable p, which gives a conformal transformation of the p plane on the plane of the complex parameter ϵ, while the locus determined in the p plane is transformed into the positive part of the real axis on the ϵ plane.

REFERENCES

1. *Fundamentals of automatic regulation. Theory.* V.V. Solodovnokov (Editor); Mashgiz (1954).
2. L.E. Mashkilleison; *Determining the speed of the voltage recovery on the contacts of a circuit-breaker at the extinction of the arc. In symposium, "High voltage apparatus design"*, United Scientific and Technical Press (1935).
3. P. Hammarlund; *Voltage recovery on the contacts of a circuit-breaker*, Gosenergoizdat (1956).

DETERMINATION OF THE LEVEL OF MAGNETIC NOISE OF D.C. MACHINES BY THE METHOD OF ELECTROMECHANICAL ANALOGY*

I.G. SHUBOV

S.M. Kirov Factory "Elektrosila"

(Received 7 May 1957)

Magnetic noise produced by d.c. machines in many cases prevails over noise of non-magnetic origin and thus determines the general noise level of the machine.

One of the fundamental problems in calculating magnetic noise is the determination of the space forms of the frame vibrations and of magnetic forces appearing in the machine air gap. Therefore, in this article, before the discussion of determination of magnetic noise by the method of electromechanical analogy, basic formulae for calculation of various types of vibrations and of periodic magnetic forces are given; basic assumptions, used for deducing these formulae, are stated.

The space forms of frame vibrations

The frame of a d.c. machine, being an elastic ring, has an infinite number of degrees of freedom, but due to the nature of exciting forces acting on the frame, only certain definite forms of vibrations are produced. These vibrations may appear in the form of a symmetrical tension – compression, bending or torsion of the ring.

In designing a d.c. machine it is necessary to pay particular attention to the possibility of coincidence of the frequency of exciting forces f_e with the frequency of natural vibrations f_n of the system, consisting of the frame with main and auxiliary poles:

$$f_e = Zn/60 \tag{1a}$$

$$f_n = 1/(2\pi\sqrt{m_e\lambda_e}) \tag{1b}$$

where m_e is the equivalent mass of the system; λ_e is the equivalent compliance of the system for various kinds of vibrations; Z is the number of slots in the armature; n is the speed of rotation of the armature. The coincidence of frequencies f_e and f_n results in a sharp increase of machine vibration, i.e. leads to a resonance of vibrations, which is highly undesirable. Let us note the similarity of formula (1b) with the formula for the frequency of natural oscillations of an electric circuit consisting of inductance L and capacitance C:

---

* *Elektrichestvo*, No. 4, 30–35, 1958.

$$f = \frac{1}{2\pi\sqrt{LC}} \tag{2}$$

In calculating the vibrations of a frame at resonance or at frequencies near to resonance it is necessary to take into account the damping resistance of vibrations in the frame:

$$r_{mf} = 2\pi f_c m_f D, \tag{3}$$

where D is the damping factor, equal for steel to 0.0525; m_f is the mass of frame.

The action of this resistance is analogous to the action of an electric resistance in a circuit r_E, L, C, to which an oscillating voltage is applied.

According to the nature of exciting forces, the space vibrations of frames are possible with the number of deformation waves equal to $\nu = 0$ and $\nu \geqslant 1$.

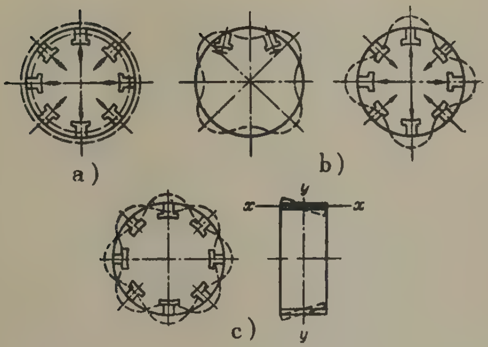

FIG. 1. Space forms of frame vibrations; (a) vibrations of the zero kind, (b) vibrations of the first kind, (c) vibrations of the second kind.

Vibrations of the zero kind ($\nu = 0$)

The frame undergoes deformations of extension and compression (Fig. 1a). Radial compliance of the frame is:

$$\lambda_{fo} = \frac{R}{2\pi ES}\,[cm/kg], \tag{4}$$

where R is the radius of the mean line of the frame (cm); E is Young's modulus of elasticity (kg/cm^2); S is the area of the transverse section of the frame (cm^2).

Vibrations of the first kind ($\nu \geqslant 1$)

The frame undergoes bending deformations (Fig. 1b). Here we have to distinguish two cases:

First case ($\nu = 1$)

The frame is clamped at two points. In this case the radial compliance of the frame is:

$$\lambda_{f1} = \frac{R^3}{2\pi E J_x \xi_1^2}\ [\text{cm/kg}], \tag{5}$$

where factor ξ_1 depends on the angle ψ of the frame clamping and may be found from Fig. 2; and J_k is the moment of inertia of the frame cross-section with respect to the x - x axis (cm^4).

Second case ($\nu \geqslant 2$)

Vibration nodes are situated at places where main poles are fixed or between them. The radial compliance of the frame in this case is given by the formula (5):

$$\xi_1 = \frac{\nu(\nu^2 - 1)}{\sqrt{\nu^2 + 1}}. \tag{6}$$

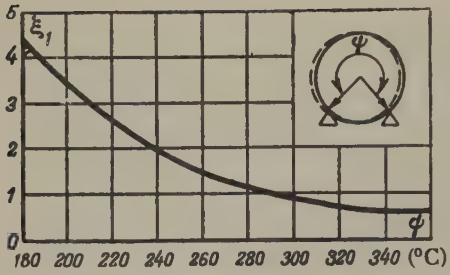

FIG. 2. Dependence of ξ_1 on ψ.

Vibrations of the second kind (Fig. 1c)

Such vibrations occur in machines with wedge-shaped armature slots or wedge-shaped pole shoes. In this case the frame executes bending and torsional vibrations.

Radial compliance of the frame is:

$$\lambda_{f2} = \frac{R l_f^2 \xi_2}{4\pi E J_y} \ [\text{cm/kg}], \qquad (7)$$

where l_f is the length of the frame (cm);
J_y is the moment of inertia of the frame transverse section with respect to the y-y axis (cm^4);

$$\xi_2 = \frac{1+\sigma}{1+\sigma+2\nu^2}; \qquad (8)$$

σ Poisson's ratio, equal for steel to 0.3.

The action of periodic magnetic forces caused by the armature teeth

All periodic magnetic forces, so far as their action on main poles and frame is concerned, can be subdivided into three groups:

(a) radial forces F_r producing radial displacements of poles and the frame vibrations of the first and second kind;

(b) bending moments M_r producing angular displacements of poles in the transverse plane of the machine and frame vibrations of first kind;

(c) torsional moments M_p producing angular displacements of poles in the longitudinal plane of the machine and frame vibrations of the second kind.

TABLE 1.

Number of teeth in a pole division and in a pole arc	Kind of the exciting force	Vibrations of the adjacent poles	Number of deformation waves on the frame circumference and the kind of vibration
$\frac{Z}{2p}=n; \quad \alpha=\frac{b_p}{t_1}=n$	Bending moment M_r	In phase	$\nu=2p$ (first kind)
$\frac{Z}{2p}=n, \quad \alpha=\frac{b_p}{t_1}=n+\frac{1}{2}$	Radial force F_r	In phase	$\nu=0$ (zero kind)
$\frac{Z}{2p}=n+\frac{1}{2}; \quad \alpha=\frac{b_p}{t_1}=n$	Bending moment M_r	In antiphase	$\nu=p$ (first kind)
$\frac{Z}{2p}=n+\frac{1}{2}; \quad \alpha=\frac{b_p}{t_1}=n+\frac{1}{2}$	Radial force F_r	In antiphase	$\nu=p$ (first kind)

Thoughout, n is an integer

The conditions for the appearance of radial forces and bending moments for the idle run of the machine are given in Table 1.

So far as torsional moments M_p are concerned, they are due to the wedge shape of the armature slots or pole shoes, this shape being used in d.c. machines to weaken the action of radial forces and bending moments.

During the run of an electric machine, superposition of different kinds of vibrations takes place, and this complicates the problem of determination of the vibration level of the frame. Nevertheless, as investigations show, for practical calculations in most cases we may only consider the influence of these forces that excite oscillations of the first kind. Nevertheless, we may only neglect the action of radial forces producing oscillations of the zero kind, and of torsional moments due to these forces, in the absence of the resonance of vibrations. Such an assumption is permissible owing to the following considerations:

(1) Radial forces producing oscillations of the zero kind are to a considerable extent attenuated by the damping action of the excitation winding.

(2) The torsional moments produce only insignificant vibrations of the frame, owing to its small torsional compliance.

Considering that radial forces and bending moments can produce only vibrations of the first kind, it is convenient in designing an electromechanical analogy to replace the action of bending moments by the action of equivalent radial forces (so far as values of deformations, which are produced by them, are concerned).

Thus a bending moment M_r applied to a pole may be replaced by an equivalent force F_{eq} applied between the poles:

$$F_{eq} = \frac{\gamma M_r}{R}, \tag{9}$$

where the value of γ for various ν may be taken from Table 2.

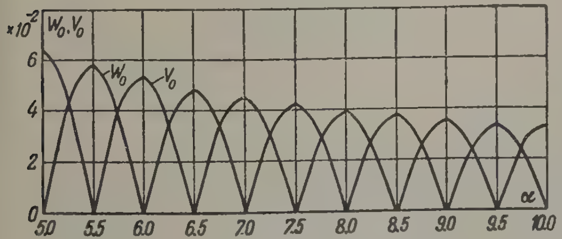

FIG. 3. Dependence of W_0 and V_0 on α.

Moreover, to simplify calculations we may neglect the action of tangential forces, since they are always smaller than radial ones.

The magnitude of periodic magnetic forces may be determined by formulae given in Table 3 for machines having rectangular or wedge-shaped armature slots, or an uniform or eccentric gap, this is often done in practice.

Formulae given in Table 3 are derived for the no-load and on-load run of the machine, on the basis of the following assumptions:

(a) the alternating magnetic field in the armature slots varies sinusoidally;

TABLE 2.

ν	2	3	4	5	6
γ	9.3	54	140	262	486

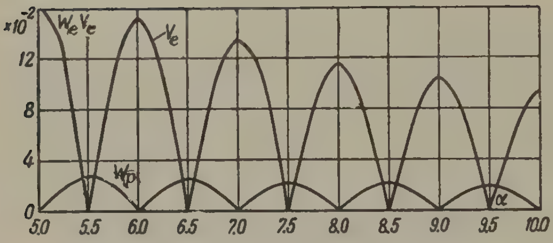

FIG. 4. Dependence of W_e and V_e on a.

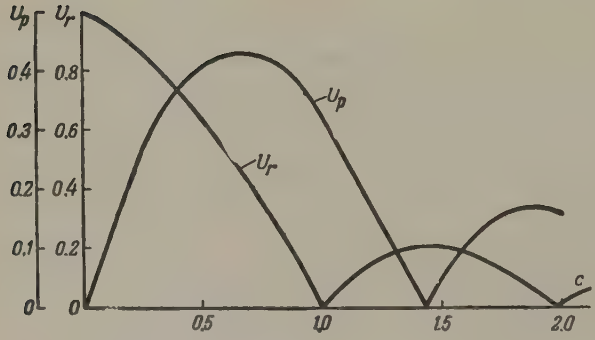

FIG. 5. Dependence of U_p and U_r on c.

(b) the magnetic system is unsaturated;

(c) the stepped shape of the curve of armature reaction is neglected.

$$F_0 = \left(\frac{B_\delta}{5\,000}\right)^2 b_p l_n \,[\mathrm{kg}].$$

where $\epsilon = k_c - 1$;

$\varkappa = \frac{Asb_p}{1{,}6\sigma B_\delta}$, the load factor; W_0, V_0, W_e, V_e are functions of $a = b_p/t_1$ (Fig. 3 and 4); U_r and U_p are functions of the slope of wedge shaped slots, c (Fig. 5); B_δ is magnetic induction in the air gap (G); b_p is width of the pole shoe (cm); l_n is the length of the pole (cm); k_c is Carter's coefficient; As is linear load of the armature (A/cm); δ is thickness of the air gap (in the case of an eccentric gap the thickness of an equivalent uniform air gap is used) (cm).

Noise due to yoke

The yoke of an electric machine may be considered as a cylindrical radiator of sound waves; its radiation power N is determined by the vibration speed of the yoke $\dot{x}_0$ and by the acoustical resistance of the yoke in air r_a [4]:

$$N = \frac{1}{2} r\, \dot{x}_0^2. \tag{10}$$

Acoustical resistance r_a may be calculated approximately by the formula [4]:

$$r_a = \pi R l_c \rho\, v_s \phi_1, \tag{11}$$

TABLE 3.

Shape of the armature slot or of the pole shoe	Kind of excitation	Value of the amplitude of forces and moments		Kind of forced vibrations
		Uniform gap	Eccentric gap	
Rectangular	Radial force	$F_r = 2F_0\epsilon\sqrt{W_0^2 + x^2V_0^2}$	$F_r = 0.36F_0\epsilon\sqrt{W_e^2 + 1.7x_e^2}$	Vibrations of the zero or first kind
	Bending moment	$M_r = F_0\epsilon b_p\sqrt{V_0^2 + x^2W_0^2}$	$M_r = 0.18F_0\epsilon b_p\sqrt{V_e + 1.7x^2W_e^2}$	Vibrations of the first kind
Wedge-shaped	Radial force	$F_r = 2F_0\epsilon U_r\sqrt{W_0^2 + x^2V_0^2}$	$F_r = 0.36F_0\epsilon U_r\sqrt{W_e^2 + 1.7x^2V_e^2}$	Vibrations of the zero or first kind
	Bending moment	$M_r = F_0\epsilon b_pU_r\sqrt{V_0^2 + xW_0^2}$	$M_r = 0.18F_0\epsilon b_pU_r\sqrt{V_e + 1.7x^2W_e^2}$	Vibrations of the first kind
	Torsional moment	$M_p = F_0\epsilon l_nU_p\sqrt{W_0^2 + x^2V_0^2}$	$M_p = 0.18F_0\epsilon l_nU_p\sqrt{W_e^2 + 1.7x^2V_e^2}$	Vibrations of the second kind

where $\rho v_s = 41.3$, the specific acoustic resistance of the air. Function ϕ_1 depends on the effective radius of the cylinder $2\pi R/\lambda$ where λ is the length of the sound wave for the frequency f_w (Fig. 6).

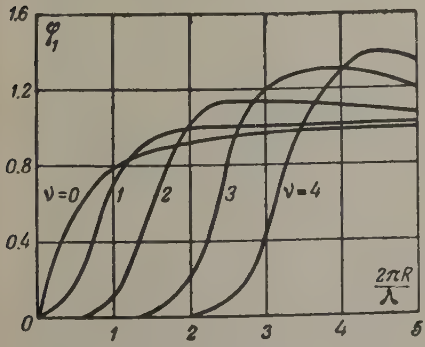

FIG. 6. Dependence of ϕ_1 on $2\pi R/\Lambda$ for different V.

Acoustical pressure of a distance d from the machine yoke in the case of open space is:

$$q = 408\sqrt{\frac{N}{4\pi(R+d)^2}}\ \text{[bar]}. \tag{12}$$

The level of the machine noise with respect to the level of the acoustical pressure $q_0 = 2 \times 10^{-4}$ bar, which is arbitrarily chosen as a zero level, will be:

$$T = 20\log\frac{q}{q_0}\ \text{[dB]}. \tag{13}$$

Electromechanical analogy

It is known that for calculating complicated mechanical and acoustical oscillating systems we often replace them by better-known systems. Such systems are electric circuits whose equations are analogous to the basic equations of motion in mechanics and acoustics.

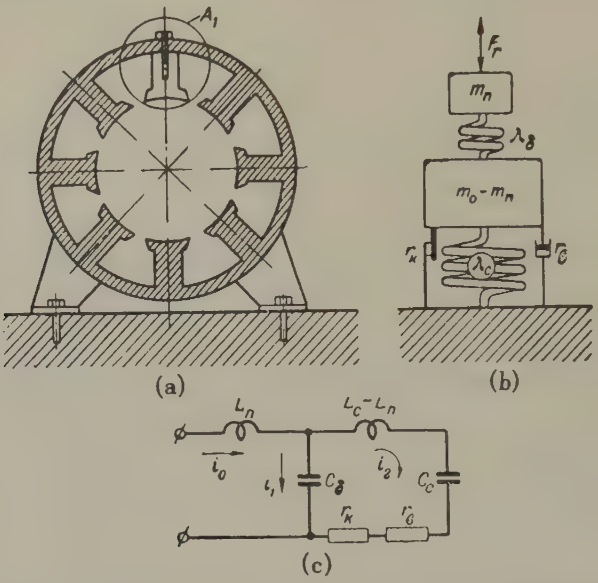

(a) (b)

(c)

FIG. 7. Equivalent circuit of the node A_1 of a vibrating d.c. machine: (a) machine; (b) mechanical system; (c) equivalent electric circuit.

In comparing these equations we see that as friction r_m, mass m and compliance λ of a mechanical system determine its motion, so resistance r_E, inductance L and capacitance C determine current in an electric circuit.

In calculating the magnetic noise produced by an electric machine, we may replace the system under investigation by a simple translational mechanical system, which in turn may be represented by an equivalent electric circuit (Fig. 7).

In designing an analogy we may neglect the compliance of poles and the mass of bolts attaching the poles to the frame. Table 4 gives the conventional symbols of mechanical and electrical systems and formulae for their calculation.

The knowledge of parameters of a mechanical system and frequency of exciting ω enables us to determine the total impedance z_m of the mechanical system by analogy with an electric circuit (Table 5). It is customary to call the units of resistance of a mechanical system "mechanical ohms"; their dimension is kg sec/cm.

For the electric circuit (Fig. 7c), we may determine the current i_2 and in consequence the speed of vibrations of the machine frame x_2.

After having performed calculations using the circuit in Fig. 7, it is interesting to find the level of magnetic noise under the condition of absolutely rigid attachment of the poles to the frame. In this case the equivalent circuit becomes a simple circuit with elements r_1, L, C connected in series; solution of this problem is quite easy.

TABLE 4.

Element of a mechanical system	Conventional symbols adopted and mathematical formulae.	
	in a mechanical system	in an electric circuit
Mass of a pole	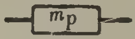	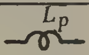
Compliance of bolts, attaching a pole to the frame, for tension:	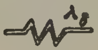	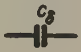
for a radial force	$\lambda_\delta = \frac{l_\delta}{kEs}$ [cm/kg];	
for an equivalent force	$\lambda_\delta = \frac{2Rl_\delta}{\gamma akEs}$ [cm/kg], where l_δ is length of a bolt in a smooth part (cm); k – number of bolts; a – width of the core of the main pole (cm) s – area of a section of one bolt (cm^2)	
Mass of the magnetic system without one main pole	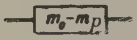	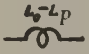
Radial compliance of the frame for tension compression (zero kind of vibrations)	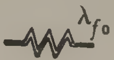 [formula (4)]	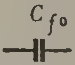
Radial compliance of the frame for bending (first kind of vibrations)	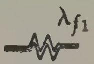 [formula (5)]	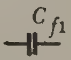
Radial compliance of the frame for tension (second type of vibrations)	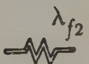 [formula (7)]	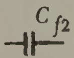
Damping resistance of the frame vibrations	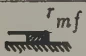 [formula (3)]	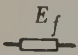
Mechanical resistance of the machine frame in air	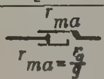 $r_{ma} = \frac{r_a}{g}$ [formula (11)]	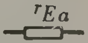

TABLE 5.

Electric circuit	Mechanical system
$z_{1E} = j\omega L_p$	$z_{1m} = j\omega m_p$
$z_{2E} = \dfrac{1}{j\omega C_\delta}$	$z_{2m} = \dfrac{1}{j\omega \lambda_\delta}$
$z_{3E} = r_E + j\omega (L_0 - L_p) + \dfrac{1}{j\omega C_f}$	$z_{3m} = r_m + j\omega (m_0 - m_p) + \dfrac{1}{j\omega \lambda_f}$

Example

Calculation of magnetic noise of a d.c. machine. 1. Initial data: $n = 1600$ rev/min, $2p = 4$; $B_\delta = 5680$ G; $As = 187$ A/cm; $Z = 42$; $t_1 = 1.72$ cm; $b_p = 12$ cm; $a = 6.8$ cm; $l_n = 14.5$ cm; $k_c = 1.23$; $c = 0$; $\delta = 0.25$ cm (uniform); $J_x = 16.6$ cm^4; $R = 20$ cm; $S = 50$ cm ^{2}.

Weights of: pole, $G_p = 13.2$ kg; magnetic system, $G_0 = 135$; frame, $G_f = 63$ kg.

Bolts: $k = 2$; $l_\delta = 1.8$ cm; $s = 1.13$ cm^2.

Calculations

1. $f_a = 42 \times 1600/60 = 1120$ c/s; $\omega = 7030$ 1/sec; $\Lambda = 29.4$ cm.

2. $\dfrac{Z}{2p} = 10.5$; $a = \dfrac{12}{1.72} = 7.0$; $c = 0$.

For these ratios vibrations of the first kind are excited by bending moments M_r with the number of waves in the circumference of the frame $\nu = 2$ (Fig. 1).

3.
$$x = \frac{187\cdot12}{1.6\cdot0.25\cdot5680} = 1.0.$$

4. $M_r = \dfrac{1}{\sqrt{2}}\left(\dfrac{5680}{5000}\right)^2 12^2\cdot14.5\cdot0.23\cdot4.5\cdot10^{-2} = 19.8$ kg/cm; $F_{equ} = \dfrac{9.3\cdot19.8}{20} = 9.2$ kg.

5.
$$\lambda\delta = \frac{2\cdot20\cdot1.8}{9.3\cdot6.8\cdot2\cdot2.1\cdot10^6\cdot1.13} = 0.24\cdot10^{-6} \text{ cm/kg};$$

$$\lambda_{c1} = \frac{20^3}{2\pi\cdot2.1\cdot10^6\cdot16.6\cdot2.69^2} = 5.1\cdot10^{-6} \text{ cm/kg};$$

$$\xi_1 = \frac{2(2^2-1)}{\sqrt{2^2+1}} = 2.69;\ \omega_f = 1\,200 \text{ 1/sec}.$$

6.
$$z_{1m} = j\,7030\frac{13.2}{981} = j0.094\cdot10^3 \text{ mech } \Omega;$$

$$z_{2m}=\frac{1}{j7\,030\cdot 0.24\cdot 10^{-6}}=-j0.595\cdot 10^{3}\ \text{mech}\ \Omega;$$

$$z_{3m}=0.0525\cdot 1\,200\,\frac{63}{981}+j\,7\,030\,\frac{135-13.2}{981}+$$

$$+\frac{1}{j\,7\,030\cdot 5.1\cdot 10^{-6}}=0.0040\cdot 10^{3}+j0.842\cdot 10^{3}\ \text{mech}\ \Omega;$$

$$r_a=\pi\cdot 20\cdot 25\cdot 41.3\cdot 1.0=6.5\cdot 10^{4}\ \text{g/cm}.$$

7. Total mechanical impedance of the machine from the circuit in Fig. 7.

$$z_m\approx 2.1\cdot 10^{3}\ \text{mech}\ \Omega$$

8. $$\dot{x}_0=\frac{9.2}{2.1\cdot 10^{3}}=4.4\cdot 10^{-3}\ \text{cm/sec}\qquad \dot{x}_2=10.4\cdot 10^{-3}\ \text{cm/sec}.$$

9. $$N=\frac{1}{2}\,6.5\cdot 10^{4}\cdot 108\cdot 10^{-6}\cdot 10^{-4}=350\cdot 10^{-6}\ \text{W}.$$

10. $$q=408\sqrt{\frac{350\cdot 10^{-6}}{4\pi(0.2+1.0)^{2}}}=1.8\ \text{bar}.$$

11. Magnetic noise $$T=20\log\frac{1{,}8}{2\cdot 10^{-4}}=79\ \text{dB}.$$

The analysis of the noise spectrum of the machine shows that the level of magnetic noise for the frequency of magnetic forces 1120 c/s is equal to 76 *dB*.

Translated by S. Szymanski

REFERENCES

1. G. Olson; Dinamicheskie analogii (Dynamical analogies), *Izd. inostrannoi lit.* (1947).
2. V.V. Furduev; *Elektroakustika (Electro-acoustics)* United State Press (1948).
3. W.P. Ermolin; Shum mashin pastiannogo toka (Noise in d.c. machines), *Izv. Lengingradshoge elektrotekhnicheskogo inst. im. Lenina* 24, (1951); 28, (1955).
4. K. Schmidt; Gehäuseschwingungen von Gleichstrom-Mashinen als Ursache magnetischen Geräusches (Frame vibrations of d.c. machines as a cause of magnetic noise), *A.F.E.* (1938).
5. Mikina; Effect of skewing and pole spacing on magnetic noise in electric machinery, *Trans. Amer. Soc. Mech. Engrs.*, 5, No. 10 (1934).
6. K. Gamata; Magnitnyi shum mashin postoiannogo toka (Magnetic noise of d.c. machines). *Elektrotechnicky obzor*, No. 6 (1954).
7. V.K. Iofe and A.A. Iasnopolskii; *Raschetnye grafiki i tablitsky po elektroakustike (Graphs and tables for electro-acoustical calculations)*, Gosenergoizdat (1954).

TRANSIENT PROCESSES IN AN ELECTRIC DRIVE FOR AN EXPONENTIAL VARIATION OF THE MAGNETIC FLUX *

Yu. P. PETROV Leningrad

(Received 11 July 1957)

In many d.c. drives transient processes occur when the magnetic flux varies exponentially: the starting of a motor when the excitation winding was not connected before the start, the control of the motor speed by varying the magnetic flux, and others, are examples of such processes. In spite of the importance of these transient processes, no convenient methods for their calculation are available. The method proposed by Kuznetsov, [1] which consists in integrating the differential equations of the motor by means of power series, requires tedious calculations. Nikitin and Kunitskii in 1943 suggested a description of the transient processes in an electric drive, for the exponential variation of the magnetic flux, by means of new, non-elementary functions [2]. The realization of this idea proved to be difficult because these non-elementary functions depend on many parameters. Consequently, their evaluation and use was not easy.

In this article the functions of one parameter (and of time) are discussed; they permit an easy calculation of transient processes.

Let us make the following assumptions:

(a) the magnetic flux in the motor increases and decreases as a strictly exponential function;

(b) the armature reaction is absent;

(c) the armature inductance is zero;

(d) the torque due to the load resistance of the drive is constant.

With these assumptions the differential equations of the drive, when the motor is started without the excitation winding being energized in advance, are:

$$\left.\begin{aligned} U &= ir_a + C\Phi\left(1 - e^{-\frac{t}{T_w}}\right)\omega; \\ Ci\Phi\left(1 - e^{-\frac{t}{T_w}}\right) &= J\frac{d\omega}{dt} + M_r, \end{aligned}\right\} \tag{1}$$

---

* *Elektrichestvo*, No. 4, 35-38, 1958.

where U is the grid voltage
r_a is the armature circuit resistance
Φ is the steady state value of the magnetic flux;
ω is the angular speed of the armature rotation;
J is the moment of inertia reduced to the motor shaft;
M_r is the torque due to the load resistance of the drive;
T_w is the time constant of the excitation winding.

We introduce the relative values for current $i_k = \frac{i}{I_{st}}$; angular speed $\omega_k = \omega/\omega_{nl}$; time $x = t/T_\omega$ and the torque $\lambda = M_r/M_{\max}$, where I_{st} is the current for for the stalled armature of the motor, ω_{nl} angular speed of an ideal no-load running and $M_{\max} = CI_{st}\,\Phi$ the maximum torque of the motor.

Dividing the first of the equations (1) by $U = r_a I_{st} = C\,\Phi.\,\omega_{nl}$ and the second by $M_{\max} = C I_{st}\Phi$, we get:

$$\begin{gathered} 1 = i_k + (1 - e^{-x})\,\omega_k; \\ i_k(1 - e^{-x}) = \frac{1}{k}\frac{d\omega_k}{dx} + \lambda, \end{gathered} \tag{2}$$

where $K = T_w/T_m$; $T_m = I\omega_{nl}/M_{\max}$, the electromechanical time constant. Eliminating i_k from the system (2) we get:

$$\frac{d\omega_k}{dx} + k(1 - e^{-x})^2\omega - k(1 - e^{-x}) + k\lambda = 0. \tag{3}$$

Equation (3) reduces to quadratures: $\omega_k = e^{-k(x-0,5e^{-2x}+2e^{-x}-1,5)} \times$

$$\times \left[f_0 + k\int_0^x (1 - e^{-x} - \lambda)\, e^{k(x-0,5e^{-2x}+2e^{-x}-1,5)} dx \right], \tag{4}$$

where f_0 is the initial condition value ω_k for $x = 0$.

The integral in equation (1) cannot be evaluated in a finite form and is inconvenient for an approximate calculation. Expression (4) can be represented as a sum of three terms:

$$\omega_k = f_1(x, k) + f_0 \cdot f_2(x, k) + \lambda \cdot f_3(x, k),$$

where

$$f_1(x, k) = f_2(x, k) \cdot k \times$$

$$\times \int_0^x (1 - e^{-x}) e^{k(x-0,5e^{-2x}+2e^{-x}-1,5)} dx;$$

$$f_2(x, k) = e^{-k(x-0,5e^{-2x}+2e^{-x}-1,5)};$$

$$f_3(x, k) = -f_2(x, k)\,k \int_0^x e^{k(x-0,5e^{-2x}+2e^{-x}-1,5)} dx.$$

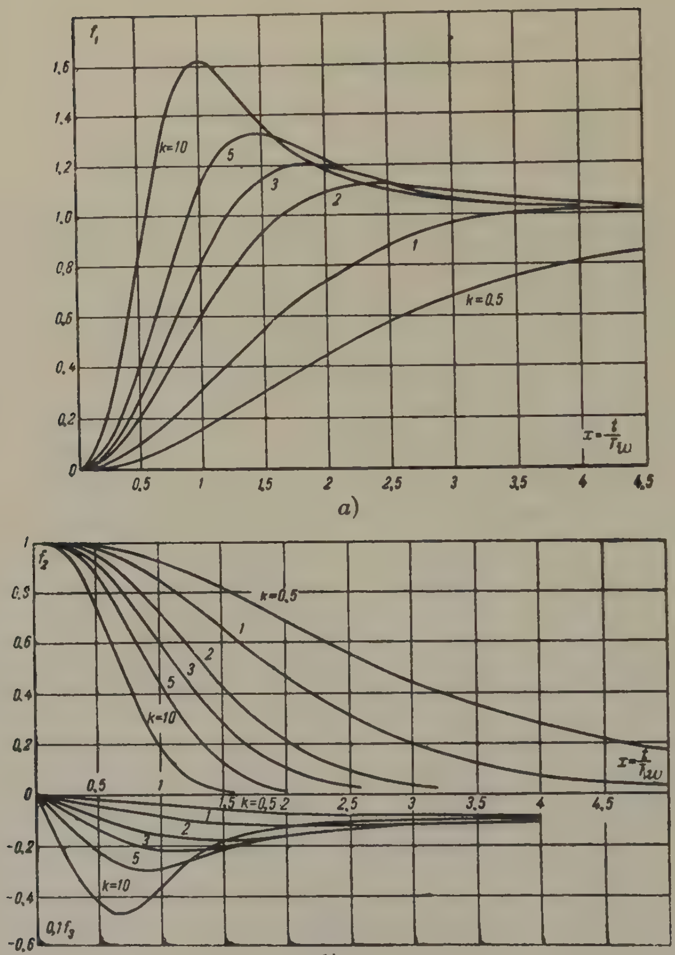

FIG. 1. Graphs of f_1, f_2 and $0.1f_3$ as functions of $x = t/T_w$.

Since f_1, f_2 and f_3 depend only on two parameters, x and k they can be represented as a family of curves.

Fig. 1 shows curves f_1, f_2 and $0.1\ f_3$. Values of $k = 0.2 - 1$ are characteristic for low power electric drives; values $k = 0.5 - 5$ are characteristic for the medium power drives.

Curves in Fig. 1 may be used for the calculation of transient processes not only for the case when $\Phi = 0$, but also for any value of the initial magnetic flux. From the expression:

$$1-(1-a)\,e^{-x}=1-e^{-(x+x_0)},$$

where $x_0 = ln/1{-}a$, it follows that, after the change of variable $x_1 = x_0 + x$, the calculation of the transient process for an initial magnetic flux not equal to zero also reduces the use of the curves in Fig. 1.

The application of the method of calculation discussed is illustrated by the following examples.

Example 1.

The start of a motor, for which $k = 1$ and $\lambda = 0.2$, is made without previous switching-on of the excitation winding.

It is required to find the current and speed.

The process of accelerating the motor begins when its driving torque becomes greater than the torque due to the load-resistance; i.e. when $1 - e^{-x} = 0.2$. Hence we find $x = -\ln(1-0.2) = 0.222$. Hence we have:

$$\omega_k = f_1(k=1,\ x=0.222) + f_0\cdot f_2(k=1).\ x=0.222) + \\ + 0.2\cdot f_3(k=1,\ x=0.222) = 0. \tag{6}$$

Since the values of f_1, f_2 and f_3 are known from Fig. 1, we find from equation (6) $f_0 = -0.06$.
Finally, for $0 < x \leq 0.222$, we have

$$[\omega_k = 0;]$$

for $x \geq 0.222$

$$\omega_k = f_1(k=1,\ x) - 0.06\cdot f_2(k=1,\ x) + \\ + 0.2\cdot f_3(k=1,\ x).$$

Having found ω_k, we use the equation $i_k = 1 - (1 - e^{-x})\omega_k$, and calculate the armature current.

Example 2.

In a motor ($k = 2$ and $\lambda = 0.1$), after shunting the resistance in the circuit of its excitation winding, the magnetic flux increases from $\Phi_0 = 0.5\,\Phi$ *to* Φ.

The initial angular speed $\omega_0 = 1.6\,\omega_{nl}$, the initial current $i_0 = 0.2\,I_{st}$. It is required to calculate the transient process, which takes place after shunting the resistance.
From (5) we find:

$$x = -\ln(1 - 0.5) = 0.696$$

Therefore, when $x = 0.696$ we have $\omega_k = \omega_0 = 1.6$.
On the other hand, at the same moment of time:

$$\omega_k = f_1(k=2,\ x=0.696) + f_0\cdot f_2(k=2,\ x=0.696) + \\ + 0.1\cdot f_3(k=2,\ x=0.696). \tag{7}$$

Having found the values of f_1, f_2 and f_3 from Fig. 1 on the basis of (7) we find $f_0 = 1.58$.

Finally we have:

$$\omega_k = f_1(k=2,\ x-0.696) + 1.58\cdot f_2(k=2,\ x-0.696) + \\ + 0.1\cdot f_3(k=2,\ x-0.696).$$

The results of calculations are given in Table 1.

TABLE 1.

$x_1 = x-0.696$	0	0.3	1.3	2.3
ω_k	1.6	1.57	1.36	1.03
i_k	0.2	0	—0.18	0.03

Example 3.

Start of the motor PN – 28.5, 110V, 2.2 kW, 1500 rev/min is made without previous connexion of its excitation winding to the generator PN-85, 115 V, 6.5 kW, 56.5 A, 1460 rev/min.

The armature resistance of the motor 0.443 ohm; armature resistance of the generator 0.141 ohm; resistance of connected leads 0.167 ohm. The magnetic flux of the motor 0.328 x 10^6 maxwell; the number of turns of the excitation winding per pole 1400. The time constant of the excitation winding, the dissipation factor being accounted for $T_w = 0.184$ sec; the electro-mechanical time constant $T_m = 0.31$ sec.; $k = 0.184/0.31 = 0.594$. The values of t_k and ω_k are calculated as in Example 1.

Table 2 gives the results of calculations and the experimental data, recorded by means of oscillograms.

TABLE 2.

x	t, (sec)	ω_k		i_k	
		calculated	experimental	calculated	experimental
0	0	0	0	1	0
1	0.184	0.183	0.177	0.885	0.880
2	0.368	0.44	0.450	0.620	0.670
3	0.552	0.68	0.700	0.350	0.400
4	0.736	0.8	0.850	0.220	0.205

TABLE 2.

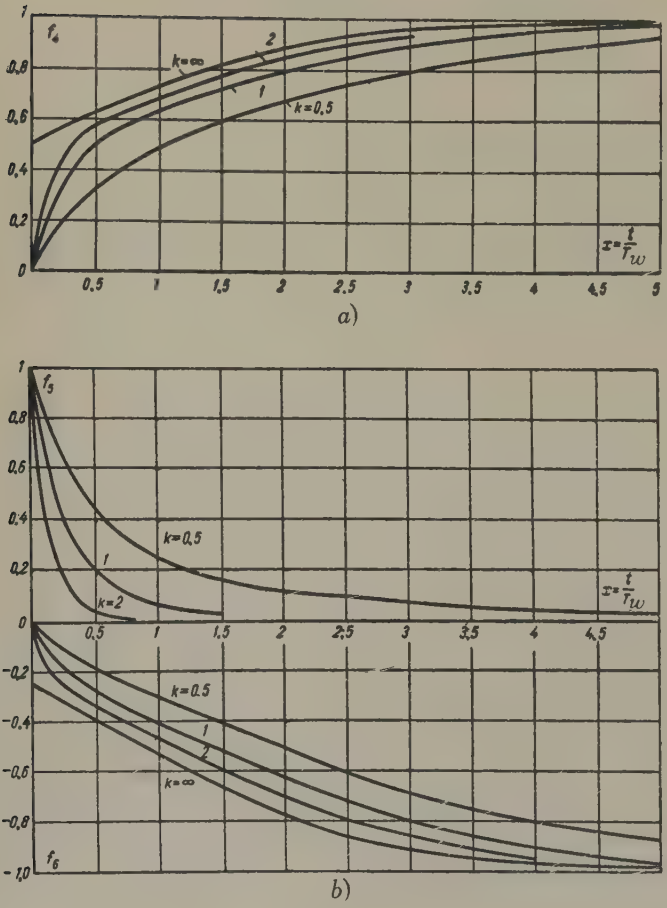

FIG. 2. Graphs of f_3, f_4, f_5 and f_6 as functions of $x = t/T_w$.

For calculation of transient processes with an exponentially decreasing flux it is necessary to introduce new functions f_4, f_5 and f_6 corresponding to functions f_1, f_2 and f_3 for the case of an increasing magnetic flux. Fig. 2 shows these functions, calculated for the case when the magnetic flux decreases according to the law:

$$\Phi = \Phi_{\text{fin}}\,(1 + e^{-x}).$$

As in the case of the increasing magnetic flux, on the basis of the equality

$$ae^{-x} + 1 = e^{-(x+x_0)} + 1,$$

where $x_0 = \ln a$,

by the change of the variable $x_1 = x + x_0$, we reduce the calculation of a transient process, for any initial value of the magnetic flux (less than twice·the value of the final flux) to the use of the curves in Fig. 2.

Example 4.

A resistance stage is introduced into the excitation circuit. The initial magnetic flux is 1.5 Φ; the initial speed is 0.6 of the steady state speed (after the end of the transient process). The time constant of the excitation winding, calculated with the introduced resistance accounted for, is $T_w = 0.2$ sec. The electromechanical time constant of the drive, calculated for the final value of the magnetic flux Φ_{fin}, $T_m = 0.15$ sec; $\lambda = 0.1$. We find $T_w/T_m = 1.33$ and $x_0 = -$ ln $0.5 = 0.696$. For $x = 0.696$ the following equation is valid:

$$\omega_\kappa = f_4(k = 1.33. \ x = 0.696) + f_0 \cdot f_5(k = 1.33, \ x = 0.696) +$$
$$+ 0{,}1 \cdot f_6(k = 1.33, \ x = 0.696) = 0{,}6.$$

Having found from curves in Fig. 2 f_4, f_5 and f_6, we find $f_0 = 6.7$ and finally we get:

$$\omega_\kappa = f_4(k = 1.33, \ x - 0.696) + 6.7 \cdot f_5(k = 1.33, \ x - 0.696) +$$
$$+ 0.1 \cdot f_6(k = 1.33, \ x).$$

Accounting for the armature inductance

The comparison of the results obtained by using curves in Fig. 1 and 2 with the experimental data shows that neglecting the armature inductance leads to an appreciable error only at the beginning of the transient process. In particular, at the start of the motor the maximum value of the current due to the armature inductance is always smaller than that for the armature stalled ($i_{k \max} < 1$), whereas by calculating by means of the curves in Fig. 1 and 2, we get $i_{k \max} = 1$. To introduce corrections into the calculation of currents at the start, appropriate curves are constructed in Fig. 3; they give the values of the maximum current at the start as functions of the factor $k = T_w/T_m$ and of the ratio T_a/T_m, where $T_a = L_a/r_a$, time constant of the armature circuit (sec).

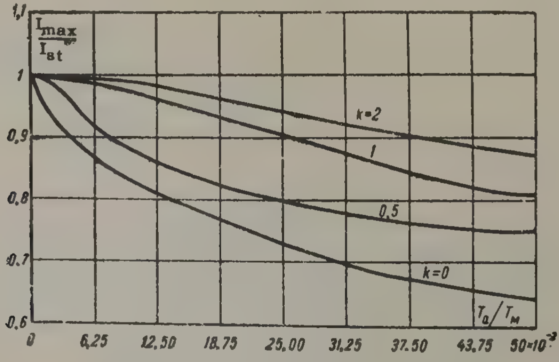

FIG, 3. Graphs of $I_{\max}/I_{st}$ as functions of T_a/T_m.

For the drive discussed in example 3, the armature inductance of the motor is 0.00357 H, of the generator armature – 0.00136 H. Hence the time constant of the armature circuit $T_a = 0.0066$ sec.

For this case, according to Fig. 3 we have $i_{k\ \max} = 0.98$, and the experimental value of $i_{k\ \max} = 0.96$.

The lower curve in Fig. 3 ($k = 0$) is constructed for the infinite rate of increase of the current, which is equivalent to the previous connexion of the excitation winding. From Fig. 3 it follows that the influence of the armature inductance in the case, when the excitation winding was not energized before the start, is less pronounced than in the case when the excitation winding was switched on before the start.

Conclusions

The above method, based on the use of special functions given by the graphs of Fig. 1 and 2 allows both quick and sufficiently accurate calculation in practice of the transient processes for the exponentially varying magnetic flux.

Translated by S. Szymanski

REFERENCES

1. P.I. Kuznetsov; Transient processes in an electric motor when the armature and excitation voltages vary simultaneously, *Avtomatika i telemekhanika*, No. 5 (1951).
2. V.P. Nikitin, V.K. Turkin and N.P. Kunitskii; An analytical method for the investigation of the operation of a shunt motor for speed control, by the excitation flux, *Izv. Akad. Nauk SSSR (Otd. tekh. nauk)*, No. 9-10 (1943).

THE USE OF ELECTROMAGNETIC POWDER COUPLINGS FOR FREQUENT REVERSALS OF A DRIVEN MECHANISM*

T.A. GLAZENKO

Leningrad

(Received 13 June 1957)

Many types of electric drives operate under conditions of frequent reversals of the direction of motion of a driven mechanism, the frequency of reversals varying within the limits 0.1 - 10 / sec. Very often in this case a quite definite graph of motion is prescribed; to comply with the specified requirements sufficiently large accelerations for starting and braking should be applied. The use of electric machines, working with a reclosing feedback, usually does not satisfy all the requirements of the drive. Owing to difficult thermal conditions and a large value of the dynamic

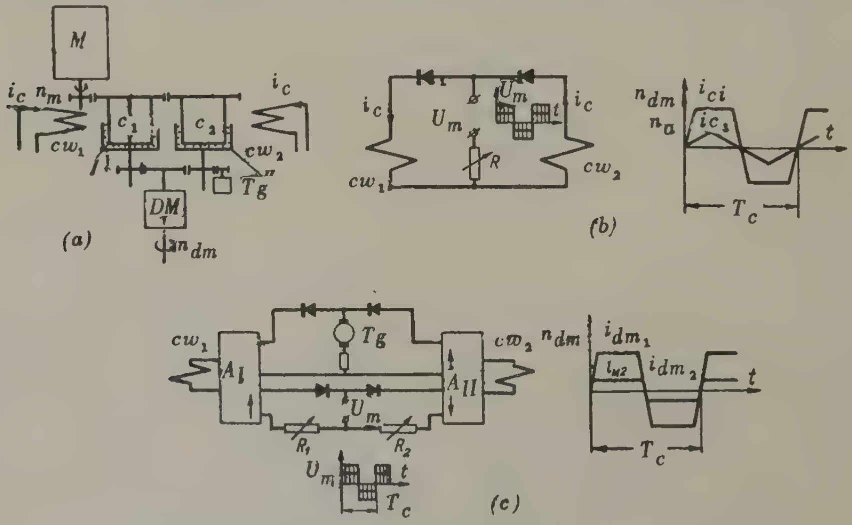

FIG. 1. Diagrams of a drive with the use of powder couplings to control a driven mechanism: M is the motor of the drive; I, II the couplings; CW_1 and CW_{11} excitation windings of the couplings; DM the driven mechanism; TG a d.c. tachogenerator; and A_1 and A_{11} amplifiers.

---

* *Elektrichestvo*, No. 4, 38-43, 1958.

torque, necessary for quick accelerating and braking, the power of a motor should be greatly increased, and special arrangements for its cooling are needed.

The use for this purpose of two powder couplings together with a mechanical reductor (Fig. 1) enables us:

(a) to decrease the power and facilitate operation of the driving motor;
(b) to use, for accelerating and braking, the kinetic energy accumulated by the rotating masses of the non-reversible part of the drive;
(c) to shorten the duration of transient processes and to decrease thermal losses in the drive;
(d) to realize the specified graph of motion and to vary the mean speed of rotation of the driven mechanism.

Transient processes in an electric drive at reversals of a driven mechanism.

The analysis of the reversal process has been carried out according to the method and assumptions which are stated in [1].

Let us adopt the following notation:

M_I, M_II are torques transmitted by couplings I and II to the shaft of the driven mechanism;

ω_I, ω_II and s_I, s_II: angular speeds and slips of non-reversible and reversible parts of the drive;

$T_{e\mathrm{I}}$, $T_{e\mathrm{II}}$, $T'_{e\mathrm{I}}$ and $T'_{e\mathrm{II}}$: equivalent time constants of the couplings I and II during the period of connecting and dis-connecting from the grid and switching in a discharge resistance;

$T_I = J_\mathrm{I}\,\omega_0/B$ and $T_\mathrm{II} = J_\mathrm{II}\,\omega_0/B$: electromechanical constants of the driving and driven parts of the drive.

The torque of the motor Bs_I, torques of both parts of the drive for no-load run $M_{0\mathrm{I}}$, $M_{0\mathrm{II}}$, torque due to the static resistance of the load, M_s, and moments of inertia on non-reversible and reversible parts of the drive, J_I, J_II, are all considered to be reduced to the shaft of the couplings.

Equations of motion of the driving and driven parts of the drive are:

$$Bs_\mathrm{I} = -J_\mathrm{I}\omega_0\frac{ds_\mathrm{I}}{dt} + M_\mathrm{I} + M_\mathrm{II} + M_{0\mathrm{I}}; \tag{1}$$

$$M_\mathrm{I} + M_\mathrm{II} = J_\mathrm{II}\frac{d\omega_\mathrm{II}}{dt} + M_{0\mathrm{II}} + M_s. \tag{2}$$

The reversal begins at the instant of disconnecting the winding of the coupling I from the grid and closing it through the discharge resistance.

In this case

$$M_{\text{I}} = M_{ss} e^{-\frac{t}{T'_{e\text{I}}}},$$

where M_{ss} is the moment of the coupling corresponding to the steady state value of the excitation current. Let us split up the process under consideration into four periods.

In the first period, slowing down begins at the instant of time

$$t = t_0 = T'_{e1} \ln \frac{M_{ss}}{M_s + M_{0\text{II}}},$$

when the decreasing torque of the coupling I becomes equal to $M_s + M_{0\text{II}}$, and lasts until the instant of switching of the winding of coupling II ($t = t_0 + t_1$). The length of this period is equal to the time t_1, of operation of the switching device. Denoting $t - t_0 = t'$, $(M_1)t_0 = M_{ss_1} + \exp(-t_0/Te_1)$ and taking into account the initial conditions, for $t' = 0$, we get

$$s_{\text{I}} = s_{\text{II}} = \frac{M_{0\text{I}} + M_s + M_{0\text{II}}}{B} = \frac{M_{0\text{I}} + M'_s}{B}$$

integrating equations (1) and (2) we get:

$$s_{\text{I}} = \frac{M_{0\text{I}}}{B} + \frac{M'_s}{B} e^{-\frac{t'}{T_{\text{I}}}} + \frac{(M_{\text{I}})_{t_0} T'_{e\text{I}}}{B(T_{\text{I}} - T'_{e\text{I}})} \left(e^{-\frac{t'}{T_{\text{I}}}} - e^{-\frac{t'}{T'_{e\text{I}}}} \right); \tag{3}$$

$$\omega_{\text{II}} = \omega_0 \left(1 - \frac{M_{0\text{I}} + M'_s}{B} \right) - \frac{M'_s}{J_{\text{II}}} t' + \frac{(M_{\text{I}})_{t_0} T'_{e\text{I}}}{J_{\text{II}}} \left(1 - e^{-\frac{t'}{T'_{e\text{I}}}} \right). \tag{4}$$

Usually the electromagnetic constant of the process of disconnexion of couplings is so small that at the end of the first period of the reversal the torque of the coupling I becomes zero. Substituting into formulae (3) and (4) the value $t' = t_1$, we shall find the values of speeds and slips at the beginning of the second period: $s_{\text{I}b}$, $s_{\text{II}b}$, $\omega_{\text{I}b}$, $\omega_{\text{II}b}$.

The second period, of reversal-braking, lasts during the time t_2 from the moment of connecting the second coupling ($t = t_0 + t_1$) till the moment of stand-still if the driven mechanism ($t = t_0 + t_1 + t_2$). The increasing torque of the coupling II brakes the reversible part, and we have to substitute into equation (2):

$$M_{\mathrm{II}} = -M_{ss\mathrm{II}}\left(1 - e^{-\frac{t''}{T_{e\mathrm{II}}}}\right) \tag{5}$$

Choosing the instant when $t = t_1 + t_0$ as a zero moment for time-counting, and denoting $t - t_0 - t_1 = t''$, we solve equations (3) and (4) with regard to the initial conditions ($t'' = 0$; $s_{\mathrm{I}} = s_{\mathrm{Ii}}$ and $\omega_{\mathrm{II}} = \omega_{\mathrm{IIi}}$)

$$s_{\mathrm{I}} = \frac{M_{0\mathrm{I}} + M_{ss\mathrm{II}}}{B} + \frac{M_{ss\mathrm{II}} T_{e\mathrm{II}}}{B(T_{\mathrm{I}} - T_{e\mathrm{II}})} e^{-\frac{t''}{T_{e\mathrm{II}}}} + \left[s_{\mathrm{I}\text{к}} - \frac{M_{0\mathrm{I}}}{B} - \frac{M_{ss\mathrm{II}} T_{\mathrm{I}}}{B(T_{\mathrm{I}} - T_{e\mathrm{II}})}\right] e^{-\frac{t''}{T_{\mathrm{I}}}}; \tag{6}$$

$$\omega_{\mathrm{II}} = \omega_{\mathrm{II}\text{к}} + \frac{M_{ss\mathrm{II}} T_{e\mathrm{II}}}{J_{\mathrm{II}}}\left(1 - e^{-\frac{t''}{T_{e\mathrm{II}}}}\right) - \frac{M_{ss\mathrm{II}} + M'_s}{J_{\mathrm{II}}} t''. \tag{7}$$

The last equation is valid up to the moment of time, when ω_{II} becomes zero.

The third period of the acceleration of the driven part in the opposite direction (t_3), lasts till the moment, when the slip between the driving and driven part of the coupling vanishes.

For $t = t_0 + t_1 + t_2 + t_3$,

$\omega_{\mathrm{I}} = \omega_{\mathrm{II}} = \omega_{\mathrm{eng}}$. Equations and formulae, given in [1] for the acceleration of the driven mechanism are also valid in this case.

In the fourth period, that of reversal, the acceleration of the driven and driving parts of the drive reaches the steady-state speed under conditions of rigid engagement (t_4).

The motion of the system is characterized by a single general equation [1]. with initial conditions: for

$t'''' = t - (t_0 + t_1 + t_2 + t_3) = 0$,

$s_{\mathrm{I}} = s_{\mathrm{II}} = s_{\mathrm{eng}}$.

The total time of the reversal will be $t_{\mathrm{rev}} = t_0 + t_1 + t_2 + t_3 + t_4$.

Calculations of the transient process and construction of the graph of the motion of the load are greatly simplified if $T_{\mathrm{II}} > 3\ T_e$.

In this case we may assume that the decrease and increase in the torques of couplings occur instantaneously and in the equations of motion (1) and (2):

$$M_{\mathrm{I}} = M_{ss\mathrm{I}} = \text{constant}; \quad M_{\mathrm{II}} = M_{ss\mathrm{II}} = \text{constant}.$$

Then the formulae for speed of the reversible parts are reduced to the form:
(a) during the period of braking:

$$\omega_{\mathrm{II}} = 1 - \left(s_{ss} + \frac{M_{ss\mathrm{II}} + M_s}{J_{\mathrm{II}}\omega_0} t''\right)\omega_0 = \omega_{ss} - \frac{M_{ss\mathrm{II}} + M'_s}{J_{\mathrm{II}}} t'' \qquad (8)$$

and

$$t_2 = \frac{J_{\mathrm{II}}\omega_{ss}}{M'_s + M_{ssII}}; \qquad (9)$$

(b) during the period of accelerating

$$\omega_{\mathrm{II}} = \frac{M_{ss\mathrm{II}} - M_s}{J_{\mathrm{II}}} t''' \text{ и } t_3 = \frac{J_{\mathrm{II}}\omega_{ss}}{M_{ss\mathrm{II}} - M'_s}, \qquad (10)$$

where s_{ss} and ω_{ss} are steady state values of the slip and angular speed of the coupling.

Fig. 2 shows curves s_{I} and $s_{\mathrm{II}} = f$ (t) and M_{I}, $M_{\mathrm{II}} = f(t)$ calculated by the above equations.

On comparing these curves with the reversal oscillograms (Fig. 3) recorded on a certain installation, we may note the analogy in the shape of the theoretical and experimental curves $\omega_{\mathrm{II}} = f(t)$. The oscillogram of the change of the motor current (Fig. 3) shows that in this system the motor works under a nearly constant load; braking and accelerating of the driven mechanism is done at the expense of the kinetic energy of the rotating masses of the non-reversible part of the drive (in this installation $J_{\mathrm{I}}, \approx 3\ J_{\mathrm{II}}$). It is easy to show that the mean speed of the driven mechanism and the torque of the powder coupling are related by the following equations:
(a) in the case when the curve (Fig. 3) has a horizontal portion;

$$\omega_{cp\mathrm{II}} = \omega_{ss} - \frac{2J_{\mathrm{II}}\omega_y^2}{T_ц} \, \frac{M_{ss}}{M_{ss}^2 - M'^2_s}; \qquad (11)$$

(b) for a triangular shape of the curve $n_{II} = f(t)$:

$$\omega_{mell} = \frac{T_c}{8J_{II}} \cdot \frac{M_{ss}^2 - M_s'^2}{M_{ss}}, \tag{12}$$

where T_c is a period of the curve $\omega_{II} = f(t)$.

Thus, varying the excitation current in the couplings, we control the mean speed of the output shaft of the installation by decreasing the steady-state torque of the coupling $(M_{ss} = ki_{sh})$. Speed control of installations has been realized by means of magnetic amplifiers connected in the excitation circuit of the couplings. To obtain a steady-speed control of the mechanism for a constant period of reversal in the circuit in Fig. 1b, a feedback coupling is necessary in systems with a variable torque of the load resistance.

If the shaft of the driven mechanism is to rotate at a constant angular speed for all values of the angle of rotation, i.e. if for all angles we want to preserve the trapezoidal shape of the curve $n_{II} = f(t)$, then a negative speed feedback has to be introduced in the system (Fig. 1c). Experimental and theoretical investigation of such a system will be the subject of another work of the author.

We may also control the speed n_{II} for a constant excitation current of the coupling by varying the speed of rotation of the driving motor. In this case the trapezoidal shape of the curve $n_{II} = f(t)$ is preserved for all the values of the speed, and the period of the reversal process decreases with the decrease of n_m [The speed of the motor].

Thermal conditions of the couplings

The heat developed during the reversal of the driven mechanism should be dissipated by the couplings, without overheating them to a temperature dangerous for winding insulation. Therefore, the dimensions and construction of the couplings should be so chosen as to ensure an adequate dissipation of heat. Losses of energy in couplings consist of losses due to slip A_{s1}, copper losses in windings A_w and friction losses during no-load running A_{n1}. Losses due to slip play the most important part in the development of heat in couplings controlling a reversible mechanism. These losses are taken as a basis for calculations.

Fig. 4 shows diagrams of power losses in couplings I and II in relation to the graph of the output shaft speed. In calculating losses due to slip we assume that the change of the torque of the coupling takes place instantaneously and the speed of rotation of the driving part of the system remains constant during the reversal process:

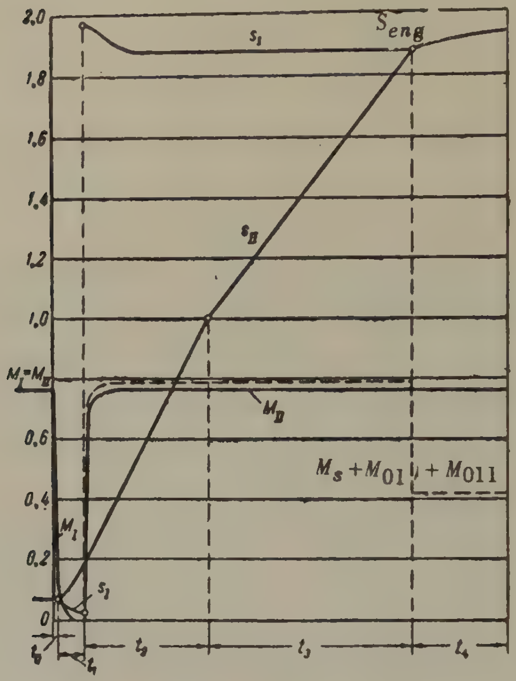

FIG. 2. Graphs for calculation of reversal parameters $S_{I}, S_{II} = f(t)$ and $M_{I}, M_{II} = f(t)$.

$\omega_I = \omega_{ss}$ = constant.

The loss of energy due to the slip in a powder coupling during the braking and accelerating processes is determined by:

$$A_{sl}\ A_b + A_a = \int_0^{t_2} M_y\,(w_1 + w_2)\,dt" + \int_0^{t_3} M_y\,(w_1 - w_2)\,dt" \tag{13}$$

Integrating this equation and taking into consideration relationships (8) - (10) we get:

$$A_{c\kappa} = \frac{3}{2} J_{II}\omega_{ss}^2 \frac{M_{ss}}{M_{ss} + M'_s} + \frac{1}{2} J_{II}\omega_{ss}^2 \frac{M_{ss}}{M_{ss} - M'_s} \tag{14}$$

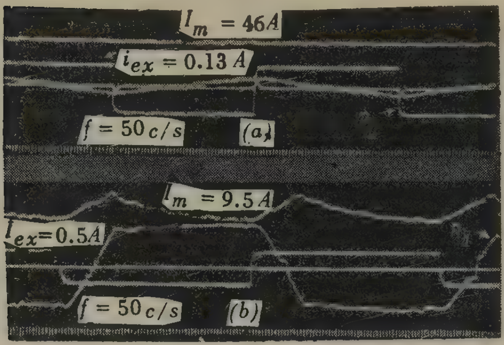

FIG. 3. Reversal oscillograms of the driven mechanism for the constant angular rotation of the motor $n_m = 8000$ rev/min (Fig. 1b): (a) I_m motor current; i_{ex} excitation current in the coupling; n_{II} mean = 16 rev/min, the mean angular velocity of the output shaft; angle of rotation of the shaft for $\frac{1}{2} T_e$ $\alpha = 120°$; reversal frequency $f = 0.4$ c/s; (b) $n_{II\,\mathrm{mean}} = 1.67$ rev/min; $\alpha = 10°$; $f = 0.5$ c/s.

Introducing the notation for the security factor of the coupling $K = M_{ss}/M_s$ and rearranging the formula (14), we get the expression for energy losses due to slip for one cycle.

$$A_{sl} = \frac{1}{2} J_{II}\omega_{ss}^2 \frac{2k(2k-1)}{k^2-1} = A_0 \cdot f(k). \tag{15}$$

The relative loss of energy due to slip

$$\alpha_{sl} = \frac{A_{sl}}{A_0} = \frac{2k(2k-1)}{k^2-1}$$

as a function of the security factor of the coupling, k is given in Fig. 5.

It is advisable to choose a value of k greater than 2. It is remarkable that within the range of values of the coupling security factor from 1.8 to ∞, the value of energy losses due to slip for the period of braking and accelerating remains nearly constant (Fig. 5) and may be considered equal to that for no-load running

$$A_{sl} = 4 \cdot \frac{J_{II}\omega_{ss}^2}{2}. \tag{16}$$

Mean power losses in the coupling for a cycle are:

$$P_{me} = \frac{A_{sl} + A_w + A_{n.l.}}{T_c}, \tag{17}$$

where

$$A_w = i_в^2 r_w \ t_{su}; \quad A_{n.l.} = M_{n.l} \Delta\omega \cdot t_{\text{off}};$$
$$\Delta\omega = 2\omega_y; \quad M_{n.l} \approx M_y \cdot (0{,}03 \ldots 0{,}08).$$

Having determined P_{mean} and chosen the method of cooling of the coupling, we may calculate the area of the external surface of the coupling, which is required for heat dissipation, from the relationship:

$$P_{me} \leqslant k_t S (t_e^\circ - t_0^\circ), \tag{18}$$

where k_t is the coefficient of thermal dissipation of the coupling surface;

$S = \pi D_{ex} \ 1 + 2 \ \frac{\pi D_{ex}^2}{4} \sim (1.7 - 2.04) \ D^2 + 2.08 \ D^2 = (3.78 - 4.12) \ D^2$, the area of the external surface of the coupling, which dissipates heat (cm²);

t_e° the permissible limiting temperature of the coupling frame;

t_0 the temperature of the ambient medium;

D mean diameter of the working layer.

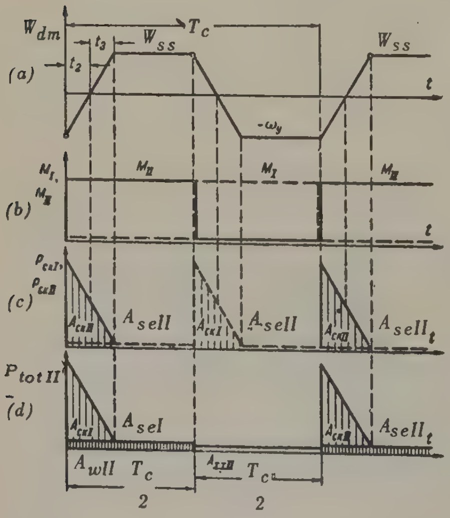

FIG. 4. Graph of the speed of the driven mechanism $w_{dm} = f(t)$, coupling torques M_I, $M_{II} = f(t)$ and power losses P_{seII}; $P_{seII} = f(t)$ and $P_{tot} = f(t)$.

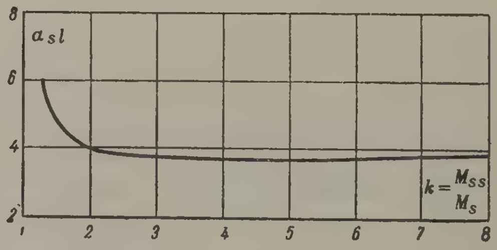

FIG. 5. Graph of the variation of relative energy losses in the coupling due to slip, during the period of braking and accelerating, as a function of the coupling safety factor $K = M_{ss}/M_s$.

The limiting temperature of overheating of the powder couplings, t_e° is determined by the type of insulation of its excitation winding and varies within the limits

70 - 130°C (The last figure applies to the couplings with a glass-mica insulation on a silicone-organic base).

Values of k_t, determined experimentally for various speeds of motion of the external surface of the coupling, are given in Fig. 6. The curve $k_t = f(v)$ is obtained from experiments with a single-gap cylindrical coupling with a smooth, zinc-plated external surface [$\delta_g = 0.35$ mm; filler carbonyl iron-talc (10:1)].

The value of the coefficient of thermal dissipation may be increased several times by blowing on the coupling surface (Fig. 6).

In installations in which the dimensions and weight of the coupling play a decisive role, it is necessary to provide the heat dissipating surface with fins and to use forced ventilation. In this case the maximum value of k_t should be taken for calculations.

In the class of drives which are discussed here, the reduction ratio from the motor shaft to the driven mechanism is rather large. In designing the drive we have to choose a place for fixing the couplings and determine the reduction ratio i_2. For this purpose we may be guided by the following considerations.

The magnitude of the area of the heat dissipating surface, S, of the coupling, which was found by formula 18, determines the dimensions (external diameter D_{ex} and the diameter of the layer) and, consequently, the torque of the powder coupling M_{ss}.

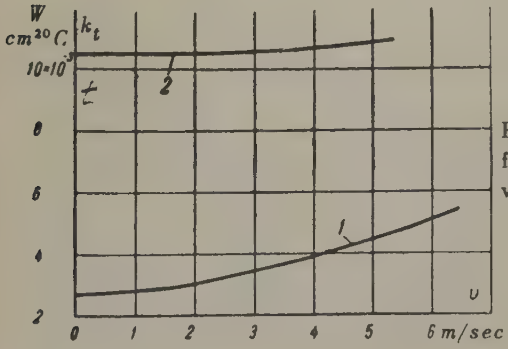

FIG. 6. Dependence of the coefficient of surface cooling of the coupling on the linear velocity of its external surface: (1) for natural cooling; (2) for forced cooling.

Knowing the torque due to the static resistance of the load, we may determine the dynamic torque on the output shaft M_{dyn}, which ensures the required acceleration of the driven mechanism during the specified period of time t_a. The ratio of these two moments determines the appropriate value of i_2.

From the above considerations we can recommend the following order for the calculation of similar electrodrive systems:

(1) Determination of the energy losses due to slip for a cycle and of the mean

power losses in the coupling;

$$A_{sl}=2\cdot 1.1\cdot J_{d.m.}\omega_{d.m.}$$

$$P_{sl}=\frac{1.05A_{sl}}{T_c};$$

Coefficient 1.1 takes into account the moment of inertia of the driven part of the coupling and toothed gears of the reductor. Coefficient 1.05 is introduced to account for losses of the no-load run of the coupling and thermal losses in the winding.

(2) The choice of the method of cooling the coupling and of the coefficient of thermal dissipation (Fig. 6) [3].

(3) Determination of the external area of the coupling surface, which is needed for the heat dissipation:

$$S=\frac{P_{me}}{k_t\,(t^{\circ}_e-t^{\circ}_0)}\,[\text{см}^2].$$

(4) The choice of the number of gaps and a preliminary calculation of the driving torque of the coupling:

(a) a single-gap coupling

$$M_{ss}\approx\frac{(\sqrt{S})^3}{48}\,[kg\ cm];$$

(b) a double gap coupling

$$M_{ss}\approx\frac{(\sqrt{S})^3}{35}\,[kg\ cm].$$

(5) Calculation of the dynamic torque of the coupling, required to achieve the acceleration of the driven mechanism during a specified period of time t_a:

$$M_{\text{dyn}}=\frac{J_{d.m.}\omega_{d.m.}}{t_a}.$$

(6) Determination of the transmission reduction ratio from the coupling shaft to the load shaft (i_2):

$$i_2=\frac{(1{,}1\ldots 1{,}25)\,M_{\text{dyn}}+M_s}{\eta M_{ss}},$$

where η is the efficiency of the reductor. Coefficient 1-1 is used in the case of a double-gap coupling, 1.25 for a single-gap one.

(7) Calculation of the basic dimensions of powder couplings and of their windings. The known data in this case are: the driving torque transmitted by the coupling to the driven shaft and operational conditions of the coupling. Comprehensive discussion of methods of calculation is given in [2-4].

(8) Checking of thermal calculations of the coupling on the basis of data obtained (moment of inertia of the reversible part of the drive, geometrical dimensions of the coupling, security factor and winding losses).
(9) Calculation of transient processes in the system and construction of the graph of motion of the driven mechanism by the above methods.

Recommendations for designing powder couplings

For the class of drives discussed above it is advisable to use powder couplings of the cylindrical type. In order to decrease dimensions and weight of the installation, high speed (n = 1000 - 2000 rev/min) double-gap couplings are constructed. Their driven part is made in a form of a hollow thin-walled shell to obtain a small moment of inertia. Labyrinth glands in the axial direction together with ordinary felt packing keep the powder mixture quite safely in the working gap.

In order to decrease the torque of the no-load running in the high speed couplings, it is necessary to decrease the volume of the frontal gaps and to separate them from the working chambers by the strip labyrinth glands, and to avoid relative speeds of rotation of the coupling components greater than 10 - 12 ,m/sec.

As a filler for the coupling gap, dry mixtures of the carbonyl iron R-8 with silicon dioxide may be recommended, the coefficient of volume filling being

$$K_{\mathrm{Fe}} = \frac{G\,F_e}{\gamma_{\mathrm{Fe}}\,V} \approx 0.34 - 0.4$$

where G_{Fe} is the weight of the carbonyl iron in the mixture, which occupies volume V (cm^3) (g);
γ_{Fe} is iron density ($\mathrm{g/cm^3}$).

The mixture of carbonyl iron with ground mica, which was proposed by Pugovkin, has also a high general and thermal stability.

The specific tangential stress, which is transmitted by dry fillers for a given value of magnetic induction in the coupling gap, and also the permeability of the mixture, are determined mainly by the properties of the ferromagnetic powder and the coefficient of its volume filling.

The values of the specific tangential stress τ, which is steadily transmitted by the dry fillers containing carbonyl iron R-8, and also the values of the relative permeability $\mu / \mu 0$ have been determined experimentally ; Fig. 7 shows them as functions of the mean value of magnetic induction in the coupling gap B_g

Within the range of induction values 0.2 - 1.2 $V.\ \mathrm{sec/m^2}$, the value of τ for powder mixtures during slip is practically independent of the relative speed of the working surfaces of the coupling. Experiments have shown that, due to the redistribution of the mixture in the coupling gap, the torque of a powder coupling with a dry filler varies during the first 2-3hr of its running-in. After that the torque remains constant.

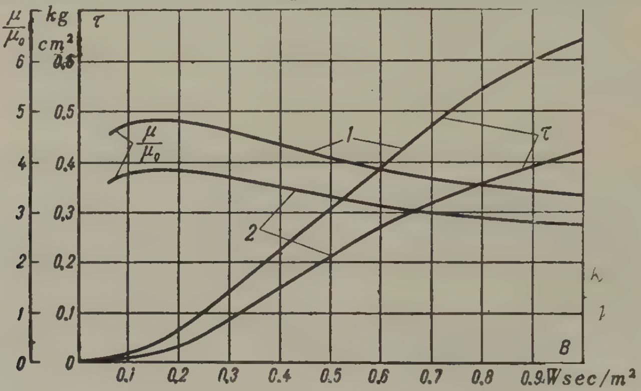

FIG. 7. Variation of the specific tangential stress τ in a layer and the relative permeability μ/μ_0 of dry fillers as functions of the inductance B in the coupling gap. (1) $k_{Fe} = 0.4$; (2) $k_{Fe} = 0.3$.

Tests of powder couplings were carried out under conditions of frequent reversal at a steady winding temperature of about 110° C. The mechanical characteristics of these couplings $M_m = f/i_{sh}/$were again recorded after 400 hr running. No decrease in the value of the torque was found.

Control characteristics of some individual couplings $M_m = f(i_{sh})$ were taken eighteen months after their filling (average working time of a coupling was 800 hr). Maximum variation of the torque did not exceed 5 per cent.

The above discussion leads to the conclusion that powder couplings with dry fillers are quite reliable elements of electric drive systems; they offer wide possibilities in the field of automatic control and regulation.

Translated by S. Szymanski.

REFERENCES

1. T.A. Glazenko; Transient processes in an electric drive equipped with an electromagnetic coupling with a ferromagnetic filler, *Elektrichestvo*, No. 12 (1954).
2. V.G. Zusman and O.N. Tatur; Electromagnetic couplings and their use in machine construction, *Elektrichestvo*, No. 3 (1956).
3. G.M. Petukhin; Characteristics and calculation of electromagnetic couplings with a ferromagnetic filler, *Elektrichestvo*, No. 3 (1956).
4. O.N. Tatur; Electromagnetic powder couplings, *Eksp. nauch.-issled. inst. metallor. stankor, tsen-byro tond. norm.* I (1956).

THE INCREASE OF THE RELIABILITY OF CONVERSION NETWORKS*

A.A. SAKOVICH

All-Union Lenin Institute of Electric Technology

(Received 10 October 1957)

In a conversion network there are elements which introduce lumped or distributed capacitances and inductances, thus forming additional oscillating circuits. In networks electrically connected with rectifiers, we have to take into account:

(1) capacitances with respect to the earth of the transformer and reactor windings, of cables, wall bushes, current transformers, anode dividers, auxiliary insulating transformers, transformers and conductors of the auxiliary circuits;

(2) dissipation reactances of the power transformer and of the anode dividers, inductances of the feeding busbars, of the blocking and smoothing reactors.

In the circuits comprising the above-mentioned reactive elements oscillations arise; harmful effects of these oscillations increase with the increase in power and voltage of the conversion installations. Oscillations arise at the beginning and at the end of commutation, when a sharp change of conditions occurs in the network; they become more prominent with the increase of the control angle, when the commutation voltage increases. As an example we may mention interference in wire communications, which arose during the transition into the inversion operation of the traction substations of the electrified railways; these disturbances were so strong that it was necessary to abandon the regeneration of energy. One of the power conversion installations, which worked quite satisfactorily during the process of adjustment, at a low voltage, could not be put into operation at a high voltage; investigations have shown a strong influence of the commutation processes on the control networks, which made the normal working of the rectifiers impossible. In many cases intermittent currents, resulting from heavy overvoltages, were observed.

Investigations, carried out directly on installations and using modern and specially designed instruments (cathode oscillographs, dividers, shunts, electronic incicators) gave a satisfactory explanation of the character of these phenomena, and their analysis helped, in the development of practical improvements to secure the normal operation of the high-voltage conversion networks and to remove or to reduce considerably disturbances caused by the operation of these networks. These results may be useful in normalizing the work of invertors on railway transport substations, in installations for methane electrocracking and in other high-voltage converting networks, working separately or in parallel with other networks.

---

* *Elektrichestvo*, No. 4, 53 – 57, 1958.

Problems connected with overvoltages arising in the case of parallel connected converting networks (for example on converting substations of d.c. transmission lines) are not discussed in this article.

Processes at the end of commutation

Let us consider a three-face bridge network, which is normally used for power conversion installations for voltages from 10 kV upwards. Taking into account complementary capacitances and inductances of the elements of the installation, we obtain a network as shown in Fig. 1a. Assume that, at the given instant, rectifier 6 is working and that current commutation takes place from rectifier 1 to rectifier 2 (Fig. 1b). At the end of the commutation period, current in rectifier 1 ceases to flow and the voltage across it becomes:

$$u_c = \sqrt{2}\cdot\sqrt{3}\,u_{ph}\sin(\alpha+\gamma). \tag{1}$$

Owing to the presence in the network of reactive elements, this voltage does not appear instantaneously, but increases gradually. Since this system consists of a complicated network, divided into branches comprising capacitances and inductances, oscillations of two or more frequencies arise; the losses in the links of the system bring about rather rapid damping of these oscillations. In the general case, the shape of the curve of the recovery voltage is determined by the equation :

$$u_{rec} = \sqrt{2}\cdot\sqrt{3}\,U_{ph}\Big\{\sin(\alpha+\gamma+\omega t) - \sin(\alpha+\gamma)\Big[A_1\sin(\omega_1 t+\psi_1)e^{-\frac{t}{\tau_1}} + \tag{2}$$
$$+ A_2\sin(\omega_2 t+\psi_2)e^{-\frac{t}{\tau_2}} + \ldots + A_c\sin(\omega_c t+\psi_c)e^{\frac{t}{\tau_K}}\Big]\Big\},$$

where A_1 and A_2 are coefficients which determine the relative value of a harmonic* ω_1 and ω_2 appropriate angular frequencies of the harmonics; ψ_1 and ψ_2 phase angles; τ_1 and τ_2 time constants, characterizing the damping of oscillations.

From formula (2) it is seen that the amplitude of the reverse voltage cannot attain the double value of the amplitude of the commutation voltage, which could happen in the simplified equivalent network (Fig. 1b) free from losses. On a real installation the reverse voltage amplitude does not exceed 140 – 160 per cent of the commutation voltage amplitude. This is due to the loss of energy in the links of the installation and also to the fact that the maxima of the individual harmonics do not coincide.

The usual method of decreasing the first amplitude of the reverse voltage and of slowing down its rate of increase is damping by additional circuits comprising capacitances and resistances (Fig. 1c). The methods of calculating damping circuits are discussed in the literature [1 – 3]. However, it is necessary to point out that we

---

* The value of the coefficients A_1, A_2 . . . . A_k is subject to the condition $\sum_{n=1}^{n=K} A_n\cdot\sin\psi_n = 1.$

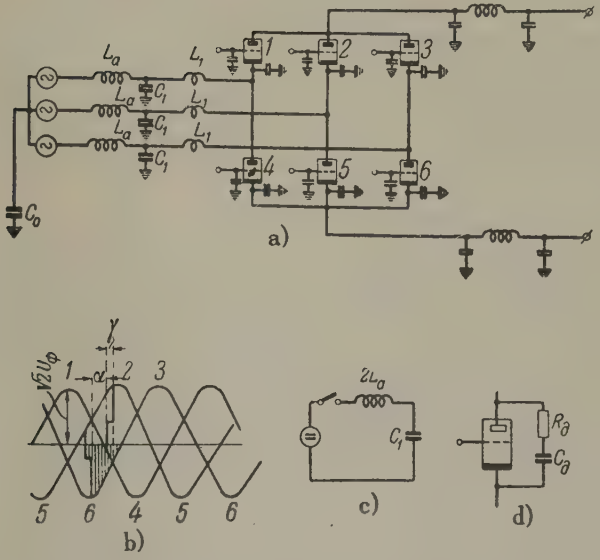

FIG. 1. Circuit showing starting-up of oscillations at the end of commutation.

cannot choose the value of the damping resistance solely on the basis of decreasing the first amplitude of the reverse voltage (the "optimum value of the damping resistance"). The value of the resistance of the damping circuit is chosen on the basis of the relationship between the rate of increase of the reverse voltage and the amplitude of its first rise, which is given by the characteristics of the rectifiers and the circuits; the condition of the ignition process should also be taken into account, and this will be discussed later. The practical value of the damping resistance is taken to be much less than that following from the conditions of the optimum damping of oscillations of the recovery voltage.

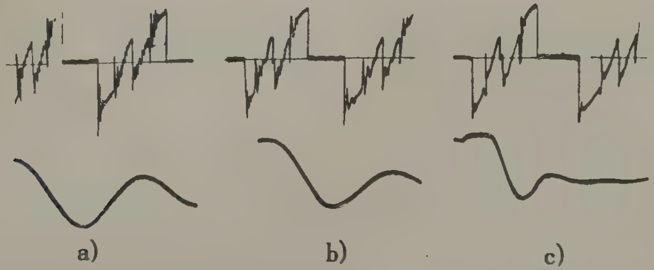

FIG. 2. Oscillogram of the recovery voltage curves for various values of the damping resistance.

Fig. 2 shows the oscillograms of the curves of the anode-cathode voltage (upper series) and the shapes of the initial rise of the recovery voltage for the same curves (lower series), recorded on a high power installation (1600 A, 10 kV).

In Fig. 2a) we see a very small value of the damping resistance-oscillations of the recovery voltage are considerable and slowly die away. Fig. 2b shows a slightly greater value of the resistance: the oscillation amplitude is decreased and damping is stronger. Finally, in Fig. 2c the resistance is near to the value for conditions of optimum damping; considerable damping takes place, but the slope of increase of the recovery voltage has increased sharply.

Taking into account the characteristics of mercury rectifiers for high voltages we may remark that the shape of the curve of the reverse voltage in the case of the optimum value of the damping resistance (Fig. 2c) is less favourable, since the slope of the voltage increase is considerably greater than that of the curve in Fig. 2b.

Processes during the ignition of rectifiers

During the ignition of the rectifiers, the discharge occurs of the capacitances connected with the rectifier anode and cathode; these capacitances are charged to the potential $u_i = \sqrt{2}\,\sqrt{3}\,U_{ph}\sin a$. Fig. 3a shows an approximate circuit diagram. In this figure the distributed inductances of the anode busbars and also the capacitances of the busbars and the connected elements of the installation are shown in the form of a chain of lumped inductances and capacitances. The capacitances, which take part in this process, have approximately the same value as those in the oscillating circuit for the recovery voltage, but inductances are considerably lower (inductances of the feeding busbars are of the order of 10^{-6} H/m.)

Owing to this fact frequencies become much higher, of the order of 10^5 - 10^6 c/s, and because of the distributive character of the capacitances and the inductances a nearly continuous spectrum of oscillations appears with individual peaks of resonant frequencies. Let us consider a simplified equivalent circuit for the dominating frequency (Fig. 3b).

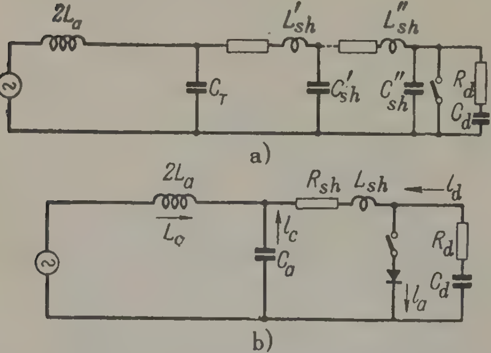

FIG. 3. Circuits showing starting-up of oscillations during the ignition process of rectifiers.

On closing of the knife switch, which is equivalent to the ignition of rectifier, the value of the current flowing in the circuit is:

$$i_s = \sqrt{3}\cdot\sqrt{2}U_{ph}\left\{\int_0^t\left[\frac{1}{2L_a+L_{sh}}\sin(\alpha+\omega t)-\right.\right.$$

$$\left.-\frac{1}{2L_a}\sin\alpha\cdot\sin(\omega_1 t+\psi_1)\,e^{-\frac{t}{\tau_1}}\right]dt+ \qquad (3)$$

$$\left.+\frac{\sin\alpha}{\omega_1 L_1}\cdot\sin\omega_1 t\cdot e^{-\frac{t}{\tau_1}}+\frac{\sin\alpha}{R_\partial}e^{-\frac{t}{\tau_2}}\right\},$$

where L_a is a lumped dissipation inductance of one phase of the power transformer with the reactance of the feeding-grid added; L_1 the inductance of the network supplying the rectifier; ω the angular frequency of the feeding voltage; ω_1 the angular frequency of oscillations; C_d the capacitance of the damping circuit; τ_1 the time constant characterizing the damping of high-frequency oscillations; ψ the phase angle of the voltage of high-frequency oscillations. Moreover, if

$$\int_0^{\frac{3\pi}{2\omega_1}} \left[\frac{1}{2L_a + L_{sh}} \sin(\alpha + \omega t) - \frac{1}{2L_a} \sin\alpha \cdot \sin(\omega_1 t + \right. \qquad (4)$$

$$\left. + \psi_1) e^{-\frac{t}{\tau_1}} \right] dt + \frac{\sin\alpha}{R_d} e^{-\frac{3\pi}{2\omega_1\tau_2}} < -\frac{\sin\alpha}{\omega_1 L_1} e^{-\frac{3\pi}{2\omega_1\tau_1}},$$

then the current in the rectifier circuit will pass through the zero value and will change direction. If a rectifier is connected in the circuit, which conducts currents only in one direction, the current in the network will be intermittent, and anode peaks of the reverse voltage will appear on the rectifier. Fig. 4 shows the oscillogram of the intermittent ignition process. Such a character of ignition is harmful to the rectifier because of increased sputtering of the anode material. Also, frequent extinctions of the excitation anode in the excitrons or of the arc of the igniter in the ignitrons take place; this is due to the high rate of voltage decrease and to the growth of reverse voltage on the main anode during the ignition process. This results in failure of operation of rectifiers and produces strong overvoltages in the control circuits, which is very dangerous for the auxiliary equipment. In the case when, during the ignition process, high frequency oscillations of a great amplitude arise, they cause strong radio interference.

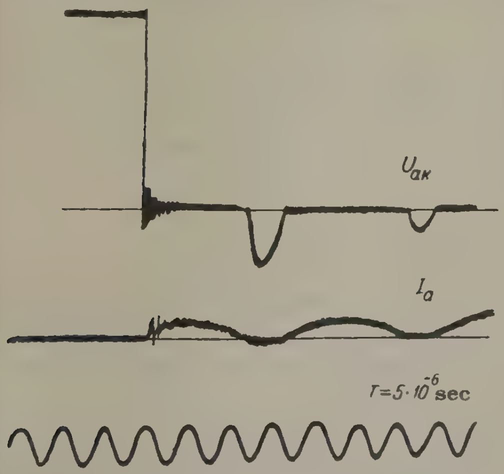

FIG. 4. Oscillogram of current and voltage oscillations during the ignition process.

To eliminate harmful effects during the ignition periods, blocking reactors are used in the anode circuits and the appropriate resistances are chosen in the damping circuit.

By connecting the reactor we decrease the oscillation frequency and the current amplitude during the ignition process. By a careful choice of the value of the damping circuit resistance, we may increase the current component of the aperiodic discharge and achieve a situation in which the anode current at ignition will decrease to zero and pass through the zero value. Fig. 5 shows the components of the anode current during the ignition process: in presence of oscillations and intermittent ignition (a), and for the normal ignition process (b).

A right choice of the parameters of the damping circuit and the blocking reactor is rather difficult. The available methods of calculation are complicated and not sufficiently tested.

Experiments with an electrical model, with an enlarged time scale, or direct detailed investigations on the installation are the proper methods for choosing the parameters. The values of inductances of the blocking reactors lie within the limits of 10^{-5} - 10^{-6} H; in the case of high power installations, reactors become rather cumbersome. The value of the capacitance of the damping capacitors of each phase is of the same order as that of all secondary windings of the transformer with respect to earth. The value of the damping resistances chosen to obtain the current, overlapping the current of high oscillations, is usually smaller than the value of resistances, that ensure the aperiodic damping of the oscillations of the recovery voltage. In choosing the value of damping resistances it is necessary to bear in mind that losses in the resistances may be heavy and may reach 0.5 - 2 per cent of the power of a conversion installation. The losses increase considerably with the increase of the ignition angle.

The influence of processes in the power network on the control network

For considerable values of the ignition angle, the rectifier ignition is accompanied by an abrupt variation of the potential of its electrodes. Abrupt variation of the cathode voltage can influence the control network and disturb the operation of the conversion circuit. Premature ignitions or ignition failures may occur in the individual rectifiers. One of the causes occurring in practice and producing these failures is shown in Fig. 6a. It can be seen from the circuit that with the ignition of the rectifier of the anode group (for example, 2), its cathode potential sharply increases and becomes equal to the anode potential. If the control networks have a considerable capacitance with respect to earth (for example, if the feeding leads are not sufficiently screened or screening is badly executed), then the change of the potential values on the corresponding conductors will be delayed (owing to the influence of

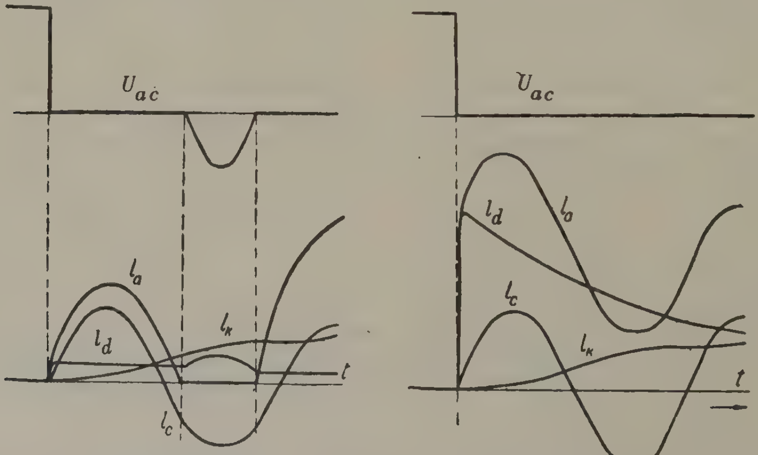

a) b)

FIG. 5. Components of the anode current of a rectifier during the ignition process.

capacitance). This will lead to the appearance on the grids of impulses of negative polarity. In consequence, of the two parallel connected rectifiers only one will work, namely that which fired first.

In the case of the oscillating growth of the anode current, the working rectifier may also be extinguished.

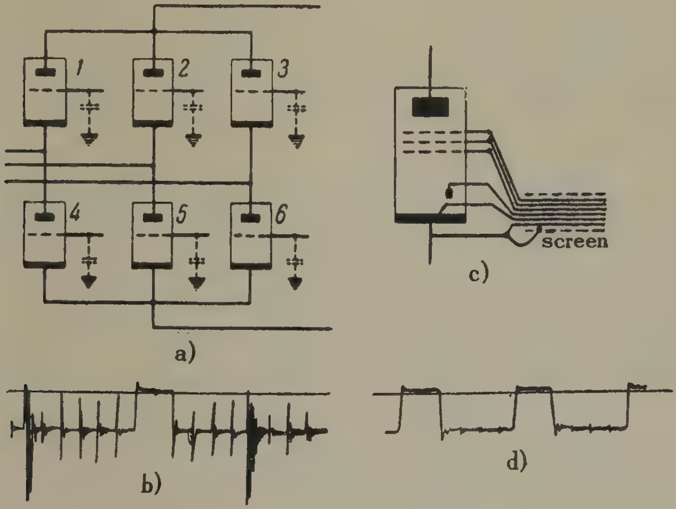

FIG. 6. The influence of processes in the power networks on the control networks of a rectifier.

Fig. 6b shows an oscillogram of the grid voltage in the above case. On the other hand, the induced voltage on the grids may cause premature ignition, for example, of the rectifier 2 when the commutation of rectifiers 3 and 4 takes place. The presence of similar induced voltages in the ignition circuit of the ignitron may also cause ignition failures and lead to the early damage of the semiconductor igniters. From the above discussion it follows that the method of construction of feeding leads of the control networks plays a very important part in high-voltage conversion networks. The screening of all in-leads is recommended, and the screen should be connected to the cathode of the corresponding rectifier, as shown in Fig. 6c. Fig. 6d, shows the voltage oscillograms of the grid circuits of the same installation (in Fig. 6a), but after alteration of its network. There is a possibility of overvoltages arising in the grid circuits due to the capacitance between the grid and the main anode. Nevertheless, for voltages on the main anode of the order of 10 kV these overvoltages are easily suppressed by connecting a small capacitor between the grid and the cathode.

Very dangerous voltages arise in the case of intermittent currents. Under such conditions, rectifiers of the anode and cathode groups fire each in turn for a short period; current impulses flow in the circuit, which is formed by the capacitance with respect to earth of all secondary windings of the transformer and the lumped dissipation inductance of the secondary windings of the transformer. With every ignition of the rectifier the periodical recharging of this capacitance takes place. Overvoltages with respect to earth are 5 – 8 times greater than the working voltage on the secondary windings; this is very dangerous for the equipment and causes breakdowns and backfires in the rectifiers. The elimination of these harmful effects, under the conditions of intermittent currents, may be achieved by one of the following methods:

(1) Earthing of the star point of the transformer and of the star point of the load through resistances, or connecting these two points through a resistance. In the case when transformer windings are delta-connected and there is no star point, artificial zero points are formed by resistances, which are either interconnected or earthed. Thus a leakage path is provided for the capacitance charges of the secondary windings of the power transformer.

(2) Wide control impulses (width 60 – 90 el deg) are used to establish conditions for re-ignition of rectifiers after their extinction by the oscillating anode current.

(3) A special control circuit is used to apply trigger pulses on the rectifiers, when the anode voltage on a given rectifier exceeds a predetermined value.

These methods have been tested on real installations and on models; positive results have been obtained in suppressing overvoltages caused by intermittent currents.

Increase of operational stability of an invertor

Recently the use of inversion installations has increased; bridge circuits controlled by various methods are also widely used; in these systems one group of rectifiers works as convertors, and another is controlled to act as invertors.

The output voltage in these networks may vary within wide limits, with a better power factor on the d.c. side than in the usual networks.

Nevertheless, ignition failures hamper the invertor operation; the occurrence of failures increases with increasing voltage.

To prevent the harmful effects of ignition failures and to increase the operational stability of the invertor, we may use the following method. Consider a three-phase network working under inversion conditions, a voltage diagram of which is shown in Fig. 7a. If the ignition of a consecutive rectifier (voltage diagram 2) fails, this causes the "reversal" of the invertor, which is not spontaneously suppressed, since the increase of current at the "reversal" leads to the increase of the commutation angle, and the transition of the current to another rectifier cannot be accomplished.

Fig. 7b shows the action of the technique of "advanced ignition". In this technique, in the case of ignition failure in a consecutive rectifier (for example 2), a trigger pulse is applied to the grid of the next rectifier, 3, with a lead of about 60 el deg. This produces a switching of the current from rectifier 1 to rectifier 3, and the invertor continues operating even in the case of a long delay in ignition. This method was tested in practice and gave positive results. The circuit for applying a trigger pulse is comparatively simple and may be realized in different ways [4].

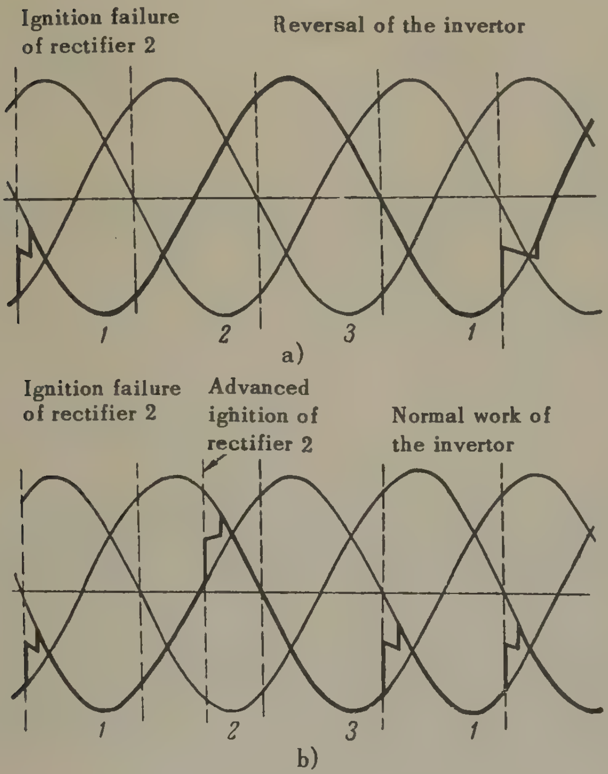

FIG. 7. Method of increasing the operational reliability of an invertor.

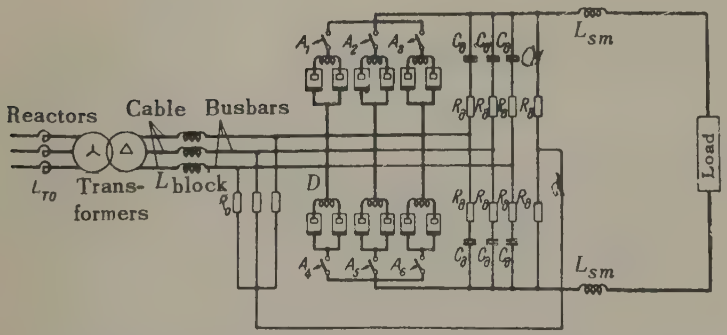

FIG. 8. Network of a high-voltage inversion installation.

Conclusion

The measures discussed above were developed as a result of research, and they were applied and tested on one of the conversion installations of about 15 MW power working at 10 kV. The result was such that this installation, which previously could not be put into operation, began to work normally. On the basis of these experiments similar measures have been undertaken on more powerful installations, where they also produced positive results. The system of advanced ignition was tested by the Direct Current Scientific Research Institute employees on the invertor substation of the transmission line from Kashira to Moscow.

Fig. 8 shows a complete network of a conversion installation with blocking reactors and damping circuits, which – as experience proves – should be regarded as an indispensable attribute of a powerful conversion network.

In carrying out the experimental part of this work the following persons participated: N.M. Maslennikov, S.M. Luzhanskii, V.P. Nadgornyi, E.P. Shmarina. L.I. Luzhanskaia and I.V. Blond.

Translated by S. Szymanski

REFERENCES

1. M.M. Akodis;. Narastanie obratnogo napryazheniia pri kommutatsii v ionnykh ventiliakh (Increase of a back voltage during the commutation period in ionic rectifiers) *Elektrichestvo*, No. 6 (1950).
2. V.B. Samodelkin; O roischete vossstanavlivaiushchegosia napriazheniia na ventiliakh v trekhfaznoi mostovoi skheme (Calculation of the recovery voltage on rectifiers in a three-phase bridge circuit), *Elektrichestvo*, No. 12 (1952).
3. V.B. Samodelkin; Dempfirovanie kolebanii vosstanavlivaiushchegosia napriazheniia v trekhfaznoi mostovi skheme (Damping of oscillations of the recovery voltage in a three-phase bridge circuit) *Elektrichestvo*, No. 4 (1954).
4. A.A. Sakovich; *Ustroistvo dla setochnogo upravleniia ventiliami inventora (Device for a grid control of rectifiers of an invertor)*, Author's Patent 84681.

CALCULATION OF CERTAIN TYPES OF COMPOUND EARTHING DEVICES *

A.B. OSLON

(Received 18 April 1957)

For calculation of compound earthing devices it is customary to make use of utilization factors, which take into account the increase of the earthing resistance due to the mutual screening of elements of an earthing device. These factors depend on many parameters (length, depth of earthing of the individual elements, their mutual position etc). Nevertheless, in many cases, we may carry out calculations of earthing devices by using simple formulae, without regard to utilization factors.

Consider a compound earthing device comprising n elements. Using the electrostatic analogy we derive a system of equations with coefficients of potential:

$$\left.\begin{aligned} \varphi_1 &= \alpha_{11}I_1 + \alpha_{12}I_2 + \ldots + \alpha_{1n}I_n; \\ \varphi_2 &= \alpha_{21}I_1 + \alpha_{22}I_2 + \ldots + \alpha_{2n}I_n; \\ &\cdot\ \cdot\ \cdot\ \cdot\ \cdot\ \cdot\ \cdot\ \cdot\ \cdot\ \cdot\ \cdot \\ \varphi_n &= \alpha_{n1}I_1 + \alpha_{n2}I_2 + \ldots + \alpha_{nn}I_n, \end{aligned}\right\} \qquad (1)$$

where $I_1 \ldots {}_n$ are currents leaking to the earth from each element of the earthing device;

α is coefficient of self and mutual potential;

$\phi_1 \ldots \phi_n$ are potentials of the elements of the earthing device.

For the parallel connexion of the elements of the earthing device $\phi_1 = \phi_2 = \ldots = \phi_n = \phi$. Solving the system of equations (1) with respect to currents, we get:

$$\left.\begin{aligned} I_1 &= \varphi(\beta_{11} + \beta_{12} + \ldots + \beta_{1n}); \\ I_2 &= \varphi(\beta_{21} + \beta_{22} + \ldots + \beta_{2n}); \\ &\cdot\ \cdot\ \cdot\ \cdot\ \cdot\ \cdot\ \cdot\ \cdot\ \cdot\ \cdot\ \cdot\ \cdot\ \cdot \\ I_n &= \varphi(\beta_{n1} + \beta_{n2} + \ldots + \beta_{nn}). \end{aligned}\right\} \qquad (2)$$

---

* *Elektrichestvo*, No. 4, 58-61, 1958

Earthing resistance of the compound earthing device is:

$$R = \frac{\varphi}{\Sigma I} = \frac{1}{\Sigma \beta}. \tag{3}$$

The determination of the coefficients of conductance is complicated in a general case, and, consequently, the calculation of resistance R by the formula is also complicated. This resistance is much more easily found if the currents in all elements of the earthing device are equal:

$$I_1 = I_2 = \ldots = I_n = I.$$

Then

$$R = \frac{\varphi}{\Sigma I} = \frac{\varphi}{nI} = \frac{\alpha_{k1} + \alpha_{k2} + \ldots + \alpha_{kk} + \ldots + \alpha_{kn}}{n}, \tag{4}$$

i.e. in this case resistance R can be found by dividing the sum of the coefficients of any of the equations (1) by the number of elements n.

If the currents of the elements of the earthing device are not equal to one another, but their corresponding ratios are known, for example

$$\frac{I_1}{I_k} = A; \quad \frac{I_2}{I_k} = B; \quad \ldots \quad \frac{I_n}{I_k} = N,$$

then

$$R = \frac{\varphi}{\Sigma I} = \frac{\alpha_{k1} A + \alpha_{k2} B + \ldots + \alpha_{kk} + \ldots + \alpha_{kn} N}{A + B + \ldots + 1 + \ldots + N}. \tag{5}$$

Thus, the problem of the calculation of compound earthing devices is reduced to the problem of finding the coefficients of self and mutual potential and the current distribution in the elements of the earthing device. Coefficients of self potential are usually much larger than of mutual potential, therefore there is no need for particularly exact determination of the latter.

In the case of linear earthing electrodes, whose transverse dimensions are small in comparison with the longitudinal, the simplest way for calculation coefficient α is to use the method of mean potentials [1].

The determination of potentials by this method is carried out on the basis of two assumptions:
(1) the current density is everywhere constant along the length of the conductors;
(2) the potential, acquired by the conductor l_2 in the field of the conductor l_1, is equal to the arithmetic mean of the potentials, produced by the field of the conductor l_1 at all points of the conductor l_2.

From the first assumption it follows that in a conducting medium of the resistivity ρ the potential of a point in the field of the linear conductor l_1 is:

$$\varphi = \frac{I_1 \rho}{4\pi l_1} \int_{l_1} \frac{dl_1}{r}, \tag{6}$$

where I_1 is the current in the conductor l_1;

r is the distance from the element dl_1 to the point where the potential is to be found.

According to the second assumption the potential of the conductor l_2 in the field of the conductor l_1 is equal to:

$$\varphi_{21} = \frac{1}{l_2}\int\limits_{l_2}\varphi\, dl_2 = \frac{I_1\rho}{4\pi l_1 l_2}\int\limits_{l_2}\int\limits_{l_1}\frac{dl_2\, dl_1}{r}. \tag{7}$$

The potential of the point A in the field of a rectilinear conductor (Fig. 1) is found in the following way:

$$\varphi = \frac{I_1\rho}{4\pi l_1}\int\limits_{l_1}\frac{dl_1}{r} = \frac{I_1\rho}{4\pi l_1}\int\limits_{x_1}^{x_2}\frac{dx}{\sqrt{x^2+y^2}} = \frac{I_1\rho}{4\pi l_1}\ln\frac{x_2+r_2}{x_1+r_1}, \tag{8}$$

where x_1 and x_2 are to be taken with their corresponding signs.

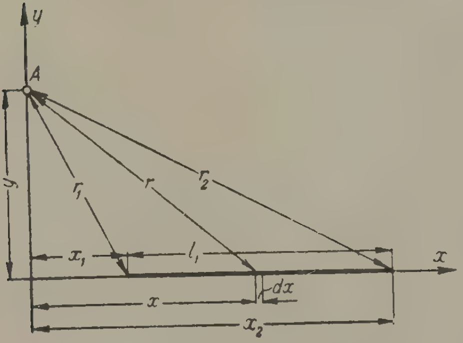

FIG. 1.

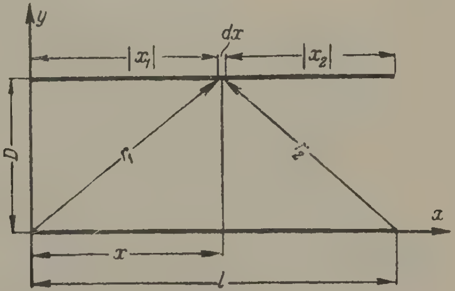

FIG. 2.

Since $x_1 = \dfrac{r_2^2 - r_1^2 - l_1^2}{2l_1}$, and $x_2 = x_1 + l_1$,

we get

$$\varphi = \frac{I_1\rho}{4\pi l_1}\ln\frac{2a+l_1}{2a-l_1}, \tag{9}$$

where $2a = r_1 + r_2$, the sum of distances from the point to the ends of the conductor l_1.

For the electrostatic field this expression has been derived [2].
From expressions (7), (8) and (9) we have:

$$\alpha_{12}=\alpha_{21}=\frac{\varphi_{21}}{I_1}=\frac{\rho}{4\pi l_1 l_2}\int\limits_{l_2}\ln\frac{x_2+r_2}{x_1+r_1}\,dl_2 \tag{10}$$

or

$$\alpha_{12}=\alpha_{21}=\frac{\rho}{4\pi l_1 l_2}\int\limits_{l_2}\ln\frac{2a+l_1}{2a-l_1}\,dl_2. \tag{11}$$

The use of this or other formulae is only a matter of convenience for calculations.

By using formula (2), let us calculate α_{12} between two parallel conductors of equal length (Fig. 2). In this case:

$$\begin{gathered}
l_1=l_2=l;\quad x_1=-x;\quad x_2=l-x;\\
r_1=\sqrt{x_1^2+D^2};\quad r_2=\sqrt{x_2^2+D^2};\\
\alpha_{12}=\frac{\rho}{4\pi l^2}\int\limits_0^l\ln\frac{x_2+\sqrt{x_2^2+D^2}}{x_1+\sqrt{x_1^2+D^2}}\,dx=\\
=\frac{\rho}{4\pi l^2}\int\limits_0^l\ln\frac{\frac{x_2}{D}+\sqrt{\left(\frac{x_2}{D}\right)^2+1}}{\frac{x_1}{D}+\sqrt{\left(\frac{x_1}{D}\right)^2+1}}\,dx=\\
=\frac{\rho}{4\pi l^2}\cdot 2D\int\limits_0^l\sinh^{-1}\left(\frac{x}{D}\right)d\left(\frac{x}{D}\right).
\end{gathered}$$

Hence

$$\alpha_{12}=\frac{\rho}{2\pi l}\left(\sinh\frac{l}{D}-\sqrt{\left(\frac{D}{l}\right)^2+1}+\frac{D}{l}\right). \tag{12}$$

For $\frac{l}{D}<1$

$$\alpha_{12}=\frac{\rho}{4\pi D}, \tag{12a}$$

and for $\frac{l}{D}>3$ we may assume, as a good approximation, that:

$$\alpha_{12}=\frac{\rho}{2\pi l}\ln\frac{l}{D}. \tag{12b}$$

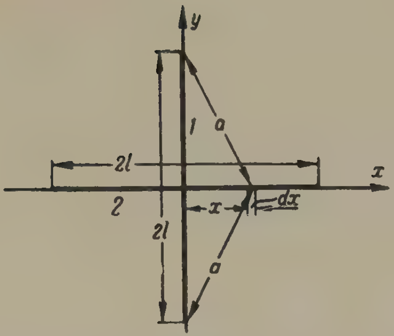

FIG. 3.

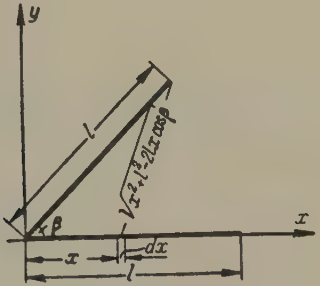

FIG. 4.

Let us apply formula (11) to find α_{12} in the case of the two conductors of the length $2l$, situated in the same plane and intersecting at right angles in the middle of their length (Fig. 3). In this case

$$l_1=l_2=2l;\quad 2a=2\sqrt{l^2+x^2};$$

$$\alpha_{12}=\frac{\rho}{4\pi 4l^2}\int_{-l}^{l}\ln\frac{2\sqrt{l^2+x^2}+2l}{2\sqrt{l^2+x^2}-2l}\,dx=$$

$$=\frac{\rho}{16\pi l^2}\int_{-l}^{l}\ln\frac{\sqrt{l^2+x^2}+l}{\sqrt{l^2+x^2}-l}\,dx.$$

Assuming

$$\sqrt{l^2+x^2}=lz,$$

we obtain:

$$\alpha_{12}=\frac{\rho}{2\pi l}\ln(\sqrt{2}+1)=\frac{\rho}{2\pi l}\,0{,}88. \qquad (13)$$

In many cases it is required to determine the coefficient of mutual potential α_{12} for two rays of equal length, diverging from a common point at an angle β (Fig. 4). In this case:

$$\alpha_{12}=\frac{\rho}{2\pi l}\ln\frac{2+\sqrt{2-2\cos\beta}}{\sqrt{2-2\cos\beta}}. \qquad (14)$$

In the case of two rays of different length diverging from a common point at a right angle (Fig. 5):

$$\alpha_{12}=\frac{\rho}{4\pi l_1 l_2}\left(l_2\sinh^{-1}\frac{l_1}{l_2}+l_1\sinh^{-1}\frac{l_2}{l_1}\right). \qquad (15)$$

The derivation of formulae (14) and (15) is given in the appendices.

The coefficient of self potential of a rectilinear conductor in a conductive medium is:

$$\alpha_{11}=\frac{\rho}{2\pi l}\ln\frac{2l}{d}, \tag{16}$$

where *d* is the diameter of the conductor [2, p.99].

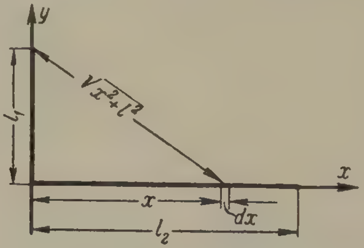

FIG. 5.

In calculating earthing devices, which are earthed to the depth t, the method of images is used, which differs from the analogous method in electrostatics in that images are of the same sign (direction of current flow) as conductors. The earthing resistance of the earthing device is twice as large as the value of the resistance, calculated by formulae (4) or (5) for a system of conductors and their images, since the current, flowing down the conductors of the earthing device, is equal only to a half of the current of this system. In future, symbols of quantities relating to images will be primed.

The above considerations enable us to calculate earthing resistance of the following earthing devices:

A four ray star (Fig. 3) By expression (4) and taking into consideration the above discussion, we get:

$$R=2\,\frac{\alpha_{11}+\alpha'_{11}+\alpha_{12}+\alpha'_{12}}{4}=\frac{\alpha_{11}+\alpha'_{11}+\alpha_{12}+\alpha'_{12}}{2}.$$

Here α_{11}, α'_{11} and α_{12} are determined on the basis of expressions (16), (12b) and (13). Hence also assuming $\alpha'_{12}=\alpha_{12}$, we get:

$$R=\frac{\alpha_{11}+\alpha'_{11}+2\alpha_{12}}{2}=\frac{\rho}{8\pi l}\ln\frac{4\,(\sqrt{2}+1)^4 l^2}{dt}=$$

$$=\frac{\rho}{8\pi l}\ln\frac{135 l^2}{dt}.$$

The exact calculation of α'_{12} gives:

$$\alpha'_{12}=\frac{\rho}{2\pi l}\ln\frac{\sqrt{2l^2+4t^2}+l}{\sqrt{l^4+4t^2}}-\frac{\rho t}{4\pi l^2}\tan^{-1}\frac{l^2}{2t\sqrt{2l^2+4t^2}}.$$

For $\frac{l}{t}=10$

$$\alpha'_{12}=\frac{\rho}{2\pi l}\,0.85,$$

i.e. the difference between α_{12} and α'_{12} is about 3 per cent.

Denote the sum of the lengths of the earthing conductors by L. Then $L = 4l$, and

$$R=\frac{\rho}{2\pi L}\ln\frac{8.45L^2}{dt}. \tag{17}$$

A right-angle For a right angle consisting of two horizontal rays, each of length l, the earthing resistance is:

$$R=\frac{\alpha_{11}+\alpha'_{11}+\alpha_{12}+\alpha'_{12}}{2},$$

where

$$\alpha_{11}=\frac{\rho}{2\pi l}\ln\frac{2l}{d};\ \alpha'_{11}=\frac{\rho}{2\pi l}\ln\frac{l}{2t}.$$

For $\beta = 90°$ from the expression (14) we get:

$$\alpha_{12}=\frac{\rho}{2\pi l}\ln(\sqrt{2}+1).$$

Assuming $\alpha'_{12} = \alpha_{12}$, we get:

$$R=\frac{\rho}{4\pi l}\ln\frac{(\sqrt{2}+1)^2l^2}{dt}=\frac{\rho}{2\pi L}\ln\frac{1.46L^2}{dt}. \tag{18}$$

A three ray star In this case

$$R=\frac{\alpha_{11}+\alpha'_{11}+2\alpha_{12}+2\alpha'_{12}}{3}.$$

For $\beta = 120°$ formula (14) gives

$$\alpha_{12}=\alpha'_{12}=\frac{\rho}{2\pi l}\ln\left(\frac{2+\sqrt{3}}{\sqrt{3}}\right)=\frac{\rho}{2\pi l}\ln 2.15.$$

As a result we get

$$R=\frac{\rho}{6\pi l}\ln\frac{2.15^4l^2}{dt}=\frac{\rho}{2\pi L}\ln\frac{2.38L^2}{dt}. \tag{19}$$

For a six-ray star similarly we get:

$$R=\frac{\rho}{2\pi L}\ln\frac{192L^2}{dt}. \tag{20}$$

For a square:

$$R=\frac{\rho}{2\pi L}\ln\frac{5.53L^2}{dt}. \tag{21}$$

For a rectangle: Denoting the long side of the rectangle l_1 and the short one l_2 and assuming

$$\frac{I_1}{I_2}=\frac{l_1}{l_2},$$

by formula (5) we get:

$$\begin{aligned}R=&\frac{1}{2+2\frac{l_2}{l_1}}\left[\frac{\rho}{2\pi l_1}\ln\frac{2l_1}{d}+\frac{\rho}{2\pi l_1}\ln\frac{l_1}{2t}+\right.\\&+4\frac{\rho}{4\pi l_1 l_2}\left(l_2\sinh^{-1}\frac{l_1}{l_2}+l_1\sinh^{-1}\frac{l_2}{l_1}\right)\frac{l_2}{l_1}+\\&\left.+2\frac{\rho}{2\pi l_1}\left(\sinh^{-1}\frac{l_1}{l_2}-\sqrt{\left(\frac{l_2}{l_1}\right)^2+1}+\frac{l_2}{l_1}\right)\right]=\\=&\frac{\rho}{2\pi L}\left[\ln\frac{l_1^2}{dt}+2\frac{l_2}{l_1}\left(\sinh^{-1}\frac{l_1}{l_2}+\frac{l_1}{l_2}\sinh^{-1}\frac{l_2}{l_1}\right)+\right.\\&\left.+2\left(\sinh^{-1}\frac{l_1}{l_2}-\sqrt{\left(\frac{l_2}{l_1}\right)^2+1}+\frac{l_2}{l_1}\right)\right].\end{aligned}\tag{22}$$

Expressions (17) -(22) can be represented in a general case by the formula

$$R=\frac{\rho}{2\pi L}\ln\frac{KL^2}{dt}.\tag{23}$$

In formula (23) the value of K depends only on the configuration of the earthing device.

For different types of earthing devices the values of K is given in Table 1.

TABLE 1.

Earthing device	K	Earthing device	K	Earthing device	$\frac{l_1}{l_2}$	K
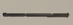	1	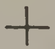	8.45	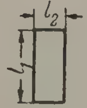	1.5	5.81
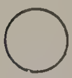	1.27*	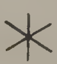	192		2	6.42
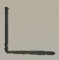	1.46	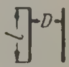	$\frac{l^2}{4D^2}$**		3	8.17
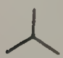	2.38	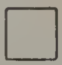	5.53		4	10.4

* $R=\frac{\rho}{2\pi^2 D}\ln\frac{4\pi D^2}{dt}$, where D is the diameter of the circle [4].

** For $D \geqslant 5t$.

The error, due to the assumption $a_{12} = a'_{12}$, is significant only for $l/t < 10$. The values of earthing resistances calculated by formula (23) are 3-5 per cent greater than those calculated by means of utilization factors. This is due to the fact that in calculating utilization factors we used less exact methods for determining the mutual influences of the elements of the earthing device [3].

Appendix

(1) *Derivation of formula (14).*

We make use of formula (11). In our case (Fig. 4).

$$2a = x + \sqrt{x^2 + l^2 - 2xl\cos\beta}.$$

We denote:

$$x^2 + l^2 - 2xl\cos\beta = X.$$

Then

$$\alpha_{12} = \frac{\rho}{4\pi l^2}\int\limits_0^l \ln\frac{x + \sqrt{X} + l}{x + \sqrt{X} - l}\,dx =$$

$$= \frac{\rho}{4\pi l^2}\left[\int\limits_0^l \ln(x + \sqrt{X} + l)\,dx - \int\limits_0^l \ln(x + \sqrt{X} - l)\,dx\right].$$

Putting:

$$du = dx,\quad v = \ln(x + \sqrt{X} \pm l),$$

we evaluate each integral by parts:

$$\int\limits_0^l \ln(x + \sqrt{X} + l)\,dx = [x\ln(x + \sqrt{X} + l)]_0^l -$$

$$-\int\limits_0 x\frac{x + \sqrt{X} - l\cos\beta}{\sqrt{X}(x + \sqrt{X} + l)}\,dx = l\ln[l(2 + \sqrt{2 - 2\cos\beta})] -$$

$$-\frac{1}{2}\int\limits_0^l \frac{xdx}{\sqrt{X}} + \frac{l}{2}\int\limits_0^l \frac{dx}{\sqrt{X}} - \frac{1}{2}\int\limits_0^l dx;$$

$$\int\limits_0^l \ln(x + \sqrt{X} - l)\,dx = l\ln(l\sqrt{2 - 2\cos\beta}) -$$

$$-\frac{1}{2}\int\limits_0^l \frac{xdx}{\sqrt{X}} - \frac{l}{2}\int\limits_0^l \frac{dx}{\sqrt{X}} - \frac{1}{2}\int\limits_0^l dx.$$

Subtracting the second integral from the first we get:

$$\int_0^l \ln\frac{x+\sqrt{X}+l}{x+\sqrt{X}-l}\,dx = l\ln\frac{2+\sqrt{2-2\cos\beta}}{\sqrt{2-2\cos\beta}} + l\int_0^l\frac{dx}{\sqrt{X}} =$$

$$= l\left(\ln\frac{2+\sqrt{2-2\cos\beta}}{\sqrt{2-2\cos\beta}} + \ln\frac{\sqrt{2-2\cos\beta}+1-\cos\beta}{1-\cos\beta}\right) =$$

$$= 2l\ln\frac{2+\sqrt{2-2\cos\beta}}{\sqrt{2-2\cos\beta}}$$

Substituting the expression obtained into formula (11), we get formula (14).

(2) *Derivation of formula (15)*. For this case (Fig. 5).

$$2a = x + \sqrt{x^2+l_1^2};$$

$$a_{12} = \frac{\rho}{4\pi l_1 l_2}\int_0^{l_2}\ln\frac{x+\sqrt{x^2+l_1^2}+l_1}{x+\sqrt{x^2+l_1^2}-l_1}\,dx = \frac{\rho}{4\pi l_1 l_2}\left[\int_0^{l_2}\ln(x+\right.$$

$$\left.+\sqrt{x^2+l_1^2}+l_1)\,dx - \int_0^{l_2}\ln(x+\sqrt{x^2+l_1^2}-l_1)\,dx\right].$$

As in the previous case, putting $du = dx$; $v = \ln(x + \sqrt{y^2+l_1^2} \pm l_1)$ and evaluating each integral separately, we get:

$$\int_0^{l_2}\ln\frac{x+\sqrt{x^2+l_1^2}+l_1}{x+\sqrt{x^2+l_1^2}-l_1}\,dx = l_2\ln\frac{l_2+l_1+\sqrt{l_2^2+l_1^2}}{l_2-l_1+\sqrt{l_2^2+l_1^2}} +$$

$$+ l_1\int_0^{l_2}\frac{dx}{\sqrt{x^2+l_1^2}} = l_2\sinh^{-1}\frac{l_1}{l_2} + l_1\sinh^{-1}\frac{l_2}{l_1}.$$

Translated by S. Szymanski

REFERENCES

1. L.R. Neiman and P.L. Kalantarov; *Teoreticheskie osnovy elektrotekniki (Theoretical principles of electric technology)* part 3, Gosenergoizdat (1948).
2. K.A. Krug; *Osnovy elektrotekhniki (Principles of electrical technology)* vol. 1, Gosenergoizdat (1946).
3. A.P. Beliakov; *Osnovaniia dlia proektirovaniia zazemlenii elektricheskikh ustanovok (Principles of earthing design of electrical installations)*, State United Scientific and

Technical Publishing House, People's Commissariat of Heavy Industry (1938).

4. I.S. Stekolnikov (Editor); Grozozashchita promyshlennykh sooruzheni i zdanii pod redaktsiei *(Lightning protection of industrial constructions and buildings)*, Izv. Akad. Nauk SSSR (1951).

SERVICE TESTS

A METHOD OF CALCULATION OF MECHANICAL CHARACTERISTICS OF ASYNCHRONOUS MOTORS UNDER CONDITIONS OF DYNAMIC BRAKING*

A.G. MIRER

Central Scientific Research Institute for Machine Technology

Generally accepted methods of calculation of mechanical characteristics of dynamic braking do not give a clear idea how the characteristics vary when the excitation current varies (direct current in the stator winding).

In this article a method of calculation of a family of mechanical characteristics for dynamic braking is given; these characteristics allow a proper choice of the excitation current, corresponding to the required characteristic.

Certain relationships which determine the operation of an asynchronous motor under conditions of dynamic braking form the basis for the calculations:

$$E_2' = I_\mu \cdot x_\mu; \tag{1}$$

$$I_2' = \frac{E_2' s}{\sqrt{R_2'^2 + x_2'^2 s^2}}; \tag{2}$$

$$I_e^2 = I_\mu^2 + I_2'^2 + 2 I_\mu I_2' \sin\varphi_2; \tag{3}$$

$$\sin\varphi_2 = \frac{x_2' s}{\sqrt{R_2'^2 + x_2'^2 s^2}}; \tag{4}$$

$$M = 2.92 \frac{I_2'^2 R_2'}{n_s s}, \tag{5}$$

where E_2' is the e.m.f. of the rotor phase, reduced to the stator winding; I_2' is the current of the rotor phase reduced to the stator winding; I_μ is the magnetizing current; x_μ is the reactance of the magnetizing circuit; I_e is the alternating current of the stator phase, equivalent to a direct current inducing in the stator winding the same m.m.f; n_s is the synchronous speed; s is the slip; x_2' is the reactance of the rotor phase reduced to a stator winding; $R_2' = r_2' + R_a'$ is the total resistance of the rotor phase, comprising the winding resistance r_2' and additional resistance r_a', all reduced to the stator winding.

---

* *Elektrichestvo*, No. 4, 65 – 66, 1958.

Under conditions of dynamic braking, the magnetic flux of the machine depends to a considerable extent on the speed of rotation, in consequence the calculation of dynamic characteristics neglecting the influence of saturation, leads to inadmissible errors. For calculation, the magnetization curve of the machine $E_2' = f(I_\mu)$ or the relationship $x_\mu = f(I_\mu)$ must be known. If these data are not available we can make use of universal curves [1, 2]. In contrast to the generally accepted methods of calculation, which consists of the solution of the simultaneous equations (1)-(5), we shall choose a set of values of the magnetizing current $I_{\mu 1}, I_{\mu 2}, \ldots, I_{\mu n}$ and calculate for each chosen value the values of I_2', M and I_e for different values of slip $s_1, s_2 \ldots s_m$.

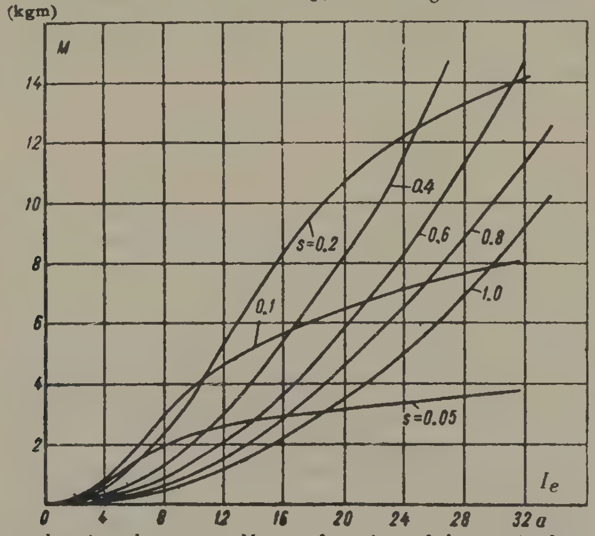

FIG. 1. Curves showing the torque M as a function of the equivalent current I_e.

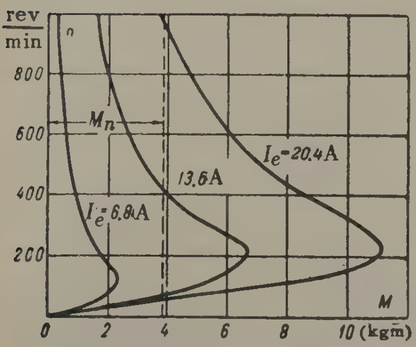

FIG. 2. Mechanical chracteristics of the dynamic braking of a motor of the MTK-12-6 type.

Using these data we may plot the relationship $M = f(I_e)$ for every value of slip $s_1, s_2, \ldots, s_m$ Fig. 1 shows such graphs calculated for a short-circuited motor of type MTK-12-6. The graphs so obtained give a clear idea of the family of mechanical characteristics of dynamic braking, and they enable us easily to construct characteristics corresponding to any equivalent current, since the ordinates of these curves, for given values of I_e, give the values of torques for slips $s_1, s_2, \ldots, s_m$ (Fig. 2).

For motors with a phase rotor we have to construct curves $M = f(I_e)$ for short-circuited rotor rings ($r_a' = 0$), from which it is easy to find corresponding natural mechanical characteristics of dynamic braking. The artificial characteristics for $r_a' \neq 0$ are determined from natural ones by simple recalculation: $s' = s. R_2'/r_2'$ for M = constant and I_e = constant, where s' and s are the values of slip for the required artificial and given natural characteristics respectively.

Relationships $M = f(I_e)$, when once calculated for a certain given type of motor, may be introduced as the catalogue data, in a similar way as for working characteristics, so as to be used for calculation of mechanical characteristics of dynamic braking.

Translated by S. Szymanski

REFERENCES

1. A.T. Golovan; *Elektroprivod (Electric drive)* Gosenergoizdat (1948).
2. S.N. Veshenevskii; *Raschet kharakteristik i soprotivlenii dlia elektrodvigotelei (Calculation of characteristics and resistances for electric motors)*, Gosenergoizdat (1955).

EXPERIMENTAL DETERMINATION OF PARAMETERS OF ELEMENTS OF AUTOMATIC CONTROL SYSTEMS*

S.Ia. BEREZIN

Leningrad

(Received 11 December 1957)

For theoretical investigation of automatic control systems it is necessary to know the parameters of the individual elements of these systems. At present many methods for the determination of the parameters of automatic control systems exist [1, 2].

The majority of these methods are cumbersome, and do not permit the determination of the parameters of elements which are characterized by differential equations of an order greater than the second. In finding these parameters we also assume that the order of the differential equation of the element is known.

The most widely used method of experimental investigation of automatic control systems is the frequency method, owing to its many advantages, which are described in [3]. In using frequency characteristics for finding the parameters of an individual element of automatic control systems it is very convenient to make use of inverse amplitude-phase characteristics, because this permits a considerable reduction of the time required for calculations. The inverse amplitude-phase characteristics of the elements under investigation can be obtained by one of the known methods, for example, those discussed in [3].

The inverse transfer function of an aperiodic link of the first order is of the form:

$$Y(p) = \frac{1}{K_0}(1 + Tp), \tag{1}$$

where K_0 is the amplification factor of the link; T is the time constant of the link. For a sinusoidal disturbance at the link input

$$Y(j\omega) = \frac{1}{K_0}(1 + Tj\omega)$$

the inverse amplitude-phase characteristic of the first order aperiodic link is a straight line parallel to the imaginary axis and passing it at a distance $1/K_0$ (Fig.1).

To find the time constant of the first order aperiodic link it is sufficient to find

---

* *Elektrichestvo*, No. 4, 66 – 69, 1958.

experimentally the phase of the vector of the inverse amplitude-phase characteristic for one frequency, say ω_i.

From Fig. 1 it follows that

$$\frac{AB}{OB} = \tan\phi = T\omega_i$$

hence

$$T = \frac{\tan\phi}{\omega_i} \tag{2}$$

The amplification factor of the link can be determined by meters or from the experimentally found amplitude and phase of the vector of the inverse amplitude-phase characteristic for the same frequency:

$$OB = \frac{1}{K_0} = OA\cos\phi$$

hence

$$K_0 = \frac{1}{OA\cos\phi}, \tag{3}$$

where OA is the amplitude (modulus) of the vector of the inverse amplitude-phase characteristic ω_i.

To check the accuracy of the parameters so found it is recommended that calculations should be repeated for other frequencies.

If the parameters found for various frequencies differ considerably one from another, and points A_i of the inverse amplitude-phase characteristic do not lie in the straight line, this will prove that the link in question is not a link of the first order.

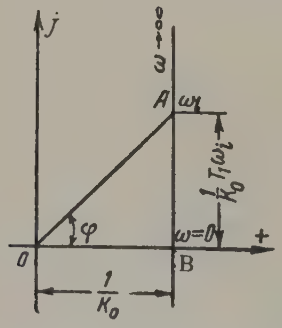

FIG. 1. The inverse amplitude-phase characteristic of an aperiodic link of the first order.

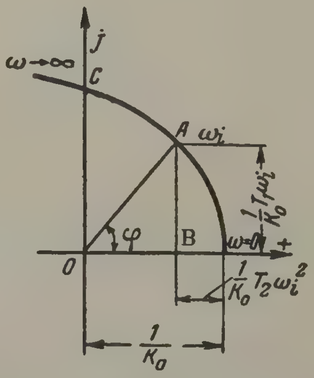

FIG. 2. The inverse amplitude-phase characteristic of a link of the second order.

The inverse complex transfer function for the second order link (aperiodic or oscillatory) is of the form:

$$Y(j\omega)=\frac{1}{K_0}(1+T_1j\omega-T_2\omega^2). \tag{4}$$

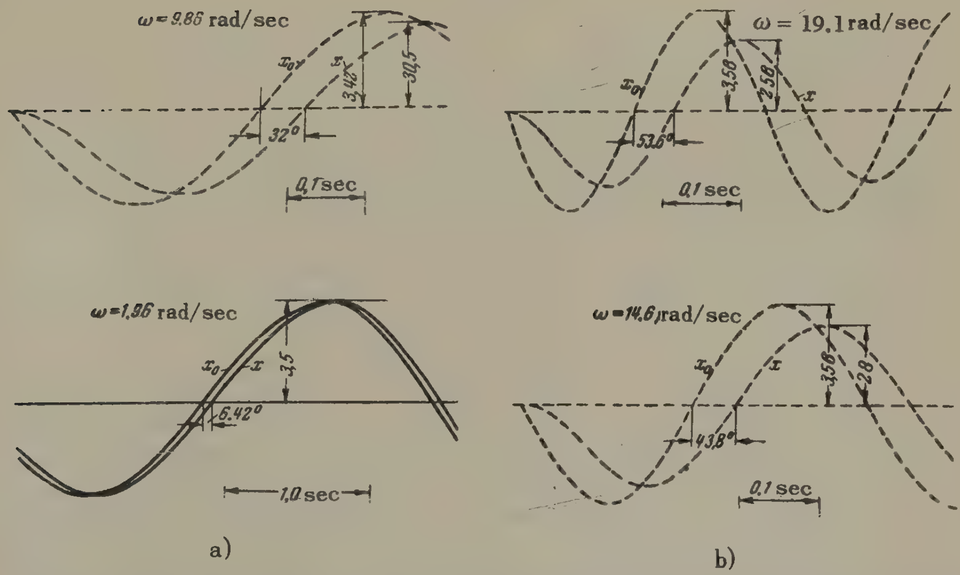

a) b)

FIG. 3. Curves of the variation of the input and output signals in the presence of sinusoidal disturbances at the input to the element under investigation.

The inverse amplitude-phase characteristic for this link is shown in Fig. 2. This characteristic lies in two quadrants.

From Fig. 2:

$$\sin\phi=\frac{AB}{OA}=\frac{T_1\omega_i}{K_0OA};\quad T_1=\frac{OA.K_0}{\omega_i}\sin\phi. \tag{5}$$

The amplitude OA and phase ϕ are found from the inverse amplitude-phase characteristics, which were experimentally determined for the frequency ω_i.

$$\cos\phi=\frac{(1-T_2\omega_i^2)}{K_0.OA}, \tag{6}$$

hence

$$T_2=\frac{1}{\omega_i^2}(1-K_0.OA\cos\phi). \tag{7}$$

The calculation of the constant T_2 can be carried out in a different way. From the triangle OAB (Fig. 2):

$$\frac{AB}{OB}=\frac{T_1\omega_i}{1-T_2\omega_i^2}=\tan\phi, \tag{8}$$

hence

$$T_2 = \frac{1}{\omega_i^2} - \frac{T_1}{\omega_i \tan\phi} \tag{9}$$

The calculation of T_2 can be considerably simplified, if we determine experimentally the frequency for which the inverse amplitude-phase characteristic intersects the imaginary axis ($\phi = 90^\circ$) (the real part of the characteristic is zero):

$$\frac{1}{K_0}(1 - T_2\omega_i^2) = 0;\quad T_2 = \frac{1}{\omega_i^2} \tag{10}$$

In this case, for a known modulus we have:

$$T_1 = \frac{OA.K_0}{\omega i}. \tag{11}$$

If the amplitude-phase characteristics are recorded at low frequencies, then, with an accuracy sufficient in practice, we may assume that

$$OA = \frac{1}{K_0}$$

and then:

$$T_1 = \frac{\sin\phi}{\omega i}; \tag{12}$$

$$T_2 = \frac{1}{\omega_i^2}(1 - \cos\phi). \tag{13}$$

But in this case, the accurate determination of the phase value is rather difficult.

In certain cases the preliminary determination of the amplification factor of the element in question is connected with many difficulties. Therefore, the determination of the parameters of this element from two points of the inverse amplitude-phase characteristic, obtained experimentally, may be recommended.

For example, if ϕ_1, ϕ_2, OA_1 and OA_2 are determined experimentally, then from (6) we find:

$$K_0 = \frac{1}{\cos\varphi_1 OA_1} - T_2\frac{\omega_1^2}{\cos\varphi_1 OA_1} = \frac{1}{\cos\varphi_2 OA_2} - T_2\frac{\omega_2^2}{\cos\varphi_2 OA_2},$$

hence

$$T_2 = \frac{\cos\varphi_1 OA_1 - \cos\varphi_2 OA_2}{\omega_2^2\cos\varphi_1 OA_1 - \omega_1^2\cos\varphi_2 OA_2} \tag{14}$$

or

$$T_2 = \frac{B_1 - B_2}{\omega_2^2 B_1 - \omega_1^2 B_2}, \tag{14a}$$

where $B_1 = OA_1 \cos\phi_1$; $B_2 = OA_2 \cos\phi_2$, the real parts of the vector of the inverse amplitude-phase characteristic for frequencies ω_1 and ω_2.

The calculation of the constant T_1 can be made by formula (8):

$$T_1 = \frac{\tan \phi i}{\omega i} (1 - T_2\omega_i^2). \tag{15}$$

The amplification factor of the link is most easily found by expression (5):

$$K_0 = \frac{T_1\omega i}{OA_i \sin \phi i}. \tag{16}$$

To check the accuracy of the values of the parameters thus found it is advisable, as in the first case, to repeat the calculations for certain other frequencies.

If from experimental determination of the amplitude-phase characteristic it follows that the phase is near to 180°, it then proves that the order of the link in question is higher than two, and the inverse amplitude-phase characteristic for high frequencies will lie in the third quadrant. The electric integrator MPT-9 was used to verify the accuracy of the above method for determining the parameters of the elements of an automatic control system. By means of the integrator several points of the amplitude-phase characteristic were obtained for a given element characterized by the equation:

$$\frac{1}{10} (1 + Tip + P_2 p^2)x = x_0$$

Fig. 3 shows the curves of variation of input and output signals in the presence of sinusoidal disturbances at the input to the element under investigation for frequencies 1.96, 9.86, 14.6, 19.1 rad/sec. The results of the analysis of the oscillograms and of the performed calculations are shown in Table 1.

TABLE 1.

ω, (rad/sec)	φ, (°)	$\frac{A_1}{A_2}$	T_1, (sec)	T_2, (sec^2)
1.96	6.42	0.1	0.057	$1.56 \cdot 10^{-3}$
9.86	32	0.112	0.0603	$5.14 \cdot 10^{-4}$
14.6	43.8	0,127	0.06	$4.7 \cdot 10^{-4}$
19.1	53.6	0.142	0.06	$4.7 \cdot 10^{-4}$

Note. Calculations of T_1 and T_2 were carried out by the approximate formulae (12) and (13).

The results of these calculations prove the high precision of the method proposed for determining the parameters of the linear elements of automatic control systems.

The error in determining the parameters is smallest for sufficiently large values of ϕ and A_1/A_2; i.e. in the region of high frequencies. Therefore, the determination of parameters should be carried out from the amplitude-phase characteristics recorded for high disturbing frequencies.

Translated by S. Szymanski

REFERENCES

1. G.L. Rabkin, B.A. Mitrofanov and Iu.D. Steinberg; *Avtomatika i telemekhanika,* No. 5 (1955).
2. E.L. Ettinger and Iu.R. Reingold; *Elektrichestvo* No. 3, (1956).
3. Iu.R. Reingold; *Elektrichestvo,* No. 4 (1954).

ELEKTRICHESTVO

Editor-in-Chief: N. G. DROZDOV

Deputy Editor-in-Chief: I. A. SYROMIATNIKOV

EDITORIAL BOARD

K. A. ANDRIANOV, N. I. BORISENKO, G. V. BUTKEVICH, M. G. CHILIKIN, A. A. GLAZUNOV, V. A. GOLUBTSOVA, E. G. KOMAR, M. P. KOSTENKO, L. R. NEIMAN, I. I. PETROV, V. I. POPKOV, A. M. FEDOSEEV

Pergamon Press are also the publishers of the following journals:

JOURNAL OF NUCLEAR ENERGY (*including* THE SOVIET JOURNAL OF ATOMIC ENERGY *on behalf of Pergamon Institute, a non-profit-making foundation*)

REACTOR TECHNOLOGY (*Journal of Nuclear Energy, Part B*)

HEALTH PHYSICS (*The Official Journal of the Health Physics Society*)

JOURNAL OF INORGANIC AND NUCLEAR CHEMISTRY

TETRAHEDRON (*The International Journal of Organic Chemistry*)

TALANTA (*An International Journal of Analytical Chemistry*)

INTERNATIONAL JOURNAL OF APPLIED RADIATION AND ISOTOPES

BIOCHEMICAL PHARMACOLOGY

*BIOPHYSICS

*JOURNAL OF MICROBIOLOGY, EPIDEMIOLOGY AND IMMUNOBIOLOGY

*PROBLEMS OF HEMATOLOGY AND BLOOD TRANSFUSION

*PROBLEMS OF VIROLOGY

*PROBLEMS OF ONCOLOGY

*SECHENOV PHYSIOLOGICAL JOURNAL OF THE U.S.S.R.

*RADIO ENGINEERING

*RADIO ENGINEERING AND ELECTRONICS

*TELECOMMUNICATIONS

*THE PHYSICS OF METALS AND METALLOGRAPHY

*THE ABSTRACTS JOURNAL OF METALLURGY

*APPLIED MATHEMATICS AND MECHANICS

CHEMICAL ENGINEERING SCIENCE

JOURNAL OF ATMOSPHERIC AND TERRESTRIAL PHYSICS

PLANETARY AND SPACE PHYSICS

GEOCHIMICA ET COSMOCHIMICA ACTA

BULLETIN GÉODÉSIQUE

ANNALS OF THE INTERNATIONAL GEOPHYSICAL YEAR

SPECTROCHIMICA ACTA

JOURNAL OF THE MECHANICS AND PHYSICS OF SOLIDS

ACTA METALLURGICA (*for the Board of Governors of Acta Metallurgica*)

INTERNATIONAL JOURNAL OF THE PHYSICS AND CHEMISTRY OF SOLIDS

DEEP-SEA RESEARCH

JOURNAL OF NEUROCHEMISTRY

JOURNAL OF PSYCHOSOMATIC RESEARCH

JOURNAL OF INSECT PHYSIOLOGY

JOURNAL OF AIR POLLUTION

INTERNATIONAL ABSTRACTS OF BIOLOGICAL SCIENCES (*for Biological and Medical Abstracts Ltd.*)

RHEOLOGY ABSTRACTS

VACUUM

OPERATIONAL RESEARCH QUARTERLY

ANNALS OF OCCUPATIONAL HYGIENE

*Translations of the Russian journals published on behalf of Pergamon Institute, a non-profit-making foundation.

Leaflets giving further details and subscription rates of each of these journals are available on request.

ELECTRIC TECHNOLOGY, U.S.S.R.

1959 VOLUME 1 JANUARY

CONTENTS

PAGE

I. M. Postnikov: A method of calculating the performance of compound synchronous motors ... 1

B. I. Nornevskii, V. F. Batko, V. E. Malishevskii, P. V. Kuropatkin and E. I. Rosin: Comparison of two-stage and three-stage rotary amplifiers with axial field ... 18

V. D. Afanas'ev and Ivobotenko: Speed control of a d.c. motor fed from a magnetic amplifier ... 28

Yu. E. Efroimovich: Model installation for remote control of electric parameters in arc furnaces ... 39

L. Ia. Stanislavskii: Turbo-generators of 30 to 200 MV power built by Khetz factory 50

V. G. Fastovskii and Iu. V. Petrovskii: On the possibility of intensification of cooling of turbo-generators ... 61

A. P. Geppe: On the surface resistance of dielectrics ... 68

K. F. Guba: The dependence of frequency of the rochelle salt piezo-electric vibrators on temperature ... 77

A. M. Kakhelnik: The use of electric locomotives with rectifiers—A review ... 81

I. A. Glebov and S. F. Zonov: Service tests—Tests of the experimental installation of an ionic excited hydrogenerator ... 89

T. A. Suetin: Ignition IVS-200/2 ... 97

B. Konorskii: Discussion: Modification of the heaviside formula ... 102

K. A. Andrianov: Synthetic compounds of high molecular weight as dielectrics ... 110

P. V. Sakharov: Apparatus for low-voltage distribution gear ... 127

G. V. Ostroumov: Investigation of transient processes in linear circuits by the method of loci ... 137

I. G. Shubov: Determination of the level of magnetic noise of d.c. machines by the method of electromechanical analogy ... 146

Yu. P. Petrov: Transient processes in an electric drive for an exponential variation of the magnetic flux ... 156

T. A. Glazenko: The use of electromagnetic powder couplings for frequent reversals of a driven mechanism ... 164

A. A. Sakovich: The increase of the reliability of conversion networks ... 177

A. B. Oslon: Calculation of certain types of compound earthing devices ... 187

A. G. Mirer: Service tests—A method of calculation of mechanical characteristics of asynchronous motors under conditions of dynamic braking ... 198

S. Ia. Berezin: Experimental determination of parameters of elements of automatic control systems ... 201

Made and printed in Great Britain by The Campfield Press, St. Albans